COMPUTER-AIDED-PROCESS DESIGN AND OPTIMIZATION (WITH COAL TO METHANOL AND OTHER EXAMPLES)

A thesis

submitted in fulfilment of

the requirements for the degree

of

Doctor of philosophy in Chemical and Process engineering

in the

University of Canterbury

by

K. A. Islam

University of Canterbury

1986

ACKNOWLEDGEMENTS

I would like to thank my supervisor Dr. W. B. Earl for his helpful advice and criticisms throughout this work. Through his kindness, tolerance and encouragement it has been possible to bring the work to a meaningful conclusion.

Thanks to Newzealand Commonwealth Scholarship Committee for granting me a commonwealth sholarship.

Thanks to Bangladesh University of Engineering and Technology for granting me a study leave during the project duration.

Thanks to Dr. R. P. Gupta for his constructive advice at the latter part of the project.

Thanks to all the postgraduates in the Chemical and Process Engineering Department for their stimulating and encuraging discussions in the seminar room.

Lastly but not the least, thanks must go to my wife and son for their patience and encouragement.

DEDICATED TO MY WIFE (ISHRAT), SON (SEEMAB)

AND

PARENTS

ABSTRACT

Steady state process modules for a Dry ash Lurgi-type moving bed coal coal gasifier, a High temperature shift reactor, a low pressure Copper based methanol reactor and a Hot gas recycle methanation reactor have been developed based on the detailed kinetics of the reactions concerned. The model results compare resonablely well with either published plant data or earlier model results. These modules were used for the following purposes:

(i) To design and/or simulate individual process units.

(ii) To examine the effects of different operating variables on individual process performance.

(iii) To optimize the operating cost of individual process units of a coal-to-methanol plant.

With minor modifications, these modules can be used as user-added subroutines in the process flowsheet packages e.g PROCESS, ASPEN, CHESS etc. In fact since this work was completed the methanol module has been incorporated as a user-added subroutine to PROCESS.

A brief state of the art analysis of different existing systems, thermodynamics, kinetics and catalysis of the gasification, shift, methanol synthesis and methanation processes are also included in the appropriate chapters.

Table of Contents

	page
(i) ACKNOWLEDGEMENTS	(i)
(ii) ABSTRACT	(ii)
1. CHAPTER I: PROCESS MODULE FOR A LURGI DRY ASH COAL GASIFIER	I-1
2. CHAPTER II: PROCESS MODULE FOR A HIGH TEMPERATURE SHIFT REACTOR ..	II-1
3. CHAPTER III: PROCESS MODULE FOR A COPPER BASED LOW TEMPERATURE LOW PRESSURE METHANOL SYNTHESIS REACTOR	III-1
4. CHAPER IV: PROCESS MODULE FOR A METHANATION REACTOR SYSTEM	IV-1
5. CHAPTER V: OPTIMIZATION OF THE REACTING SYSTEMS OF A COAL-TO-METHANOL PLANT	V-1
6. SUGGESTIONS FOR FURTHER WORK	VI-1

Listing of the computer programs of all the modules are given in volume II.

CHAPTER I

PROCESS MODULE FOR A LURGI COAL GASIFIER

ABSTRACT

A steady state heterogeneous model of the Lurgi dry ash moving bed coal gasifier has been developed based on detailed kinetics of the different reactions involved. A shell progressive (SP) model is used to describe the relatively faster combustion and char-steam reactions, whearas the rest of the reactions are considered to be controlled by their respective intrinsic reaction rates. Devolatilization, drying and heating are assumed to take place at finite rates using relatively simple models to describe these phenomena. This process module takes into account the above processes systematically and can be used to analyse and model the operation of the gasifier and to determine the optimum operating ranges of the controllable variables for trouble-free operation. This module is more robust than the existing modules available in the literature, and yet resonably simple structurally. It can also be easily extended to simulate the BGC-Lurgi slagging coal gasifier by using a ash segregated model for combustion and char-steam reactions along with some other minor modifications. The module has been tested with illinois(U.S.A) bituminous coal and model results compare well with published plant data as well as with other model results. By changing the relative reactivity factor for the coal (as proposed by Johnson, J. L., 1974 and Kasoka et al., 1983) the model could be fitted to other coal types.

TABLE OF CONTENTS

		page
(i)	ABSTRACT	
1.0	INTRODUCTION	I-1
2.0	DEVELOPMENT OF THE MODEL	I-8
2.1	Description of the Lurgi pressurized dry-ash moving bed coal gasifier	I-8
2.2	Some important assumptions in the model ..	I-11
2.3	Fundamental experimental kinetics measurements	I-14
2.3.1	Combustion and gasification reactions	I-14
2.4	Devolatilization	I-16
2.5	Drying and heating of coal	I-19
2.6	Development of model equations and solution methodology	I-22
2.7	Flow diagram of the gasifier process module	I-28
3.0	RESULTS AND DISCUSSION	I-31
3.1	Composition and temperature profiles	I-36
3.2	Effects of coal particle size	I-36
3.3	Effects of Steam/Oxygen ratio	I-42
3.4	Effects of Fixed carbon/Oxygen ratio	I-42
3.5	Effects of Blast gas (Steam/Oxygen) inlet temperature	I-49
4.0	CONCLUSIONS & SUGGESTIONS	I-52
4.1	Limitations of the model and Suggestions for furher work	I-53
5.0	NOMENCLATURE	I-55
6.0	REFERENCES	I-59
7.0	APPENDIX I-A: Three point moving averaging technique.	I-63

1.0 INTRODUCTION

Gasification can be defined as the reaction of solid fuels with air, oxygen, steam, carbon dioxide or mixtures of these to yield gaseous products that are suitable for use either as a source of energy or as raw materials for the synthesis of chemicals, liquid fuels, or other gaseous fuels. Thus gasification yields a product that can be handled with maximum convenience and minimum cost, and greatly extends the uses of solid fuels. Gasification processes may be classified in a variety of ways:

A. By the method of supplying the heat required for the gasification reactions.

(i) Internal heating

(a) Autothermic (b)cyclic (c)Heat carrying fluids or solids.

(ii) External heating; heat transferred through walls of reaction vessel.

B. By the method of contacting reactants.

(i) Moving bed

(ii) Fluidized bed

(iii) Entrained bed

C. By the flow of reactants.

(i) Cocurrent

(ii) Countercurrent

D. By the gasifying medium.

(i)Steam with oxygen or air or oxygen enriched air

(ii) Hydrogen

E. By the condition of residue removal.

(i) Dry ash

(ii) Slag in slagging operation

Coal gasification reactors are designed to convert as large a fraction of the coal as possible to combustible gases. Several commercially available coal gasification reactors are Lurgi moving bed pressurized gasifier, British Gas-Lurgi slagging gasifier, Kopper-Totzek entrained bed gasifier and the Winkler fluidized bed gasifier.

There are several advantages to a moving bed process over entrained flow and fluidized bed gasifiers. These are low pressure drop, high thermal efficiency, high carbon conversion, low entrainment of solids in the gas; effective utilization of sensible heat both at the upper and lower parts of the gasifier and in cases where the product gases are used for fuel there is direct enhancement of heating value due to the production of rich gases during devolatilization. The operation of the moving bed gasifier is relatively simple.

There are also a number of disadvandages of fixed bed gasifiers. Caking coals can not be used without pretreatment to render them nonagglomerating or without modifying the mechanical design or operating conditions of the gasifier. Sized coals must be used for maximum efficiency. The proportion of fines in the feed must be relatively low to avoid excessive entrainment of solids in the gases. The tar and oil produced in the lower temperature zones near the top of the bed add extra costs for gas purification. The production of hydrocarbons in these zones is undesirable when the gas is to be used for sythesis purposes. A fixed bed with diameter greater than 4 m has not been demonstrated commercially because of difficulty in uniformly distributing coals to the bed while fluids beds with diameter greater than 9 m are commonplace in other applications.

The Lurgi pressurized dry-ash gasifier is chosen for modeling because it is a commercially proven process e.g many Lurgi gasifiers have been in operation in Sasol, South Africa for many years and there are data available in the open

literature for model validation and comparison purposes. The Lurgi gasifier is shown diagramatically in fig.1. The moving grate at the bottom acts as a blast gas distributor and removes dry powdered ash. Dry ash removal necessitates operation below the ash clinker formation temperature.

The performance and efficient operation of these coal gasifiers depend on many variables e.g coal properties, reactor configuration, composition and temperature of the blasting medium, operating pressure, feed and blast rates. Because of the difficulty and cost of analyzing the operation of a gasifier in actual experimental conditions over a wide variety of operating conditions several qualitative models of fixed bed coal gasifiers have been developed e.g. Rudolph (1972, 1973) and Hoogendorn (1973).

Quantitative models reported in the literature can be divided into two distinct categories i.e.
(i)Equilibrium based models
(ii)Kinetic based models.

Equilibrium based models:

Gumz (1950) was the first to develop an equilibrium model of a coal gasifier. Woodmansee (1976) extended Gumz's model to calculate the exit gas temperature by adding a simple devolatilization model. Desai and Wen (1978) developed a comprehensive equilibrium model of fixed bed coal gasifiers by dividing the gasifier into three zones e.g. combustion, gasification and devolatilization and using different approach factors for reactions at different zones. With a given coal composition and feed rate, air and steam feed rates, this model can be used to calculate the composition and temperature of the gases leaving the gasifier. Using Yoon's (1978) model Denn et al. (1979) showed that temperature and composition profiles throughout the gasifier are sensitive to certain model inputs e.g. CO/CO_2 (mole $mole^{-1}$) ratio in the combustion reaction and coal particle size, but the effluent gas composition and temperature are insensitive to large variations in the same inputs. Based on these findings they developed a simple kinetic free (KF) model that could provide

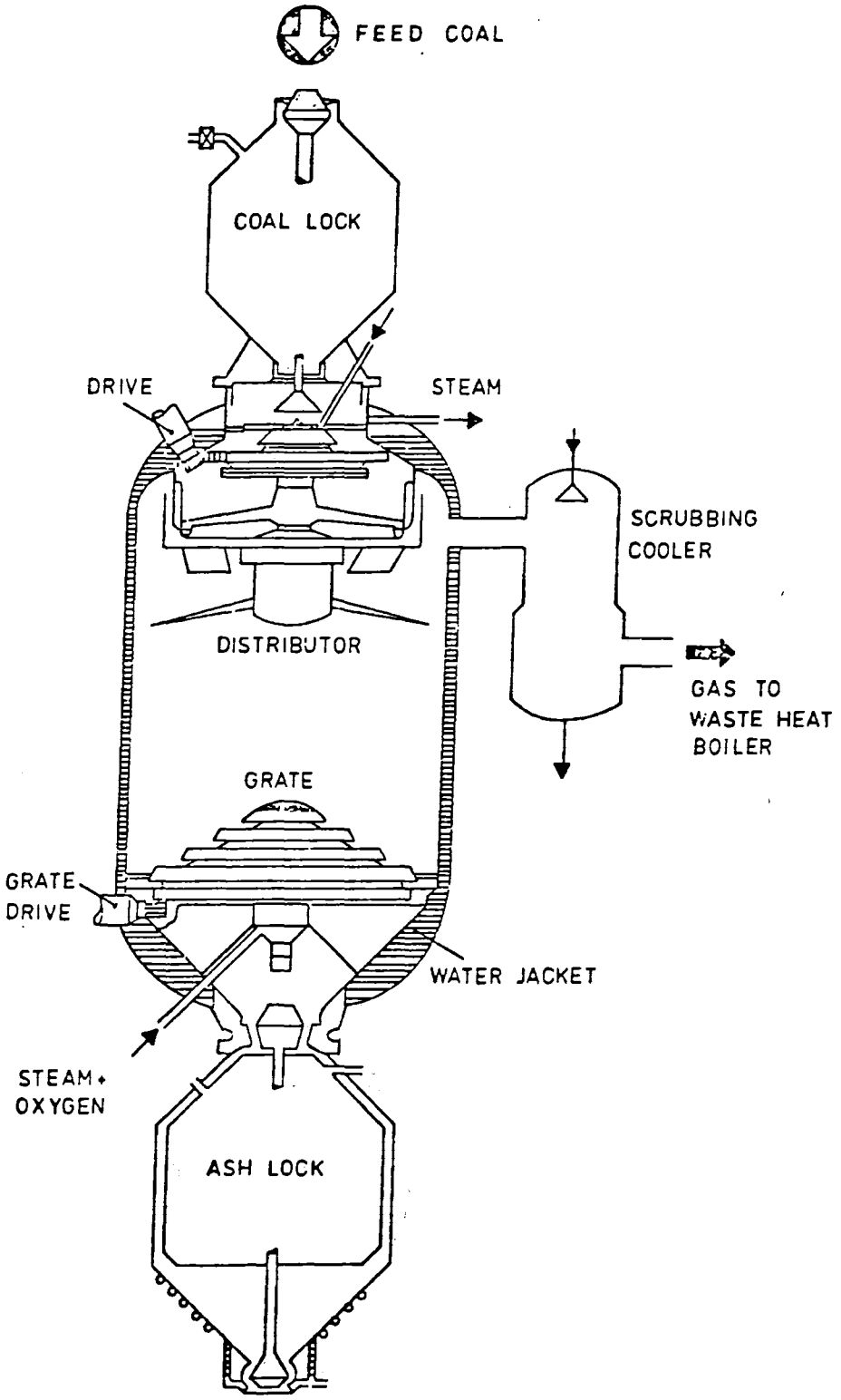

Fig. 1 : Typical Lurgi gasifier cross-section.

a rapid means for estimating overall gasifier performance under conditions of efficient carbon utilizations. Kosky and Floess(1980) devoloped a global model of a countercurrent coal gasifier assuming that the water-gas shift was at equilibrium in the exit gases before devolatilization and concluded that:-

(i) The heating value of the exit gas rises nearly 40% due to the rise in blast temperature from 450 K to 850 K, whearas the temperature at the end of gasification zone rises only from 1180 K to 1320 K implying a beneficial conversion of blast sensible heat to heating value of product gases.

(ii) Heat loss from the gasifier primarily affects the sensible heat of the product gas without affecting its heating value.

The applicability of all these equilibrium based models are limited in studying the performance of the gasifier. These models can not be used to show the effects of particle size, steam/oxygen ratio, blast medium inlet temperature, fixed carbon/oxygen ratio on maximum temperature and its position in the bed and neither can they be used for the design of the gasifier.

Kinetics based models:

Rate models are important not only for simulation of the gasifier but also for its design e.g height and diameter calculations. Since the rate models are based on hydrodynamics and detail kinetics of the reactions involved, they can be used to determine the capacity of the gasifier as it is limited by the phenomena in the reaction zones which can lead to gas channeling, clinker formation and carbon burn-up. Walker et al. (1937) presented a coal gasifier model by formulating an expression relating the maximum bed temperature to the reduction of reactants by accounting for the amount of heat conducted and radiated, as well as convected from the oxidation zone. Woodmansee (1976) discussed the merits and demerits of both the Gumz equilibrium model and the Walker et al. rate model and concluded that by combining these two models one can better predict the variation of maximum

temperature with blast rate and steam concentration. Amundson and Arri (1978) developed a model for the countercurrent char gasifier based on a detailed single char particle model (Arri and Amundson, 1978) and showed the effect of blast rate and blast temperature, steam/oxygen feed ratio, solid feed rate, radiation loss from coal particles, coal reactivities, ash layer depth, and ash layer temperature gradient, operating pressure on both conversion of coal and on some operating characteristics of the gasifier e.g. maximum temperature in the bed, its location and its relation to the thickness of the ash layer at the bottom of the reactor. Amundson and Arri(1978) did not compare the model results with plant data, and this model is also mathematically more complex than other existing models. Biba et al. (1978) formulated a detail heterogeneous model of a pressurized coal gasifier based on the following main assumptions:

(i)The gasifier consists of four distinct zones e.g. combustion, gasification, devolatilization and drying where specific processes take place.

(ii)The rates of the fluid-solid reactions are either chemical reaction, or, pore diffusion, or boundary layer diffusion controlled based on some limiting temeratures and characteristics of the coal concerned.

(iii) Devolatilisation and drying rates are finite and constant.

(iv) Heat of reactions affect the gas phase temperature only.

(v) Heat loss from the bed affects the gas phase temperature only.

The limiting temperatures used by Biba et al. (1978) to determine the rate determining step of the reaction may be difficult to obtain for different coals having different reactivity. Also the solid phase temperature gradient in the combustion zone is so high (30000 K m^{-1}), it may be difficult to apply the limiting temperature criterion to determine the rate of reactions without avoiding numerical instability as

well as oscillatory solution. Biba et al. did not use their model to predict the effects of different input parameters (e.g steam/oxygen ratio, blast gas inlet temperature, fixed carbon/oxygen ratio) on reactor performance. They checked the validity of their model only by comparing outlet gas composition and exit gas temperature with those of plant data. But outlet gas composition and temperature are not appropriate variables for checking the validity of the model as these variables are insensitive to large variation in certain input parameters (Denn et al., 1979).

Desai and Wen (1978) developed a steady state homogeneous model of the countercurrent coal gasifier of Morgantown Energy research center, taking into consideration the kinetics of the various reactions as well as the dimensions of the gasifier and obtained comparable results to plant results. This model failed to give a stable solution for a steam/oxygen case even for a very small integration step size because of inappropriate combustion and carbon-steam reaction rate expressions.

Yoon et al. (1978) developed a comprehensive steady state homogeneous model of moving bed coal gasifier and analyzed the effects of fixed carbon/oxygen feed ratio, feed gas temperature, steam to oxygen feed ratio on location of maximum temperature and gasifier performance. They obtained good agreement of their model predictions with plant data. This model is based on the assumption that solid and gas phase temperature are the same all throughout the reactor, which is not valid (Rudolph, 1973), particularly at the bottom and top parts of the reactor bed. Because of this assumption there is considerable doubt regarding the validity and usefulness of the model results. Cho and Joseph (1981) extended Yoon's model for unequal gas and solid temperatures and formulated a heterogeneous steady state model.

2.0 DEVELOPMENT OF THE MODEL

2.1 Description Of The Lurgi Pressurized Moving Bed Gasifier

The Lurgi gasifier is a reactor designed for countercurrent gasification of coal in a slowly moving bed. The reactor is equiped with the following devices as shown in fig.1.

- An automated coal lock chamber for feeding coal from a coal bin to the reactor.
- A rotating coal distributor for uniform distribution of coal throughout the bed. Blades are mounted to the rotating distributor when processing caking coal.
- A revolving grate for introducing gasifying agents as well as for extracting the ash.
- An ash lock chamber for discharging the ash from the pressurized reactor to an ash bin.
- A water jacket for protecting the gasifier wall from overheating. This also produces steam.

Following Rudolph(1973) the descending path of coal particles can be divided into five zones where distinct chemical and physical processes take place.(shown in fig.2.)

(i) The first zone from the top is where the coal is preheated and dried by hot rising gases.

(ii) The second zone is the devolatilization zone where volatile products (gases, tar, and decomposition water) are separated from coal.

(iii) The second zone is followed by the gasification zone, which occupies most of the gasifier space. In this zone several reactions occur simultaneously between char and gases. The following reactions are cosidered for modeling purposes.

$$C + H_2O \rightleftarrows CO + H_2 \qquad (1)$$

$$C + CO_2 \rightleftarrows 2CO \qquad (2)$$

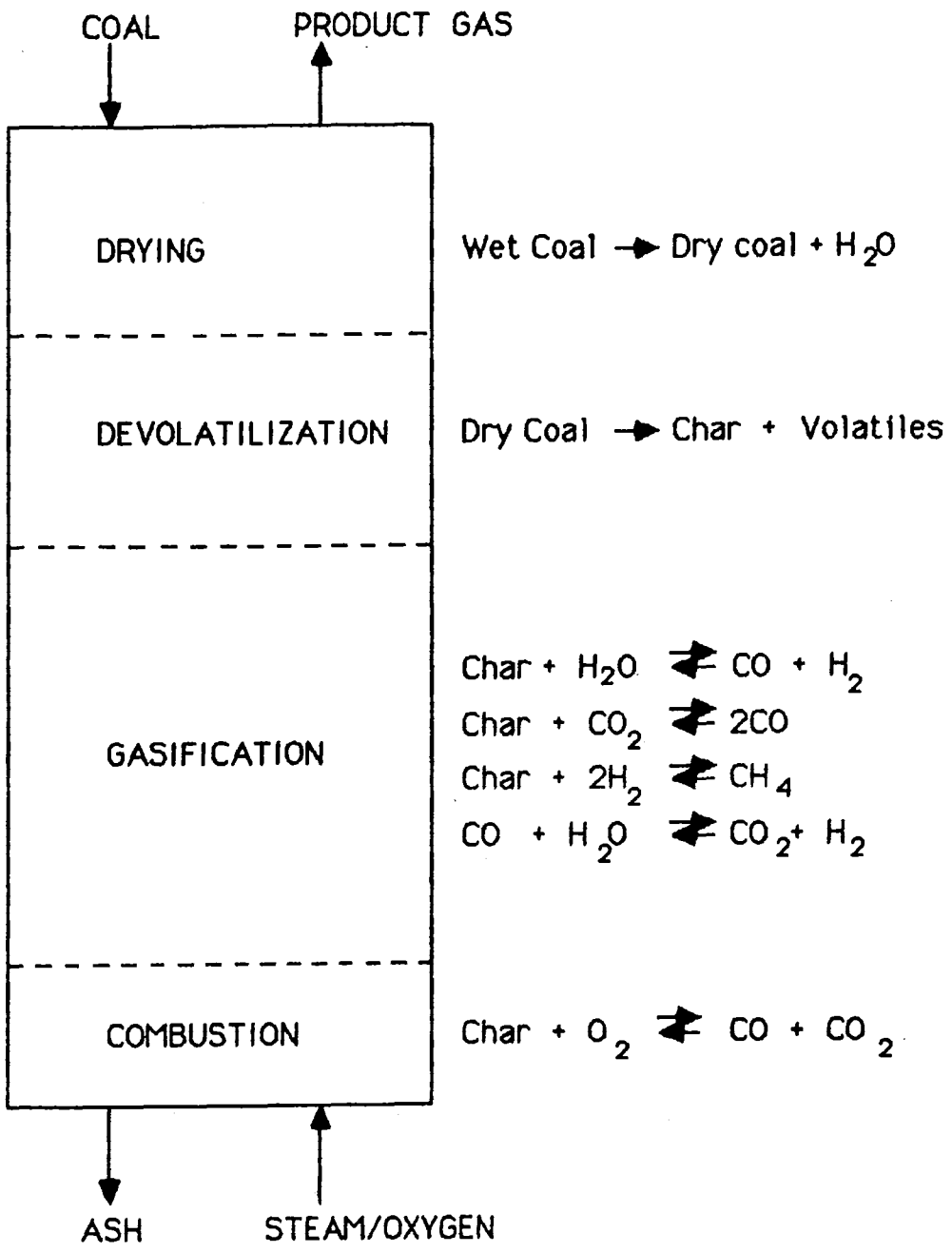

Fig. 2 Physical and chemical reactions in gasifier zones

$$C + 2H_2 \rightleftharpoons CH_4 \qquad \text{(3)}$$

$$CO + H_2O \rightleftharpoons CO_2 + H_2 \qquad \text{(4)}$$

(iv) The next zone is the oxidation zone where the highly exothermic oxidation reaction between char and oxygen takes place.

$$C + \frac{2 + \lambda}{2(1 + \lambda)} O_2 \leftrightarrows \frac{\lambda}{\lambda + 1} CO + \frac{1}{\lambda + 1} CO_2 \qquad \text{(5)}$$

This highly exothermic reaction supplies the heat for sustaining the endothermic gasification reactions.

(v) The last zone is the gas preheating zone where the entering gas mixture is heated rapidly by hot outgoing ash.

In the actual operation of the gasifier the above mentioned zones are not so distinct but rather depend on the type of coal and the operation of the gasifier and are overlapping. In the model development each zone is not considered separately but the physical and chemical processes distinct to each zone effectively define each zone. Since there is a water jacket surrounding the gasifier wall a considerable amount of heat is transferred from the gasifier bed to the jacket water. But because the thermal conductivity of the bed is low, most of the cross-section of the bed is unaffected by this heat loss. Thus the heat loss effect is confined to a thin layer near the gasifier wall. Yoon et al. (1978) considered this thin boundary layer seperately and solved the mass and heat balance differential equations seperately for the adiabatic core and for the boundary layer. This almost doubled the computational time of their model, although the quantitative results were not affected to any observable extent. In this work, the boundary layer is not considered seperately, but the effect of heat loss to the water in the jacket is taken into account by using a heat loss term in the heat balance equation of gas phase in a way similar to that of Cho and Joseph(1981).

2.2 Some Important Assumptions In The Model.

The ratio of CO to CO_2 (λ) in combustion reaction:

λ is a system constant dependent on particle surface temperature (Arri and Amundson, 1978; Desai and Wen, 1978). Arthur (1951), Rossberg (1956) expressed this molar ratio of CO/CO_2 as an Arrhenius type expression, $CO/CO_2 = \lambda = k_{ox} \exp^{-E^2_{ox}/(RT_s)}$ the parameters k_{ox}, E_{ox} (particularly k_{ox}) depend on oxygen pressure, carbon burn-off and surface oxide coverage (Phillps et al., 1969, 1970). Arri and amundson (1978) assumed $\lambda = 0$ since they assumed CO_2 is the only combustion product. Yoon et al. (1978) assumed λ is a constant equal to 1. Cho and Joseph(1981) used Rossberg's Arrhenius type correlation. Desai and Wen (1978) used $\lambda = 10^{3.4} \exp^{-12000/(RT_s)}$ In this work by comparing model results with plant data $\lambda = 100 \exp^{-12000/(RT_s)}$ was used.

Gas phase oxidation of CO and H_2:

Due to the comparatively high partial pressure of oxygen in the combustion zone, the gas phase oxidation reactions of H_2 and CO, viz;

$$H_2 + \frac{1}{2} O_2 \longrightarrow H_2O \qquad \text{(6)}$$

$$CO + \frac{1}{2} O_2 \longrightarrow CO_2 \qquad \text{(7)}$$

may occur. There is considerable doubt regarding the extent to which these reactions take place in the coal gasifier during the short residence time of the combustion zone. Yoon et al. (1978) did not consider these reactions and gave the following reasons to support their consideration:

(i) If the gas phase combustion take place to any considerable extent, the temperature rise will be much higher than is observed in practice. This does not happen in practice which is supported by Rudolph's work (1973) in which the observed temperature is found to be considerably lower than the theoretically attainable maximum temperature. (shown in fig.8)

(ii) Attainment of higher temperature because of significant gas phase combustion would be independent of coal type and reactivity. In contrast Yoon et al. (1978) found considerable difference in temperature profiles and maximum temperatures with different coals having different reactivities.

Arri and amundson (1978) allowed the gas phase combustion of CO and H_2 to proceed to completion so long as the oxygen concentration remained above a certain minimum.

Cho and Joseph (1981) modeled the coal gasifier both considering and neglecting the gas phase oxidation and concluded after comparison with plant data that the gas phase combustion does not occur to any significant extent in the gasifier.

In this work the gas phase oxidations are neglected.

Water-gas shift reaction:

There is considerable difference of opinion among researchers regarding the water gas shift reaction. Some assume it to be at equilibrium whearas some assume that it proceeds at a finite rate. Yoon et al.(1978); Amundson and Arri(1978) assumed that the water gas shift reaction is in equilibrium at all positions of the gasifier. Biba et al.(1978); Desai and Wen(1978); Cho and Joseph(1981) included a rate expression for the shift reaction. In this work the water gas shift reaction was assumed to take place at a finite rate. It was found in this work that water gas shift reaction takes place to a considerable extent in the gasification zone, but come to near equilibrium at the end of the gasification zone.

Composition of char:

The term char is generally used to represent coal after drying and devolatilization. Arri and Amundson (1978); Biba et al. (1978); Woodmansee, (1976); Yoon et al. (1978); Haynes (1982) assumed char to be pure carbon and ash. Kosky and Floess (1980) assumed that char contains a small mass of

hydrogen in addition to carbon and ash. Cho and Joseph (1981) approximated char by $CH_{\alpha}O_{\beta}$ and ash, where α and β are calculated from the ultimate analysis of coal and material balance around the devolatilization. Desai and Wen(1978) assumed a complex structure of char of the form $C_{\alpha}H_{\beta}N_{\delta}S_{\gamma}$.

There are no concrete data available at present regarding the actual composition of char relevant to a Lurgi gasifier. The researchers who assume that char contains components other than carbon and ash base their analysis on purely arbitary assumptions. Their analysis become complex without much improvement in terms of numerical results. For simplicity char is assumed in this model to consist entirely of carbon and ash. If the composition of a char is precisely known, it is not difficult to accomodate the effects of these minor components on the model as has been done by Desai and Wen(1978).

2.3 Fundamental Experimental Kinetics Measurements.

Because of the complicated nature of the gasification reactions, most experimental researchers have employed mainly high purity, relatively low porous carbons which were reacted at one or a combination of low pressures, low temperatures or high gas flux for studying chemical kinetics of these reactions. Also there are large variations in the experimental results published in the literature depending on experimental technique, type of heating used, temperature and pressure ranges, partial pressure of reactants and type of char used. As a consequence there is considerable doubt regarding the validity of the results of these kinetics studies to the high pressure Lurgi gasifier.

2.3.1 Combustion And Gasification Reactions.

The physical and chemical behavior of coal particles during combustion and gasification reactions can be described either by Shell progressive model (SP) (also sometimes known as the Shrinking core model) or by an Ash segregated model(AS). Yoon et al. (1978) indicated that better prediction of a dry ash Lurgi gasifier performance is obtained by a Shell progressive model (shown schematically in fig.3).
In the SP model it is assumed that the ash retains its structure and remains on the coal particle to form an ash layer surrounding an unreacted core. Char-oxygen (5) and char-steam (1) reactions are faster than char-carbon dioxide and char-hydrogen reactions (Lowry, 1963), so are affected by both gas film diffusion and pore diffusion as well as intrinsic reaction rates. It is assumed that char-oxygen (5) and char-steam (1) reactions are controlled by diffusion and reaction rates in the SP model, while slower char-carbon dioxide (2), char-hydrogen (3) reactions are controlled by their intrinsic reaction rates.

With the SP model the rate equation for char-oxygen (5) and char-steam (1) reactions are given by (Aris and Amundson, 1973)

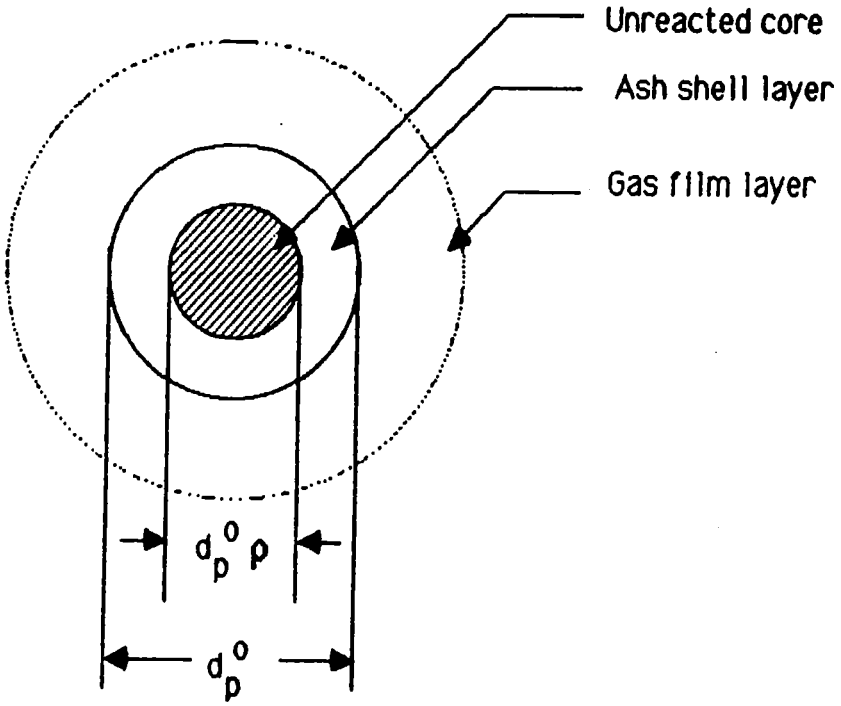

Fig. 3 Schematic of Shell Progressive model (SP)

$$r_j = \frac{(1 - \varepsilon)\ (P_i - P_i^*)}{\frac{d_o}{6K_{pi}} + \frac{d_o^2(1 - \rho)RT_s}{12\ \rho\ D_{mi}} + \frac{1}{\eta_j\ \rho^3 k_i C_o}} \qquad (8)^{**}$$

Here P_i^* is the equilibrium partial pressure of reactant i; for oxygen, P_i^* is practically zero; for steam it can be determined from equilibrium constant expression.

k_j is the intrinsic reaction rate coefficient for the reaction j;it is assumed to follow the Arrhenius law,

$$k_j = k_{jo} \exp^{-E_j/(RT_s)}$$

the parameter values, (constant, k_{jo} and activation energy E_j) for some or all reactions are given by Desai and Wen (1978); Wen and Tone (1978), Gibson and Euker (1975); Sergent and Smith (1977); Zahradnik and Grace (1974); Dobner (1976); Dutta and Wen (1979).

** In equation (8), j can be either 1 (for char-steam reaction), or 5 (for char-oxygen reaction). For j=1, i stands for steam, and for j=5, i stands for oxygen.

In this model the kinetic parameter values used by Yoon et al.(1978) are used; and for the water gas shift reaction, parameter values used by Rase(1977) are used.

K_{pi} is the film mass transfer coefficient for the gaseous element i in the reaction, which can be obtained from a j-factor correlation given by Gupta and Thodes (1963)

$$K_{pi} = \frac{2.06}{\varepsilon P} Sc^{-0.092} (PD_i/dRT_g)^{0.575} F_g^{0.425}$$

η_j is the effectiveness factor for the reaction j in the core of the particle. For a spherical core, η_j is given by the expression

$$\eta_j = \frac{1}{\phi_j} \left(\frac{1}{\tan h\ (3\phi_j)} - \frac{1}{3\phi_j} \right)$$

The modulus ϕ_j for reaction j is defined by

$$\phi_j = \frac{d^0 \rho}{6} \sqrt{\frac{k_j C_o}{\gamma_j D_{ej}/(RT_s)}}$$

The effective diffusivities in the outer shell and also in the core of the particle are estimated by the following formula proposed by Walker et al. (1959).

Shell : $D_{mj} = D_i\ \theta_s^2$

core : $D_{ej} = D_i\ \theta_c^2$

Where θ_s and θ_c are void fractions of the particle in the shell and core respectively. The following expressions proposed by Sotirchos and Amundson (1984) are used in this model.

$$\theta_s = W_b + \varepsilon_{po} (1 - W_b)$$

$$\theta_c = \varepsilon_{po} + X_c (\theta_s - \varepsilon_{po})$$

2.4 Devolatilization.

Devolatilization or pyrolysis of coal is defined as a process by which coal is thermally decomposed into char, gas, and liquid products.

For inclusion in the gasifier model, the devolatization model should :

----- be structurally simple with a minimum number of unknown parameters.

----- give an estimation of the total volatile yields under comparable gasifier operating conditions.

----- give approximate rate of devolatilization (this chracteristic is not very important unless devolatilization is a very slow process).

----- give the distribution of volatiles e.g., coal gas, chemical water, tar and oil; distribution of coal gas; estimation of tar cracking; estimation of supercritical hydrogasification of char.

----- give an estimation of heat of reaction.

Anthony and Howard (1976) gave an extensive review of coal devolatilization and hydrogasification. They also formulated a model to describe these phenomena. The expression for total volatile yields proposed by them contain ten unknown parameters, all of which have to be determined experimentally for a specific coal. This limitation restricts the applicability of this model. Also this model did not give any estimation of distribution of volatiles, cracking of tar. Following Anthony et al. (1976), Russel et al. (1977) modeled the devolatilization of coal in the presence of high pressure hydrogen. This model suffers from limitations similar to the model of Anthony and Howard (1976). Desai and Wen (1978) formulated a simple model of devolatilization based on Gregory and Littlejohn's correlation of total yields. Kalson and Briggs (1978) studied theoretically the devolatilization of a single coal particle. They explained the fundamental roles of pressure, particle size and heat transfer on product yields and distribution, but failed to give any expression that could be used either to predict total volatile yields or its distribution. In the literature there are other relatively simple devolatilization models e.g., Howard and Essehigh (1967), Juntgen et al. (1968), Wen et al.

(1974) and Badzioch and Hawksley (1970).

The yield of volatiles and the rate of devolatilization depend not only on the volatile content of the coal but also on the rank of coal, operating temperature and pressure, rate of heating, size of coal particles and constituents of the carrier gases. There is no definite evidence regarding the heat of reaction of devolatilization phenomena. Most researchers (Badzioch et al., 1970, Wen et al., 1978, Anthony and Howard, 1976) approximate the overall process of devolatilization as a first order decomposition process occuring uniformly throughout the particle. Thus the rate of devolatilization is expressed as

$$\frac{dV}{dt} = k_v (V^* - V) \text{ where } V \longrightarrow V^* \text{ when } t \longrightarrow \infty \qquad \text{——— (9)}$$

k_v is typically correlated with temperature by an Arrhenius equation $k_v = k_{v0} \exp^{-E_v/(RT_s)}$. Values of k_{v0} and E_v are tabulated by Anthony and Howard (1976) for different coals and conditions.

Yoon et al. (1978), Desai and Wen (1978) assumed devolatilization to be instantaneous and they just added the devolatilization products to the gaseous stream coming from the gasification zone. Biba et al. (1978) considered the devolatilization process as taking place at a constant rate and added the devolatilization products with a predefined composition to the gaseous stream from the gasification zone.

In this model devolatilization was assumed thermally neutral and was modeled as a finite process in the following way:

(i) The fractional yield of volatile matter at high pressure was determined from a correlation proposed by Wen and Chaung (1979)

$$V_P = V_{101\ kPa} (1 - 0.066 \ln (P/101.325)) \qquad \text{——— (10)}$$

(ii) An approximate height required for devolatilization (ΔZ_v) was determined from the first order rate expression with the parameter values of Wiser et al. (1967) at an average

temperature of 800 K. and the boundary of this zone was set using $Z_{devo} = Z_{dry} - \Delta Z_v$.

$$\frac{dV}{dt} = 47.5 \exp^{-15000/(RT_s)} \qquad \text{——} \qquad (11)$$

(iii) Typical devolatilization data given by Yoon et al. (1978) was used to determine the devolatilization product distribution.

(iv) An elemental mass balance was used to adjust the coal gas composition on the assumption that all H, O, N, S in raw coal are transferred in the devolatilization process.

(v) Fractional volatile products were added to the gaseous stream in each step of height ΔZ according to the residence time of coal in that step until the total yield becomes equal to the total amount of volatiles to be evolved.

2.5 Drying And Heating Of Coal.

For inclusion in the gasifier model the drying and heating model should possess the following characteristics :-

(i) The model should be structurally simple and contain few unknown parameters.

(ii) The unknown parameters in the model should be either easily determinable experimentally or functions of readily available coal properties e.g, coal rank, C/H ratio, volatiles content etc.

(iii) The model should predict the approximate drying time taking into account the effects of particle size, coal properties, heating rate, operating temperaure and pressure, composition and flow rate of drying medium.

There are few representive models for coal drying and heating in fixed beds in the literature. Mcintosh (1976) formulated a model of drying for Australian brown coal. This model could be used to predict the instantaneous moisture content with drying time, drying gas exit temperature and also the effects of particle size, gas temperature and gas velocity on drying rate of brown coal. Mcintosh's(1976) model is valid

for brown coal but it may not give consistent results for other types of coal which are expected to have different drying characteristics. Based on the assumption that the heat transfer rate through the dry shell is the rate controlling step for drying, Yoon et al. (1978) developed a shell progressive drying model. Main findings of this model are :

____ drying time is proportional to moisture content of coal and the difference between gas and solid temp.

____ drying time is not sensitive to Biot number , B_i (hd/K_g), which is a measure of heat tranfer coefficient between gas and solid phases.

____ drying time is proportional to the square root of the average particle diameter.

They determined the drying time for a coal particle in the typical dry ash Lurgi gasifier conditions to be between sixty and ninety seconds (negligible compared to the 1 hour residence time of coal in the gasifier). Yoon et al.(1978) did not give the value of heat transfer coefficient between solid and gas phases. In this work it is found that the effective heat transfer coefficient between gas and solid phases is approximately 1/6th of the theoretical heat transfer coefficient. Also there are added difficulties in coal drying due to bulk diffusion, pore diffusion depending on coal particle. All these complexities tend to increase the drying time. The effects of all these complications are lumped into the heat transfer coefficient term, assuming that the effective heat transfer coefficient is around 1/30th of the theoretical heat transfer coefficient, this gave results comparable to Biba et al.'s (1978) drying height. Biba et al. (1978) assumed a constant drying rate.

In this model a simplified countercurrent heat exchanger type calculation has been used to account for the heat transfer from gas to solid phase and also the moisture transfer, which is proportional to the amount of heat transferred from gas phase to solid phase.

The drying module is summarized below:

It has two parts:

A. calculation of approximate height of bed necessary for heating and drying of the coal.

(i) The total heat load(Q_d) for this purpose was determined by adding (1) the heat required for heating the coal from 298 K to 500 K (moisture evaporation temperature, typical to a Lurgi gasifier), (2) the heat required for moisture evaporation, and (3) the heat required for final heating of dry coal to devolatilization temperature, 723(K), (temperature at which devolatilization starts taking place to a significant extent).

(ii) Using typical solid and gas phases terminal temperatures between the inlet of coal and the begining of devolatilization, the log mean temperature difference, T_{lmd} for heat transfer between gas and solid phase was calculated.

(iii) The heat transfer coefficient (convective and radiative) between gas and solid phases were calculated from theoritical correlations (Gupta and Thodes, 1963; Perry ,1973) using average temperature and flow rates. The effective heat transfer coefficient was determined by multiplying the theoretical heat transfer coefficient with the factor previously mentioned.

(iv) Using the convective heat transfer relationship

$$\dot{Q}_d = h_d \frac{6(1-\varepsilon)}{d} \frac{\pi D^2 \Delta Z_d}{4} T_{lmd} \qquad \text{---- (12)}$$

the approximate drying and heating height of the bed ΔZ_d was calculated and thereby boundary of this zone was determined by using $Z_{dry} = Z_{bed} - \Delta Z_d$.

B. Drying calculation.

(i) When the drying height Z_{dry} was reached the amount of moisture that has been transferred from the solid at each step of height ΔZ was calculated from the amount of heat transferred from gas to solid phase in that step and added to the solid phase. This process was continued until the total amount of moisture transferred back to the solid becomes equal

to moisture content of coal.

(ii) When the total moisture transferred became equal to the moisture content of the solid, heat transfer phenomena was allowed to continue from gas phase to solid phase similar to a countercurrent heat exchanger till the bed height Z_{bed}.

(iii) The gas phase temperature was calculated in each volumetric element of height ΔZ of the bed from an overall heat balance in that element since the solid phase temperature was known from the assumed profile.

2.6 Development Of Model Equations And Solution Methodology.

The basic assumptions used in the model development are given below:

(1) Steady state.

(2) Plug flow both in solid and gas phases. (i.e there are no radial gradients in either temperature or concentration)

(3) Drying of coal takes place at a rate proportional to the amount of heat transferred to the solid phase from the gas phase.

(4) Devolatilization reactions are first order and thermally neutral.

(5) Since reactions (1), (2), (3) and (5) take place either on the surface or within the particle, heat of reaction of these reactions contribute to the solid phase temperature.

(6) Water gas shift reaction (4) takes place solely in the gas phase and its heat of reaction goes into the gas phase.

(7) Gaseous reactants enter the solid phase at the bulk gas temperature and products leave at the solid phase temperature.

(8) Heat loss from the gasifier affects only the gas phase temperature.

Material balance equations:

Taking a small cylindrical section of height ΔZ of the gasifier (shown in fig.4) one can according to Bird et.al (1960) derive the following mass balance equations for all the components involved.

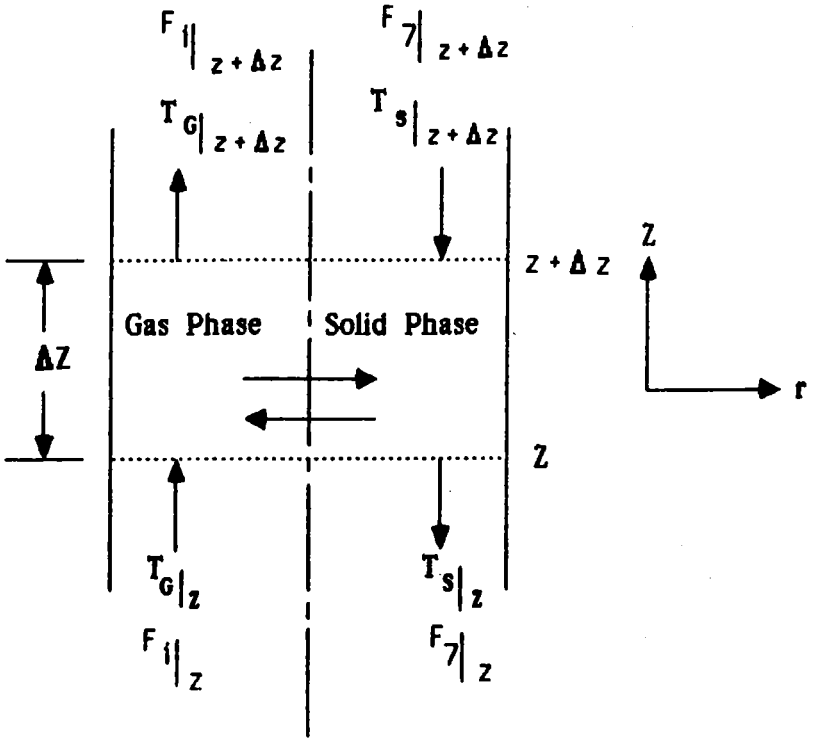

Fig. 4 Schematic diagram of the volumetric element of height ΔZ

Carbon monoxide:

$$\frac{dF_1}{dZ} = \frac{\lambda}{(1+\lambda)} r_5 + r_1 + 2r_2 - r_4 \qquad \text{(13)}$$

Carbon-di-oxide:

$$\frac{dF_2}{dZ} = \frac{1}{(1+\lambda)} r_5 + r_4 - r_2 \qquad \text{(14)}$$

Hydrogen:

$$\frac{dF_3}{dZ} = r_1 + r_4 - 2r_3 \qquad \text{(15)}$$

Methane:

$$\frac{dF_4}{dZ} = r_3 \qquad \text{(16)}$$

Oxygen:

$$\frac{dF_5}{dZ} = \frac{2 + \lambda}{2(1 + \lambda)}(- r_5) \qquad \text{(17)}$$

Steam:

$$\frac{dF_6}{dZ} = - r_1 - r_4 \qquad \text{(18)}$$

Carbon:

$$\frac{dF_7}{dZ} = r_5 + r_1 + r_2 + r_3 \qquad \text{(19)}$$

Heat balance equations:

For the solid phase:

$$\frac{dT_s}{dZ} = (\Delta H_1 r_1 + \Delta H_2 r_2 + \Delta H_3 r_3 + \Delta H_5 r_5 + H_{gs} + \xi\, ha(T_s - T_g))/ H_s \qquad \text{(20)}$$

For gas phase:

$$\frac{dT_g}{dZ} = (\Delta H_4 r_4 + H_{sg}' + \xi\, ha(T_s - T_g) - \xi\, U\, a'(T_g - T_w))/ H_g \qquad \text{(21)}$$

Where, h = Overall heat transfer coefficient (both convective and radiative) between solid and gas phases. Convective part was determined from Gupta and Thodes's (1963) correlation, radiative part was determined from Perry et al. (1973).

H_{gs} = amount of heat transferred from the gas to the solid phase due to the gaseous reactants diffusing into solid particles.

H_{sg}' = amount of heat transferred from the solid to the gas phase due to gaseous products diffusing out of the solid particles.

ξ = A constant of proportionality .
Cho and Joseph(1981) used ξ= 0.3;
In this work ξ= 0.16 was used which was found to give results comparable to plant data.

U = Overall heat transfer coefficient between gas

phase and water in the jacket. This is determined from Perry et al. (1973)

ξ' = A constant of proportionality. In this work ξ' =0.4 was used. This gave steam production in the jacket comparable to the Lurgi gasifier.

To eliminate the stiffness of the problem the pseudo-steady assumption proposed by Cho and Joseph (1981) was applied for the solid phase i.e the temperature derivative was set to zero since the contribution of the derivative term multiplied by solid heat capacity is negligible compared to other terms. Consequently the equation (20) becomes an algebraic equation.

$$T_s = T_g - (\Delta H_1 r_1 + \Delta H_2 r_2 + \Delta H_3 r_3 + \Delta H_5 r_5 + H_{gs}) / (\xi h a) \quad \text{----- (22)}$$

It is evident from the above equation (22) that it can give erroneous result when the rates of reactions are negligible or nearly zero, at the upper part of the bed. Cho and Joseph (1981) did not face this problem since they assume that both devolatilization and drying operations are instantaneous (also it is doubtful that how they could satisfy the boundary condition at $Z = Z_{bed}$, $T_s = T_{so}$). Efforts have been made to switch over to the orginal solid phase energy balance equation (20) but this did not produce stable solutions even for very small integration steps, due to the large amount of heat transfer from the gas phase to the solid phase and as a result of which both solid and gas temperatures rapidly decreased. To tackle this problem a four constant rational function was fitted for the solid temperature profile using four data points: (Z_{end}- 0.1, T_{s1}), (Z_{end}, T_{s2}); (Z_{devo}, T_{s3}); (Z_{bed}, T_{so}). After comparing with plant data Z_{end} was chosen to be 2.0 m. Thus a profile of solid phase temperature was obtained from Z_{end} to the end of the bed, Z_{bed}.

Method of solution:

The differential mass and energy balance equations (13 - 19, 21) and the algebraic equation (22) are to be solved numerically with the following boundary conditions.

at Z=0
$$T_g = T_{go}$$
$$F_5 = F_{5o}$$
$$F_6 = F_{6o}$$
$$F_1 = F_2 = F_3 = F_4 = 0.$$
$$F_7 = F_s (1 - X_{cf})$$

at $Z = Z_{bed}$
$$T_s = T_{so}$$
$$F_7 = F_{7o}$$

Since the boundary conditions are split, some iterative technique needs to be used to solve the system of differential equations. The Shooting method as used by Yoon et al. (1978) along with a variable step size 4th order Runge-Kutta-Gill method (Carnahan et al., 1969) was tried but failed to give adequate results even for very small step size (less than 0.001 m). The differential equation (20) is so stiff (since H_s is nearly 20 to 30 times less than H_g) that it became unstable in the combustion zone or at the transition between the combustion and gasification zones making the whole system unstable. To cope with this stiff differential equation (20) the pseudo- steady state assumption of Cho and Joseph (1981) was applied. This stabilised the system greatly but failed on occations to provide consistant results. It also caused the solution to become oscillatory when the overall heat transfer coefficient between solid and gas phases, h was decreased below a critical level suggested by Cho and Joseph(1981). The reasons of failure of this method can be summarized below:

To solve the system of differential equations for each volumetric step of height ΔZ one has to assume both the inlet solid temperature and exit gas temperature for the volumetric element concerned beforehand. It is found that these initial estimates have a profound impact on the performance of the model. If the initial estimates are not accurate enough, the results will be erroneous and there is every possibility that these errors propagate as the solution marches up through the bed and can ultimately make the system unstable.

To tackle this problem one has to put some bound to these errors on the values of inlet solid and exit gas temperatures for each volumetric element.The following solution methodology was used:

- Based on the initial estimates of solid and gas temperature solve the differential equations corresponding to mass balance equations, (14) - (19) and the gas phase temperature equation, (22) to get better estimate of gas phase temperature.

- Using this better gas phase temperature estimate calculate better estimate of solid phase temperature from the algebraic equation (23) and compare with the initial estimate to check wheather the difference is below a certain level or not. If not apply Wegstein's convergence technique to get better initial estimate of solid phase temperture. Repeat the above two steps until the difference meets the convergence criterion.

- Using these better solid and gas phases temperature estimates perform an overall heat balance for the volumetric element of height ΔZ to recalculate the gas phase exit temperature. In this work it was found that this recalculated gas phase exit temperature differed considerably from its earlier value obtained from the initial solution of differential equation (22), particularly in the combustion zone (contrary to Cho and Joseph, 1981). This greatly dampens any error in the value of solid phase temperature (because of high heat content of gas phase).

This stabilised the solution somewhat but still failed to give resonable results for some cases using low heat transfer coefficients between gas and solid phases.

Finally to make the solution technique more robust and to reduce the oscillatary nature of the solution a three point averaging technique was applied to both solid and gas temperatures. This provided much better performance.

* A brief description of the three point moving averaging technique is given in appendix I-A.

2.7 Flow Diagram Of The Gasifier Process Module

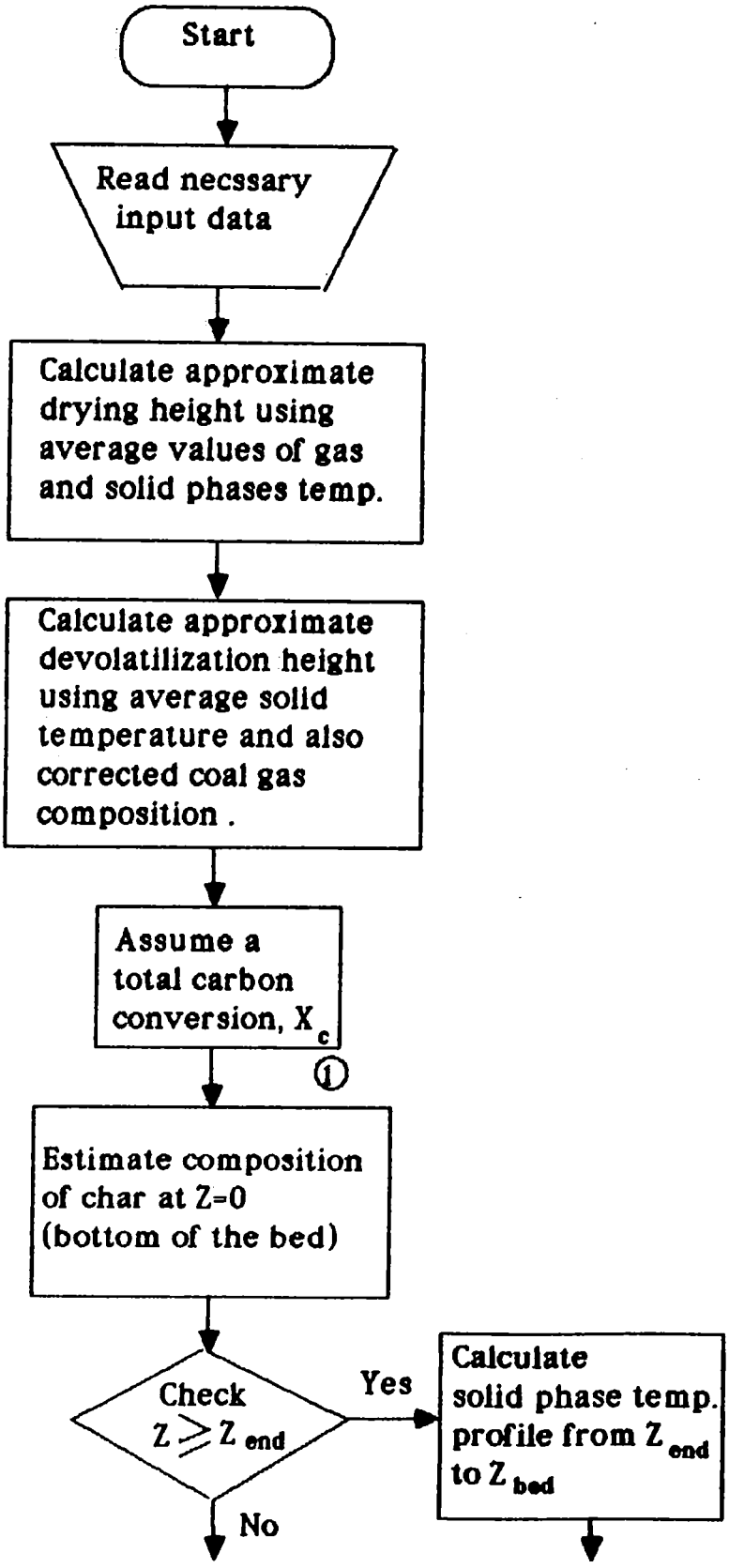

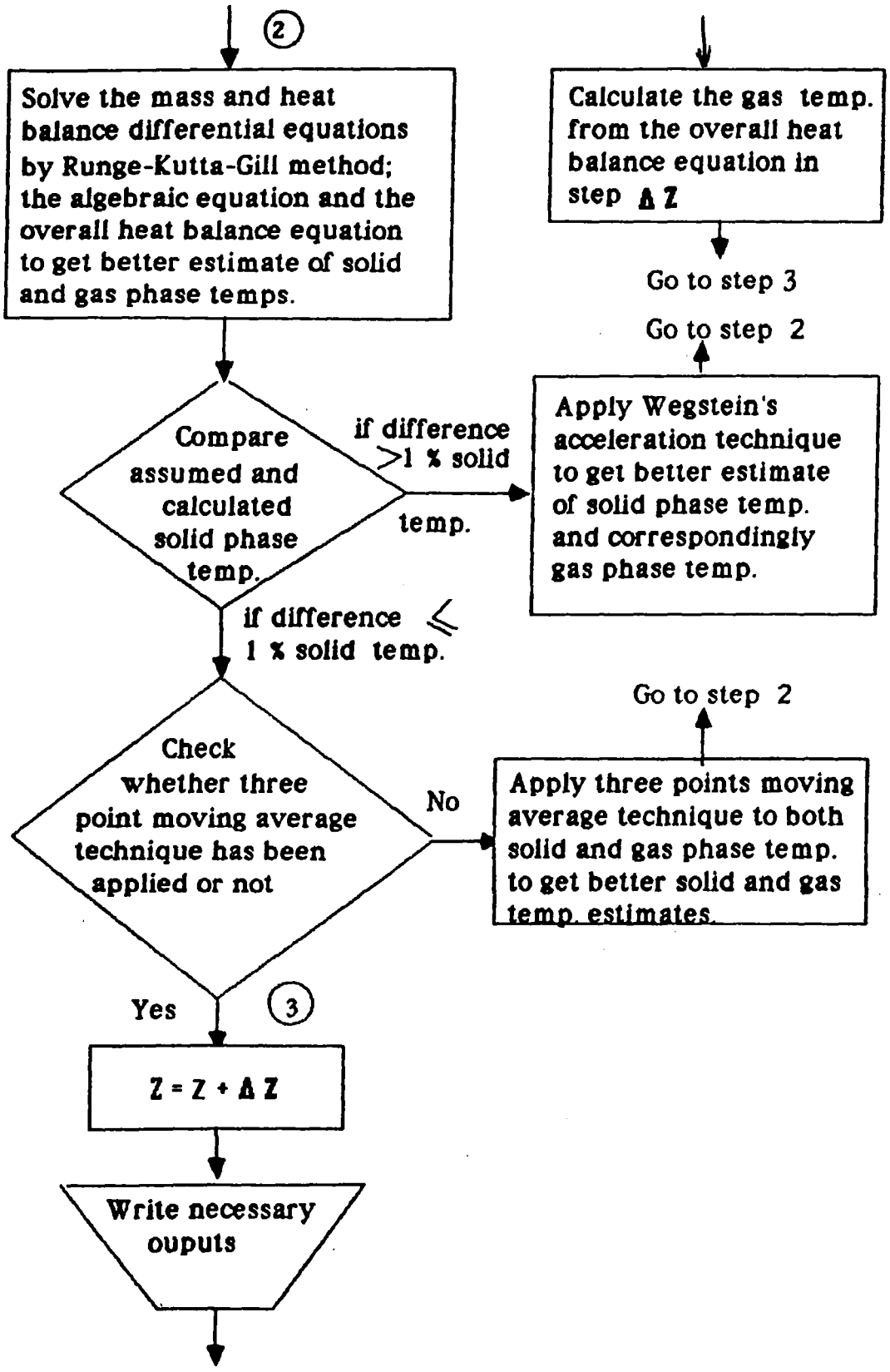
2
Solve the mass and heat balance differential equations by Runge-Kutta-Gill method; the algebraic equation and the overall heat balance equation to get better estimate of solid and gas phase temps.
Calculate the gas temp. from the overall heat balance equation in step Δ Z
Go to step 3
Go to step 2
Compare assumed and calculated solid phase temp.
if difference >1 % solid temp.
Apply Wegstein's acceleration technique to get better estimate of solid phase temp. and correspondingly gas phase temp.
if difference ≤ 1 % solid temp.
Go to step 2
Check whether three point moving average technique has been applied or not
No
Apply three points moving average technique to both solid and gas phase temp. to get better solid and gas temp. estimates.
Yes
3
Z = Z + Δ Z
Write necessary ouputs

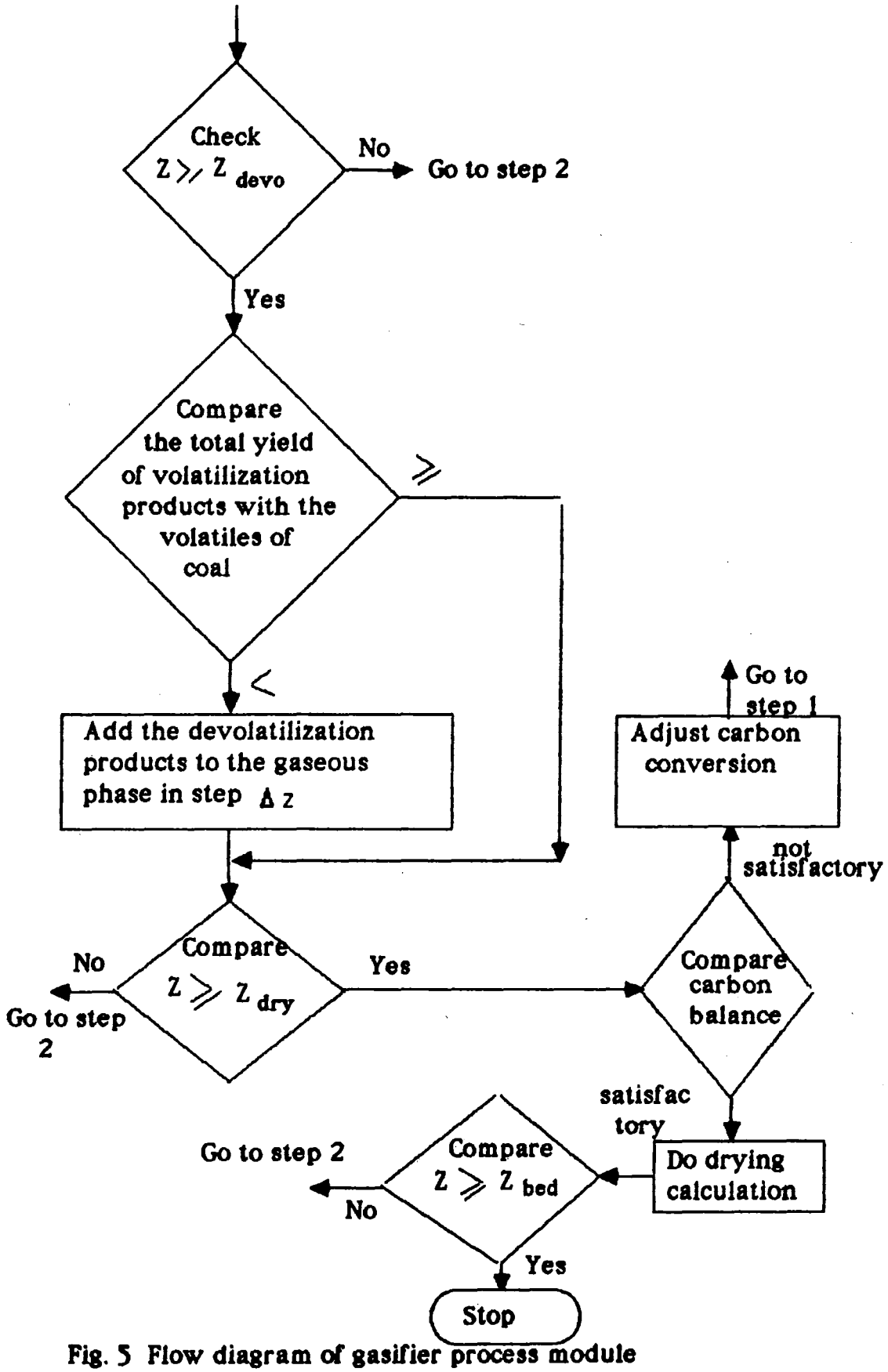

Fig. 5 Flow diagram of gasifier process module

3.0 DISCUSSIONS AND RESULTS

The model has been used to simulate a typical dry ash Lurgi coal gasifier. Operating conditions and the necessary data are given in tables I to VI. All other data are included in the respective figure.

Table I.

Operating conditions used in simulation.
(Yoon et.al,1978)

Parameter	Data
reactor bed height	3.05 m
reactor diameter	3.66 m
operating pressure	2500 kPa
bed porosity	0.52

Table II.

Coal type, properties and compositions.

coal type	:	Illinois low reactive Bituminous coal.
Initial porosity of the char particle	:	0.5445
Density of coal	:	1300.0 Kg m^{-3}
Proximate analysis(Wt. %) :		
Moisture	____	10.23
Ash	____	9.10
Fixed carbon	____	45.97
Volatile Matters	___	34.70
Ultimate analysis(Wt. %, dry basis)		
C	———	71.47
H_2	———	4.83
O_2	———	9.02
N_2	———	1.35
S	———	3.13
Ash + other minor onstituents	-	10.20

Table III.

Typical Devolatilization data (Yoon et al., 1978)

Fractional distribution of volatiles (Wt. %)	
Tar, Oil etc.	20
Chemical water	23
Coal gas	57
Distribution of coal gas (Wt. %)	
CO	29.04
CO_2	13.51
H_2	1.33
CH_4	40.51
H_2S	7.70
N_2	3.38
C_2H_6	4.53

Table IV.

Reaction rate contant expressions. (Yoon et al., 1978; Rase, 1977)

Reaction	Expression, k_i
1. Carbon - Steam	$k_1 = 613 \exp(-1.757 \times 10^5/(R_g \times T_s))$ (kmoles kmole C^{-1} atm^{-1} S^{-1})
2. Carbon - Carbon dioxide	$k_2 = 0.6 \; k_1$
3. Carbon - Hydrogen	$k_3 = 8.36 \times 10^{-4} \exp(-6.715 \times 10^4/(R_g \times T_s))$ (kmoles kmole C^{-1} atm^{-2} S
4. Water gas shift	$k_4 = Exp (12.88 - 1855.56/T_g)$
5. Combustion	$k_5 = 1.79 \times 10^6 \exp(-1.130 \times 10^5/(R_g \times T_s))$ (kmoles kmole C^{-1} atm^{-1} S^{-1}

Table V.
Equilibrium constant expressions.
(Yoon et al., 1978; Rase, 1977)

Reaction	Expression (K_i)
1. Carbon - steam	$K_1 = 3.098 \times 10^7 \times \exp(- 1.358 \times 10^5/(R_g \times T_s))$
2. Carbon - Carbon dioxide	$K_2 = 1.222 \times 10^9 \times \exp(-1.686 \times 10^5/(R_g \times T_s))$
3. Carbon - Hydrogen	$K_3 = 1.472 \times 10^{-6} \times \exp(9.144 \times 10^4/(R_g \times T_s))$
4. Water gas shift	$K_4 = \exp(- 4.72 + 4800.0/ T_g)$

Table VI.
Modified rate expressions:

1. Carbon - Steam:

$$r_1 = \frac{(1-\varepsilon)(P_{H_2O} - P_{H_2O}^{*})}{0.222\left(\frac{d}{6K_{p6}} + \frac{d^2(1-\rho)RT_s}{12\rho D_{m6}} + \frac{1}{\eta_1 \rho^3 k_1 C_o}\right)}$$

2. Carbon - Carbon dioxide:

$$r_2 = 5.0\, k_2\, C\, (P_{CO_2} - P^2_{CO}/K_2)$$

3. Carbon - Hydrogen:

$$r_3 = 5.0\, C\, k_3\, (P^2_{H_2} - P_{CH_4}/K_3)$$

4. Water gas shift:

$$r_4 = 6.1077\times10^{-6}(1-\varepsilon)X_{ash}k_4(Y_{CO}Y_{H_2O} - Y_{CO_2}Y_{H_2}/K_4)$$

5. Combustion:

$$r_5 = \frac{(1-\varepsilon)(P_{O_2} - P_{O_2}^{*})}{0.222\left(\frac{d}{6K_{p5}} + \frac{d^2(1-\rho)RT_s}{12\rho D_{m5}} + \frac{1}{\eta_5 \rho^3 k_5 C_o}\right)}$$

3.1 Composition And Temperature Profiles.

Typical composition and temperature profiles are shown in fig. 6 and 7. (Temerature profiles of Cho and Joseph's (1981) work are included in fig.7). For comparison purposes temperature profiles of a dry ash Lurgi coal gasifier, (Rudolph, 1973) are shown in fig.8. Compositions of product gas are compared with plant data, and some other model resuls in table VII.

Table VII.
Product gas composition on dry basis (% v/v)

Component	This simulation	Rudolph (1973) (plant data)	Hoogendorn (1973) (plant data)	Moe (1974) (plant data)	Yoon et.al (1978) (plant data)
CO	20.8	24	22	20.3	21.0
CO_2	26.0	28	28	28.6	27.8
H_2	42.5	38	39	37.9	43.9
CH_4	9.0	10	9	11.4	6.4
others	1.7	0	2	1.8	1.2

3.2 Effects Of Coal Particle Size.

Fig.9 and 10 show the effects of average coal particle size on solid phase temperature profiles and reactor performance respectively.

from fig.9 and 10, it is obvious that:

- Carbon conversion, thermal efficiency of the reactor (thermal efficiency = heating value of the product gas / heating value of coal) maximum temperature, position of maximum temperature from the grate, gas throughput (kmol s^{-1}) decrease with the increase in coal particle size.
- Sensible heat of the product gas increases with the increase in particle size because of less

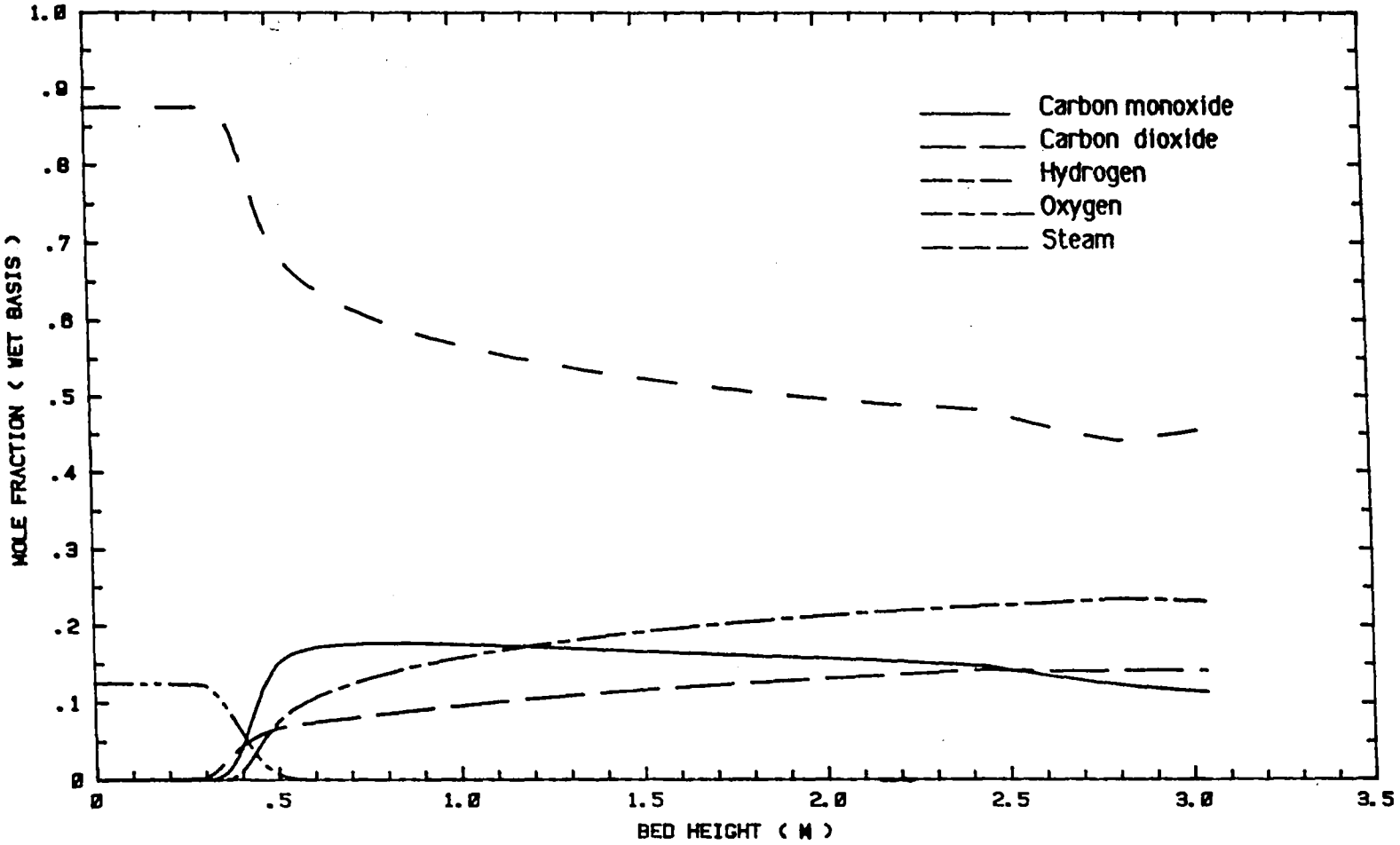

Fig. 6 : Composition profiles with a typical bituminous coal. Operating conditions of table I - VI, along with oxygen feed rate = 0.0508kmol S^{-1} ; fixed carbon/oxygen (mole $mole^{-1}$) =2.73 ; steam/oxygen (mole $mole^{-1}$) = 7.0 ; average particle diameter = 0.01 m;blast gas inlet temperature=644 K

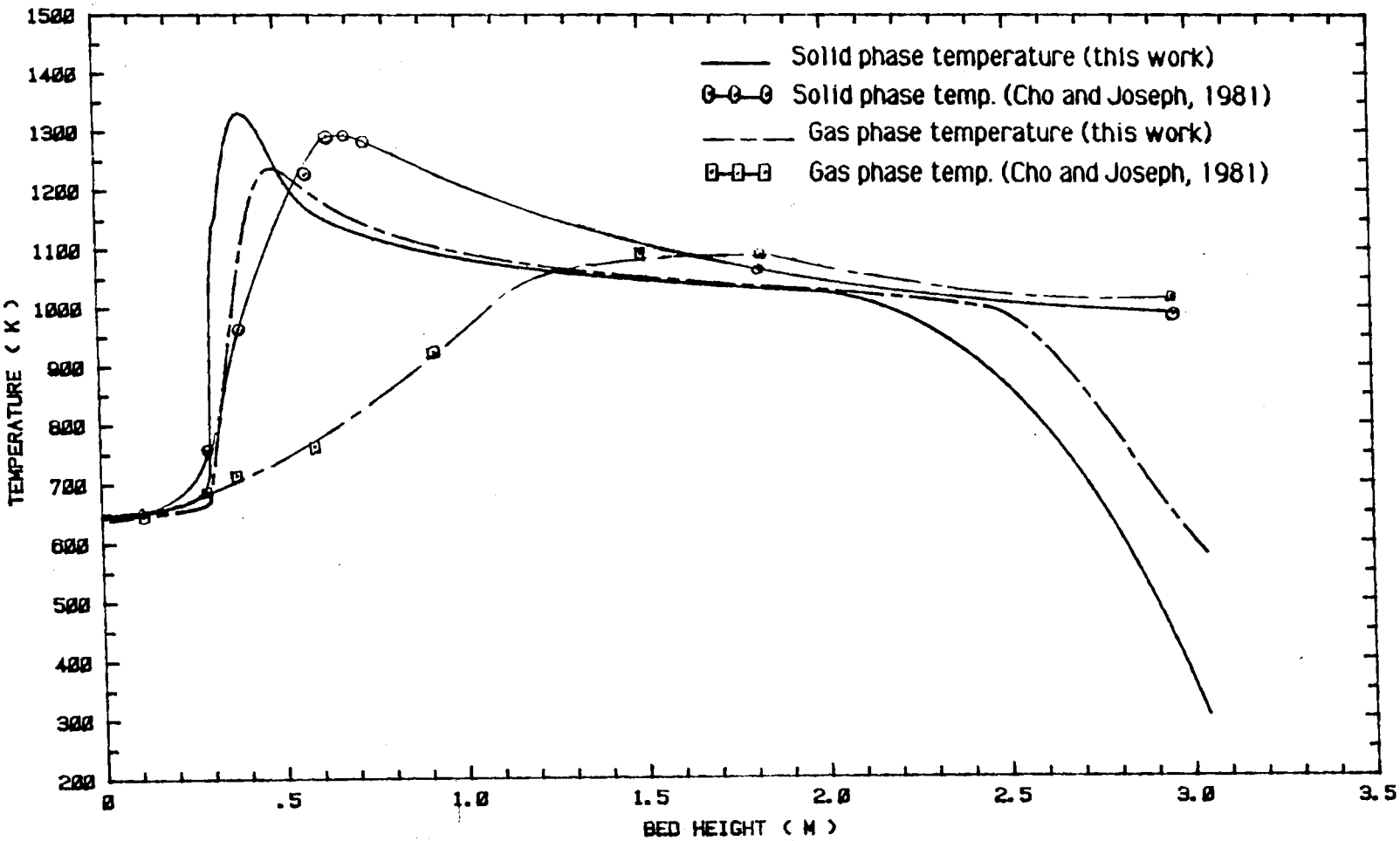

Fig. 7 : Temperature profiles with a typical bituminous coal for the same conditioins as fig. 6. and comparison with Cho and Joseph's (1981) work.

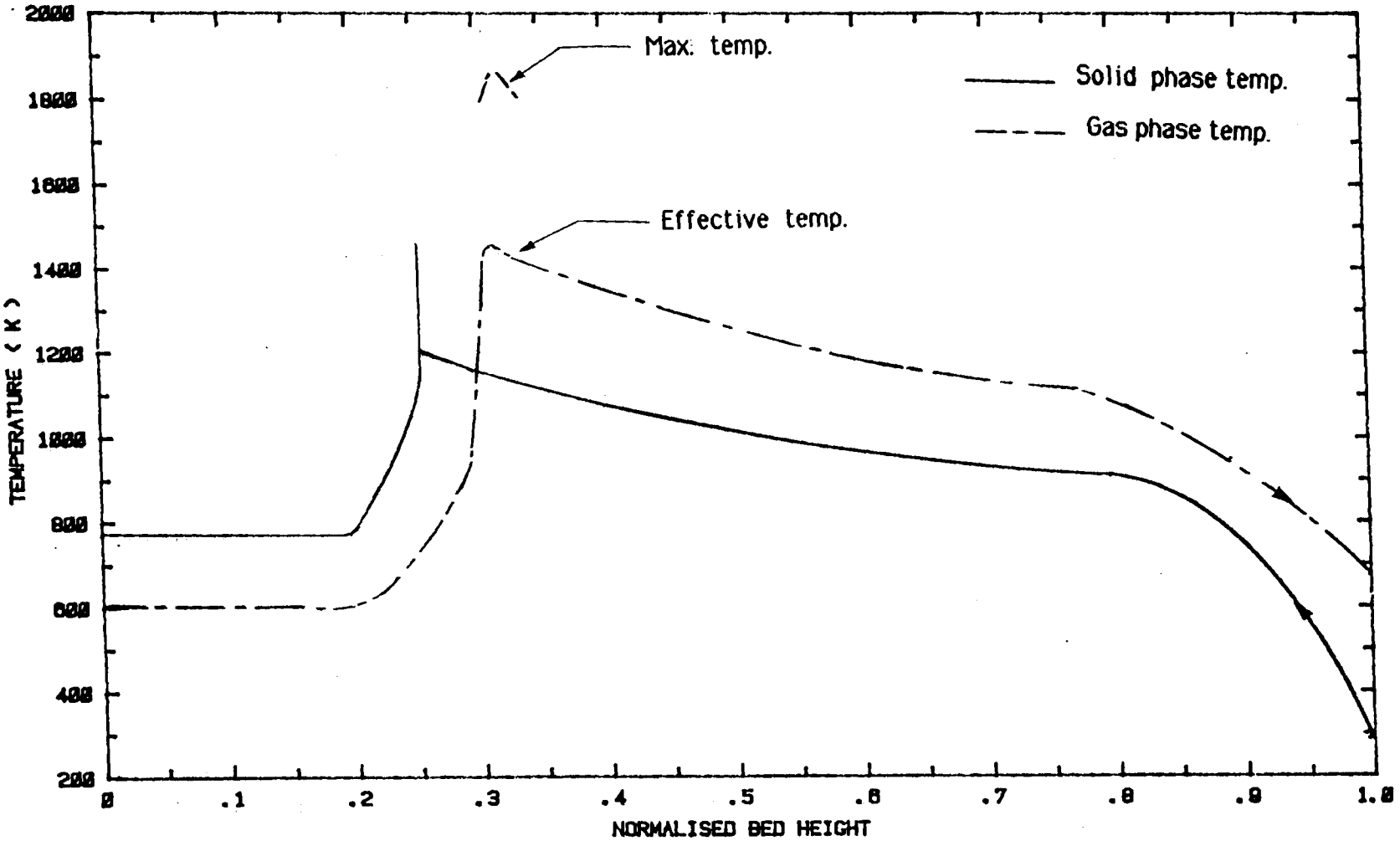

Fig. 8 Temperature profiles of a typical Lurgi gasifier (Rudolph, 1973)

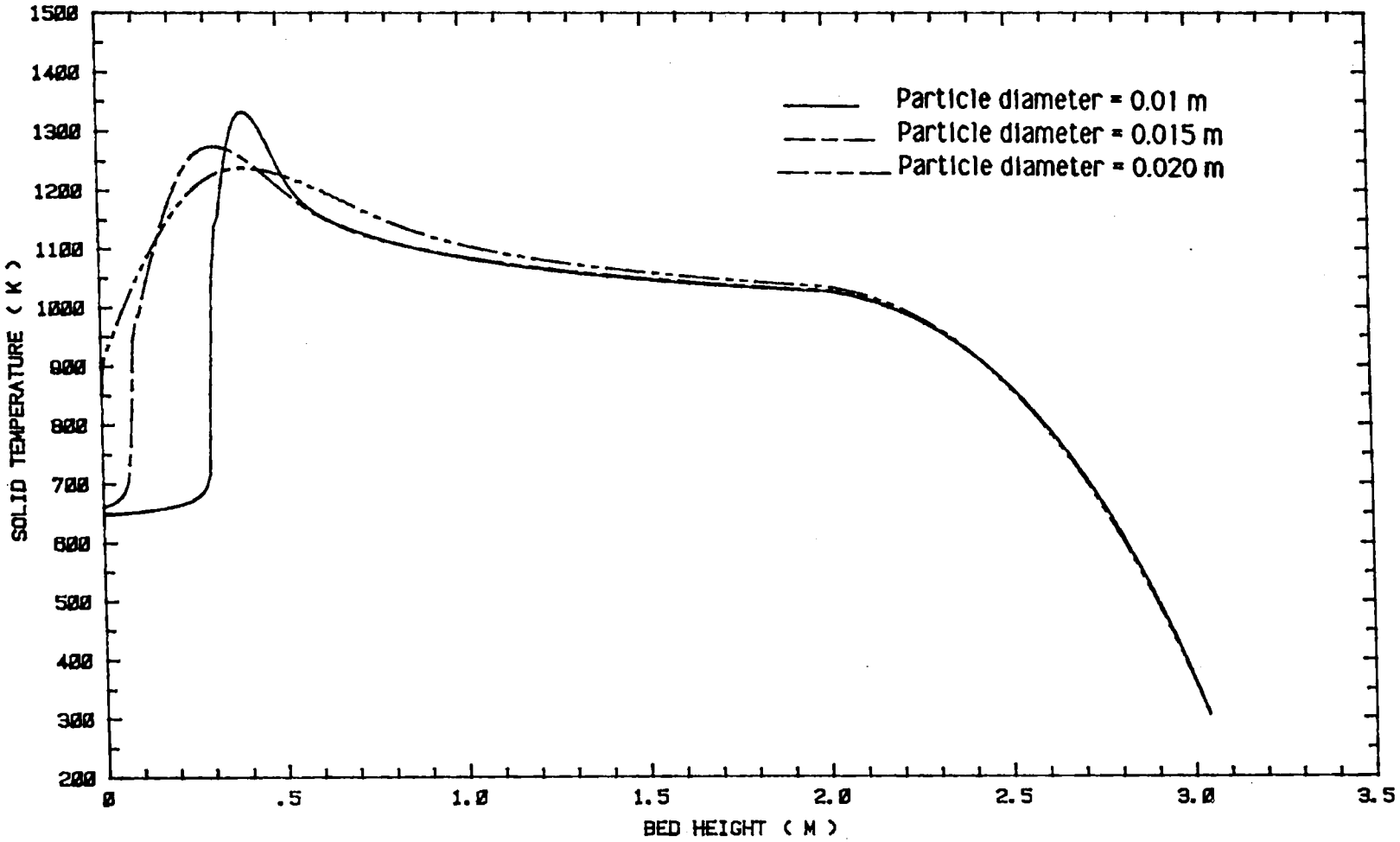

Fig. 9 : Effects of particle diameter on solid phase temperature profiles for the same conditions as fig. 6.

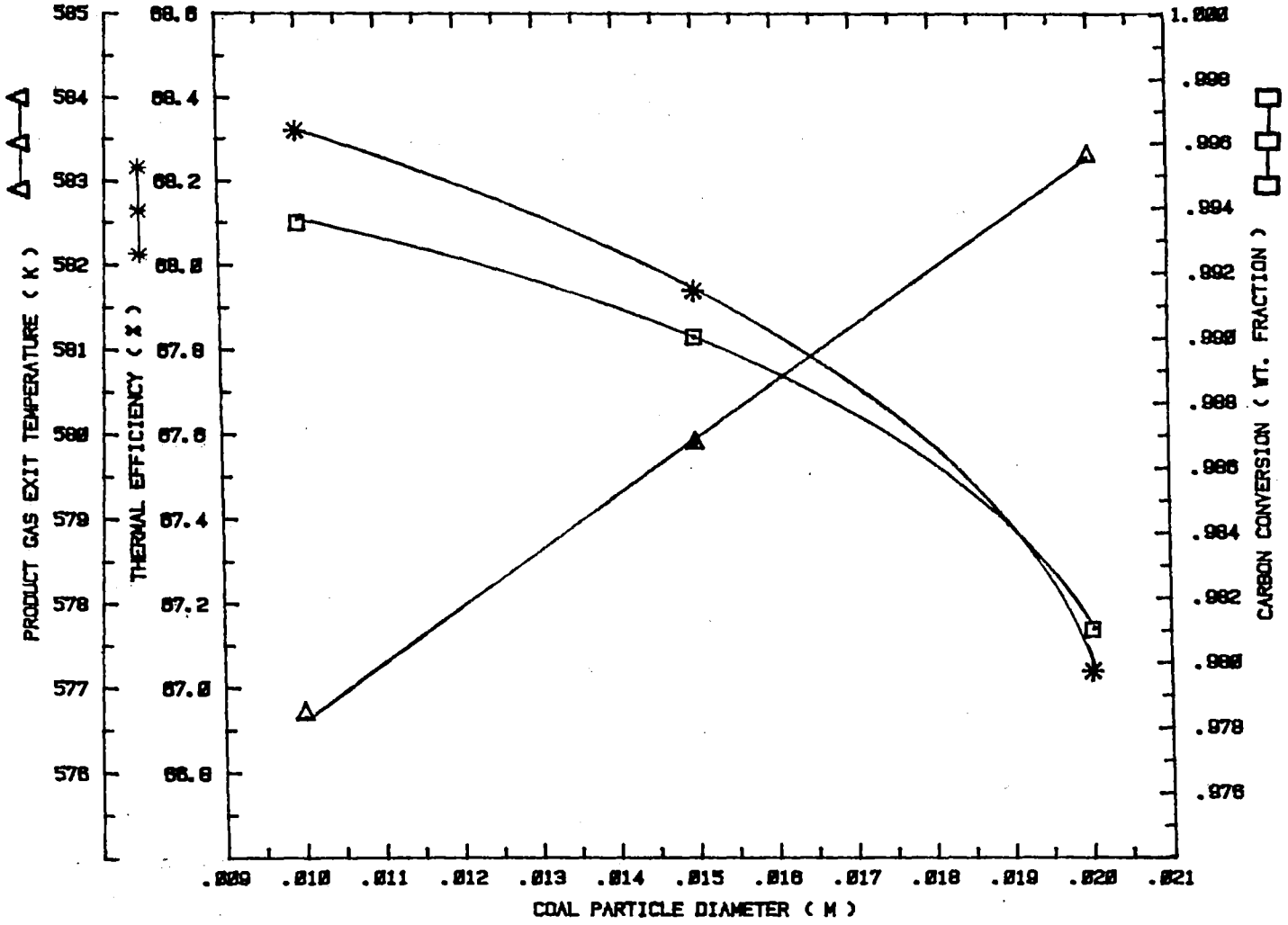

Fig. 10 : Effects of particle diameter on reactor performance for the same conditions as fig. 6.

endothermic reactions.

_____ Product gas compositions and heating value of the product gas (kJ $kmol^{-1}$), dry basis are almost independent of particle size.

3.3 Effects Of Steam/oxygen Ratio.

Fig.11, 12 and 13 show the effects of steam/oxygen ratio in the blast gas on solid phase temperature profiles and reactor performance respectively.

From fig.11, 12 and 13, it is obvious that:

_____ Carbon conversion, thermal efficiency of the reactor, Maximum temperature, position of maximum temperature from the grate decrease with the increase in steam/oxygen ratio.

_____ Product gas exit temperature, Hydrogen/Carbon monoxide ratio in the product gas increase with the increase in steam/oxygen ratio.

3.4 Effects Of Fixed Carbon/Oxygen Ratio.

Fig.14, 15 and 16 show the effects of Fixed carbon/Oxygen ratio on solid phase temperature profiles and reactor performance.

From fig. 14, 15 and 16 it is obvious that :-

_____ Carbon conversion, efficiency of the reactor, position of maximum temperature from the grate, product gas exit temperature decrease with the increase in Fixed carbon/Oxygen ratio.

_____ Heating value of the product gas (kJ $kmol^{-1}$), product gas rate (kmol s^{-1}) increase with the increase in Fixed carbon/Oxygen ratio.

_____ Maximum solid temperature and Hydrogen/Carbon monoxide ratio in the product gas remain almost constant.

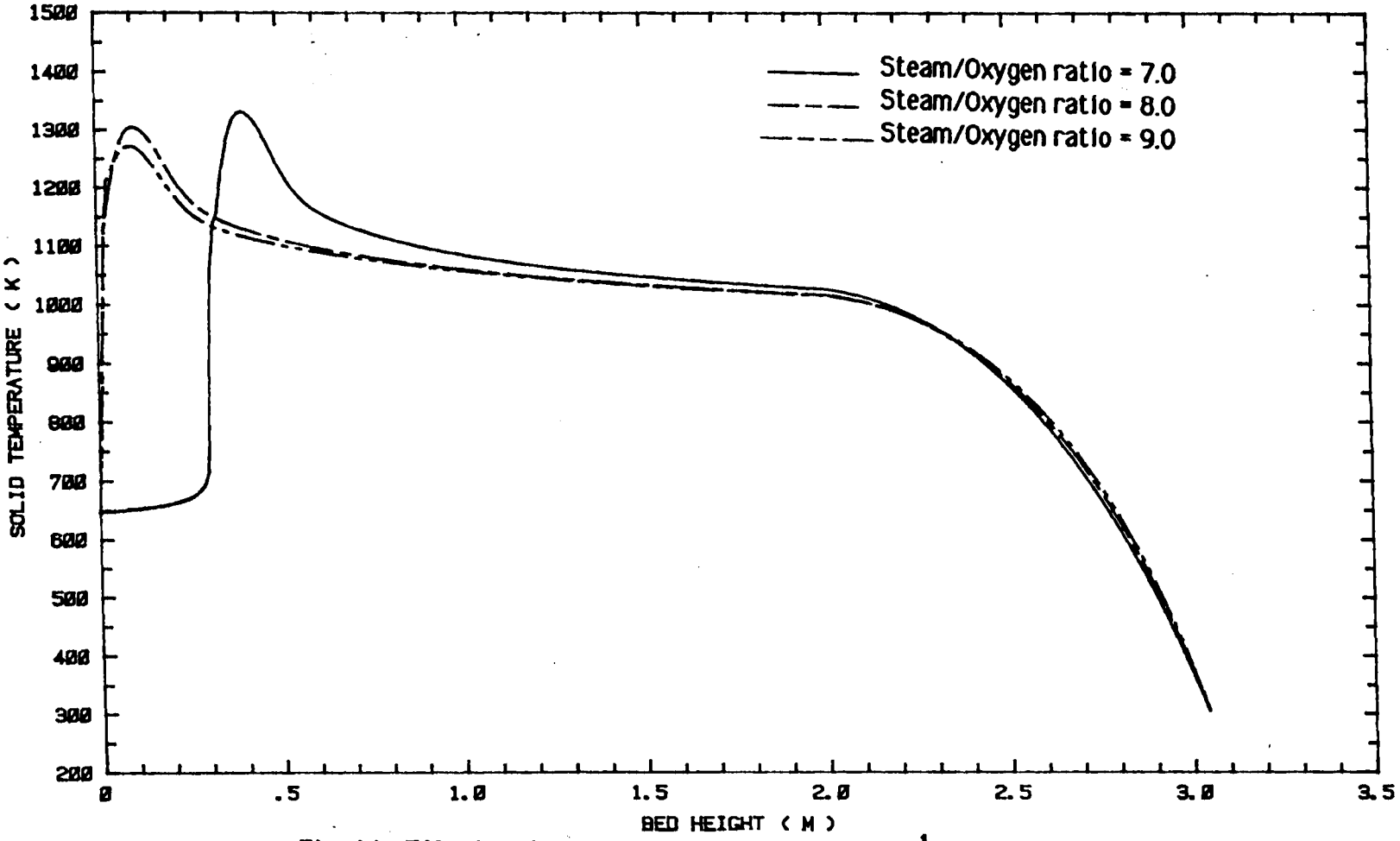

Fig. 11 : Effects of steam/oxygen (mole mole^{-1}) ratio on solid phase temperature profiles for the same conditions as fig. 6.

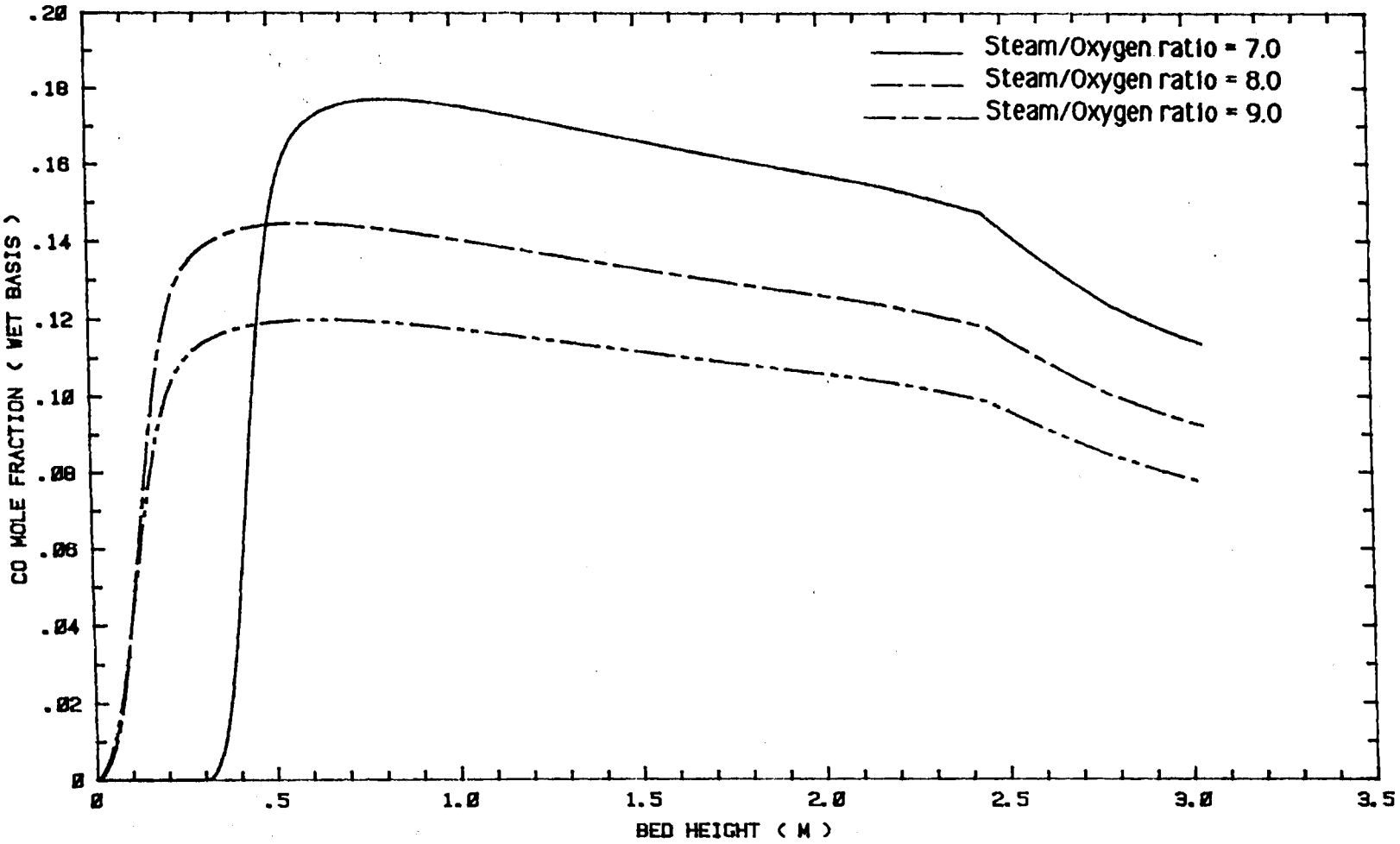

Fig. 12: Effects of steam/oxygen (mole $mole^{-1}$) ratio on carbon monoxide concentration profiles for the same conditions asfig. 6

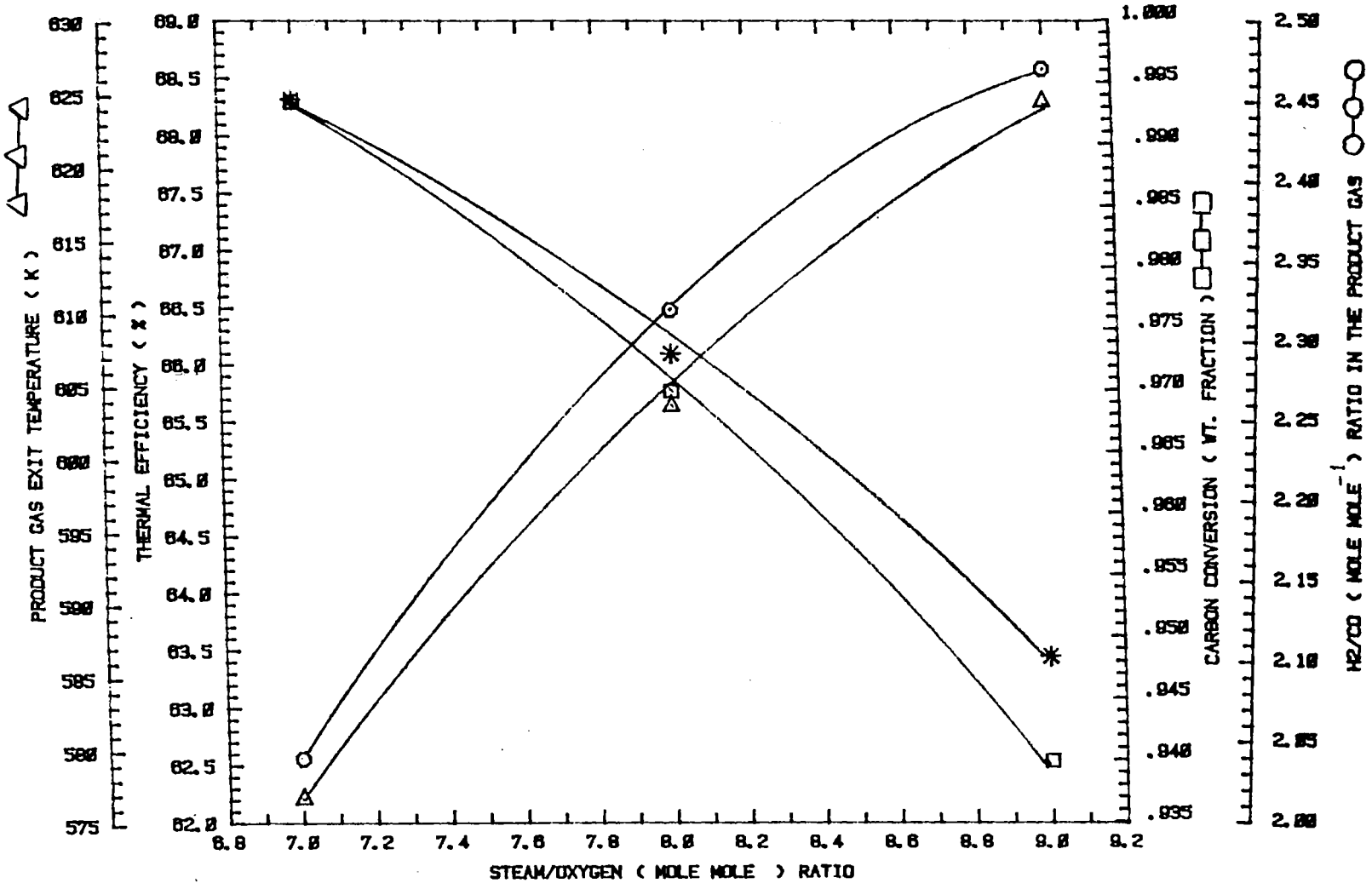

Fig. 13 : Effects of steam/oxygen (mole mole^{-1}) ratio on reactor performance for the same conditions as fig. 6.

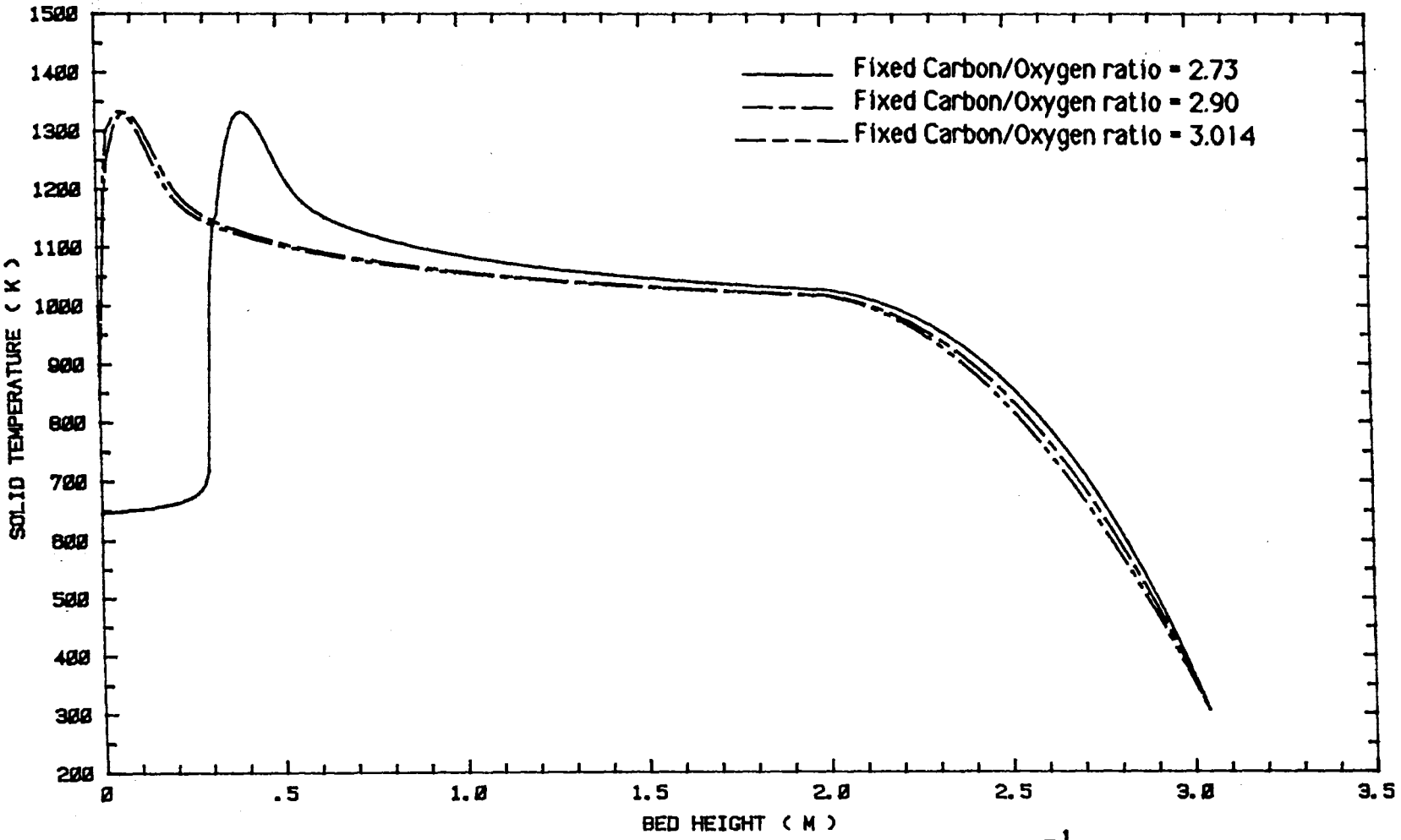

Fig. 14 : Effects of fixed carbon/oxygen (mole mole^{-1}) ratio on solid phase temperature profiles for the same conditions as fig. 6

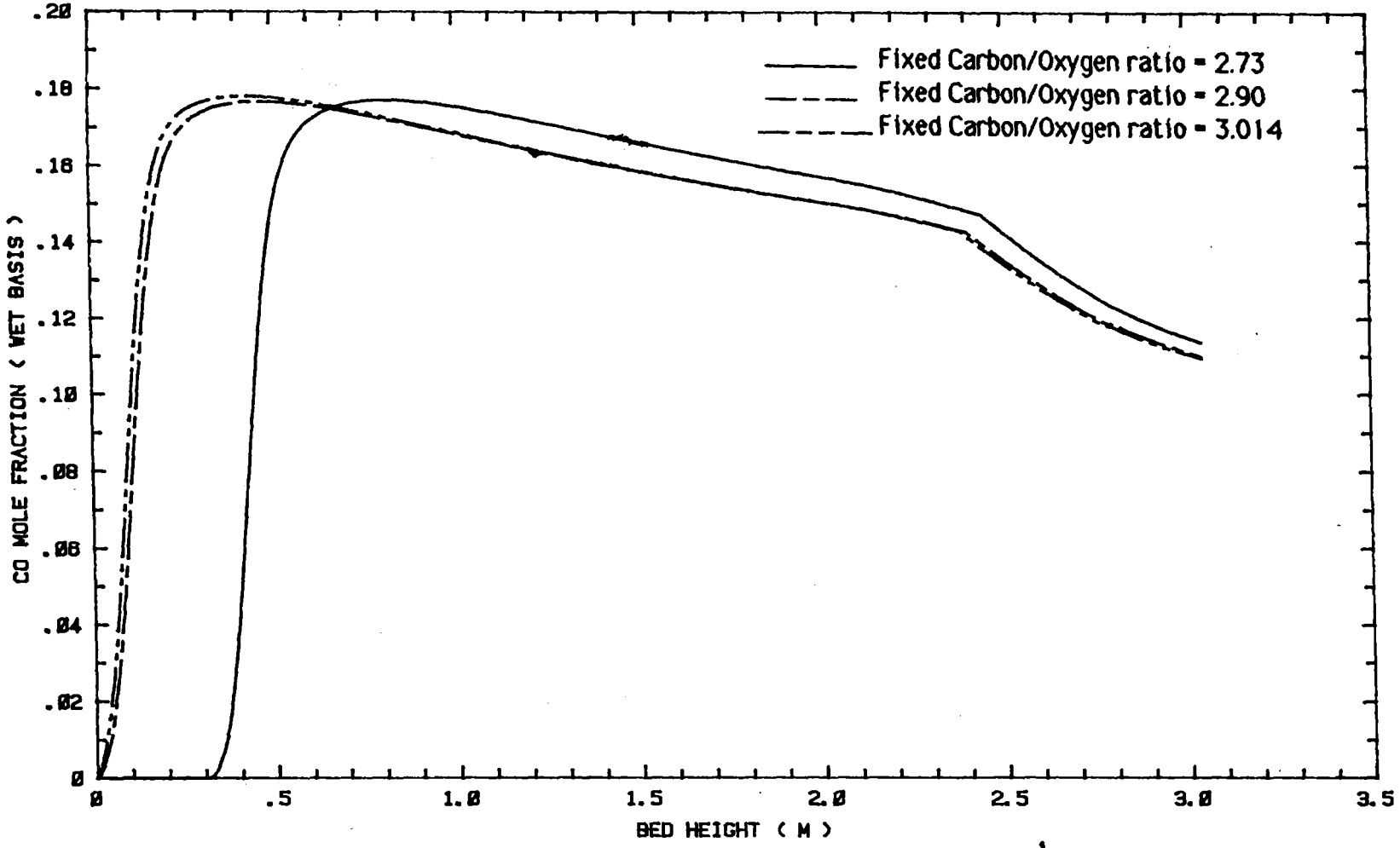

Fig. 15: Effects of fixed carbon/oxygen (mole $mole^{-1}$) ratio on carbon monoxide concentration profiles for the same conditions as fig. 6.

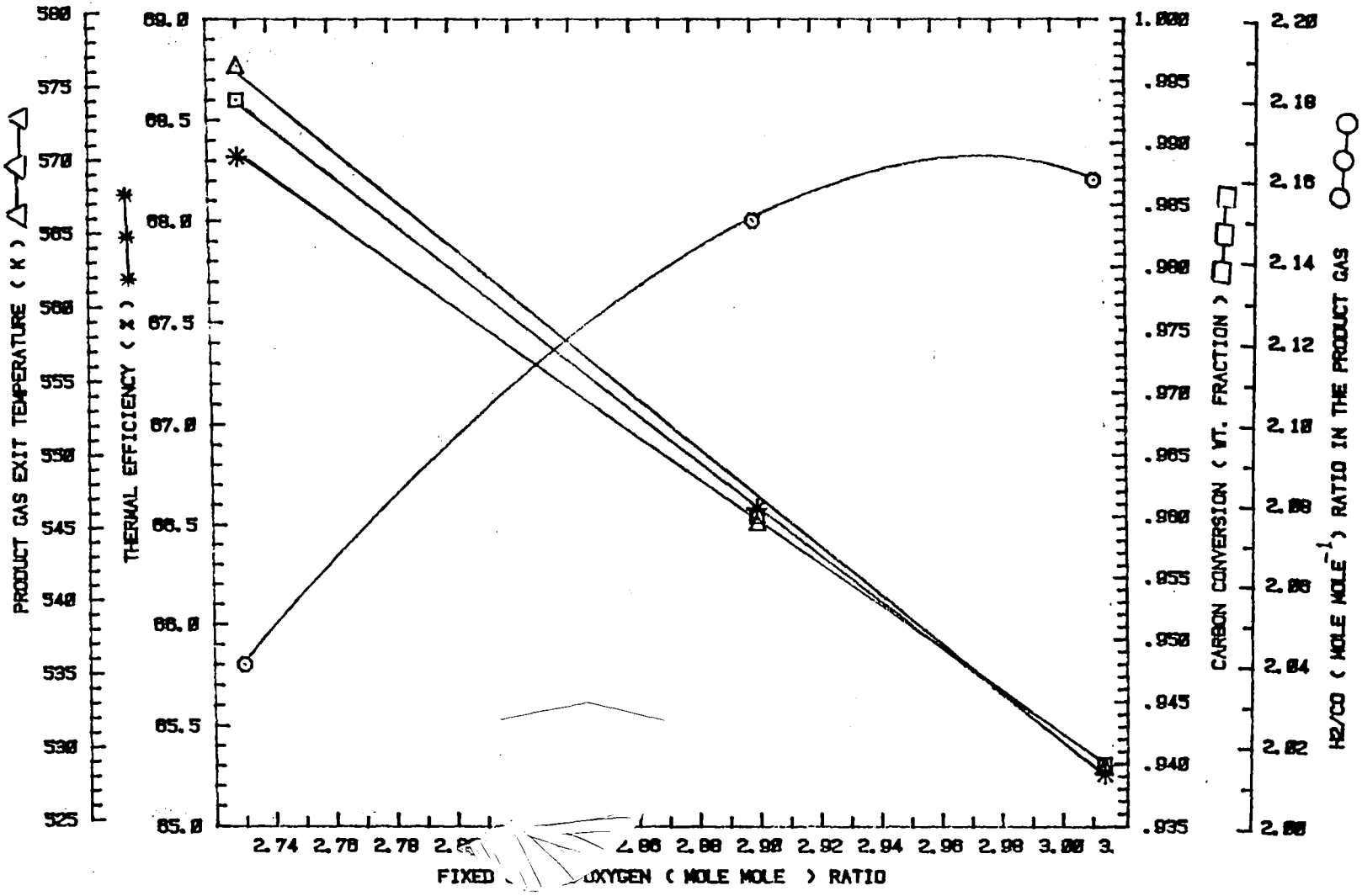

Fig. 16 : Effects of fixed carbon/oxygen (mole $mole^{-1}$) ratio on reactor performance for the same conditions as fig. 6.

3.5 Effects Of Blast Gas(Steam/Oxygen) Inlet Temperature.

Fig.17 and 18 show the effects of blast gas inlet temperature on solid phase temperature profiles and reactor performance respectively.

From fig.17 and 18 it is obvious that :-

_____ Carbon conversion, thermal efficiency, product gas heating value (kJ $kmol^{-1}$), product gas rate, position of maximum temperature from the grate decrease with the decrease in blast gas inlet temperature.

_____ Hydrogen/ Carbon monoxide ratio in the product gas increases with the decrease in blast gas inlet temperature.

_____ Maximum temperature in the bed is almost independent of blast gas temperature (provided it is above a certain value).

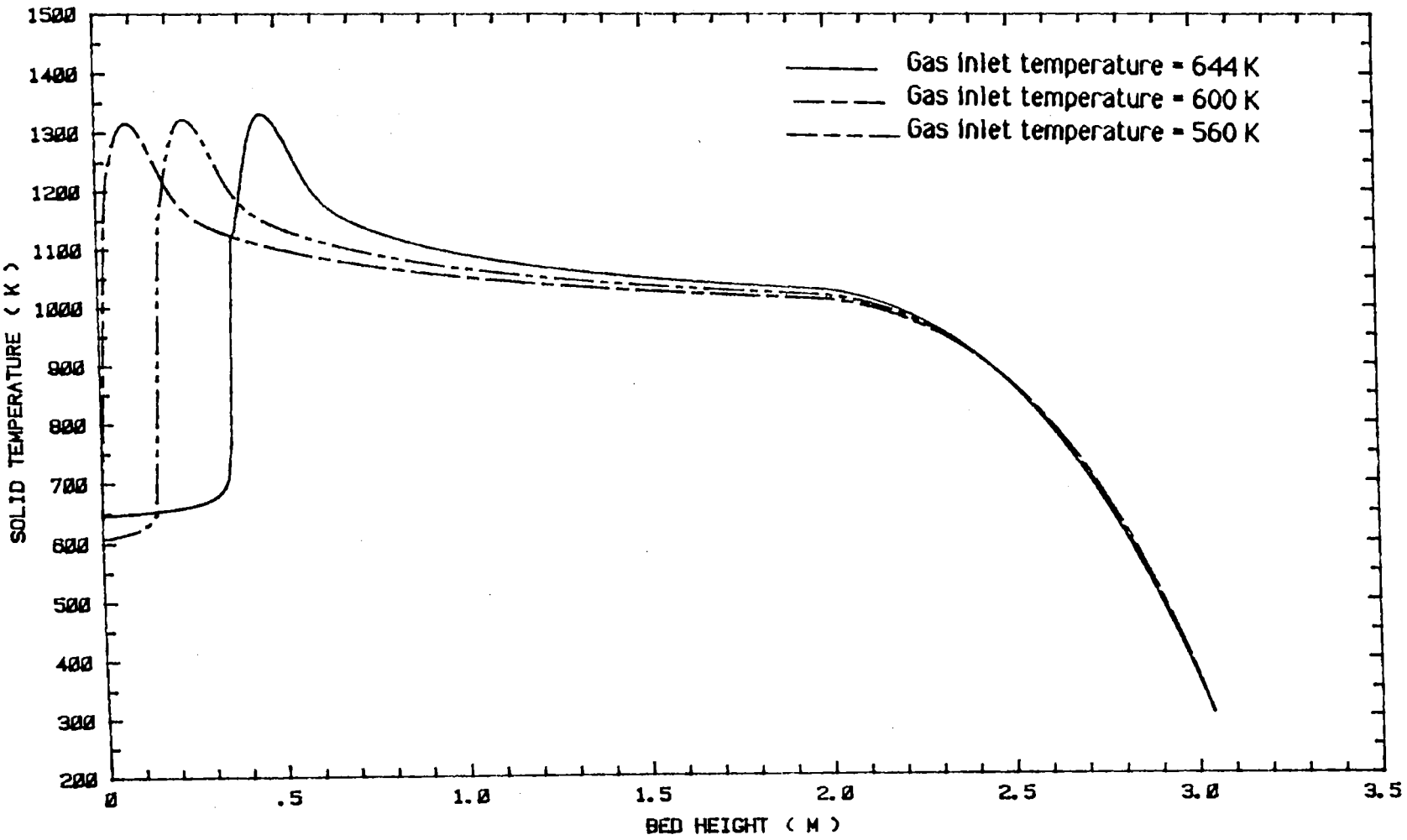

Fig. 17 : Effects of blast gas inlet temperature on solid phase temperature profiles for the same conditions as fig. 6.

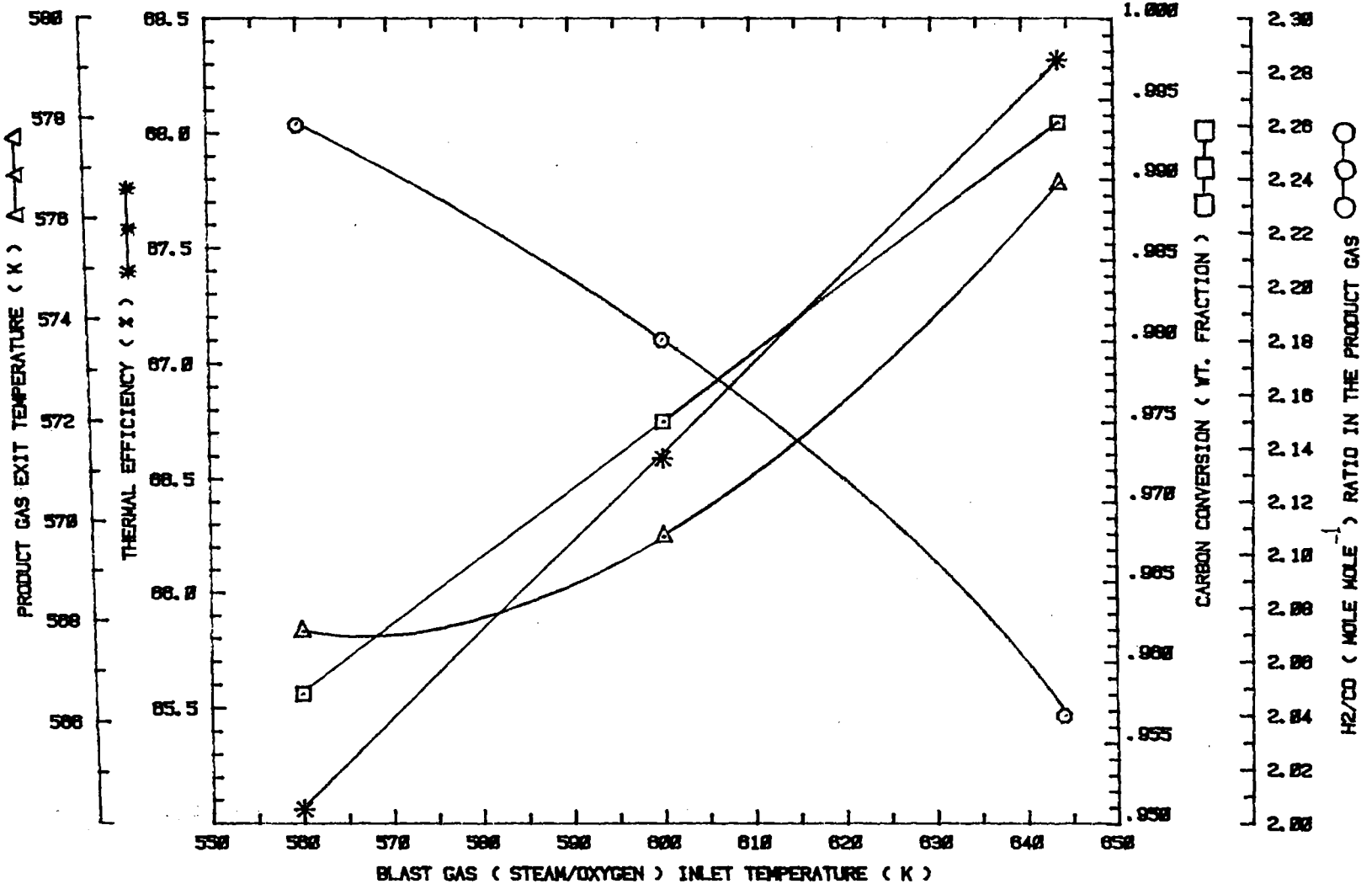

Fig. 18 : Effects of blast gas inlet temperature on reactor performance for the same conditions as fig. 6.

4.0 CONCLUSIONS AND SUGGESTIONS

For a dry ash Lurgi coal gasifier throughput is limited mainly by the following operating and controllable variables :-

_____ Flow rate of blast gas (Steam/Oxygen); this must be below a certain level depending on operating pressure, temperature, particle size , coal properties and gasifier dimension , otherwise excessive entrainment of fine particles and gas pressure drop will result.

_____ Maximum temperature in the bed; this must be below the ash softening temperature, otherwise ash clinker may form and the operation of the reactor will be seriously hampered.

_____ Product gas exit temperature; this must be above the condensation temperature of steam and tar in the product gas, otherwise reactor operation will be affected.

The following conclusions can be drawn from the model results.

(i) Maximum temperature is a strong function of Steam/Oxygen ratio, coal particle size but almost independent of blast gas inlet temperature and Fixed carbon/Oxygen ratio.

(ii) For efficient operation of the reactor and coal concerned the position of the maximum temperature should be maintained between 0.2 m to 0.5 m above the grate using suitable Steam/Oxygen ratio ($\sim$ 7.0), blast gas inlet temperature ($\sim$644 K), particle diameter ($\sim$0.01 m), Fixed carbon/Oxygen ratio ($\sim$2.73 for oxygen flow rate of 0.0508 kmol s^{-1}).

(iii) Thermal efficiency and carbon conversion can be increased by decreasing particle size, decreasing Steam/Oxygen ratio or by increasing the blast gas inlet temperature. (particle size should not be decreased below 0.01 m and Steam/Oxygen ratio should not be decreased below 7.0 to avoid ash clinker formation.

Blast gas inlet temperaures should not be increased above 644 K, because of insignificant improvement).

(iv) With the assumption of no entrainment of coal particles the reactor throughput can be increased by increasing coal, oxygen and steam feed rate in such a way that Fixed carbon/Oxygen, Steam/Oxygen ratio remain at 2.73 and 7.0 respectively.

(v) Below a certain blast gas inlet temperature (nearly 540 K), most of the reactor bed will be needed for lighting up. Consequenly reactor pereformance will be adversely affected.

4.1 Limitations Of The Model And Suggestions For Further Work

The model can be made more robust and its area of application can be widened by making improvement in the following two areas:-

(i) This model has been devoloped on the assumption that ash outlet temperature is almost in equilibrium with blast gas inlet temperature. This is valid when the position of maximum temperature is sufficiently high from the grate; this is the case for high carbon conversion (more than 0.99 wt. fraction of carbon). When the carbon conversion is less than 0.99 (wt. fraction), the position of maximum temperature comes close to the grate due to the highly exothermic combustion reaction between oxygen and excess unreacted carbon, as a result the ash exit temperature can not reach equilibrium with entering blast gas temperature. Due to the uncertainty in the prediction of solid phase exit temperature and also that of heat transfer coefficient near the grate (which will be greater near the grate than other part of the bed due to highly turbulent motion of the entering blast gas) the solid phase temperature profile becomes oscillatory in the model near the grate for low carbon conversion.

(ii) Reactor throughput can be increased by increasing coal, oxygen and steam flow rate at the expense of increased particle entrainment and gas phase pressure drop. This model can not be used to determine maximum allowable gas superficial velocity in the reactor. This limitation can be ovecome by incorporating minimum fluidized velocity type correlation in the model.

. These two limitations can better be overcome by comparing the model results with actual gasifier data operating over a wider range of conditions thereby introducing some empirical factors in the model for matching the model output with actual plant output.

(iii) At very high carbon conversion (X_{cf} greater than 0.996) the model failed to give consistent results because most of the bed will be occupied by ash layer.

5.0 NOMENCLATURE

a = specific area of the reactor bed (= $6(1 - \varepsilon)/d$), $m^2\ m^{-3}$

a = wall heat transfer area per unit volume of bed (= $4/D$), $m^2\ m^{-3}$

C = carbon concentration (= $(1 - \varepsilon)\ X_c \rho_c$), kmol m^{-3} (o refers to initial condition)

D = diameter of the reactor, m

D_i = bulk phase effective diffusivity of gaseous component i, $m^2\ s^{-1}$

FC = fixed carbon in the coal, wt. fraction

d = average diameter of the coal particle, m

F_i = specific molar flow rate of gaseous component i up through the bed (i= 1 to 6), kmol $s^{-1}\ m^{-2}$ (o refers to inlet condition)

F_7 = specific molar flow rate of carbon down through the bed, kmol $s^{-1}\ m^{-2}$ (o refers to inlet condition)

F_g = total molar flux of gases, kmol $m^{-2}\ s^{-1}$

F_s = Weight of char leaving the reactor, kg s^{-1}

h = overall heat transfer coefficient (convective and radiative) between gas and solid phases, kW $m^{-2}\ K^{-1}$

H_i = enthalpy of gaseous component i at temp. T, kJ $kmol^{-1}$

H_g = specific enthalpy flow rate of gaseous phase (= heat capacity of gas x gas flux), kW $K^{-1}\ m^{-2}$

H_s = specific enthalpy flow rate of solid phase (= heat capacity of solid x solid flux), kW $K^{-1}\ m^{-2}$

H_{gs} = amount of heat transferred from the gas to solid phase due to the gaseous reactants diffusing into solid particles, kJ m^{-3} s^{-1}

H_{sg} = amount of heat transferred from the solid to gas phase due to gaseous products diffusing out of the solid particles, kJ m^{-3} s^{-1}

h_d = effective heat transfer coefficient between gas and solid phases in the drying and heating zone, kW K^{-1} m^{-2}

ΔH_j = heat of reaction j, kJ $kmol^{-1}$

ΔZ = incremental bed height, m

ΔZ_d = approximate bed height for drying and heating of the coal, m

ΔZ_v = approximate bed height for the devolatilization the coal , m

i = subscript for component (i=1 for CO, i=2 for CO_2 (i=3 for H_2, i=4 for CH_4, i=5 for O_2, i=6 for H_2O, i=7 for C)

j = subscript for reaction

K_g = thermal conductivity of the gaseous phase, kW $m^{-1}K^{-1}$

K_j = equilibrium constant for reaction j

K_{pi} = film mass transfer coefficient of component i

k_j = Arrhenius type rate constant for reaction j

k_{ox}, E_{ox} = Arrhenius parameters in the expression of λ

k_v = rate constant of devolatilization reaction s^{-1}

k_{vo}, E_v = Arrhenius parameters in the expression of k_v

P = total pressure, kPa

P_i = partial pressure of component i, kPa
(o refers to inlet condition)

Q_d = total heat load for drying and heating of the coal, kW

R = universal gas constant, kJ $kmol^{-1}$ K^{-1}

r_j = rate of reaction j, kmol m^{-3} s^{-1}

T_g = gas phase temperature, K
(o refers to inlet condition)

T_s = solid phase temperature, K
(o refers to inlet condition ; other subscripts refers to different positions of the bed)

T_{lmd} = log mean temperature difference in drying and heating of the coal, K

T_w = temperature of boiling water in the jacket of gasifier, K

t = instantaneous time, s

U = overall heat transfer coefficient between gas and water in the jacket, kW m^{-2} K^{-1}

V, V^* = wt. fraction of coal lost as volatililes at time t and ∞

VM = volatiles content of coal, wt. fraction

W_b = initial carbon content of the char, kg kg^{-1}

X_{ash} = ash in coal, wt. fraction

X_c = wt. fraction of carbon in coal kg kg^{-1}

X_{cf} = ultimate carbon conversion , wt. fraction

Y_i = mole fraction of gaseous component i

Z = instantantaneous bed height at time t, m

Z_{bed} = bed height, m

Z_{end} = bed height at which assumed solid phase temperaure profile started, m

Z_{devo} = bed height at which devolatilization started, m

Z_{dry} = bed height at which drying of the coal started, m

Greek letters:

λ = ratio of CO and CO_2 in combustion reaction, mole $mole^{-1}$

θ_s = porosity in the shell of the coal particle

θ_c = porosity in the core of the coal particle

ε = porosity of the bed

ε_{po} = initial porosity of the char particle

ρ = fraction of particle which is unreacted

ρ_c = density of carbon in coal, kmol m^{-3}

ξ, ξ' = constants of proportianality

γ_j = stoichiometric coefficient of carbon in reaction j

6.0 REFERENCES

Amundson, N. R. and L. E. Arri, "Char gasification in a counter current reactor," AIChE J.,vol. 24, no. 1 pp 87-101, (1978).

Anthony, D. B and J. B. Howard, "Coal devolatilization and hydrogasification," AIChE J. vol. 22, no. 4 , pp 625-656, (1976).

Aris, R. and N. R. Amundson, "Mathematical methods in chemical engg.," vol. 2, pp 316-328, Prentice Hall, N. J., (1973).

Arri, L. E and N. R. Amundson, "Analytical study of single particle char gasification," AIChE J. vol. 24, no. 1, pp 72-86, (1978).

Arthur, J. R., "Reaction carbon and oxygen", Trans. Faraday Soc., vol. 47, pp 164-, (1951).

Badzioch, S. and P. B. W. Hawksley, Ind. Eng. chem. Process Des. Dev. vol. 9, pp 521-, (1970).

Biba, V., et al., "Mathematical model for the gasification of coal under pressure," Ind. Eng. chem. Process Des. Dev. vol. 17, pp 92-, (1978).

Carnahan, B. et al., "Applied Numerical methods", J Wiley & sons, N.Y., (1969).

Cho, Y. S. and B. Joseph, "Heterogeneous model for moving bed coal gasification reactors," Ind. Eng. chem. Process Des. Dev. vol. 20, no. 2, pp 314-318, (1981).

Denn, M. M. et al., "A kinetic free model of coal gasifiers," Ind. Eng. chem. Fundam. vol. 18, pp 286-, (1979).

Desai, P. R, C. Y. Wen, "Computer modeling of the Morgantown energy research center's fixed bed gasifier," Dept. of Chemical engg., West Virginia university, Morgantown, W. Virginia, (March, 1978).

Dobson, S., "Modeling of entrained bed gasification : The issues", EPRI, Palso Patlo, Calif., (Jan. 15, 1975).

Gibson, M.A. and C.A. Euker, Jr. "Mathematical modeling of fluidized bed coal gasification," paper presented at AIChE meeting, L.A., Calif., (Nov., 1975).

Gumz, W., "Gas producers and blast furnaces", Wiley, N.Y., (1950).

Hoogendorn, J. C. "Gas from coal with Lurgi gasification at Sasol," IGT symp. papers, " Clean fuels from coal",pp 111-, (1973).

Howard, J. B and R. H. Essenhigh, Ind. Eng. Chem. Proc. Des. Dev., vol. 6, pp 74-, (1967).

Johnson, J. L., "Kinetics of Bituminous coal char gasification with gases containing steam and hydrogen," Adv. chem. ser., vol. 131, ACS, pp 145-178, (1974).

Juntgen, H. K and K. H. Vanheek, Fuel, vol. 47, pp 103-, (1968).

Kalson, P. A. and D. E. Briggs, "Coal devolatilization: fundamental and modeling," Canadian chemical engg. conference - coal and coke session (28th), Halifax, Nova Scotia, (1978).

Kasoka, S. et al., "The development of rate expressions and the evaluation of reactivity for gasification of various coal chars with steam and oxygen," Intern. chem. engg. vol. 23, no. 3, pp 477-485, (July, 1983).

Kosky, P. G and J. K. Floess, "Global model of countercurrent coal gasifiers," Ind. Eng. Chem. Process Des. Dev., vol. 19, no. 4, pp 586-592, (1980).

Loison, R. and F. Chauvin, chem. Ind. (Paris), 91, 269, (1964).

Lowry, H. H., "Chemistry of coal utilization", Supplemetary vol., J. Wiley, N.Y, (1963).

Perry, R. H and C. H. Chilton, "Chemical Engineer's handbook," 5th edn., McGraw-Hill, (1973).

Phillips, R., et al.,"Factors affecting the product ratio of the carbon-oxygen reaction, I and II, Carbon, 7, 479, (1969); 8, 205, (1970).

Rase, H. F., "Chemical reactor design for process plants," vol. II, pp 44-60, J Wiley & sons, (1977).

Rossberg, M. Z., Electrochem., 60, 952, (1956).

Rudolph, P., "The Lurgi process, the route to S.N.G from coal," Proc. 4th symp. synthetic pipeline gas, Chicago, Illinois (1972).

Rudolph, P., "Gas from coal", Chemical Economy & engg. review, vol. 5, no. 10, (Oct, 1973).

Sergent, G. D. and I. W. Smith, "Combustion rate of Bituminous coal char in the temperature range 800 to 1700 K," Fuel, vol. 52, pp 52-, (1973).

Sotirchos, S. V. and N. R. Amundson, "Dynamic behavior of a porous char particle burning in an oxygen- containing environment," AIChE J., vol. 30, pp 537-, (1984).

Walker, P. L. Jr. et al., "Gas reactions of carbon," Advan. Catalysis, 2, 134, (1959).

Walker, W. H. et al., "Principles of chemical engg.," McGraw-Hill, N.Y., (1937).

Wen, C. Y. et al., "Production of low Btu gas involving coal pyrolysis and gasification," Coal gasification, Adv. chem. ser., vol. 131, pp 6-, (1974).

Wen, C. Y. and S. Tone, "Coal conversion reaction Engg.," ACS symp. ser., vol. 72, pp 56-, (1978).

Wen, C. Y. and T. Z. Chaung, "Entrainment coal gasification modeling," Ind. Eng. chem. Process Des. Dev., vol. 18, pp 684-, (1979).

Wegstein, J. H. , " Accelerating convergence of iterative processes," Comm., Assoc. Comput. Mach., vol. 1, no. 6, pp 9- , (1958).

Wiser, W. H. et al., "Kinetic study of the pyrolysis of a high-volatile Bituminous coal," Ind. Eng. chem. Process Des. Dev., vol. 6, pp 133-, (1967).

Woodmansee, D. E, "Modeling of fixed bed gas producer performance," Energy communications, vol. 2, pp 13-, (1976).

Yoon, H., et al., "A model for moving bed coal gasification reactors", AIChE J., vol. 24, pp 885- , (1978).

Zahradink, R. L. and R. J. Grace, Adv. chem. ser., no. 131, pp 126-, (1979).

7.0 APPENDIX I-A:

Three point moving averaging technique:

This technique was used to get nonoscillatary solution in the dry ash Lurgi gasifier modeling.

Reason of application:

Gasifier modeling is an example of split boundary value problem. For this problem one has to assume solid and gas phase temperatures at $Z + \Delta Z$ (refer to fig. 4) to solve the necessary equations in order to get the values of all the unknowns at $Z + \Delta Z$. These initial estimates of solid and gas phase temperatures have significant impact on the solution, because of two competing sets of reactions e.g., exothermic reaction (char-oxygen reaction), endothermic reactions (char-steam, char-carbon dioxide reactions). Exothermic reaction may become predominant if the initial estimates are too low, whearas endothermic reactions may become predominant if the initial esimates are too high. Consequently, there is a high probability of getting oscillatary and unstable solution. To get good estmites of both solid and gas phase temperatures three point moving averaging technique was applied in the following way:

Step 1: Starting from Z, all the necessary equations were solved to get values of solid and gas phase temperatures at $Z + \Delta Z$, and at $Z + 2\Delta Z$ e.g., $T_s|_{Z + \Delta Z}$, $T_g|_{Z + \Delta Z}$, $T_s|_{Z + 2\Delta Z}$, and $T_g|_{Z + 2\Delta Z}$.

Step 2: Solid and gas phase temperature values at Z, $Z + \Delta Z$, and $Z + 2\Delta Z$ were averaged using:

$$T_{s,av} = \frac{T_s|_Z + T_s|_{Z + \Delta Z} + T_s|_{Z + 2\Delta Z}}{3.0}$$

$$T_{g,av} = \frac{T_g|_Z + T_g|_{Z + \Delta Z} + T_g|_{Z + 2\Delta Z}}{3.0}$$

Step 3: Using the average solid and gas phase temperatures, $T_{s,av}$ and $T_{g,av}$ as modified initial estimates of solid and gas phase temperatures, all system equations were solved to get the values of all the unknowns at $Z + \Delta Z$.

Step 4: The above steps were repeated till the end of devolatilization zone.

CHAPTER II

PROCESS MODULE FOR A HIGH TEMPERATURE SHIFT REACTOR

ABSTRACT

A process module has been developed for high temperature shift reactors based on a simple steady state one dimensional rate model. This module can be used for the design and simulation of the high temperature shift reactors, used as an important process in Methanol synthesis, Ammonia synthesis, SNG manufacturing from any carboneceous materials either to adjust CO/H2 ratio or to get rid of CO. This module is tested with published plant data and simulates plant behaviour results resonably well.

It is possible to extend this module for low temperature shift reactors by using different rate parameters as proposed by Singh and Saraf(1980); and Rase (1977).

TABLE OF CONTENTS

		page
(i)	ABSTRACT	
1.0	INTRODUCTION	II-1
1.1	Earlier models of shift reactors	II-4
2.0	THERMODYNAMICS	II-5
3.0	KINETICS AND REACTION RATE EXPRESSIONS	II-8
3.1	Effects of some important variables on reaction rate	II-9
4.0	MODEL DEVELOPMENT	II-11
4.1	Model equations and method of solution	II-11
4.2	Flow diagram of the computer program .	II-13
5.0	RESULTS AND DISCUSSIONS	II-15
5.1	Effects of Steam/CO ratio on shift reactor performance	II-18
5.2	Effects of feed gas inlet temperature on shift reactor performance	II-21
5.3	Effects of CO_2 concentration level on shift reactor performance	II-21
6.0	CONCLUSIONS AND SUGGESTIONS	II-26
7.0	NOMENCLATURE	II-27
8.0	REFERENCES	II-29
9.0	APPENDICES	II-31

1.0 INTRODUCTION

The carbon monoxide shift conversion:

$$CO + H_2O \rightleftarrows CO_2 + H_2 \qquad \text{(1)}$$

is one of the most important industrial reactions in high temperature gas processing. The shift reaction is a process by which a part or most of the carbon monoxide in synthesis gas is converted to CO_2 and H_2 by reaction with steam either to adjust the H_2/CO ratio (in the synthesis of SNG or Methanol) or to make H_2 gas.

Two types of shift catalysts are in industrial use: e.g.

(i) High temperature (iron oxide catalyst based) shift catalysts.

(ii) Low temperature (zinc and copper oxides based) shift catalysts,

depending on the operating conditions and specific needs. Comparative chracteristics of the two types of catalysts are given in table 1.

Table 1
Comparative characteristics of high and low temperature catalysts. (Rase, 1977)

	High temperature catalysts	Low temp. catalysts
Compositions	Chromia promoted iron oxides(Fe_2O_3, 85-95%) Cr_2O_3, 5-15%))	Copper-Zinc oxide (CuO, ZnO)
Max. operating temperature(K)	750	550
Bulk density (kg m^{-3})	1121	1442
Particle density (kg m^{-3})	2019	2484
Relative cost	1	3.8
Catalyst life (yrs.)	3 yrs and over depending on care in startup and operation.	2 to 3 years.
Catalyst poisons	Inorganic salts, boron, oils, phosphorus compounds liquid H_2O is a temporary poison, Sulphur compounds in an amount greater than 50 ppm.	Sulphur and Halogen and unsaturated Hydrocarbons.
Operating advantages & disadvantages	High operating temperature favors high CO content at equilibrium. So it is suitable for converting the bulk of the CO to H_2; down to concentrations of round about 1. to 4.%.	Because of lower operating temp.,it is suitable for converting CO to a concntration of less than 0.3%.

High temperature shift catalysts were chosen for modeling purpose over low temperature shift catalysts because,

____ these catalysts are more favorable in term of cost for reducing the bulk CO content to a level suitable for both methanol and SNG synthesis, (i.e.10% to 20%, dry basis).

____ high temperature shift catalysts are relatively more resistant to sulphur compounds.

Because of the low heat of reaction of the shift reaction either single bed adiabatic tubular reactors or multi bed adiabatic tubular reactors with interstage cooling (shown in fig.1) are used according to the amount of CO to be converted.

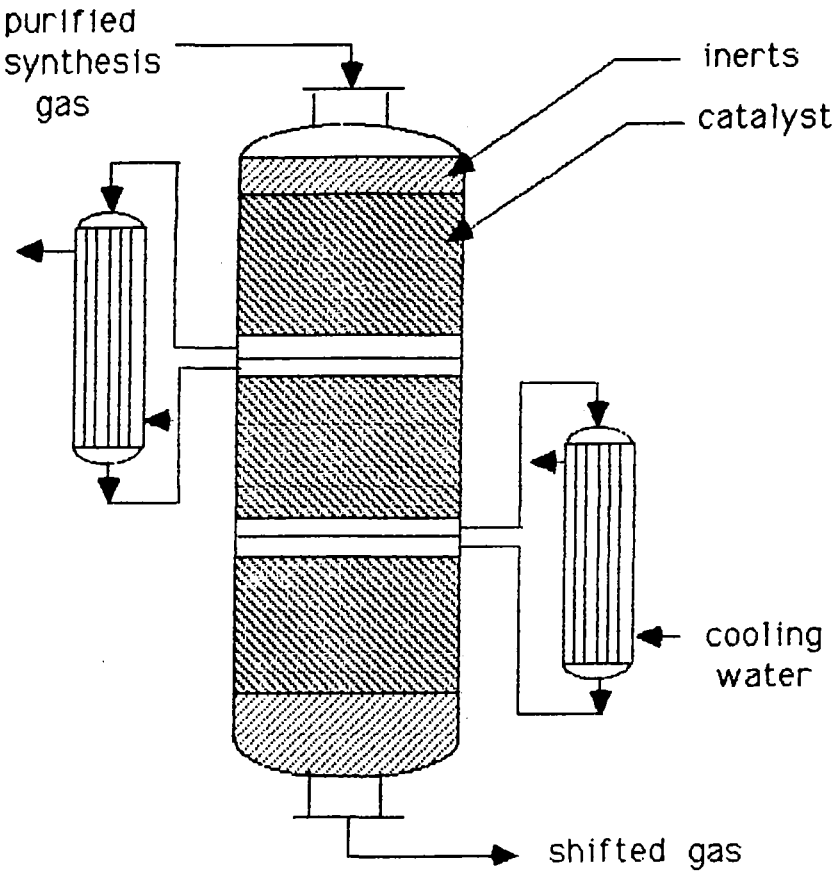

Fig. 1 Multi bed adiabatic reactor with interstage cooling

1.1 Earlier Models Of Shift Reactors.

Wen and Kim (1970) developed first order models of both single and multibed with interstage quench shift reactors. They tested both the pseudo first order rate expression of Ruthven (1969) as well as the second order rate expression of Girdler chemical company (1965) in their models but did not find any noticeable difference in reactor performance. Singh and Saraf (1977) developed simple first order models of both high and low temperature shift reactors based on pseudo first order rate expressions and obtained results comparable to plant results. Rase (1977) developed simple models of both high and low temperature shift reactors based on second order rate expressions of Girdler chemical company (1965). Employing modified version of Goodridge and Quazi's (1967) second order rate expression, Duffuor and Stewart (1979) developed a relatively complex model of shift reactors using the "two-tier" modeling technique. Main features of this model are :

____ Solution of material, energy and momentum balance differential equations for the volumetric section ΔV to get temperature, concentration and pressure at the end of each section of the bed.

____ Using the calculated temperature, concentration and pressure, solution of two coupled second-order differential equations describing the tempearture and concentration changes within the catalyst pellet to evaluate the effectiveness factor at each section of the bed.

____ Updating of concentration and temperature for each section of the bed using the calculated effectiveness factor.

They concluded that results comparable to plant results can be obtained using either an average effectiveness factor for each bed or a mathematical function representing the effectiveness factor with bed height in the model, rather than solving the coupled differential equations in each section of the bed.

2.0 THERMODYNAMICS

The shift reaction $CO + H_2O \rightleftharpoons CO_2 + H_2$, ΔH^0 =9180 kcal/kmol CO conversion is a slightly exothermic reaction. For this reaction one can plot the equilibrium CO mole percent in the exit gas vs. adiabatic reaction temperature and also the adiabatic operating line for a given feed condition and a given feed temperature in the following way (Rase, 1977; Ting and wan, 1969; Levenspiel, 1972): One such plot from Rase(1977) is shown in fig. 2.

The method of obtaining such a plot is as follows :-

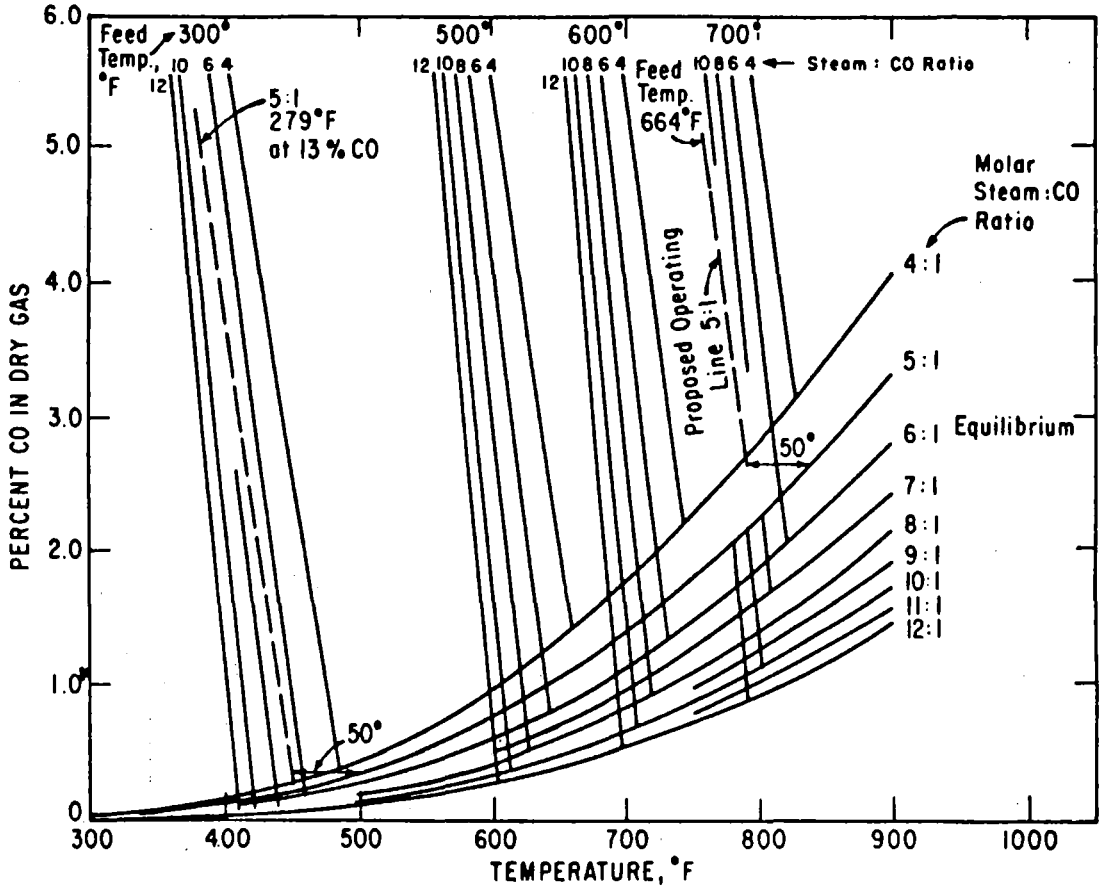

Fig. 2 Adiabatic plot for shift conversion at various steam-to-CO ratios.

Step A. Plot of an equilibrium conversion curve of mole percent vs.adiabatic temperature:

(i) A series of temperatures relevent to the operating temperature of the shift reactor were arbitrarily selected and then the equilibrium mole percent (dry basis) of CO was calculated from the following expressions.

$$K = \frac{Y_{CO_2}^{*}\, Y_{H_2}^{*}}{Y_{CO}^{*}\, Y_{H_2O}^{*}} K_v$$

$$= \frac{(F_{CO_2}^{0} + \Delta_{CO})\,(F_{H_2}^{0} + \Delta_{CO})}{(F_{CO}^{0} - \Delta_{CO})\,(F_{CO}^{0} B - \Delta_{CO})} \times K_v \quad \text{---} \quad (2)$$

Percentage CO in dry gas

$$= \frac{F_{CO}^{0} - \Delta_{CO}}{100 + \Delta_{CO}} \times 100$$

The fugacity correction term, K_v can be taken as one. Some expressions of K are given in table 2.

Table 2. Equilibrium constant expressions for the shift reaction.

Singh and Saraf (1977),
$K = \text{Exp}\,[(9998.22/T - 10.213 + 2.7465 \times 10^{-3}T$
$-0.453 \times 10^{-6} T^2 - 0.201 \text{ Ln } T) / R']$
Rase (1977),
$K = \text{Exp}\,(-4.72 + 4800/T)$ for $422 < T < 589$
or
$= \text{Exp}\,(-4.33 + 4577.8/T)$ for $589 < T < 756$

(ii) Then mole percent of CO vs. temperature was ploted.

Step B. Plot of an adiabatic operating line:

(i) For an arbitrary equilibrium mole percent of CO (close to the exit value), the exit gas composition and the equilibrium adiabatic temperature were calculated (from the plot of mole percent of CO vs. equilibrium temperature) and

hence the actual outlet temperature (outlet temperature= equilibrium temperature - equilibrium approach temperature (approx. 30 K)).

(ii) The average specific heat capasity, C_p of the gaseous mixture was calculated from inlet and approximate outlet conditions.

(iii) From the average heat of reaction $-\Delta H$, the slope of the operating line was determined using (slope = $C_p/(-\Delta H)$)

(iv) The adiabatic operating line was drawn starting from the feed temperature.

Step C. Determination of the adiabatic equilibrium point for given feed conditions from the intersection of the equilibrium curve and the adiabatic operating line.

From these plots one can approximately predict for given feed composition and temperature, the capability of a particular shift reactor to meet required CO conversion.

One can also calculate from thermodynamic principles the fraction of raw gas to be shifted for a particular requirement (One such calculation is given in appendix II-A).

3.0 KINETICS AND REACTION RATE EXPRESSIONS.

Bohlbro (1966), Temkin (1979) have discussed the detailed mechanism of the shift reaction. Numerous rate expressions have been proposed by different researchers. (some of these expressions are given in table 3.)

Table 3. Rate expressions of shift reaction.

Goodridge and Quazi (1967),

$$(-r_{CO}) = A \exp^{-E/(RT)} P_{CO}^{a} P_{H_2O}^{b} P_{CO_2}^{c} P_{H_2}^{d}/3600$$

Values of A, E, a, b, c, and d vary widely depending on the catalyst type and operating temperature range.

Moe (1962); Rutheven (1969); Wen and Kim (1970),

$$-\frac{dP_{CO}}{dt} = k_a (P_{CO} - P_{CO}^{*})$$

Singh and Saraf(1977),

$$(-r_{CO}) = \eta\ 2.32 \times 10^{13} \exp^{-116147.84/(RT)} R_a A_{gf} P_f, S_f (Y_{CO} - Y_{CO}^{*}) (P/101.325) \rho_c / (3600R^{'} T)$$

This rate expression takes into account the effects of catalyst reducing temperature, pressure, sulphur concentration, age of the catalyst etc.

Rase (1977); Girdler catalysts company(1965),

$$(-r_{CO}) = P_f \exp(15.95 - 4900/T) (Y_{CO} Y_{H_2O} - Y_{CO_2} Y_{H_2} / K) / 23.654/3600$$

This rate expression takes into account the effect of pressure on the activity of the catalyst.

Duffuor and Stewart (1979),

$$(-r_{CO}) = \text{Goodridge and Quazi's expression x} \left(1 - \frac{P_{CO_2} P_{H_2}}{K P_{CO} P_{H_2O}} \right)$$

Podoloski and Kim (1974) examined a number of representative rate expressions e.g. Langmuir-Hinshelwood, Eiley-Rideal, Oxidation-Reduction, Hulvert-Vasan, Kodama, emprical or power law models of shift reaction and concluded that the Langmuir-Hinshelwood and the Power-Law models could adequately describe the reaction behavior.

Wen and Kim (1970) used both the pseudo first order expression of Ruthven and the second order rate expression of Girdler to optimize the fixed bed shift converter; they did not find any noticeable difference between the cases and found both of them suitable in the usual operating range. Rase (1977) used the second order rate expression of Girdler and found it adequate.

In this work the rate equation proposed by Girdler chemical company (1965) is used for the design of shift reactors because it adequately represents the behavour of shift reactors (Wen and Kim, 1970; Rase, 1977). For simulation the effects of catalyst age, suphur concentration are taken into account in the model from Singh and Saraf's work (1977).

3.1 Effects Of Some Important Variables On The Reaction Rate.

A. Pressure

According to Moe (1962); Wen and Kim (1970) the activity of the catalyst increased up to 28 atm. and then remained constant. Based on extensive pilot plant data of a high temperature based shift reactor, Ting and Wan (1969) concluded that reaction rate decreased according to the factor $P_f = P^{-1.5}$ near atmospheric presure, Where P is in atm. Analyzing published kinetic data of commercial high temperature shift catalysts Ruthven (1969) proposed three pressure factor expressions depending on diffusional resistance for pressure in the range of 1 to 25 atm. Wilson et al. (1968) conducted some kinetic studies over standard high temp. catalyst and showed that rate rose sharply as pressure increased from 1 atm. to 8 atm. then rose slowly till 21 atm. Rase (1977) correlated the activity of high temperature shift catalyst by the following correlation:

$$P_f = 0.816 + 0.184\ (P/101.325) \quad \text{for } P < 1196$$
$$= 1.53 + 0.123\ (P/101.325) \quad \text{for } 1196 < P < 2027$$
$$= 4.0 \quad \text{for } P > 2027$$

where, P is in kPa.

Most of these pressure factors except that of Ting and Wen (1969) are in close agreement with each other.

B. Sulphur compounds and dust

Wilson et al. (1968) conducted an experiment on shift conversion of synthesis gas containing the sulphur compounds, COS, CS_2, C_2H_5SH, H_2S, dust and CO_2 and reached the following conclusions:

(i) CO conversion was lower than with purified gas at atm. pressure but was comparable when the residence time was increased by raising the pressure (up to 21 atm.).

(ii) Dust in the gas did not decrease catalyst activity,but dust concentration of 400 grains per 100 s.cft or more increased the pressure drop and reduced the gas flow appreciably through the converter.

(iii) conversion of CO was generally independent of the type of sulphur compounds.

Singh and Saraf (1977) used an expression proposed by Banerjee et al. (1972) regarding the effect of H_2S concentration in the synthesis gas on the activity of iron based catalyst which is given by:

$$f_s = -0.276 \, \text{Log}_{10} \, ([H_2S] + 2.78) + 1.127$$

where $[H_2S]$ represents concentration of H_2S in ppm.

C. Age of catalyst and reduction temperature.

The activity of freshly prepared shift catalyst undergoes a rapid decline during the first 24 to 72 hours of operation. Thereafter the rate of decline becomes gradual depending on operating conditions (Moe, 1962 ; Singh and Saraf, 1977). This characteristic of the catalyst complicates the selection of the rate constant which will be used for design purposes. Rase (1977) used a rate constant which represents midlife activity proposed by Girdler (1965). Singh and Saraf (1977) used the following two expressions for the effects of reduction temperature and age of catalyst respectively.

$$R_a = \text{Exp} \, (-89.1 + 5.553 \times 10^4/T)$$

$$\text{Log}_{10} \, A_{gf} = (4.66 \times 10^{-4} - 2.0 \times 10^{-6} T) \, \tau$$

4.0 MODEL DEVELOPMENT.

The mathematical model for the high temperature shift reactor has been developed based on the following assumptions:

1. Steady state.
2. No temperature or concentration gradient in the radial direction of the reactor i.e. temperature and concentration are uniform at any cross-section.
3. No axial diffusion of mass or heat.
4. The differences in temperature and concentration between the bulk gas phase and the catalyst surface are negligible. This assumption has been confirmed by Wen and Kim (1970) for typical shift catalysts. So bulk conditions were used in the rate expression.
5. Since the pressure drop in the reactor is relatively small (approx. 69 kPa (Rase(1977)) the average value of inlet and outlet pressures was used in the rate expression i.e. momentum balance was neglected.

4.1 Model Equations And Method Of Solution:

The various processes taking place in the reactor can be described mathematically (Bird et al., 1960) by perfoming a material and a energy balance for CO over a differential element ΔZ of the reactor (shown in fig.3) along with the previously mentioned assumptions.

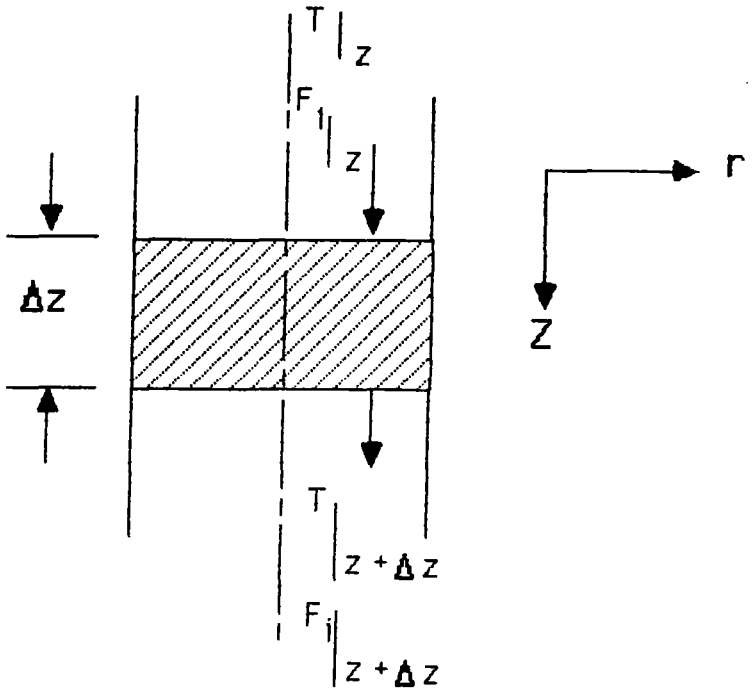

Fig. 3 Schematic diagram of a differential reactor element for heat and material balance.

Mass balance:

$$\frac{dF_{CO}}{dZ} = - r_{CO} \qquad \text{——————} \qquad (4)$$

$$F_i = F_i \pm \Delta F_{CO}$$

Heat balance:

$$\frac{dT}{dZ} = \frac{\Delta F_{CO}\ \Delta H}{\sum_{i=1}^{n} (F_i\ Cp_i)} \qquad \text{——————} \qquad (5)$$

These two coupled first order differential equations (4 and 5) are solved by a fourth order Runge-Kutta-Gill method (Carnahan et al., 1969) starting from the top at Z=0. with initial conditions; $F_i = F_{io}$ and $T = T_o$

4.2 Flow Diagram Of The Computer Program.

A computer program of the shift reactor process module has been developed. This program can be summarized by the following flow diagram:

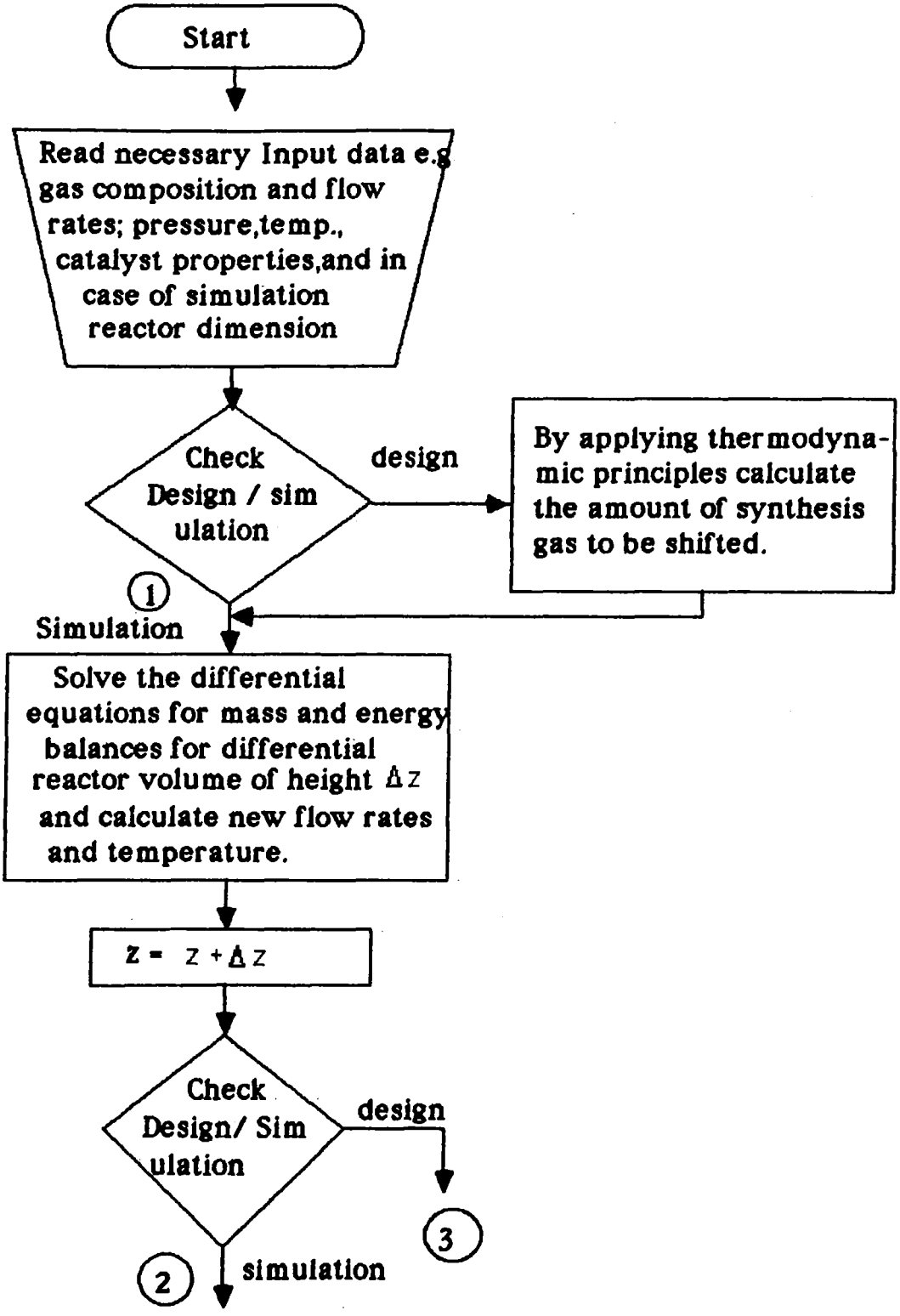

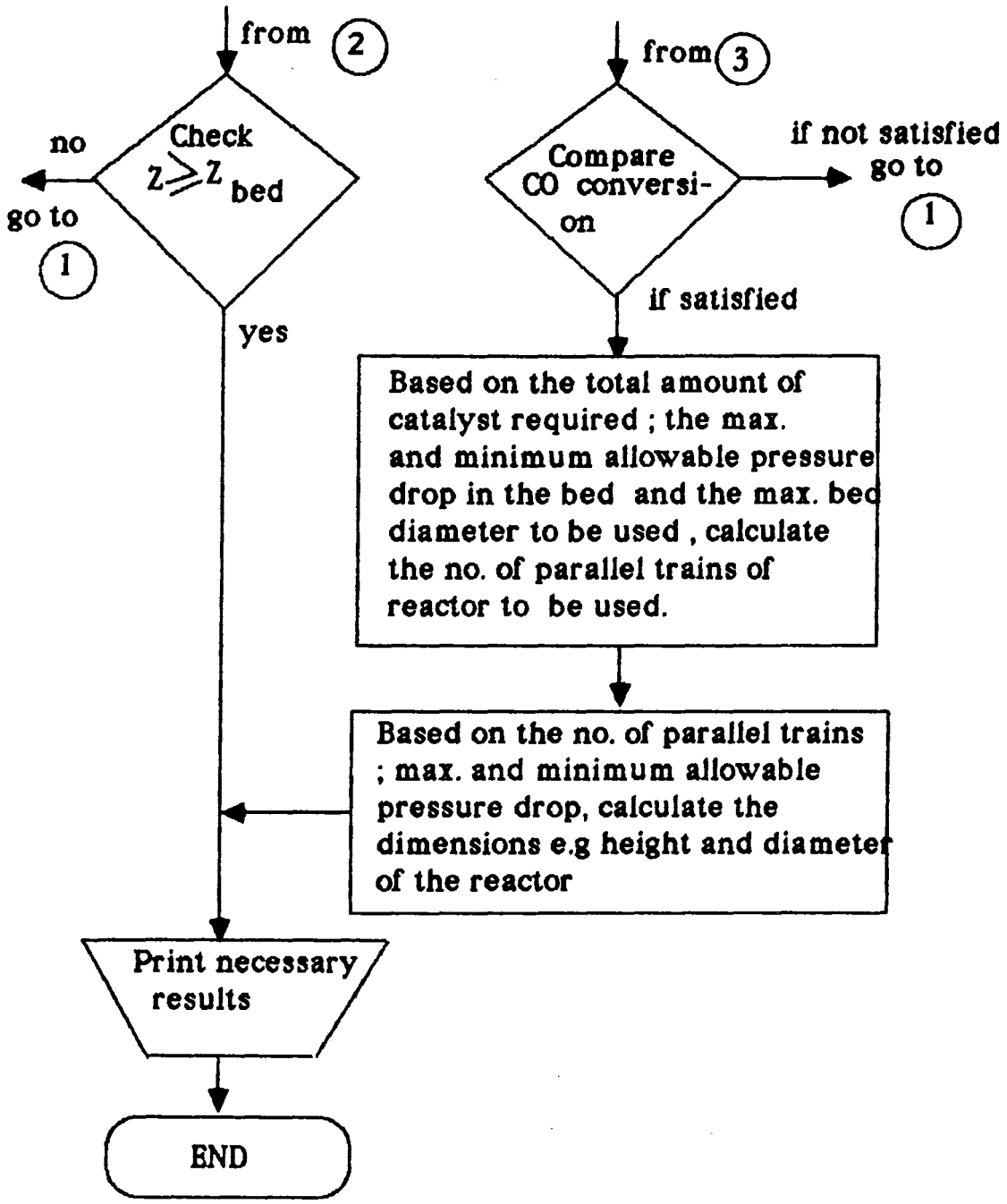

Fig. 4 Flow diagram of the shift reactor process module

5.0 RESULTS AND DISCUSSIONS

The model was used to design a high temperature shift reactor to shift purified gas from Lurgi gasifiers to produce enough synthesis gas for the production of 1200 tonne of methanol per day. (operating conditions are given in table 4.)

Assumptions in the design:

A new bed with interstage cooling is used if the experimental equilibrium constant (calculated from instantaneous mole fraction of the components) becomes equal to or greater than 1/10th of the theoretical equilibrium constant or if the bed temperature becomes equal to or greater than the maximum allowable temperature (727 K).

Typical composition profiles are shown in fig. 5

Table 4. Operating condition for the high temperature shift reactors

Gas feed rate	-----	3.0 kmol s^{-1}
Pressure	-----	2400 kPa

Gas composition (mole fraction, dry basis)

	inlet	Product gas after removal of necessary amount of CO_2 and H_2O
CO ---	0.21	0.1377
CO_2 ---	0.27	0.0736
H_2 ---	0.40	0.6463
CH_4 ---	0.10	0.1295
H_2S ---	0.01	0.0000
N_2 ---	0.01	0.0129

Feed gas was passed through a Rectisol unit to remove all H_2S and the necessary amount of CO_2 before introducing to the shift reactor.

The model was also used to simulate an existing shift reactor (operating conditions are shown in table 5. (Singh and Saraf, 1977). Comparative results with temperature profile are shown in table 5 and fig.6.

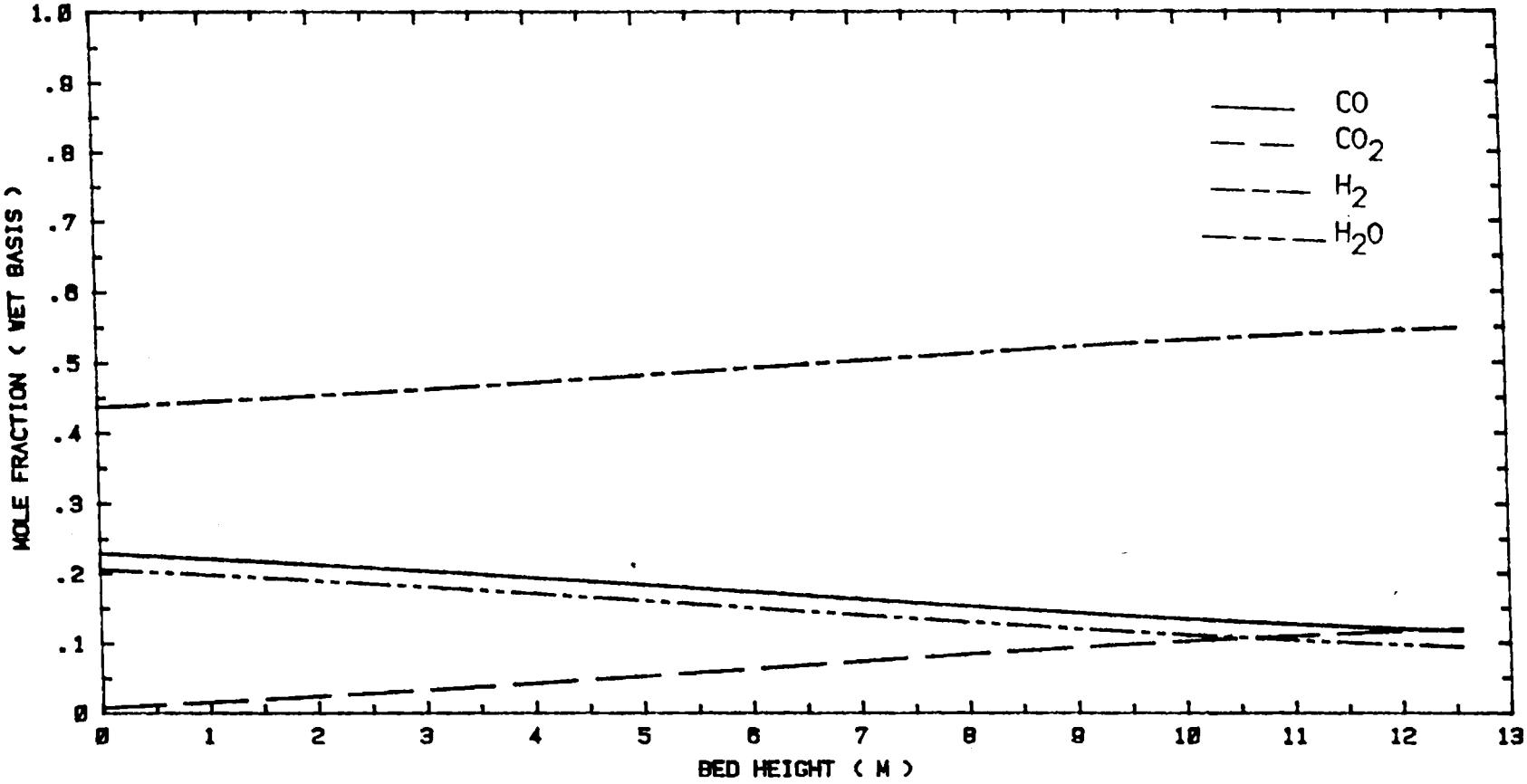

Fig .5 Composition profiles in a shift reactor. Operating conditions in table 4., along with Steam/CO ratio = 0.9 (mole $mole^{-1}$); mole fraction of CO_2 in the feed (dry basis) = 0.01; feed gas inlet temperature = 540 K.

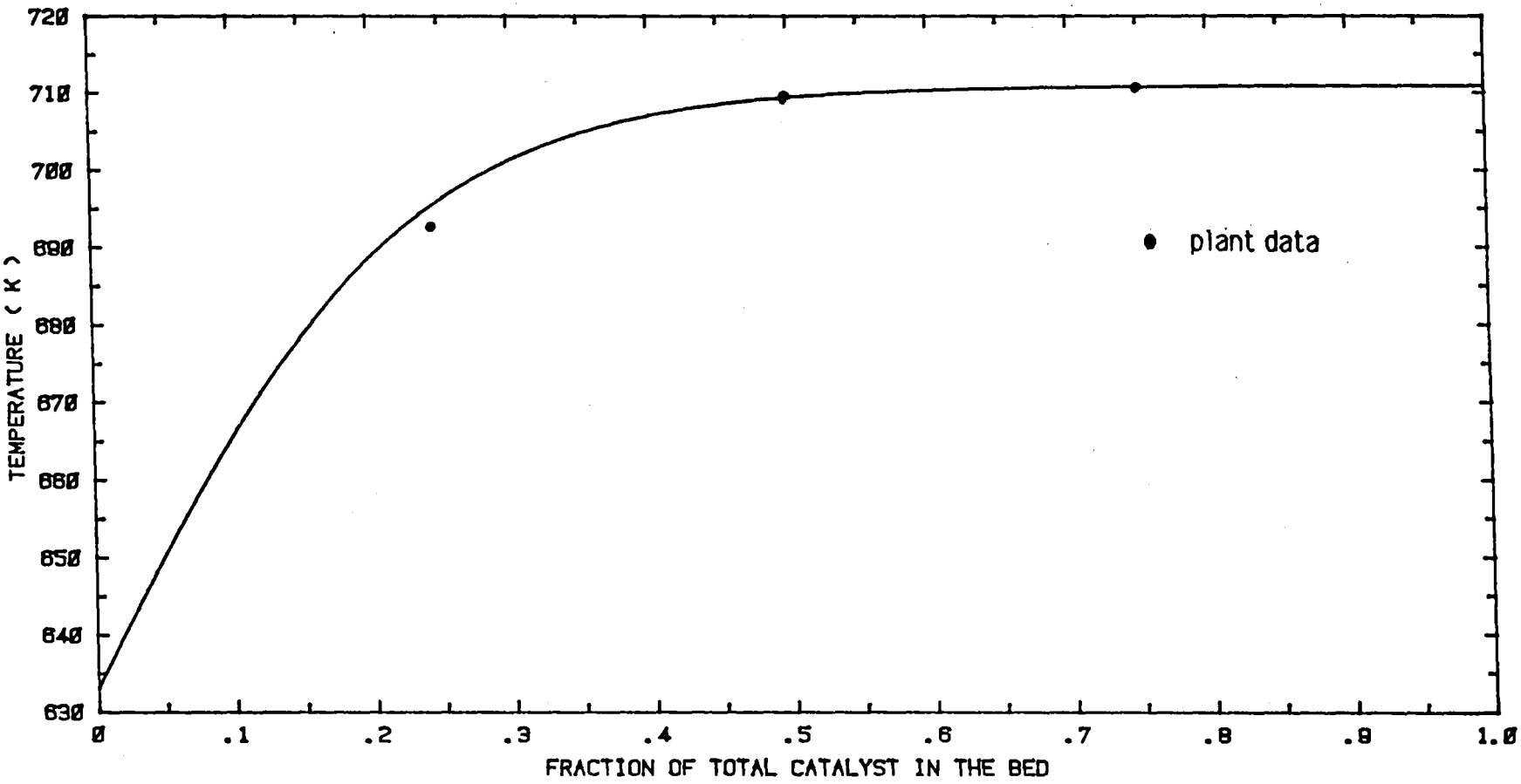

Fig. 6 Comparison of reactor tempearure profile to some plant data. Operating conditions in table 5.

Table 5. Comparison of experimental and calculated results

Give data:	Dry feed rate	---	1.0611 kmol s^{-1}	
	Inlet steam/gas ratio	--	0.693	
	Pressure	---	2280	kPa
	H_2S	---	0.5	ppm
	Age of catalyst	---	115	days
	Volume of catalyst	---	58.2	m^3

Composition of gas (mole percent, dry basis)

	inlet	outlet		
		this model	Singh & Saraf	plant data
CO	15.10	2.81	2.79	3.2
CO_2	11.41	20.86	20.80	20.50
H_2	51.83	56.97	56.73	56.70
CH_4	0.34	0.30	0.33	0.35
N_2	21.32	19.04	19.35	19.35
Temp. K	633.0	710.8	708.5	705.0

5.1 Effects Of Steam/CO Ratio On Shift Reactor Performance.

It is clear from the equilibrium constant expression (2), the rate expressions (table 3.), and the fig.2 that higher Steam/CO ratio favors the shift reaction.

Fig. 7 and 8 show the effects of Steam/CO ratio on temperature profiles and the catalyst requirement for the required CO conversion. It is evident from these figures that :

___ Temperature gradient in the bed increases with the increase in Steam/CO ratio because of higher reaction rates and consequently lower bed height.

___ Exit temperature decreases with the increase in Steam/CO ratio because of higher heat capasity of the gaseous stream.

___ Catalyst requirement decreases with the increase in Steam/CO ratio because of higher reaction rates and favourable equilibrium condition. This decrease in catalyst requirement is quite sharp in the range of Steam/CO ratio 0.6 to 1.5; beyond 1.5 the effects of Steam/CO ratio becomes insignificant.

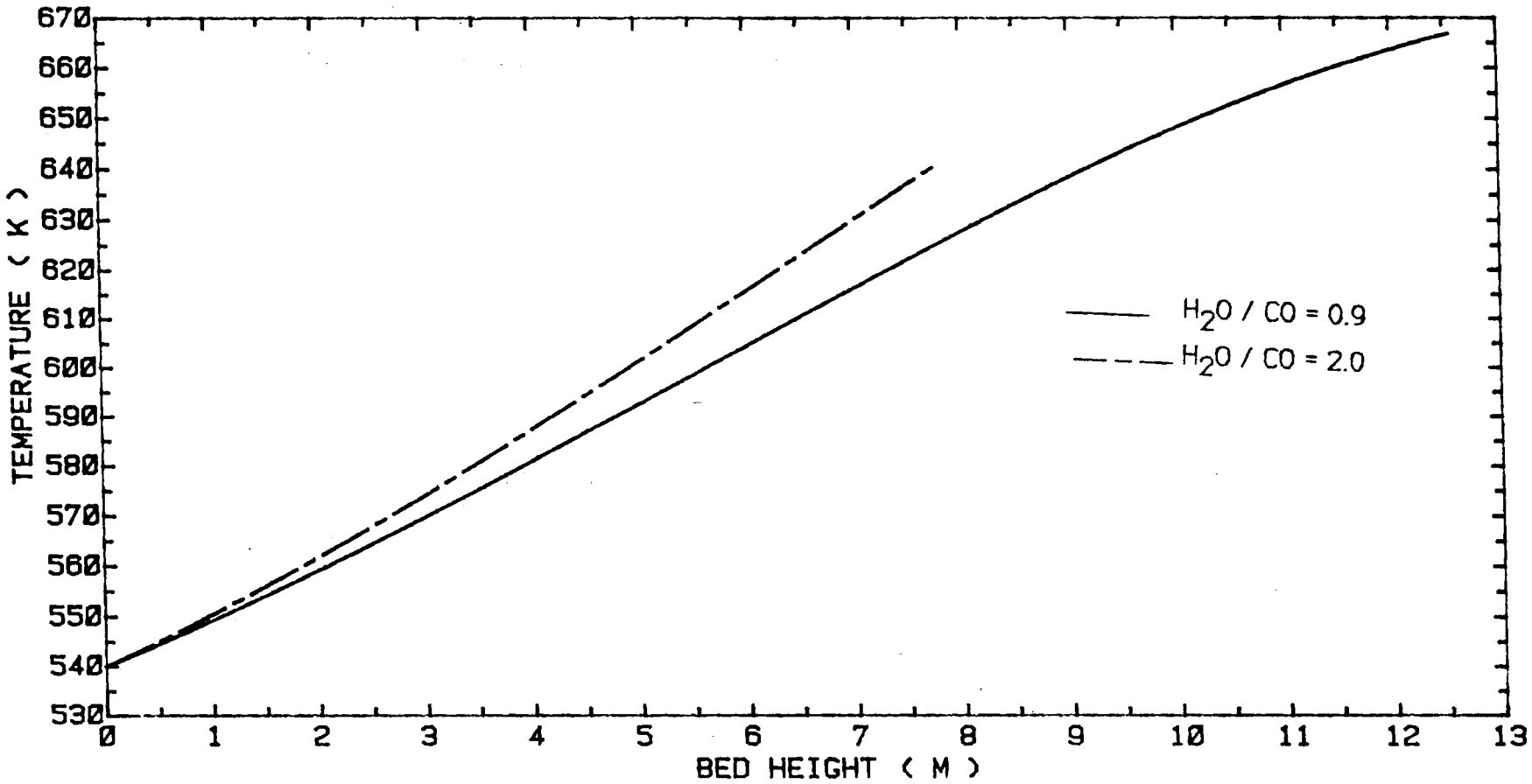

Fig. 7 Effects of Steam/CO ratio(mole $mole^{-1}$) on temperature profiles for the same conditions as fig. 5.

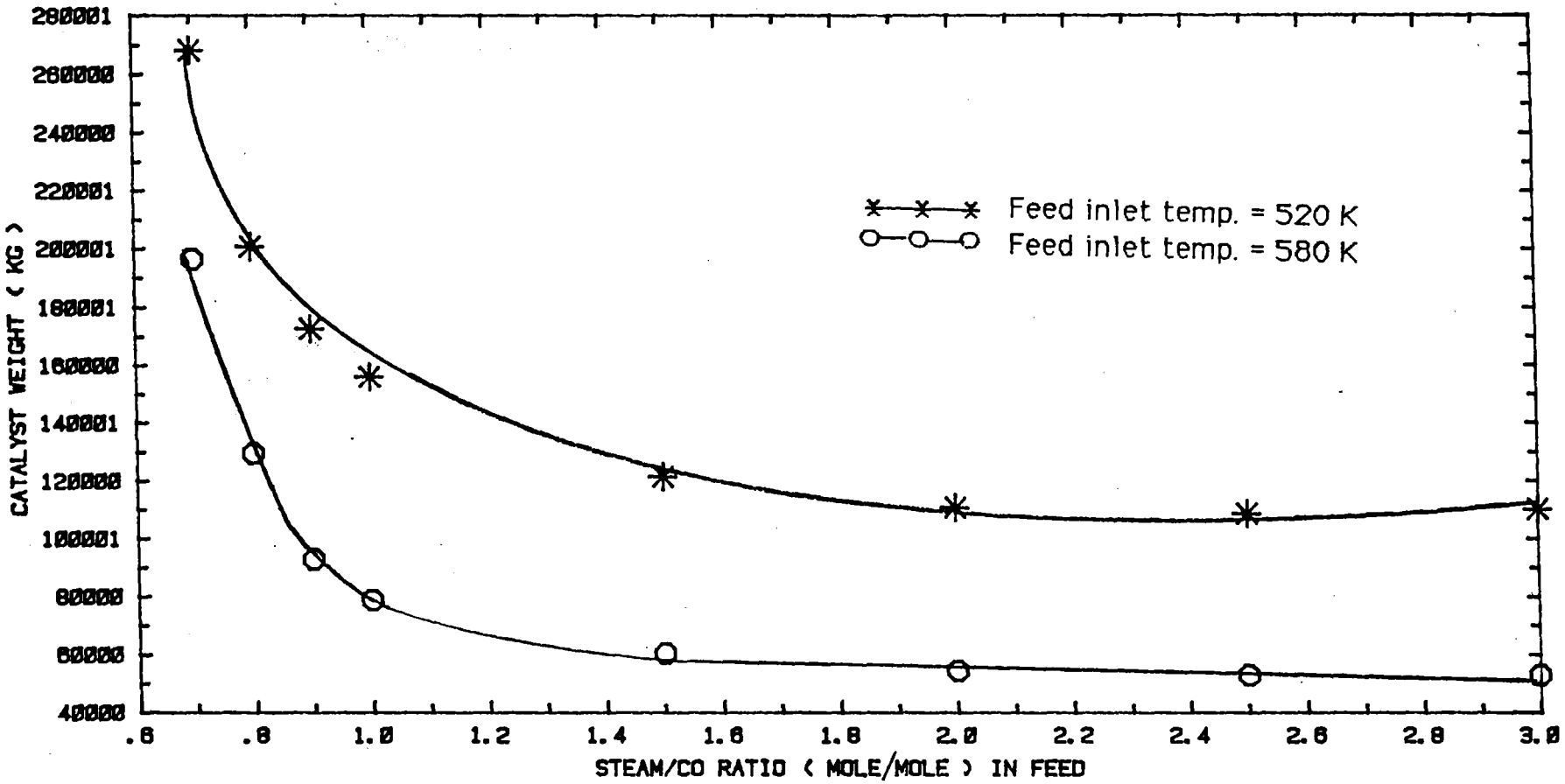

Fig. 8 Effects of Steam/CO ratio(mole $mole^{-1}$) on catalyst requirement for the same conditions as fig. 5.

5.2 Effects Of Feed Gas Inlet Temperature

Lower operating temperature favors the equilibrium but slows down the rate of shift reaction. So one has to be careful in selecting the feed gas inlet temperature.

Fig. 9 and 10 show the effects of feed gas inlet temperature on temperature profiles and the catalyst requirement for the required CO conversion. It is obvious from these figures that :

___ Temperature gradient and the exit bed temperature increase with the increase in feed gas inlet temperaure.

___ 600 K is nearly the maximum feed gas inlet temperature that can be used to achieve the required CO conversion in a single adiabatic bed.

___ Catalyst requirement decreases with the increase in feed gas inlet temperature because of higher reaction rates, but beyond 600 K feed gas inlet temperature, catalyst requirement becomes almost constant.

5.3 Effects Of CO_2 Level In The Feed

Lower CO_2 level in the feed favours the equilibrium and the rate of shift reaction. Fig.11 and 12 show the effects of CO_2 concentration level on temperature profiles and on the catalyst requirement for the required CO conversion. It is obvious from these figures that :

___ Temperature gradient in the bed and the exit bed temperature increase with the decrease in CO_2 concentration level because of higher reaction rates and as well as low heat capasity of the gaseous mixture.

___ Catalyst requirement decreases with the decrease in CO_2 concentration level. This decrease is insignificant below 0.01 CO_2 mole fraction (dry basis).

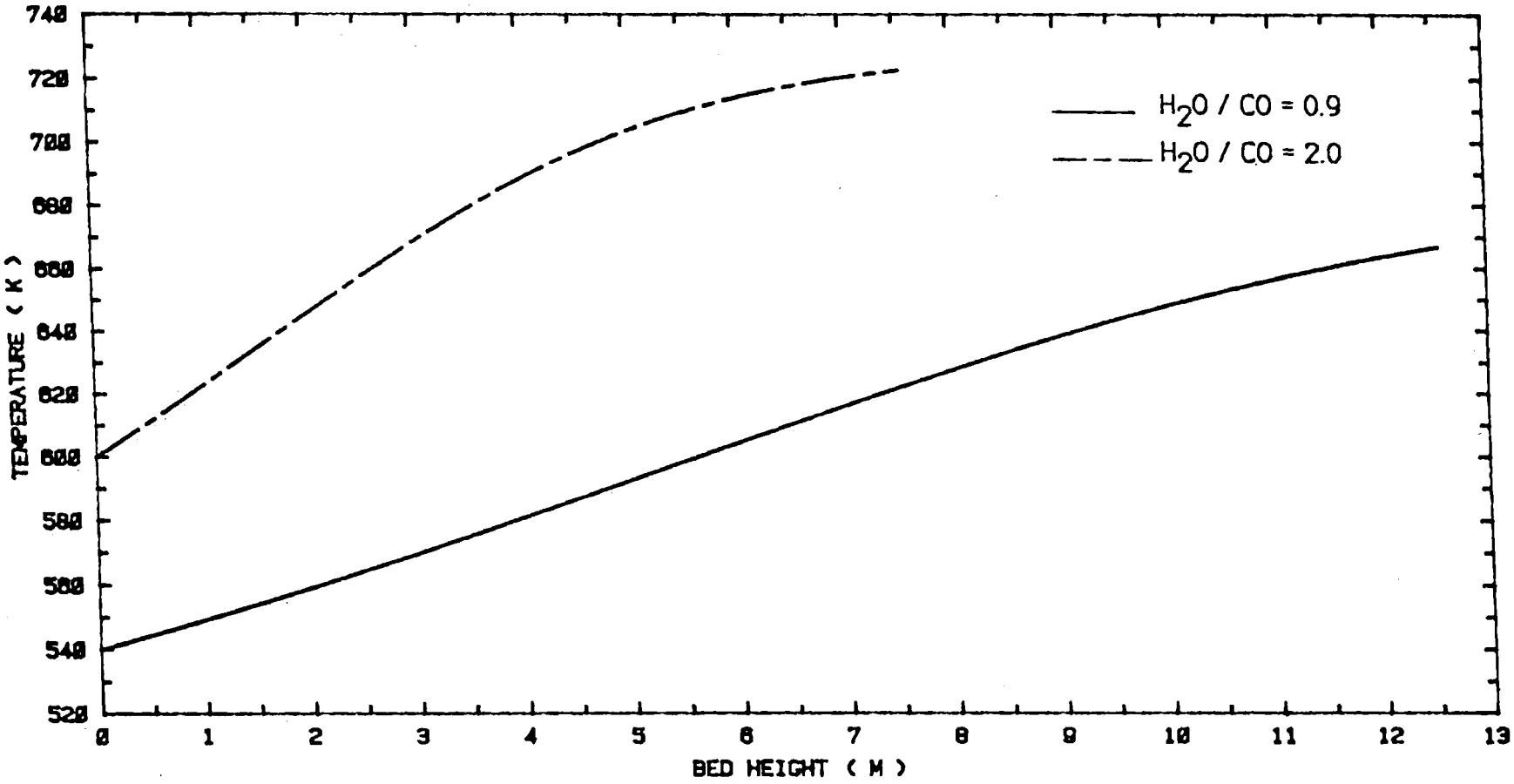

Fig. 9 Effects of feed inlet temperature on temperature profiles for the same conditions as fig. 5.

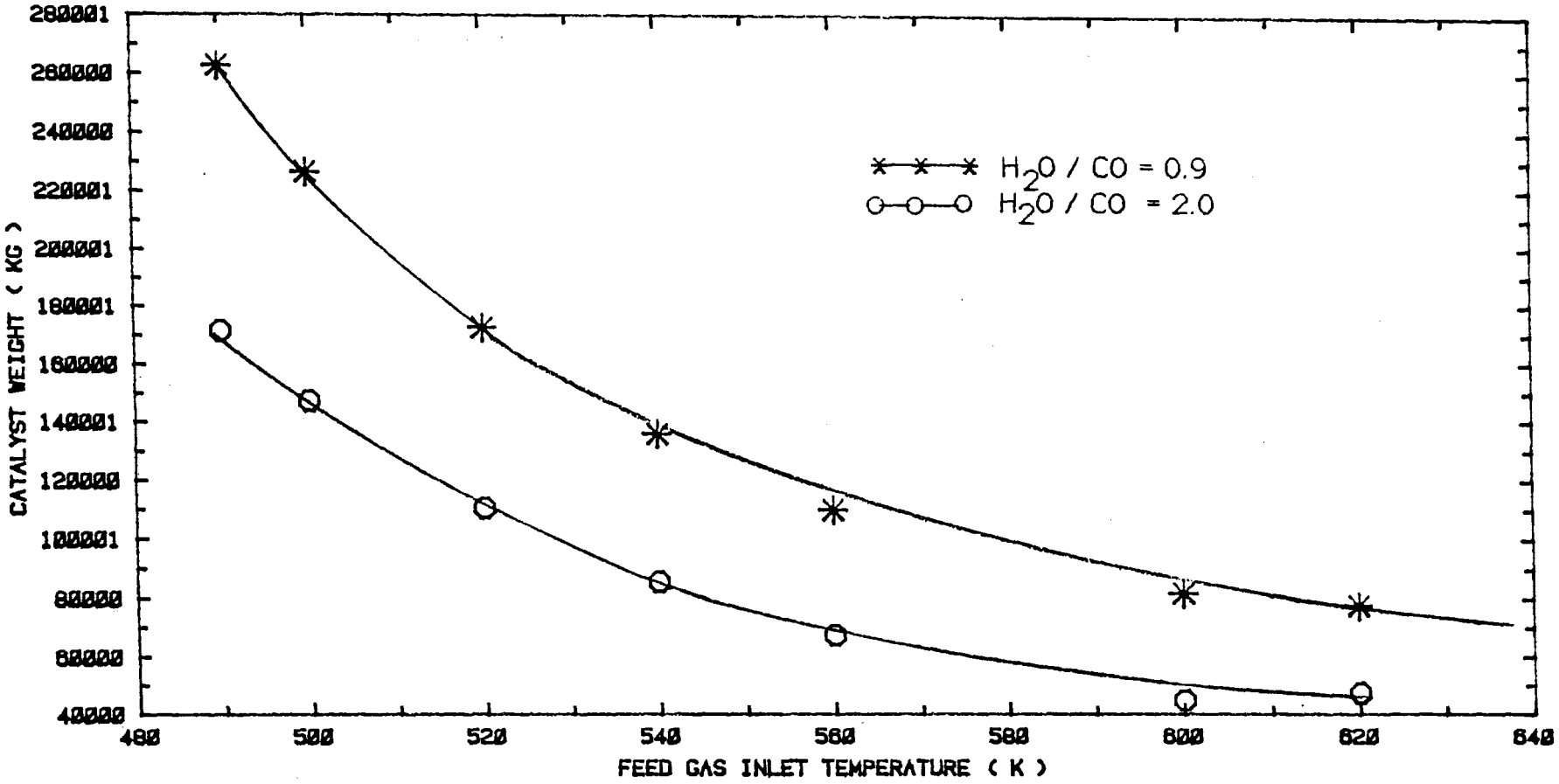

Fig. 10 Effects of feed gas inlet temperature on catalyst requirement for the same conditions as fig. 5.

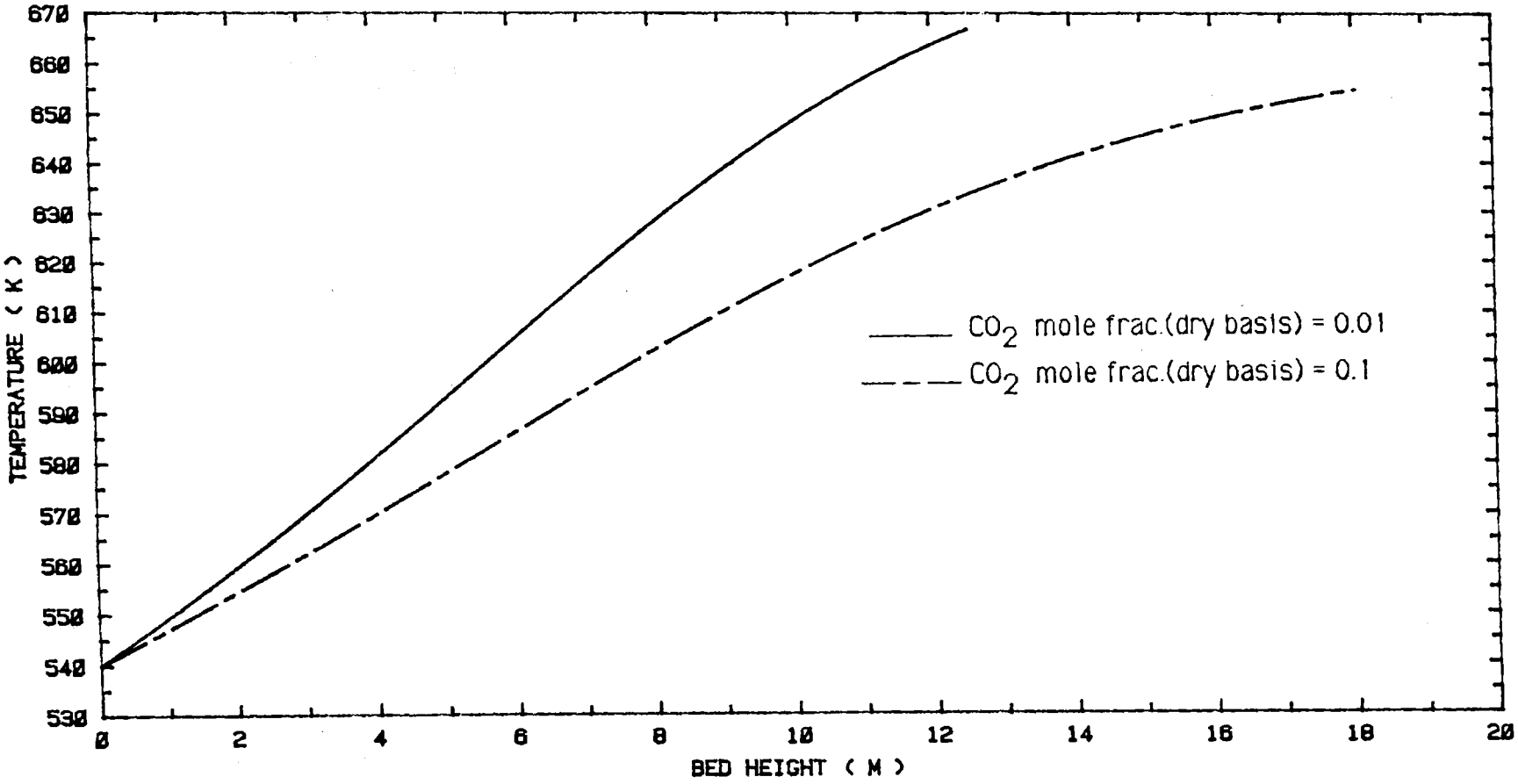

Fig. 11 Effects of CO_2 concentration level in the feed (dry basis) on temperature profiles for the same conditions as fig. 5.

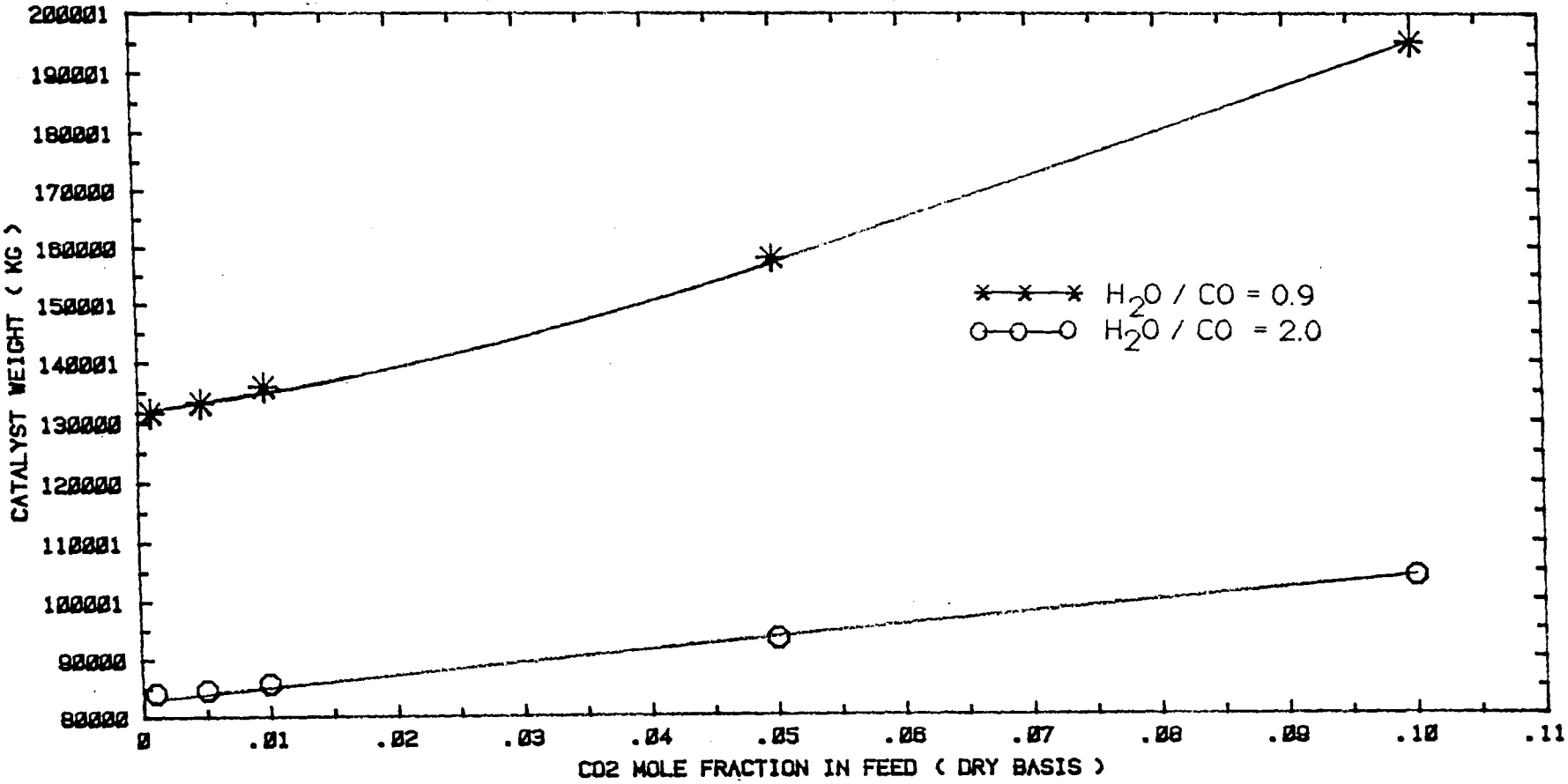

Fig. 12 Effects of CO_2 concentration level in the feed (dry basis) on catalyst requirement for the same conditions as fig. 5.

6.0 CONCLUSIONS AND SUGGESTIONS

Higher Steam/CO ratio (not above 1.5), higher feed gas inlet temperature (not above 600 K) and lower CO_2 concentration level (not below 0.01) are significantly beneficial for the shift reaction in term of catalyst requirement to meet a certain CO conversion. If the Steam/CO ratio is below 0.8 ,or the feed gas inlet tempearture is above 600 K, or the CO_2 mole fraction (dry basis) in the feed is above 0.10, then multibed adiabatic reactors with interstage cooling may be needed to meet the required exit gas composition (H_2/ (CO + CO_2)= 3.05; CO/CO_2=1.87, after necessary removal of CO_2). It is not possble to find the optimum operating conditions without taking into account the cost of all the relevent items. Detail of such an optimization study is given in the optimization chapter V.

Limitations and Suggestions

Gas from Lurgi gasifiers contain sulphur compounds at a level which is much higher than the maximum allowable sulphur compounds for present day shift catalysts. So the raw gas is to be purified by a Rectisol unit before passing through the shift reactor. This process greatly increases the operating cost of the shift reactor system because :

____ All the unconverted steam in the raw gas is lost, which could otherwise be used as process steam in the shift reactor.

____ Large amount of process steam is to be added in the shift reactor.

These disadvantages could be overcome by using sulphur resistant shift catalysts, therby bypassing the Rectisol unit before the raw gas is passed through the shift reactor. No data are available for shift catalyst operating at higher pressure comparable to that of either methanol synthesis or SNG synthesis (70 to 100 bar). More work needs to be carried out to get rate expression data for shift catalysts operating in the high pressure range.

7.0 NOMENCLATURE.

A,E = Arrhenius parameters in the rate constant

A_{gf} = catalyst age factor

A_x = cross sectional area of the shift reactor m^2

B = Steam/CO (mole $mole^{-1}$) ratio in the feed

C_p = average specific heat of the gaseous mixture, $kJ\ kmol^{-1}\ K^{-1}$

C_{pi} = specific heat of component i, $kJ\ kmol^{-1}\ K^{-1}$

ΔH = heat of reaction, kJ $(kmol\ CO\ conversion)^{-1}$
(o refers to standard conditions, 1 atm, 298 K)

ΔZ = differential reactor length, m

dV = differential reactor volume, m^3

Δ_{CO} = total change in number of moles of CO in the reactor

ΔF_{CO} = change in number of moles of CO in reactor volume, ΔV

F_i = molal flux of component i, $kmol\ m^{-2}\ s^{-1}$
(i = 1 for CO; i=2 for CO_2; i=3 for H_2;
i=4 for CH_4; 1=5 for O_2; i=6 for H_2O;
i=7 for C_2H_6; i=8 for H_2S; i=9 for N_2;
i=10 for CH_3OH)
(o refers to inlet conditions)

K = shift reaction equilibrium constant

K_a = Apparent rate constant of the catalyst, hr^{-1}

K_v = fugasity correction term

k = shift reaction rate constant

P = pressure, kPa

P_i = partial pressure of component i, kPa
(* refers to equilibrium values)

P_f = pressure factor for catalyst activity

$-r_{CO}$ = rate of shift reaction, $kmol\ m^{-3}\ s^{-1}$

R = gas constant, 8.314 $kJ\ kmol^{-1}\ K^{-1}$

R' = gas constant, 1.987 $kcal\ kmol^{-1}\ K^{-1}$

R'' = gas constant, 82.05 cm^3 atm $gm\text{-}mole^{-1}\ K^{-1}$

R_a = reduction temperature factor for the catalyst

S_f = sulphur factor for the catalyst

Z = instantaneous bed height, m

Greek letters:

η = catalyst effectiveness factor

ρ_c = bulk density of the catalyst, kg m^{-3}

τ = catalyst age, days

8.0 REFERENCES

Bohlbro, H, "An investigation of the kinetics of the conversion of carbon monoxide with water vapour," Gjelrup, Copenhagen, (1966).

Bird, R. B, W. E. Stewart and E. N. Lightfoot, "Transport phenomena," John Wiley & sons, N.Y., (1960).

Carnahan, B., H. A. Luther and J. O. Wilkes, "Applied Numerical Methods," John Wiley & sons , N.Y., (1969).

Duffuor, K and G. Stewart, "Mathematical model of the shift reactor in an Ammonia plant," Summer computer simulation conference, Toronto, Ontario, Canada, July 16-19, (1979).

Girdler catalysts technical data, Chemetron chemicals, Louisville, Kentucky, (1965).

Levespiel, O, " Chemical reaction engineering", 2nd edition, chap. 8, Wiley Interscience edn., (1972).

Moe, J. M, "Design of water-gas shift reactors," Chemical Engg. Progress, vol. 58, no. 2, pp 33- , (1962).

Podolski, W. F and Y. G. Kim, "Modeling the water gas shift reaction," Ind. Eng. & chem. proc. des. & dev. vol. 13, no. 4, pp 415-, (1974).

Rase, H. F, "Chemical reactor design for process plants," vol.II, John Wiley & sons, N.Y., (1977).

Singh, C. P. P and D. N. Saraf, "Simulation of High temperature shift reactors," Ind. Eng. Chem. proc. des. & dev., vol. 16, no. 3, pp 313-, (1977).

Singh, C. P. P and D. N. Saraf, "Simulation of Low temperature shift reactors," Ind. Eng. Chem. proc. des. & dev., vol. 19, no. 3, pp 393-, (1980).

Temkin, M. I., "The kinetics of some industrial heterogenous catalytic reactions," Advances in catalysis, Vol. 28, pp 263-267, Academic press, (1979).

Ting, A. P, and S. W. Wan, "Sizing CO shift converters," Chemical Engg., May 19, pp 185-, (1969).

Wen, C. Y and H. N. Kim, "Optimization of fixed bed water-gas shift converter for production of pipeline gas," preprints of papers, Amer. chem. Soc., Div. of Fuel Chemistry, vol. 14, no. 3, pp 57-86, (1970).

Wilson, M. W. and K. D. Plants, "Shift conversion of synthesis gas containing sulphur, Dust and carbon dioxide," Ind. Eng. & Chem. proc. des. dev., vol. 7, no. 4, pp 526- , (1968).

9.0 APPENDICES

Appendix II-A :

Calculation of the fraction of synthesis gas to be shifted:

The fraction of raw gas to be shifted to meet a certain specified requirement can be calculated from thermodynamic principles and a material balance. One such analysis of a shift reactor system used for methanol synthesis is shown below:

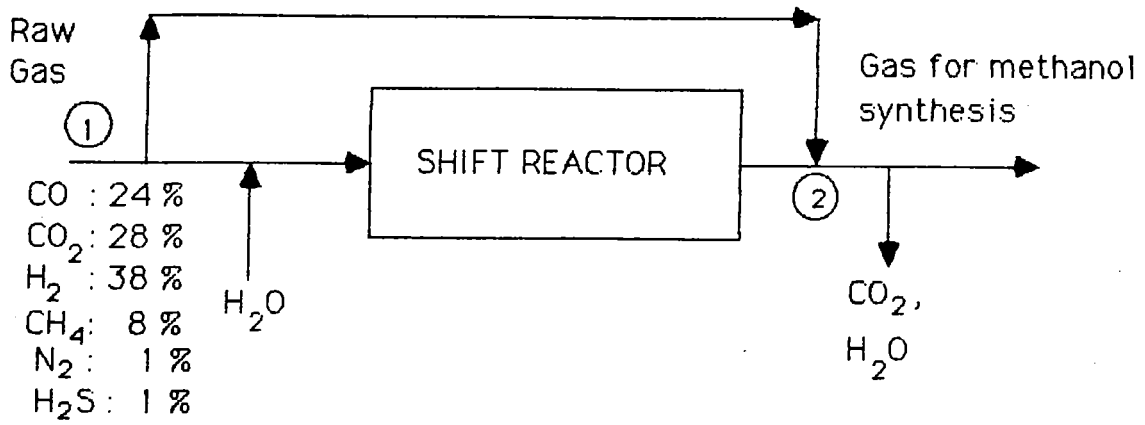

Fig. 13 Block diagram of a shift reactor

Basis : 100 kmol of Dry feed gas

Calculation of composition of gases after the shift reactor (after mixing both shifted and unshifted gases and removal of necessary CO_2) to meet the requirements:

$$CO/CO_2 = 1.87 \text{ and } H_2/ (CO + CO_2) = 3.05$$

Let X kmole of CO to be shifted and Y kmole of CO_2 is to be removed from the gas after the shift reactor. Then

$$\frac{CO}{CO_2} = \frac{24 - X}{28 + X - Y} = 1.87$$

or $28.36 + 2.87X - 1.87Y = 0.0$ _____ (7)

$$\text{and} \quad \frac{H_2}{CO + CO_2} = \frac{38 + X}{52 - Y} = 3.05$$

or $X + 3.05Y - 120.6 = 0.0$ _____ (8)

Solving (7) and (8) one can get X = 13.1 and Y = 35.3

Thus the composition of the gas before CO_2 removal, to be maintained after mixing shifted and unshifted gas:

	kmoles	Mole percent (dry basis)
CO	10.9	9.64
CO_2	41.1	36.34
H_2	51.1	45.19
CH_4	8.0	7.07
N_2	1.0	0.88
H_2S	1.0	0.88

Calculation of the maximum CO conversion possible in one shift reactor:

Maximum operating temperature of the reactor = 727 K (30 K less than the allowable maximum temperature of high temperature shift catalysts).

K (at 727 K) = 7.15

Let, n moles of CO can be converted;

Steam/CO ratio = 5:1

So after shift moles of the components:

	kmoles
CO	24 - n
CO_2	28 + n
H_2	38 + n
CH_4	8
H_2O	120 - n
H_2S	1
N_2	1

From equilibrium contant expression (2)

$$7.15 = \frac{(28 + n)(38 + n)}{(24 - n)(120 - n)}$$

or $n^2 - 178.15n + 3175.28 = 0$ _____(9)

One can get n = 20.1 or 158.06; the second value

is absurd, so n = 20.1 kmols.

Composition after the maximum CO conversion: (dry basis)

	mole %
CO :	3.25
CO_2 :	40.05
H_2 :	48.39
CH_4 :	6.65
H_2S :	0.83
N_2 :	0.83

Calculation of the fraction of synthesis gas to be shifted

Let R_1 fraction of the synthesis gas is to be shifted,

Making a CO balance at point (2) of fig. 13

$$\frac{(100R_1 + 20.1R_1)0.0325 + (1 - R_1)24}{(\ 100 + 20.1R_1\ )} = 0.0964 \quad (10)$$

solving equation (12) $R_1 = 0.65$ is obtained.
So 65% of the raw gas is to be shifted.

Calculation of reactor exit temperature.

Total feed to the reactor = 65 kmols
Feed temperature = 630 K
Maximum allowable temperaure = 727 K
So average temperature = 679 K

Based on feed compositions and the equilibrium conversion possible the following exit gas composition can be obtained:

	Feed (kmols)	Exit gas (kmols)
CO	15.6	2.54
CO_2	18.2	31.76
H_2	24.7	37.76
CH_4	5.2	5.2
N_2	0.65	0.65
H_2S	0.65	0.65
H_2O	78.0	64.95

Heat capasity of the exit gas = $AF_{i,avr}\ C_{pi,avr}$
$= 5487.67\ kJ\ K^{-1}$

Heat of reaction $= 38827\ kJ\ (kmol\ CO\ conversion)^{-1}$

So rise in temperature per kmol of CO converted =
$= 38827/5487.67 = 7.075\ K$

Total rise in temperature in the bed $= 7.075\ (\ 15.6 - 2.54\ )$
$= 92.44\ K$

So the outlet temperature of the adiabatic reactor =
$= 630 + 92.44 = 722.44\ K < 727\ K$

Thus the single adiabatic reactor can meet the required CO conversion without violating the maximum allowable temperature.

CHAPTER III

PROCESS MODULE FOR A COPPER OXIDE BASED LOW TEMPERATURE LOW PRESSURE METHANOL SYNTHESIS REACTOR

ABSTRACT

A pseudo-homogeneous steady state one dimensional process module for a copper oxide based low temperature, low pressure methanol synthesis section is developed. This module is based on the detailed kinetics of two reactions, methanol synthesis from carbon monoxide hydrogenation and shift reaction. The methanol reactor considered is a typical ICI multibed axial reactor with a number of lozenge quench gas distributors between consecuitive beds. This module can be used to

(i) analyze and understand the methanol synthesis section at different operating conditions e.g., different $H_2/(CO+CO_2)$, CO/CO_2 ratios, recycle ratios, quench fraction and distributions, feed and, cold gas temperature, feed gas composition etc.

(ii) optimize the synthesis section to find the optimum operating conditions.

After some small modifications it can be used as an useradded subroutine with any steady state simulation package e.g., PROCESS, ASPEN, etc. This has recently been done with PROCESS in the Department of Chemical and Process engineering, University of Canterbury, New zealand (Gupta, 1985)

Module results compared well to some actual operatiing plant data.

TABLE OF CONTENTS

Page

(i) ABSTRACT .....

1.0 INTRODUCTION III-1

1.1 Different LP - Processes III-2

1.2 Different industrial reactors III-6

1.3 Existing models of methanol reactors III-9

2.0 THERMODYNAMICS III-11

2.1 The effects of temperature, pressure, and inlet gas temperature upon the equilibrium methanol content in the effluent III-14

2.2 The effects of CO_2 concentration on methanol synthesis III-15

3.0 KINETICS AND RATE EXPRESSIONS FOR METHANOL SYNTHESIS III-17

4.0 CATALYSIS III-23

5.0 MODEL DEVELOPMENT III-25

5.1 Model equations and method of solution III-25

5.2 Algorithm for simulation of a 4 - bed quench cooling methanol reactor III-27

6.0 RESULTS AND DISCUSSIONS III-30

6.1 The effects of different variables on reactor performance III-33

7.0 CONCLUSIONS AND SUGGESTIONS III-38

8.0 NOMENCLATURE III-42

9.0 REFERENCES III-44

1.0 INTRODUCTION

Methanol is one of the most important petrochemicals. Prior to the 1920's it was mainly obtained from distillation of wood. Some is still derived from this source, but the amount is now negligible compared with methanol made synthetically from hydrogen and carbon oxides. In the U.S.A alone more than 4 million tonne of methanol is produced annually (Chem. and eng. news, Jan 31, 1977, p-11). Single train plant with capacity of 2000 tonne/day is common today. Formaldehyde production is currently the largest consumer of methanol. Other important uses of methanol are as a methylating agent and as a solvent. Methanol can be used as a fuel, either directly or in association with other liquid fuels e.g., gasoline; so one of its large scale future uses may therefore be as an energy carrier and as an alternative to natural gas and petroleum. It has often been termed as "The transport fuel of the future".

In 1923, BASF was successful in producing methanol on a commercial scale by hydrogenating CO over certain mixed catalysts containing ZnO and Cr_2O_3 at high pressure (30000 kPa) and high temperature. From that time until the mid 1960's methanol synthesis was performed at high pressures typically 30000-37500 kPa and at temperatures of 600-650 K over $ZnO-Cr_2O_3$ catalysts. In 1967 ICI introduced their low pressure methanol synthesis process using a copper based catalyst ($CuO/ZnO/Cr_2O_3$) operating at pressure 5066 to 8100 kPa and temperature 500 to 550 K. After a few years Lurgi also introduced their low pressure methanol technology based on copper containing catalysts at pressure 4135 to 4652 kPa and at temperature 473 to 573 K.

Due to subtantial savings in both operating and capital costs of low pressure processes over high pressure processes, all new methanol plants built since 1970 have used low pressure methanol synthesis technology (Bolton and Hanson, 1969; Rogerson, 1973).

The following discussion is based on low pressure processes.

1.1 Different LP-processes

1. ICI LP process:

This process was introduced by Imperial chemical industries in 1967. A simplified flow diagram of this process is shown in fig.1 (Smith et al. , 1984).

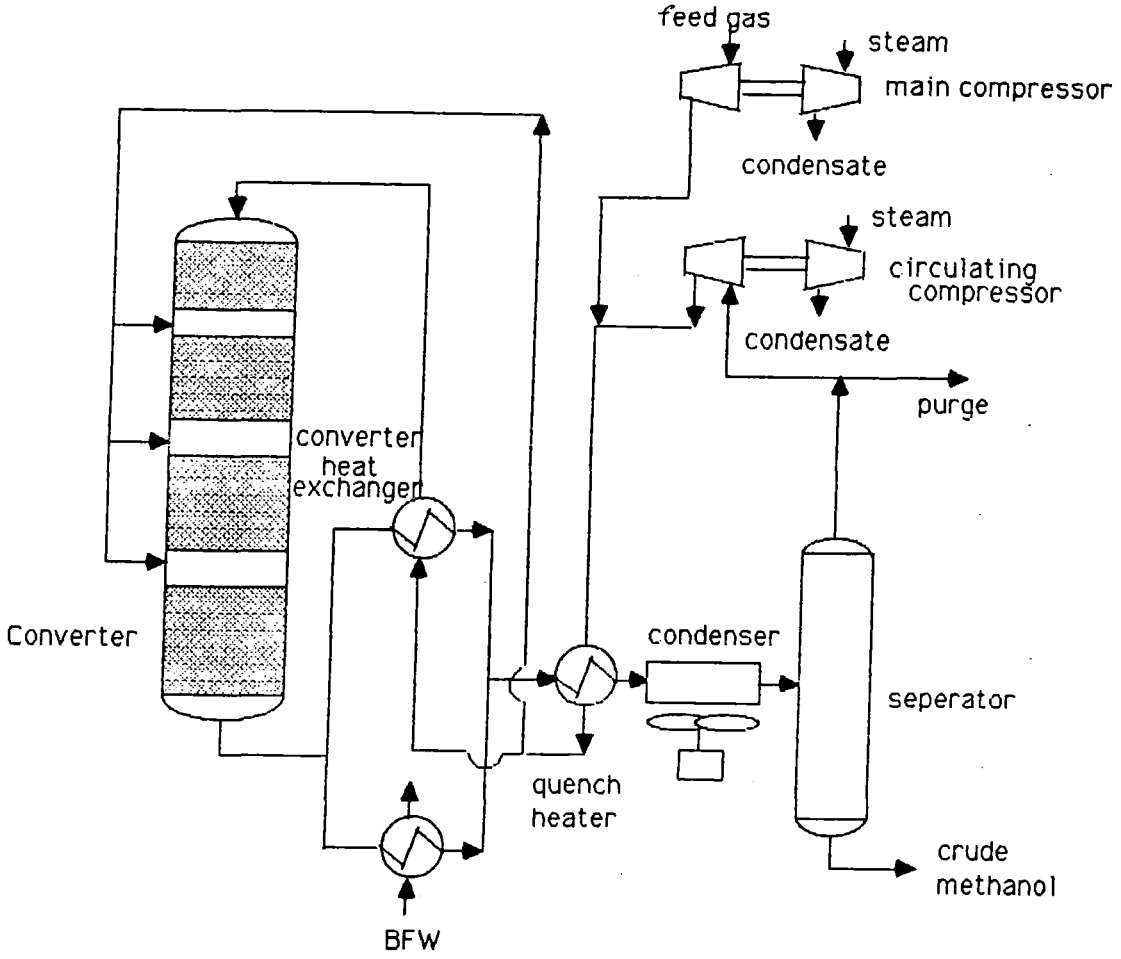

Fig. 1 ICI Low Pressure Methanol Process

2.Lurgi LP process:

A simplified flow diagram of this process is shown in fig.2 (Hiller and Marchner, 1970).

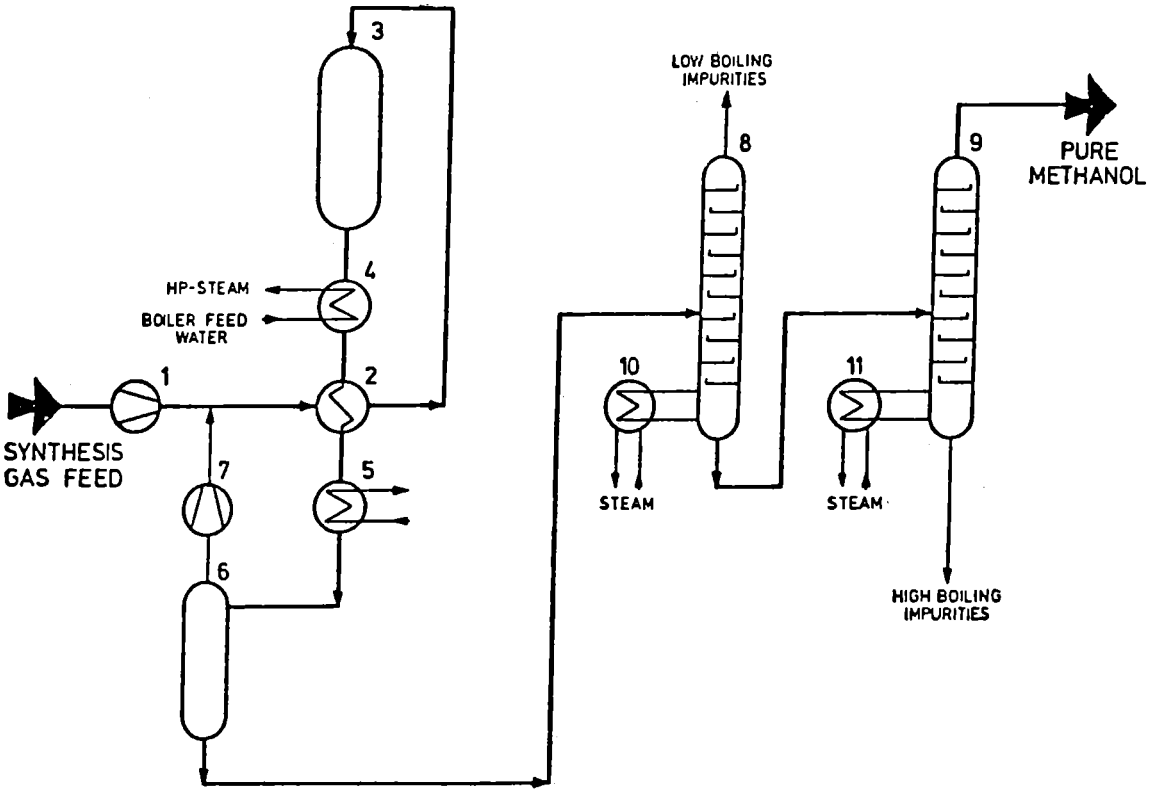

Fig. 2 Lurgi Low pressure methanol synthesis process.

Main features of these two processes are given in table 1.

Table 1. Main features of ICI and Lurgi LP processes.

	ICI	Lurgi
(i) Catalyst:	Initially $CuO/ZnO/Cr_2O_3$ (Davies and Snowdon, 1967) At present Alumina replaces Chromic oxide (Casey and Chapman, 1974)	Copper based catalyst
(ii)Temp:	500-540 K	473-573 K
(iii)Pressure:	5000-10000 kPa	4000-5000 kPa
(iv) Reactor:	Multibeds single tubular reactor with quench cooling between beds.(shown in fig.3)	Tubular Single bed axial type shell and tube reactor, with catalyst in tube side and boiling water in shell side. (shown in fig. 4)
(v)Single train capasity: (tonne/day)	up to 3000	up to 1250
(vi)Catalyst beds pressure drop: (kPa)	500-600	500-600
(vii)Crude Product specification:	Almost pure methanol and water	Other than water, product contains dimethyl ether, methyl formate, other lowboiling impuriies, higher alcohols.
(viii)Commercial plants:	31 reactors	16 reactors

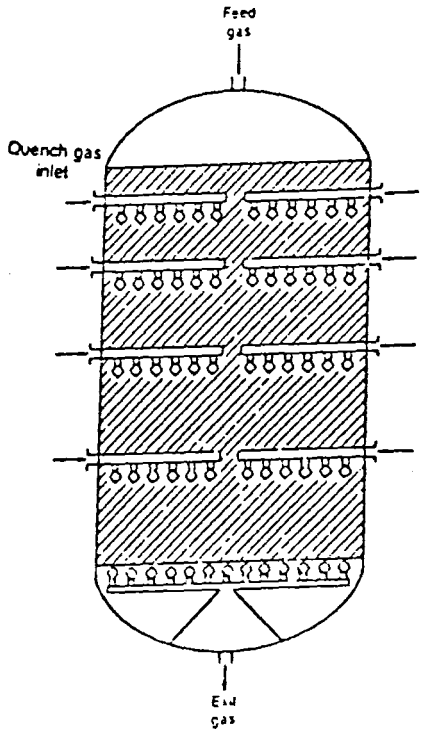

Fig. 3 Quench reactor showing quench gas inlets

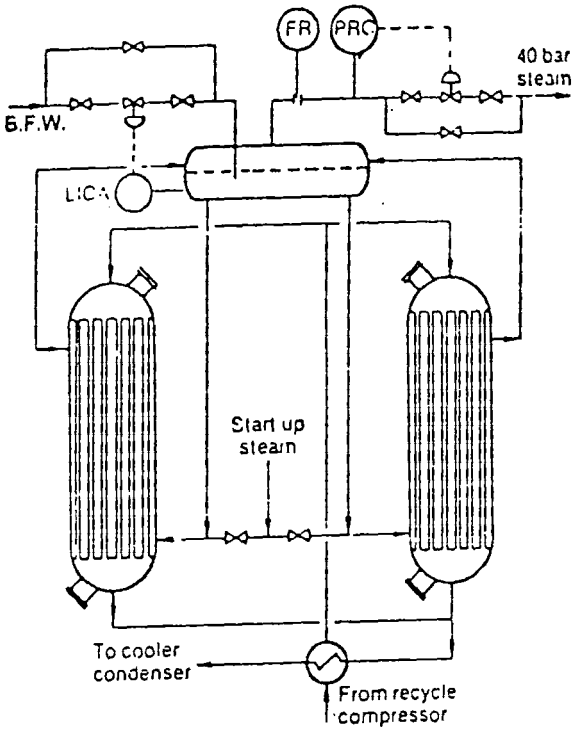

Fig. 4 — Lurgi tubular single bed axial methanol reactor.

1.2 Different Industrial Reactors
(Zardi, 1982;Smith, 1984)

(i) ICI fixed bed quench reactor:

This type of reactor is used in the commercial ICI low pressure process. The Fixed bed quench reactor has the potential for scaling to large capacity, but in order to avoid an excesive pressure drop across the catalyst beds, the reactor height to diameter ratio is not usually greater than 2:1. This requires large diameter high pressure vessels with thick wall for large capacities (more than 3000 tonne/day); this causes difficulties in mechanical design, fabrication and transportation.

(ii) Lurgi tubular single bed axial reactor:

This uses a special patented shell and tube reactor. The major advantage of this reactor is the gentle treatment of the catalyst, which is kept at relatively constant temperature by the high pressure boiling water in the shell side. Reaction heat is transformed into 4000 kPa steam. The main disadvantages are,

1. The length of the reactor tends to be fixed and scale-up to large plant capacities on a single reactor basis is impossible.
2. From a mechanical design standpoint, a fixed tube sheet tubular reactor is a difficult problem. Special tubesheet designs are required and the choice of shell and tube materials is critical to insure that thermal expansion can be accomodated without the need for expansion bellows on the shell side.
3. Special operating procedures and control equipments are needed to ensure that water is always present under pressure in the shell while reaction is taking place in the tubes.

(iii) Fluidized bed reactors:

Essentially an isothermal reaction can be obtained without the complication of a multi tubular type reactor (Lurgi type), through removal of reaction heat by steam generation coils immersed in the fluid bed. Major disadvantages are,

1. Catalyst may be erroded by attrition.
2. For larger capacity, the reactor will be a thick wall vessel and also have the additional complication of a catalyst support grid, feed gas distribution manifolds and catalyst recirculation from cyclone collectors.

(iv) Topsoe radial reactor (shown in fig.5)

Three radial beds in seperate vessels with external heat exchanger between vessels are used in this system. Because of radial movement of gases pressure drop in the catalyst beds is relatively lower than both quench type and multi-tubular type reactors. Maximum capacity can be up to 5000 tonne/day.

5. Ammonia Casale axial-radial low pressure reactor (shown in fig.6)

In this type of reactor, the catalyst is contained in cylindrical annular baskets, which are closed at the bottom and open at the top. The sides of the basket are perforated to allow gas to pass through. In the top of the bed, the gas flow is predominantly axial acting as a seal for the greater part of the bed which is contacted by gas flowing radially (shown in fig. 7). The use of this type of reactor removes the pressure drop limitations as in any axial type reactor and significantly reduces the vessel diameter and wall thickness,thus easing the fabrication and transportation problems.Pressure drop in the beds is also much lower (100-200 kPa). Another important feature of the reactor system is the indirect cooling rather than direct quench mixing; this further simplifies the reactor system by leading to fewer cooling stages. Large column-like, low pressure drop reactors can be designed up to a single train capacity of 5000 tonne/day.

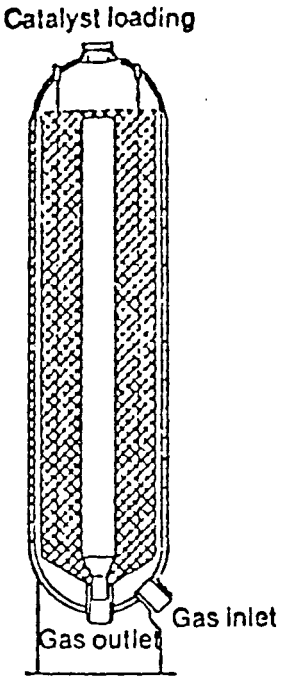

Fig. 5 – Topsoe radial methanol reactor.

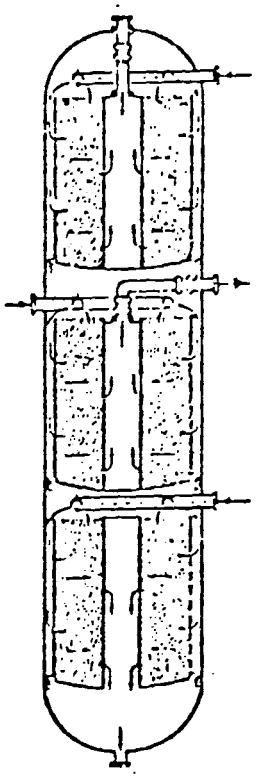

Fig 6 Ammonia Casale axial- radial low pressure methanol reactor.

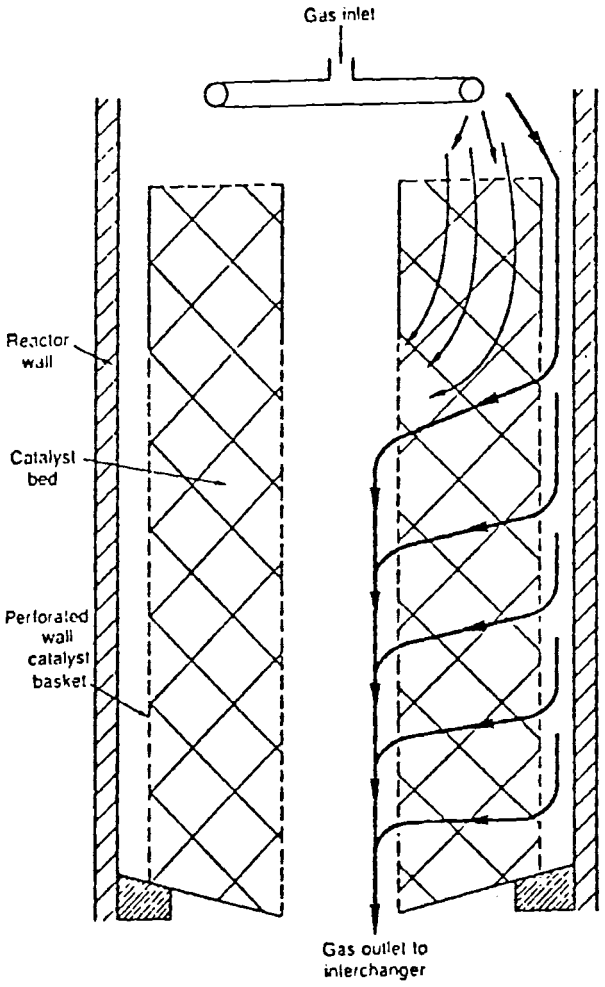

Fig 7 Ammonia Casale mixed flow concept

1.3 Existing Models Of Methanol Reactors

Most of the existing models of methanol synthesis reactors are based on the older high pressure, high temperature technology. There are no details of low pressure models published in the open literature. Some of the earlier and recent models are described briefly.

Bakemeier et al.(1970) developed a comprehensive model of the high pressure methanol synthesis based on BASF invented commercial catalysts (ZnO/Cr_2O_3= 78:22 wt.%). This model takes into account the main methanol synthesis reaction along with three side reactions; shift, methanation and dimethyl ether production.

Shah et al.(1970) formulated a model of a generalized high pressure methanol synthesis reactor consisting of a number of catalyst beds with quench in between beds, with or without heat exchange in the catalyst section based on detail kinetics of reactions involved. This model can be used for computer control and optimization of a high or medium pressure based methanol plant.

Cappelli et al. (1972) developed a mathematical model of Fauser Montecatini high pressure methanol reactors based on ZnO/Cr_2O_3(75.3:11.6 wt.%) catalysts to prepare a computer simulation programme for checking the operation of the industrial plants.

Stephens(1975) described briefly a steady state as well as a dynamic model of the ICI LP-process based on kinetics of methanol synthesis reaction from CO and reverse shift reaction. These models were used to optimize the methanol converter and to calculate its stability margins for trouble free operations.

Ballman and Gaddy(1977) developed a steady state process module of a medium pressure (20 mPa) methanol synthesis system to optimize the plant by linking it with a flow sheet simulation package (PACER).

Knudsen et al. (1982) described briefly mathematical models of ICI methanol synthesis reactor of different complexities considering mainly the methanol synthesis reaction from CO and the reverse shift reaction. These models were used to simulate ARCO chemical company's new 2000 tonne/day methanol plant linking with a flowsheet simulation package (ASPEN).

2.0 THERMODYNAMICS

(Strelzoff,1970; Natta,1955; Klier,1982; Denny and Whan,1978; Stiles,1977)

Carbon monoxide and hydrogen may react to give several end products. A thermodynamic approach to the equilibria related to all the possible reactions is quite useful in order to understand the reasons why the synthesis of methanol requires the use of a highly selective catalyst, specific temperature and pressure ranges. The following reactions for the synthesis of methanol from carbon oxides are of interest.

$$CO + 2H_2 \rightleftarrows CH_3OH \qquad \Delta H^0 = -90642 \text{ j mol}^{-1} \quad \ldots\ldots (1)$$

$$CO_2 + 3H_2 \rightleftarrows CH_3OH + H_2O \qquad \Delta H^0 = -53664 \text{ j mol}^{-1} \quad \ldots\ldots (2)$$

The reaction (2) may be considered as a composite equilibrium, whose individual reactions are conversion of CO_2 into CO by reverse of shift reaction,

$$CO + H_2O \rightleftarrows CO_2 + H_2 \qquad \Delta H^0 = -41162 \text{ j mol}^{-1} \quad \ldots\ldots (3)$$

and the synthesis of methanol from carbon monoxide through reaction (1) Carbon oxides and hydrogen can react in many other ways:

$$CO + 3H_2 \rightleftarrows CH_4 + H_2O \quad \ldots\ldots (4)$$

$$2CO + 2H_2 \rightleftarrows CO_2 + CH_4 \quad \ldots\ldots (5)$$

$$nCO + (2n+1)H_2 \rightleftarrows C_nH_{2n+2} + nH_2O \quad \ldots\ldots (6)$$

$$2CO \rightleftarrows CO_2 + C(\text{solid}) \quad \ldots\ldots (7)$$

If the above reactions occur then the following secondary reactions may also proceed:

$$2CH_3OH \rightleftarrows CH_3OCH_3 + H_2O \quad \ldots\ldots (8)$$

$$CH_3OH + nCO + 2nH_2 \rightleftarrows C_nH_{2n+1}CH_2OH + nH_2O \quad \ldots\ldots (9)$$

$$CH_3OH + nCO + 2(n-1)H_2 \rightleftarrows C_nH_{2n+1}COOH + (n-1)H_2O \quad \ldots (10)$$

Except for reactions (1), (2) and (3), all other reactions are undesirable in the case of methanol synthesis. By using a selective catalyst and by choosing a set of appropriate operating conditions, the formation of methanol can be made

predominant.

Dependence of the standard free energy of formation on temperature for the synthesis of some typical products from hydrogenation of carbon monoxide with water as byproduct is shown in fig.8.

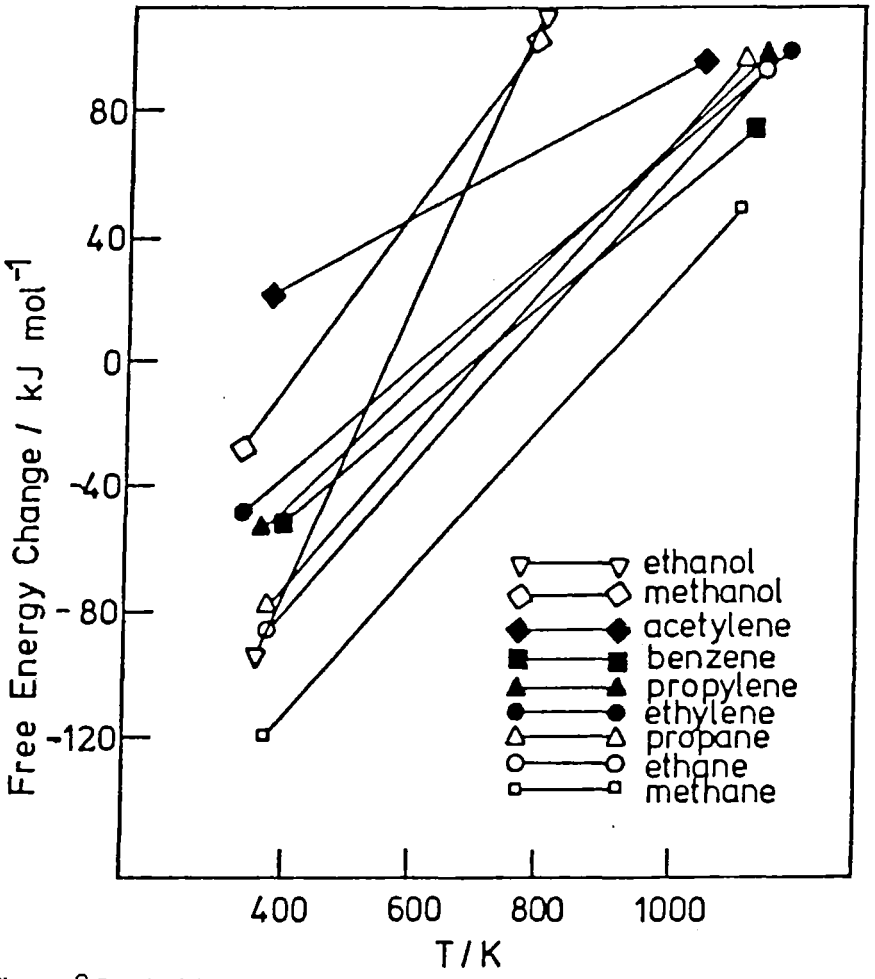

Figure . 8 *Standard free energies of formation for synthesis of hydrocarbons and alcohols from carbon monoxide and hydrogen with water as byproduct* (Denny and Whan, 1979)

It is evident that in the hierarchy of products obtainable from carbon oxides hydrogenation, methane is thermodynamically the most favored; longer chain hydrocarbons are next, followed by higher molecular weight alcohols and methanol is thermodynamically one of the least stable products. Although ΔF^{o} of reaction (1) at standard operating conditions is positive, synthesis of methanol is made possible by the use of high pressure, since this reaction is associated with a

considerable volume contraction. The equilibrium constant of reaction (1) is written as

$$K_f = \frac{f_{CH_3OH}}{f_{CO} \times f_{H_2}^2} \qquad \ldots\ldots\ldots\ldots\ldots\ldots (11)$$

K_f, a function of absolute temperature is independent of pressure, and can be calculated from the heat of reaction and entropy change using the following equations,

$$K_f = \exp^{-\Delta F^0/RT} \qquad \ldots\ldots\ldots\ldots\ldots\ldots (12)$$

$$\Delta F^0 = \Delta H^0 - T\Delta S^0 \qquad \ldots\ldots\ldots\ldots\ldots\ldots (13)$$

Generally K_f is reported in terms of K_p^0 based on the partial pressure of the reactants and products at a total pressure of 1 atm. ($K_f = K_p^0$). The equilibrium expression can be converted to a suitable form by using a formula proposed by Lewis and Randal through the use of the fugacity coefficient .

$$\gamma = \frac{\phi}{P} = \frac{f}{P} \qquad \ldots\ldots\ldots\ldots\ldots\ldots (14)$$

or $f_i = P_i \gamma_i$

So equation (11) becomes,

$$K_f = K_p^0 = \frac{P_{CH_3OH}\, \gamma_{CH_3OH}}{P_{CO}\gamma_{CO}\, (P_{H_2}\gamma_{H_2})^2}$$

$$= \frac{\gamma_{CH_3OH}}{\gamma_{CO}\, \gamma_{H_2}^2} K_\gamma \qquad \ldots\ldots\ldots\ldots (15)$$

$$= K\, K_\gamma$$

or $K = K_p^0 / K_\gamma$

Where K is the equilibrium constant for reaction (1) in terms of partial pressure of the reactants at the operating pressure.

Similarly for the shift reaction it is possible to relate the equilibrium constant,

$$K_f = \frac{P_{CO_2}\, P_{H_2}}{P_{CO}\, P_{H_2O}} \times \frac{\gamma_{CO_2}\, \gamma_{H_2}}{\gamma_{CO}\, \gamma_{H_2O}} = K'\, K_\gamma'$$

$$\text{or } K' = K_p^{o\prime} / K_\gamma' \qquad \text{.....(16)}$$

Klier et al. (1982) gave the values of K_p^o and K_γ for reaction (1), (2) and reverse of reaction (3); these values are compiled in table 2.

Table 2. values of equilibrium constants and K_γ for different reactions.

Reaction	K_p^o	K_γ
(1)	$3.27\times10^{-13}\exp^{11628/T}$	$1 - 1.95\times10^{-4}\ \exp^{1703/T}$
(2)	$3.826\times10^{-11}\exp^{6851/T}$	$\dfrac{1 - 1.95\times10^{-4}\ \exp^{1703/T}}{1 - 4.24\times10^{-4}\ \exp^{1107/T}}$
reverse of (3)	$1.17\times10^{2}\exp^{-4827/T}$	$1 - 4.24\times10^{-4}\ \exp^{1107/T}$

2.1 The Effects Of Temperature, Pressure And Inlet Gas Composition Upon The Equilibrium Methanol Content In The Effluent.

Equation (5), which can be rearranged to

$$Y_{CH_3OH} = \frac{K_p^o\, Y_{CO}\, Y_{H_2}{}^2 P^2}{K_\gamma} \qquad \text{.....(17)}$$

sets the upper limit to the methanol content Y_{CH_3OH} in the effluent from the catalyst bed for a given set of temperature, pressure and inlet conditions.

From Equation (7) the following conclusions can be drawn:

(i) Since K_p^o decreases with temperature increase (table 2) and K_γ increases with temperature increase (table 2), Y_{CH_3OH} decreases with temperature rise.

(ii) Y_{CH_3OH} increases with pressure to the second power.

According to Strelzoff (1970) the highest methanol content at equilibrium is obtained in the effluent from an inlet mixture having a H_2/CO ratio of 2:1 which corresponds to the stoichiometric mixture according to reaction (1).

Natta (1955) concluded that H_2/CO ratio in the synthesis gas should be higher than two because of higher adsorption of CO on the catalyst surface, to obtain a stoichiometric H_2/CO composition in the adsorbed phase.

2.2 The Effects Of CO_2 Concentration On Methanol Synthesis

The synthesis gas prepared from natural gas, naptha or solid fuels contain a considerable amount of CO_2 in addition to CO and H_2. CO_2 is converted to methanol according to either the one step reaction(direct hydrogenation through reaction (2)) or the two step reactions (first coversion of CO_2 to CO by reverse shift reaction and subsequently converted to methanol by reaction (1)). There is considerable debate in the literature regarding this. The two step process is not strictly valid, but it serves the practical purpose of obtaining a close approximation of the real kinetics of the methanol synthesis as carried out in industrial plants. Lender et al. (1973) stated that the temperature profiles calculated from the combination of the reverse shift reaction and methanol synthesis from CO agree well with their experimentally determined temperature profiles in an adiabatic converter. The presence of small quantities of CO_2 in the gas has a favorable effect on the conversion to methanol, when the reaction is performed at high space velocities (Natta, 1955). Small concentrations of CO_2 have a true promotional effect on the methanol synthesis from CO and H_2 over copper based catalysts at low pressure (5000-10000 kPa); rather than its involvement through direct hydrogenation to methanol, that

would be faster than the hydrogenation of CO (Herman et al., 1979; Andrew, 1980; Klier et al., 1982). At high concentrations, CO_2 acts as a retardant of the synthesis (Klier et al., 1982). When synthesis is performed with recycle of reacting gases, it is not convenient to work with gaseous mixtures containing a high percentage of CO_2, because a large amount of CO_2 may be dissolved in the produced methanol during seperation. Klier et al., (1982) carried out an experiment regarding the effects of CO_2 on the synthesis of methanol over CuO-ZnO and observed a maximum synthesis rate at $CO_2/CO/H_2$ = 2/28/70 (molal ratio). At lower concentrations of CO_2 catalyst is deactivated by overreduction and at higher concentrations of CO_2, the synthesis is retarded by a strong adsorption of this gas. Andrew(1980) reported that the rate of methanol synthesis reached a maximum at the CO_2 to CO partial pressure ratio around 0.01 for Cu-ZnO-alumina catalysts and decreased as the CO_2 partial pressure further increased. It was also indicated that the methanol synthesis rate would decline at very small concentrations of CO_2.

Natta (1955) mentioned the following factors responsible for the promotional effect of CO_2:

(i) It causes a decrease in the formation of dimethyl ether.

(ii) It prevents the conversion of CO to CO_2 by shift reaction in the presence of water.

(iii) By allowing the reverse shift reaction (which is endothermic) it helps reduce the temperature rise thereby reduces the risk of the catalyst overheating.

3.0 KINETICS AND RATE EXPRESSIONS FOR METHANOL SYNTHESIS

The kinetics of the methanol synthesis reaction is the most difficult phase for experimentation as well as for discussion. Kinetics are influenced by a variety of factors e.g gas composition, catalyst shape, type, pore chracteristics, age, internal depositions within the catalyst particle, operating temperature and pressure etc. (Stiles, 1977). Because of the above mentioned difficulties and the high pressure involved there have been very few kinetics studies of this industrially important reaction reported in the open literature. Most of the earlier kinetics studies deal with high pressure and high temperature methanol synthesis based on $ZnO\text{-}Cr_2O_3$ catalysts. Natta (1955), Chrednichenko and Tempkin (1957), Uchida and Ogino (1958), Pasquon and Dente (1962), Bakemier et al. (1970), Shah and Stillman (1970), Cappelli et al. (1972) have performed kinetics studies of high pressure methanol synthesis reaction over $ZnO\text{-}Cr_2O_3$ catalysts and propose different rate expressions. These studies will not be discussed here; instead attention will be mainly focused on commercially important Copper based catalysts. Natta (1955) was the first to perform a thorough and systematic study of methanol synthesis reaction with a mixture of CO and H_2 using a copper based catalyst of composition $ZnO:CuO:Cr_2O_3=2:1:1$ (wt. basis) at high temperature range (570-600 K) and at high pressure (30 mPa). The following rate expression was proposed by Natta:

$$r_{CH_3OH} = \frac{\gamma_{CO}P_{CO}\ \gamma_{H_2}{}^2P_{H_2}{}^2 - \dfrac{\gamma_{CH_3OH}\ P_{CH_3OH}}{K}}{\left(A + B\ \gamma_{CO}P_{CO} + C\ \gamma_{H_2}P_{H_2} + D\ \gamma_{CH_3OH}P_{CH_3OH}\right)^3} \quad \ldots\ldots\ldots (18)$$

The four constants A, B, C, D are all positive and are functions of temperature only. Using Natta's graphical representations these constants can be correlated by the following expressions:

$$A = \frac{(44.7302-0.0846T)}{(1.0-1.18278\times10^{-3}\ T)}$$

$$B = \frac{(5.4245-9.1618\times10^{-3}\ T)}{(1.0-1.6723\times10^{-3}\ T)}$$

$$C = \frac{(0.1502-3.7484\times10^{-4}\ T)}{(1.0-1.889\times10^{-3}\ T)}$$

$$D = \frac{(5.2498-0.0115\ T)}{(1.0-1.8287\times10^{-3}\ T)}$$

Schermuly and Luft(1977) reported a preliminary investigation of the low pressure methanol synthesis in a driving jet reactor. A copper based catalyst of unstated composition was employed. Nine gas mixtures with CO content from 7 to 25 %, CO_2 contents from 1 to 15 % and H_2 between 60 and 70% were tested at temperatures from 225 to 265 deg. C at pressure from 20 to 80 bar. They analyzed their data and obtained a rate expression similar to Natta(1955):

$$r_{CH_3OH} = \frac{\gamma_{CO}P_{CO}\ \gamma_{H_2}{}^2P_{H_2}{}^2 - \dfrac{\gamma_{CH_3OH}\ P_{CH_3OH}}{K}}{\left(A + B\ P_{CO}\gamma_{CO} + C\ P_{H_2}\gamma_{H_2} + D\ P_{CH_3OH}\gamma_{CH_3OH} + E\ P_{CO_2}\gamma_{CO_2}\right)^2} \quad \ldots\ldots\ldots (19)$$

By regression analysis they obtained the values of the constants A, B, C, D and E at different temperatures. These constants were represented in terms of Arrhenius expressions,i.e $K_0\ \exp^{-E_0/RT}$. The values of K_0 and E_0 are given below in table 3.

Table 3. Parameter values of Schermuly and Luft's (1977) rate expression.

	K_0	E_0 (kJ/kmole)
A	6.63×10^{14}	128.3×10^3
B	2.28×10^{-3}	-39.4×10^3
C	2.12×10^{-6}	-65.0×10^3
D	8.14	3.9×10^3
E	2.03×10^{-11}	-116.0×10^3

Wainright (1978) proposed the following rate expression for a Raney copper catalyst at around 70 bar and between 260 and 280 deg. C.

$$r_{CH_3OH} = \frac{f_{CO} f_{H_2}^{\ 2} - f_{CH_3OH} / K}{A + B f_{CO} + C f_{H_2} + D f_{CH_3OH} + E f_{CO_2}} \quad \ldots\ldots (20)$$

The values of the constants are not mentioned in the paper.

Leonov et al. (1973) put forward a kinetic rate equation for the low pressure copper-zinc oxide-alumina catalyst for temperatures between 220 and 260 deg C. The rate equation was

$$r_{CH_3OH} = k \left(\frac{P_{CO}^{\ 0.5} P_{H_2}}{P_{CH_3OH}^{\ 0.66}} - \frac{P_{CH_3OH}^{\ 0.34}}{P_{CO}^{\ 0.5} P_{H_2} K} \right) \quad \ldots\ldots\ldots (21)$$

Where k is the rate constant for the forward reaction.

A rate expression that does contain an empirical CO_2-dependent term for the Cu-ZnO-Alumina catalysts has been proposed by Andrew(1980) in the form,

$$r_{CH_3OH} = k\, P_{H_2}^{0.7}\, P_{CO}^{0.2 \text{ to } 0.6} \phi_{CO_2} \qquad \ldots\ldots(22)$$

Where ϕ_{CO_2} is an empirical parameter which varies with CO_2 concentration.

Klier et al.(1982) made a thorough study of the kinetics of low temperature low pressure methanol synthesis over a Cu/ZnO (30/70 atomic ratio) catalyst. They formulated a kinetic model based on their experimental study as well as on the following findings:

(i) The catalyst can exist in a reduced state A_{red} and in an oxidized state A_{ox}. The oxidized state is active and the reduced state is inactive. The proportion of A_{red} and A_{ox} is controlled by the ratio of CO_2 and CO in the synthesis gas.

(ii) Several active centers A_{ox} are involved in each reaction step. These centers may be identified with copper solute species in zinc oxide.

(iii)All three components of the synthesis gas CO, H_2 and CO_2 react in the adsorbed layer. CO_2 competes for active sites with at least one of the reactants CO and H_2. The adsorption strengths are in the order $CO_2 > CO > H_2$.

(iv) The products CH_3OH, H_2O, CH_4 are adsorbed weakly; their effects on these reaction rate are taken into consideration by kinetic terms for the reverse reaction but not for product desorption in the forward reaction. They considered the following three cases in deriving the rate expression.

Case 1. CO, CO_2, H_2 compete for the same active sites of catalyst.

Case 2. CO and H_2 are adsorbed on different sites and CO_2 competes for the hydrogen sites.

Case 3. CO_2 competes for both the CO sites and the H_2 sites.
For case 1. the following rate expression was derived:

$$r_{CH_3OH} = k A_0^3 \frac{K_a^3 (P_{CO_2}/P_{CO})^3}{[\,1 + K_a (P_{CO_2}/P_{CO}\,]^3} \times \frac{K_{CO} K_{H_2}^2 \left(P_{CO} P_{H_2}^2 - P_{CH_3OH}/K\right)}{\left(\,1 + K_{CO} P_{CO} + K_{CO_2} P_{CO_2} + K_{H_2} P_{H_2}\,\right)^3} + k' \left(P_{CO_2} - \frac{P_{CH_3OH} P_{H_2O}}{K,\ P_{H_2}^3}\right) \quad \ldots\ldots(23)$$

Values of all the constants varies depending on pressure, temperature, etc.

Villa et al.(1985) performed a kinetic study of the low pressure methanol reaction over a commercial $Cu/ZnO/Al_2O_3$ ($CuO:ZnO:Al_2O_3:CO_2$ = 54.6 :19.0:9.1:8.9, wt.%) catalyst with temperatures, pressures and gas compositions typical of industrial operations (temp., 388-418 K; pressure, 3000-9500 kPa; gas composition,CO, 8-10%; CO_2, 5-6%;, the balance hydrogen) considering the synthesis of methanol reaction from CO (1) and reverse of shift reaction (3). They fit their data with Langmuir-Hinshelwood-Hougher-Watson model, similar to Natta (1955) and proposed the following rate expression

for reaction (1),

$$r_{CH_3OH} = \frac{f_{CO} f_{H_2}^2 - f_{CH_3OH}/K}{60\left(C_1 + C_2 f_{CO} + C_3 f_{CO_2} + C_4 f_{H_2}\right)^3} \times \quad \ldots\ (24)$$

for reverse shift reaction,

$$r_{CO} = \frac{(f_{CO_2} f_{H_2}^2 - f_{CO} f_{H_2O}/K_r'')}{60\ C_6} \quad \ldots\ (25)$$

where parameters C_1 to C_4 and C_6 are exponential function of temperature and a reference temperature (506 K).

Agny and Takoudis (1985) studied the kinetics of methanol synthesis over a commercial catalyst (C79-2-01 of United catalysts Inc., Kentucky of composition, Cu/Zn/Al=40.6:50.3:9.1 wt%) in a differential reactor at pressures in the range of 300 to 1500 kPa and temperatures between 523 and 563 K and H_2/CO ratio between 2.1 and 2.4. They found the best possible fit to their experimental data from the rate expression,

$$r_{CH_3OH} = k(P_{CO}P_{H_2}^{2} - P_{CH_3OH}/K) (P_{CO}P_{H_2}^{0.5})^{n} \quad \ldots\ldots (26)$$

Where k is the rate constant represented by an Arrhenius type correlation and n is equal to -1.3 ± 0.03

Denny and Whan (1978) tabulated different rate expressions of methanol synthesis reaction from CO hydrogenation over both ZnO,Cr_2O_3 and CuO,ZnO based catalysts.

In this work the rate expression (19) of Schermuly and Luft (1977) is used for reaction (1) and Rase's (1977) rate expression is used for shift reaction along with an activity factor f_{ac}, which takes into account of all uncertainties.

$$-r_{CO} = f_{ac}\ 1.1746\times10^{-5} \times 4.33 \exp^{(12.88 - 1855.56/T)} (Y_1Y_6 - Y_2Y_3/K'')/\rho_c \quad \ldots\ldots (27)$$

f_{ac} equal to 150 gave comparable to plant results.

4.0 CATALYSIS

Natta(1955) summarized the development of methanol synthesis catalysts that took place before 1950, but these were mainly high temperature, high pressure based ZnO/Cr_2O_3 catalysts with little reference to some copper based catalysts operating at similar conditions. Since Natta's work much progress has been made in this field particularly with highly active copper based catalysts. Discussion here will be confined to findings related to the current commercial catalysts, $Cu/ZnO/Cr_2O_3$ and $Cu/ZnO/Al_2O_3$. Kung (1980) pinpointed a number of requirements for an active, stable oxide based methanol synthesis catalyst. Firstly the catalyst must be stable against reduction, since the catalyst is used in a reducing atmosphere. Secondly the catalyst must be able to activate CO without dissociating the molecules and at the same time also able to activate H_2. Finally based on the mechanism that the synthesis reaction proceeds via surface methoxide, an active and selective catalyst must not form a very stable metal methoxide. For the synthesis reaction to occur at a resonable rate at 523 K,the activation energy for the rate limiting step should not be higher than about 60 kJ $mole^{-1}$.

Also for increased productivity the catalyst must possess the following qualities: (stiles, 1977)

(i) resistance to deactivation by sintering.

(ii) resistance to deactivation by common poisons.

(iii) operate efficiently at pressures as low as 5.2 to 6.9 mPa; and as high as 34.5 to 51.0 mPa depending on equipment size and heat exchange.

(iv) tolerate high amounts of CO_2 in the synthesis gas by either effciently converting CO_2 to CO by the reverse shift reaction or directly hydrogenating to methanol.

Klier (1982) tabulated some of the important copper based catalysts. These are presented in tables 5 and 6. Marsden et al. (1980) and Friedrich et al. (1982) demonstrated that novel catalysts of the raney type produced by the caustic

extraction of Al/Cu/Zn alloys show high activity and selectivity for methanol synthesis similar to a commercial copper based catalyst.

TABLE 5
Cu/Zn/Cr Oxide Catalysts Used in the Synthesis of Methanol (Klier, 1982)

Composition[a] (wt. %)	Reactants[b]	Temp. (°C)	Pressure (atm)	Space velocity (hr^{-1})	Yield (kg $liter^{-1}$ hr^{-1})	Company
11:70:19	3	250		4000		Power-Gas Corp.
15:48:37	3	270	145	10,000	1.95[c]	Jap. Gas-Chem. Co.
31:38:5	3	230	50	10,000	0.755	BASF
	4	230	50	10,000	1.275	BASF
33:31:36	3	250	150	10,000	1.1	Academic
	3	300	150	10,000	2.2	Academic
40:10:50	1	260	100	10,000	0.48[c]	T. HFA
40:40:20	2	250	40	6000	0.26	ICI
	2	250	80	10,000	0.77	ICI
60:30:10	1	250	100	9800	2.28	Metall-Gesellschaft

[a] $CuO:ZnO:Cr_2O_3$.
[b] 1, $H_2 + CO + CO_2$; 2, $H_2 + CO + CO_2 + CH_4$; 3, $CO + H_2$; 4, $CO + H_2 + O_2$; N_2 is sometimes used as a diluent.
[c] Kilograms per kilogram per hour.

TABLE 6
Cu/Zn/Al Oxide Catalysts Used in the Synthesis of Methanol (Klier, 1982)

Composition[a] (wt. %)	Reactants[b]	Temp. (°C)	Pressure (atm)	Space velocity (hr^{-1})	Yield (kg $liter^{-1}$ hr^{-1})	Company
12:62:25	2	230	200	10,000	3.290	BASF
	2	230	100	10,000	2.086	BASF
23:46:30	3	240		20,000	2.5	CCI
24:38:38	2	226	50	12,000	0.7	ICI
35:45:20	1	250				Academic
53:27:6	1	250	50			ICI
60:22.8	1	250	50	40,000	0.5	ICI
	2	226	100	9600	0.5	ICI
64:32:4	3	250	50	10,000	0.3	Academic
	3	300	50	10,000	0.9	Academic
66:17:17	1	275	70	200[d]	4.75	DuPont
[c]	1	250	50	10,000		Academic

[a] $CuO:ZnO:Al_2O_3$.
[b] 1, $H_2 + CO + CO_2$; 2, $H_2 + CO + CO_2 + CH_4$; 3, $CO + H_2$; N_2 is sometimes used as a diluent.
[c] SNM-1 catalyst.
[d] Moles per hour.

5.0 MODEL DEVELOPMENT

The mathematical model for the methanol synthesis section was developed assuming:

1. Steady state.
2. No temperature or concentration gradient in the radial direction of the reactor i.e temperature and concentration are uniform at any cross section.
3. No axial diffusion of mass and temperature.
4. Global rate expressions for methanol synthesis and shift reaction were used neglecting heat and mass transfer within the catalyst and also from bulk phase to the catalyst surface.
5. Momentum balance in the reactor was neglected. Pressure drop in each catalyst bed was calculated using average values of inlet and outlet bed conditions.
6. Adiabatic catalyst beds i.e no heat loss from the reactor bed wall.

5.1 Model Equations And Method Of Solution.

The various physical and chemical processes taking place in the reactor can be described mathematically by performing mass balances for CH_3OH and CO_2 and also an overall energy balance over a differential section of catalyst, Δw (Bird et al., 1960), shown in fig. 9.

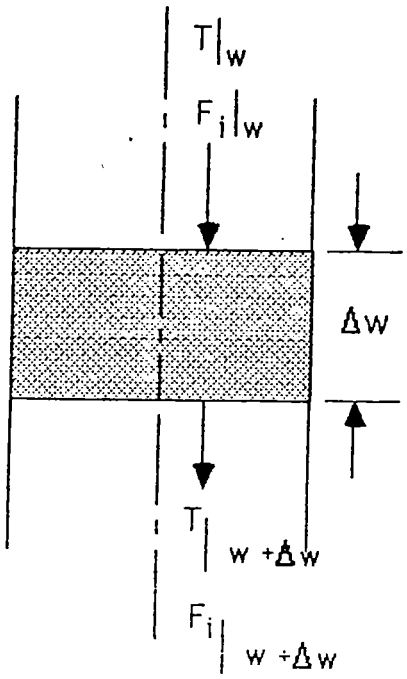

Fig. 9 Schematic diagram of differential catalyst section of weight Δw in the reactor

Mass balances:

1. For CH_3OH

$$\frac{dF_{CH_3OH}}{dw} = r_1 \qquad \text{.....(28)}$$

2. For CO_2

$$\frac{dF_{CO_2}}{dw} = r_2 \qquad \text{.....(29)}$$

Energy balance:

$$\frac{dT}{dw} = \frac{\sum_{j=1}^{m} \Delta H_j \, r_j}{\sum_{i=1}^{n} F_i \, C_{pi}} \qquad \text{.....(30)}$$

These three coupled first order non-linear differential equations were solved simultaneously by a variable step size fourth order Runge-Kutta-Gill method (Carnahan et al., 1969)

with initial conditions:

at w=0 (at top of the bed), $F_i=F_{io}$ and $T=T_o$

The flow of other components were determined from the stoichiometry of the reactions involved for each Δw. At the end of each bed, a fraction of reactant gases (cold shot) was added, then the composition and temperature of the gas mixture were calculated from an overall mass and heat balance in the quenching zone; the above steps were repeated for each subsequent bed.

5.2 Algorithm For Simulation Of A 4-bed Quench Cooling Methanol Reactor

Input data:

1. Composition of the fresh make up feed gas.
2. Initial estimate of recycle compositions, seperator operating pressure and temperature, approx. crude product compositions to determine initial recycle compositions.
3. Methanol production rate and its specifications.
4. Average operating pressure of the reactor.
5. Amount of catalyst used in different beds.
6. Fractions of total feed used in different beds as feed/cold shot.
7. Catalyst properties.
8. Parameters used for Wegstein convergence acclerating technique.
9. Fresh make up feed rate, recycle ratio.

Algorithm:

1. The flow and compositions of reactor total feed were determined from the flow and compositions of fresh feed and recycle.

2. The amount of feed used in the first bed was calculated.

3. For first bed at point w of the bed:

(a) Rates of methanol synthesis and shift reactions were calculated.

(b) Differential equations (28), (29), and (30) were solved by a variable step size fourth order Runge-Kutta-Gill method.

(c) Molal flow rates of other components over Δw, were calculated from reaction stoichiometry.

(d) The above steps are repetaed until the first bed was completed.

4. The quench at the inlet to bed II was added and the composition of the mixed feed was determined and from the heat balance the temperature of the gas mixture at the inlet of bed II aws also determined.

5. Steps 3 and 4 were conitinued through bed II.

6. At the outlet of the last bed the fraction of methanol in the product was calculated and the mole fraction of methanol and water in the recycle were also estimated.

7. The amount of crude methanol to be condensed and its composition were calculated.

8. The amount of recycle and its composition, and the purge rate were calculated.

9. Assumed and calculated recycle compositions were compared and the sum of absolute difference for each component in the recycle was calculated.

10. Convergence criteria were checked.

11. If the convergence criteria were not satisfied, Wegestein acclerating technique was applied to the individual component of recycle and the new recycle composition was calculated and then returned to step 1.

12. When the convergence criteria were satisfied the ratio of the actual amount of product to that to be produced was calculated, then the amount of feed gas, catalyst to be used in different beds and the amount of "cold shot" to be used were adjusted.

6.0 RESULTS AND DISCUSSIONS

The model was used to simulate an operating methanol reactor producing around 1200 tonne methanol/day. Operating data and comparative results are given in tables 7 and 8 and fig.10.

Table 7. Operating plant data.

Make up feed gas rate : 2.06 kmol s^{-1}

Make up gas composition(Mole fraction):

CO	: 0.165
CO_2	: 0.082
H_2	: 0.715
CH_4	: 0.029
H_2O	: 0.001
N_2	: 0.008

Catalyst : ICI 51-Z (a copper oxide/zinc oxide/alumina catalyst)

Age : nearly 8 months

Equivalent particle diameter(cylidrical shape) : 0.006 m

Bed porosity : 0.28

catalyst bulk density : 1200 kg m^{-3}

Catalyst used in different beds(m^3) :

Bed (1)	: 14.7
Bed (2)	: 20.2
Bed (3)	: 27.6
Bed (4)	: 34.6

Reactor: ICI 4- bed quench reactor

Height (tan to tan) : 7.9 m

Inside diameter : 4.575 m

Recycle ratio (recycle/make up feed, mole $mole^{-1}$) : 5.98

Cold shot temperature : 383.5 K

Distribution of feed/cold shot in beds (fraction of total mixed feed, mole basis) :

Bed (1)	: 0.423
Bed (2)	: 0.138
Bed (3)	: 0.203
Bed (4)	: 0.236

Seperator operating peressure : 8200 kPa

Seperator operating temperature : 313.2 K

Table 8. Comparative plant and model and plant results.

Reactor outlet gas compositions:	Plant results	Model results
CO :	0.0103	0.0093
CO_2 :	0.0111	0.0145
H_2 :	0.7397	0.7431
CH_4 :	0.1466	0.1416
H_2O :	0.0131	0.0125
N_2 :	0.0389	0.0387
CH_3OH :	0.0403	0.0403
Pure methanol production in different beds (kg methanol m^{-3}cat. s^{-1}) :		
Bed (1)	0.2194	0.2516
Bed (2)	0.1639	0.1974
Bed (3)	0.1333	0.1532
Bed (4)	0.1611	0.1176
Purge (fraction of make up feed):	0.1896	0.1941
Crude methanol production (kmol s^{-1}):	0.6520	0.6624
Methanol mole fraction in the crude product:	0.7547	0.7511
Pure methanol production (kmol s^{-1}):	0.4921	0.4975

The model was used to design a methanol reactor system to produce roughly 1200 tonne methanol per day by purified synthesis gas obtained from coal gasification. To make the analysis simple the same reactor used for simulation was used, but the required production was obtained by changing process conditions. Operating conditions and results are shown in table 9.

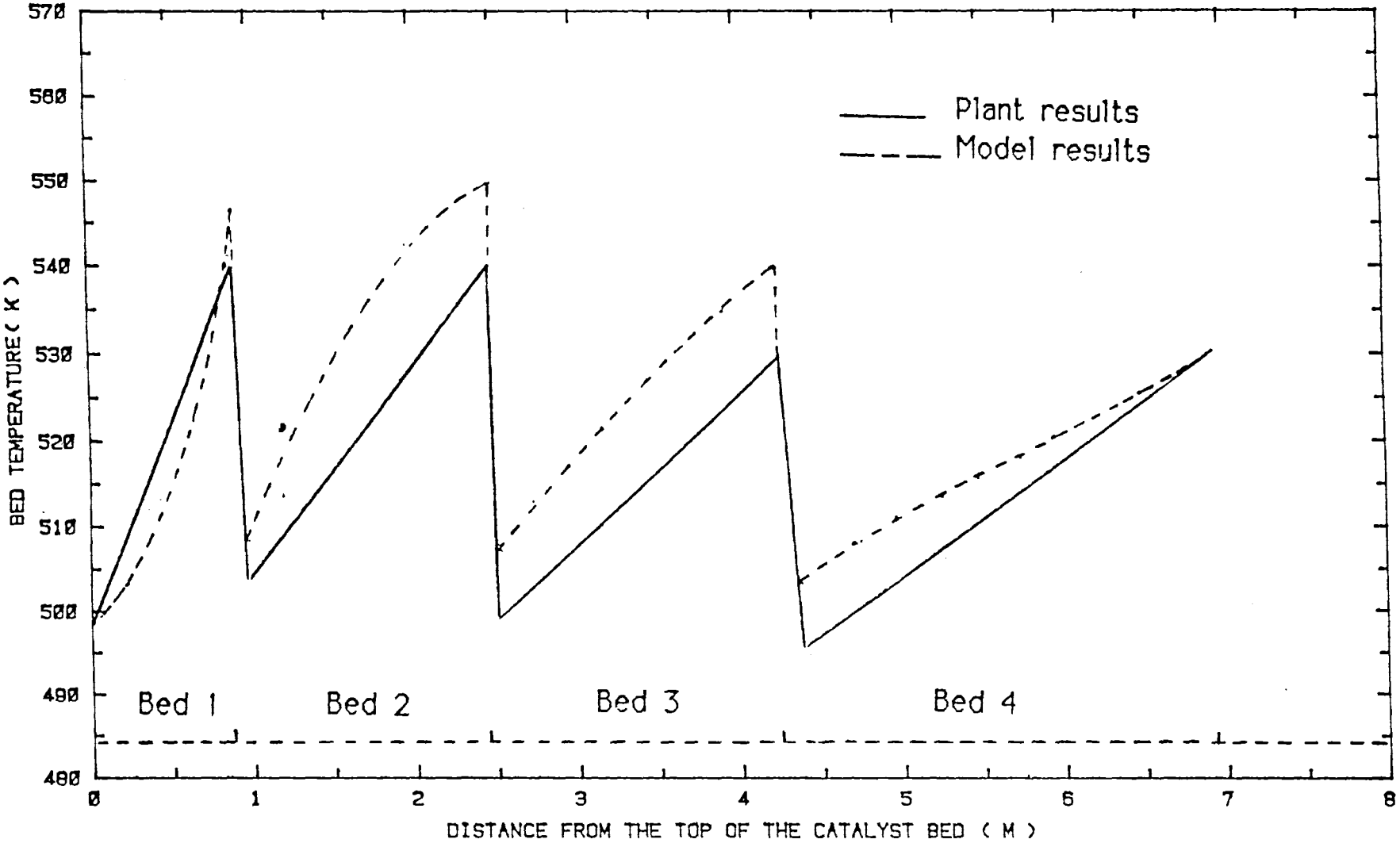

Fig. 10 Temperature profiles in the methanol reactor for the conditions of table 7.

Table 9. Operating conditions and results of design case.

Make up feed flow rate	:	2.5 kmol s^{-1}
Make up feed compositions (mole fractions)		
CO	:	0.1379
CO_2	:	0.0737
H_2	:	0.6460
CH_4	:	0.1285
H_2O	:	0.001
N_2	:	0.0129
Inlet pressure to first bed	:	8552 kPa (abs.)
Cold gas temperature	:	416 K
Recycle ratio	:	4.5
Distribution of feed/cold shot in the beds (fraction of total mixed feed)		
Bed (1)	:	0.40
Bed (2)	:	0.18
Bed (3)	:	0.19
Bed (4)	:	0.23

Inlet, outlet bed temperature (K) and methanol production in each bed (kg m^{-3} cat. s^{-1})

	Inlet temp.	Outlet temp.	Methanol production
Bed (1)	498	543	0.2312
Bed (2)	506	544	0.1964
Bed (3)	516	544	0.1464
Bed (4)	518	542	0.1241

Purge (fraction of make up feed)	:	0.3480
Crude methanol production rate (kmol s^{-1})	:	0.6497
Methanol mole fraction in the product	:	0.7500
Pure methanol production (kmol s^{-1})	:	0.4873

6.1 Effects Of Different Variables On Reactor Performance

The model was used to examine the effects of some important variables e.g, recycle ratio, feed/cold shot distribution, cold shot temperature, and make up feed compositions on

reactor performance on the basis of following assumptions:

1. Maximum allowable temperature in the bed is 545 K.
2. Maximum cold shot temperature available is 420 K.
3. The reactor is fixed but all other process equipment can be changed to have the required process conditions.
4. The temperature distribution in the beds is kept within the allowable levels 496 - 545 K by manipulation of distribution and temperature of feed/cold shot.

Effects of recycle ratio on reactor performance

Effects of recycle ratio on reactor performance are shown in table 10.(feed and reactor dimensions are same as in table 9.)

Table 10. Effects of recycle ratio on reactor performance.

	Case I	Case II	Case III
Recycle ratio	4.0	4.5	5.0
Cold shot temp. (K)	400	416	420
Distribution of feed/ cold shot in the beds (fraction of total mixed feed)			
Bed (1)	0.41	0.4	0.4
Bed (2)	0.18	0.18	0.18
Bed (3)	0.19	0.19	0.184
Bed (4)	0.22	0.23	0.23
1st bed inlet temp. (K)	496	498	503
Last bed exit temp. (K)	542	542.4	538
Crude methanol production (kmol s^{-1})	0.6432	0.6497	0.6564
Methanol mole fraction in the product	0.7521	0.7500	0.7488
Pure methanol production (kmol s^{-1})	0.4838	0.4873	0.4915

It is evident from the table 10. that :

____ Methanol production increases slightly with the increase in recycle ratio.

____ Methanol fraction in the product decreases with the increase in recycle ratio.

____ Cold shot temperatures have to be increased significantly to keep reaction rate at a resonable level with the increase in recycle ratio.

Effects of Feed/Cold shot distribution on reactor performance

The effects of the feed in the first bed and consequently of cold shot in subsequent beds are shown in table 11.

Table 11. Effects of feed/cold shot distribution on reactor performance(feed flow, composition, recycle ratio, cold shot temperature, reactor are same as in table 9.).

Case I			Case II			Case III		
Inlet and outlet temp.(K) and feed/ cold shot distribution in the beds (fraction of total mixed feed):								
Inlet	Outlet	distb.	Inlet	Outlet	distb.	Inlet	Outlet	distb.
Bed (1)								
498	542	0.42	498	543	0.40	498	544	0.38
Bed (2)								
506	544	0.18	506	544	0.18	505	543	0.18
Bed (3)								
517	545	0.19	516	544	0.19	513	543	0.20
Bed (4)								
522	544	0.21	518	542	0.23	515	540	0.24
Crude methanol production (kmol s^{-1}):								
0.6484			0.6497			0.6502		
Mole fraction of methanol in the product :								
0.7498			0.7500			0.7504		
Pure methanol production (kmol s^{-1}):								
0.4862			0.4873			0.4879		

It is evident from table 11. that:

____ Production of methanol and the fraction of methanol in the product increase slightly with the decrease in feed to the first bed because of relatively lower temperature in the latter beds which favors the equilibrium of methanol reaction.

Effects of Make up feed gas compositions on reactor performance

The effects of CO/CO_2 ratio and $H_2/(CO+CO_2)$ ratio in the make up feed gas on reactor performance are shown in tables 12 and 13.

Table 12. Effects of CO/CO_2 (mole $mole^{-1}$) ratio on reactor performance (CO, H_2O, and N_2 were kept constant; $H_2/(CO+CO_2)$ ratio was kept at 3.052; rest was balanced by CH_4 ; other variables, not mentioned here are same as in table 9.)

	Case I	Case II	Case III
CO/CO_2	1.5	1.87	2.5
Make up feed gas compositions (mole fraction):			
CO :	0.1379	0.1379	0.1379
CO_2 :	0.0919	0.0737	0.0512
H_2 :	0.7015	0.6460	0.5773
CH_4 :	0.0548	0.1285	0.2197
H_2O :	0.001	0.001	0.001
N_2 :	0.0129	0.0129	0.0129
Cold shot temp.(K)	395	416	420
1st bed inlet temp. (K)	496	498	504
Crude methanol production (kmol s^{-1}):	0.7646	0.6497	0.5270
Methanol mole fraction in the product	0.7166	0.75	0.8036
Pure methanol production (kmol s^{-1}):	0.5479	0.4873	0.4235

Table 13. Effects of $H_2/(CO+CO_2)$ ratio in the make up gas on reactor performance (CO, CO_2, H_2O, N_2 were kept constant; H_2 varied; rest was balanced by CH_4, all other variables were same as in table 9.)

	Case I	Case II	Case III
$H_2/(CO+CO_2)$	2.9	3.053	3.2
Make up feed gas compositions (mole fraction):			
CO :	0.1379	0.1379	0.1379
CO_2 :	0.0737	0.0737	0.0737
H_2 :	0.6136	0.6460	0.6771
CH_4 :	0.1609	0.1285	0.0974
H_2O :	0.001	0.001	0.001
N_2 :	0.0129	0.0129	0.0129
Cold shot temp.(K)	420	416	410
1st bed inlet temp. (K)	502	498	496
Crude methanol production (kmol s^{-1}):	0.6227	0.6497	0.6669
Methanol mole fraction in the product	0.7563	0.75	0.7460
Pure methanol production (kmol s^{-1}):	0.4709	0.4873	0.4975

It is evident from tables 12 and 13 that:

____ Methanol production increases significantly with the increase in $H_2/(CO+CO_2)$ ratio.

____ Methanol fraction in the product decreases with the increase in $H_2/(CO+CO_2)$ ratio and with the decrease in CO/CO_2 ratio because of favorable reverse shift reaction.

____ Methanol production decreases significantly with the increase in inert level in the make up feed because of decrease in reactants partial pressure.

____ Higher cold shot temperatures are needed as the inert level in the make up feed increases to keep the reaction rate at an acceptable level.

7.0 CONCLUSIONS AND SUGGESTIONS

For a particular make up feed gas and a catalyst with a certain activity level, recycle ratio, feed/cold shot distribution in the beds, cold shot temperature etc. are not effective variables in changing the methanol production level. When the catalyst activity changes or when it changes differently in different beds, it may be possible to maintain methanol production at a certain level by proper manipulation of the above mentioned variables. $H_2/(CO+CO_2)$ ratio and the inert level in the make up feed significantly affect the methanol production. Methanol production increases subtantially with an increase in $H_2/(CO+CO_2)$ ratio and with a decrease in inert level in the make up feed. For a fixed $H_2/(CO+CO_2)$ ratio the methanol fraction in the product decreases with a decrease in CO/CO_2 ratio in the make up feed gas.

Limitations of the model and suggestions for further work

As is clear from the comparative results of table 8 and fig.10, that considerable uncertainties exist in the kinetic parameters of the rate expressions because of following reasons:

- The copper based catalyst used by Schermuly and Luft(1977) may be different from the industrial catalyst, since the type and compositions of the former catalyst are unknown.
- Schermuly and Luft(1977) did not consider either reverse shift reaction or direct hydrogenation of CO_2 in their analysis; any one of these two reactions take place in the reactor to a considerable extent as is evident from the large amount of H_2O in the reactor exit gas.
- The CO concentration levels in the feed (7 to 25 %) in Schermuly and Luft's experiments are higher than that used in an industrial reactor (2 to 4%).
- Schermuly and Luft's rate expression is intrinsic, i.e it does not take into account heat and mass transfer limitations between bulk phase and catalyst surface.

____ The effects of catalyst activity decay with time was not taken into account in Schermuly and Luft's rate expression.

The above limitations can be overcome by doing the following model fitting analysis either from laboratory data of from pilot plant data or preferably from actual operating plant data over a wide range of process conditions:

The rate expressions can be written as,

$$r_{j,k} = f_k(t)\ ff_j(\ P_{i,av},\ T_{av}\ )_k$$

and then rearranged to,

$$r_{j,k} - f_k(t)\ ff_j(\ P_{i,av}, T_{av}\ )_k = FF_{op} \quad \ldots (31)$$

Where,

$f_k(t)$ = catalyst activity decay function in bed k.

$ff_j(\ P_{i,av}, T_{av}\ )_k$ = rate expression for reaction j in bed k.

$r_{j,k}$ = measured average rate for reaction j in bed k.

n = no. of data points avaiable in a bed.

$P_{i,av}$ = average partial pressure of component i in a bed.

T_{av} = average temperature in a bed.

Using suitable rate expressions for reactions involved and decay functions for catalyst activity in the beds, it is possible to calculate the unknown parameter values employing an optimization technique e.g, (constrained Box method, (Box, 1965)) by minimizing the square of the function, FF_{op} within a certain domain.

Convergence of recycle

There are two criteria for checking the recycle convergence e.g,

(i) Sum of absolute difference between the assumed and calculated molal flow rates of each component in the recycle (D_{su}, expressed as a percentage of total recycle).

(ii) Absolute difference of inerts in the fresh make up feed and in the purge (D_{in}, expressed as a percentage of total inerts in the make up feed).

It is very difficult to apply both these criterion for checking recycle convergence. Also one has to be very careful in selecting the absolute values of the convergence criterion. For example when both D_{su} and D_{in} were chosen equal to 0.1 % , the steady state solution was found to be wrong, which was verified by starting the model from different initial conditions; whearas 0.01 % was found to be adequate up to a recycle ratio of 6.

Two different methods were used to solve the recycle convergence. In the first method, purge was fixed as a fraction of the recycle and the model used to find the recycle ratio. This method was found to be difficult to apply because recycle ratio is a strong function of purge fraction, so if the initial recycle ratio and corresponding cold shot temperature and feed/cold shot distribution are not chosen correctly, this method fails to give any solution. If all the necessary variables were chosen reasonably, in this method the second convergence criterion was satisfied rapidly but the first convergence criterion was difficult to satisfy.

In the second method, recycle was fixed and the model used to calculate the purge rate. This method is easy to apply because it is relatively straight forward to choose cold shot temperature, feed/cold shot distribution in the beds based on the chosen recycle ratio. In this method the first convergence criterion was satisfied quite rapidly depending on

the recycle ratio. (the greater the recycle ratio the more difficult it was to satisfy the convergence criterion). The second convergence criterion was difficult to satisfy, because it was not used explicitly for convergence acceleration.

In this work the second method was used and only the 1st criterion was used for recycle convergence checking (D_{su} < 0.01 %).

Based on the 2nd method (fixed recycle), a better solution may be obtained by satisfying both convergence criterion in the following way:

(i) Starting from the initial conditions satisfy only the first convergence criterion (D_{su} < 0.01). At this stage the solution comes very close to steady state values.

(ii) Check the second convergence criterion, if not satisfied, apply wegestein's acceleration technique to each component and calculate the new recycle ratio (it will be very close to the chosen recycle ratio).

(iii) Proceed as usual and check both the convergence criteria.

8.0 NOMENCLATURE

A, B, C, D, E = constants in rate Eqns. (8), (9) and (10)

$C_1 \rightarrow C_6$ = constants in rate Eqns. (24) and (25)

Cp_i = specific heat capasity of component i, kJ $kmol^{-1}$ K^{-1}

ΔH_j = heat of reaction, j, kJ $kmol^{-1}$
(o refers to standard conditions 1 atm, 298 K)
(j=1 for reaction (1), j=2 for reaction (3))

ΔF = free energy change of reaction, kJ $kmol^{-1}$
(o refers to standard conditions)

ΔS = entropy change of reaction, kJ $kmol^{-1}$ K^{-1}

Δw = differential catalyst weight in the bed, kg

F_i = molal flux of component i , kmol m^{-2} s^{-1}
(o refers to inlet conditions)
(i=1 for CO; i=2 for CO_2; i=3 for H_2;
i=4 for CH_4; i=5 for O_2; i=6 for H_2O
i=7 for C_2H_6; i=8 for H_2S;
i=9 for N_2; i=10 for CH_3OH)

f_i = fugacity of component i , kPa

k = rate constant for reaction (1)

K = equilibrium constant for reaction (1)

K' = equilibrium constant for reaction (2)

K'' = equilibrium constant for reaction (3)
(r refers to reverse reaction)

K_f = equilibrium constant of reaction in terms of fugacity

K_γ = expression in terms of fugacity coefficients to take into account the effects of pressure on reaction equilibrium constants.

K_p^o = equilibrium constant in terms of partial pressure at atmospheric pressure.

K_a, K_i, k', K, = constants in rate eqn. (23)

P = total pressure, kPa

P_i = partial pressure of component i , kPa

r_j = rate of reaction j , kmol kg cat^{-1} s^{-1}
(j=1 for reaction (1); j=2 for reaction (3))

R = universal gas constant

T = instantaneous gas temperature, K
(o refers to inlet condition)

w = instantaneous catalyst weight in the bed, kg

Y_i = mole fraction of component i

Greek letters

γ_i = fugasity coefficient of component i

Φ_{CO_2} = an empirical factor in rate Eqn. 22

ρ_c = bulk density of the catalyst, kg m^{-3}

9.0 REFERENCES

Agny, R. M and C. G. Takoudis, "Synthesis of methanol from carbon monoxide and hydrogen over a copper-Zinc oxide-Alumina catalyst," Ind. eng. chem. prod. res. dev., vol. 24, no. 1 pp 50-55, (1985).

Andrew, S. P. S, Post congress symposium of the 7th Intern. Congr. catal., Osaka, Japan, July 7, (1980).

Bakemeier, H., P. R. Laurer, W. Schroder
Chem. eng. prog. symp. ser., vol. 66, no. 98, pp 1-10,(1970).

Bolton, D. H and D. Hanson, "Economics of low pressures in methanol plants," Chem. Eng. pp 154-158, (Sept., 1969).

Capelli, A., A. Collina and M. Dente, "Mathematical model for simulating behavior of Fauser-Montecatini industrial reactors for methanol synthesis.," Ind. eng. Chem. proc. des. & dev., vol. 11, no. 2, pp 184-190, (1972).

Cherdnichenko, V. M and M. I. Temkin, Zh. fiz. khim., 31, pp 1072-, (1957).

Denny, P. J and D. A. Whan, "The heterogeneously catalysed hydrogenation of carbon monoxide," Catal. spec. period. rep., chem. soc. London, vol. 2, pp 46-86, (1978).

Friedrich, J. B., M. S. Wainwright and D. J. Young, "Devolopment of raney type low temperature methanol synthesis catalysts," Chem. Eng. Commun., vol. 14, pp 279-288, (1982).

Gupta, R. P., personal communication, Dept. of Chemical and Process engg., University of Canterbury, Newzealand, (1985).

Herman, R. G., K. Klier, G. W. Simmons, B. P. Finn, J. B. Bulko and T. P. Kobyunski, J. catalysis, vol. 56, pp 407-, (1979).

Hillier, H., F. Maschner, "Lurgi makes low pressure methanol," Hydrocarbon processing, pp 281-285, (sept., 1970).

Klier, K., J. Chatikanij, R. G. Herman and G. W. Simmons, "Catalytic synthesis methanol from CO/H_2 IV. The effects

of Carbon dioxide.," J. catalysis, vol.74, pp 343-360, (1982).

Klier, K., "Methanol synthesis", Advances in catalysis, vol. 31, pp 243-313, (1982).

Knudsen, R. A., T. Bailey and L. A. Fabino, "Experience with ASPEN while simulating a new methanol plant," AIChE sympos. series, vol. 78, no. 214, pp 38-55, (1982).

Kung, H. H., "methanol synthesis," Catal. rev. sci. Eng., vol. 22, no. 2, pp 235-259, (1980).

Marsden, W. L., M. S. Wainwright and J. B. Friedrich, "Zinc promoted raney copper catalysts for methanol synthesis," Ind. Eng. chem. prod. res. dev., vol. 19, no. 4, pp 551-556, (1980).

Natta, G., "Methanol synthesis," Catalysis, editor, P. H. Emmet, vol. III, chapter 8, Reinhold, New york, (1955).

Schermuly, O., "Unterschung der Niederdruck-methanolsynthese in triebstrahlreaktor"- Dessertation, Dr. of Ing. (1977), Institut fur chemische technologie, Technical Hochschule Darmstadt, W. germany, -obtained by personal communication with prof. Dr. G. Luft.

Schermuly, O. and G. Luft, "Examination of the low pressure methanol synthesis in a driving jet reactor," Chemie Ing. techn. MS 536/77, (1977).

Shah, M. J., R. E. Stillman, "Computer control and optimization of a large methanol plant," Ind. Eng. & chem., vol. 62, no. 12, pp 59-75, (Dec, 1970).

Smith, R. E. et al., "Optimize large methanol plants," Hydrocarbon Processing, pp 95-100, (May,1984).

Stephens, A. D., "Stability and optimization of a methanol converter," Chem. Eng. sci., vol. 30, PP 11-19, (1975).

Stiles, A. B., "Methanol, past, present and speculation on the future," AIChE J., vol. 23, no. 3,pp 362-375, (May, 1977).

Uchida, H and Ogino, Y, Bull. chem. soc., Japan, vol. 31, pp 45, (1958).

Villa, P., P. Forzatti, G. Buzzi-Ferraris, G. Garone and I. pasquon, "Synthesis of alcohols from carbon oxides and hydrogen. 1.kinetics of the low pressure methanol synthesis.," Ind. Eng. chem. proc. des. & dev., vol. 24, no. 1, pp 12-19, (1985).

Wainwright, M. S., "Raney copper-A potential methanol synthesis catalyst," Sympos. on alcohol fuels, Sydney, Australia, (Aug.9-11, 1978).

CHAPTER IV.

PROCESS MODULE FOR A METHANATION REACTOR SYSTEM

ABSTRACT

A steady state one dimensional pseudo-homogeneous rate model of a methanation reactor system, comprising a hot gas recycle reactor and a multibed polishing reactor with interstage cooling has been developed. This model is particularly applicable for the design and with some modifications for the simulation of the methanation section of a SNG plant from a synthesis gas containing large amounts of CO and CO_2 (typical of synthesis gas from coal gasification). This model can also be used to observe the effects of different parameters e.g recycle ratio, feed composition and temperature, operating pressure etc. on reactor design and performance.

A brief state of the art review of the different methanation processes, thermodynamics, kinetics and catalysis of the methanation reaction is also included here.

Table of Contents

	page
(i) ABSTRACT	
1.0 INTRODUCTION	IV-1
2.0 THERMODYNAMICS	IV-2
3.0 KINETICS	IV-14
4.0 CATALYSIS	IV-19
5.0 MODEL DEVELOPMENT	IV-21
6.0 FLOW DIAGRAM OF THE COMPUTER PROGRAM	IV-24
7.0 RESULTS AND DISCUSSIONS	IV-27
7.1 The effects of recycle ratio on reactor performance	IV-31
7.2 The effects of main reactor feed inlet temperature on reactor performance	IV-32
7.3 The effects of polishing reactor feed inlet temperature on reactor performance	IV-33
7.4 The effects of H_2/CO ratio in the feed on reactor performance	IV-34
7.5 The effects of CO_2 concentration in the feed on reactor performance	IV-36
7.6 The effects of H_2O concentration in the feed to the main reactor on reactor performance ...	IV-37
7.7 The effects of H_2O concentration in the polishing reactor feed on reactor performance ..	IV-38
8.0 CONCLUSIONS AND SUGGESTIONS FOR FURTHER WORK	IV-40
9.0 NOMENCLATURE	IV-41
10.0 REFERENCES	IV-42
11.0 APPENDIX IV-A	IV-45

1.0 INTRODUCTION

Nearly all of the processes for manufacturing synthetic natural gas (SNG) from coal require a catalytic methanation step for upgrading the raw synthesis gases to a high heating value pipeline gas (calorific value 36000 kJ m^{-3}) as well as for meeting strict SNG specifications (H_2 less than 1% and residual CO less than 0.1% by volume). Methanation can be defined as a process of making methane by hydrogenating carbon oxides according to the following reactions:

$$CO + 3H_2 \rightleftharpoons CH_4 + H_2O \quad \text{.....(1)}$$

$$CO_2 + 4H_2 \rightleftharpoons CH_4 + 2H_2O \quad \text{.....(2)}$$

These reactions are used among other things for the commercial removal of traces of carbon oxides from NH_3 synthesis gas. But the environments for the methanation process in SNG manufacturing are quite different from that in NH_3 synthesis with respect to CO concentration, sythesis gas composition, pressure level etc. Thus a completely new set of rules and design parameters are imposed for the operation and design of the methanator in SNG production (Allen, 1973). The magnitude of methanation will vary considerably depending on the choise of the primary gasification process.

Sabatier and Senderens (1902) are the pioneers in the synthetic manufacturing of methane from CO hydrogenation using nickel based catalysts. At present there are several processes available at different stages of operation. Some are described below:

(i) Hot gas recycle method

(ii) Cold gas recycle method

(iii) Liquid phase approach

(iv) Steam moderated method
  (a) RM process
  (b) High carbon monoxide process(HCM)

The above methods may use either fixed or fluidized beds.

The four method itemised above are considered in more detail below:

(i) Hot gas recycle method: (Iammartino(1974), Moeller(1974))

This process was developed by Lurgi Mineraloeltechnik GMBH. A simple flow diagram of this process is shown in fig.1

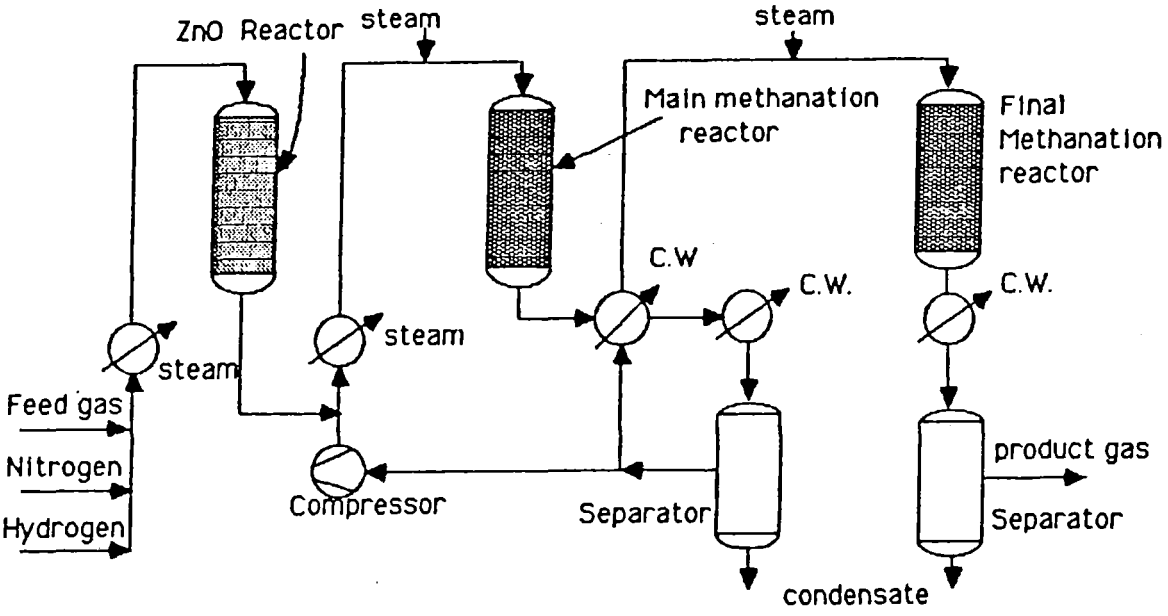

Fig. 1 Lurgi process (Hot gas recycle method)

This process is commercially proven. Thirteen commercial SNG plants based on this process are operating worldwide. (Hydrocarbon Processing, 1973)

(ii) Cold gas recycle system (Iammartino, 1974):

This system has been developed by the Institute of Gas Technology as the final step of its Hygas coal gasification route. A series of fixed bed adiabatic methanators are used rather than a single large reactor. This reduces recycle rate considerably. In this system the temperature is controlled in the reactor by regulating carbon monoxide content in the inlet gases to each stage, through proportioning fresh feed, cold

recycle and off-gases from the previous stage.

(iii) Liquid phase approach (Iammartino, 1974):

This liquid methanation scheme was developed by Chem. systems, Inc. A circulatig stream of inert liquid absorbs the heat generated in the reactor (as shown in fig.2). It flows upward through the reactor cocurrent with the synthesis gas feed, fluidizing the catalyst bed. The liquid mainly picks up sensible heat, but some vaporizes depending on volatility. The vaporized inert liquid is condensed and is then recycled.

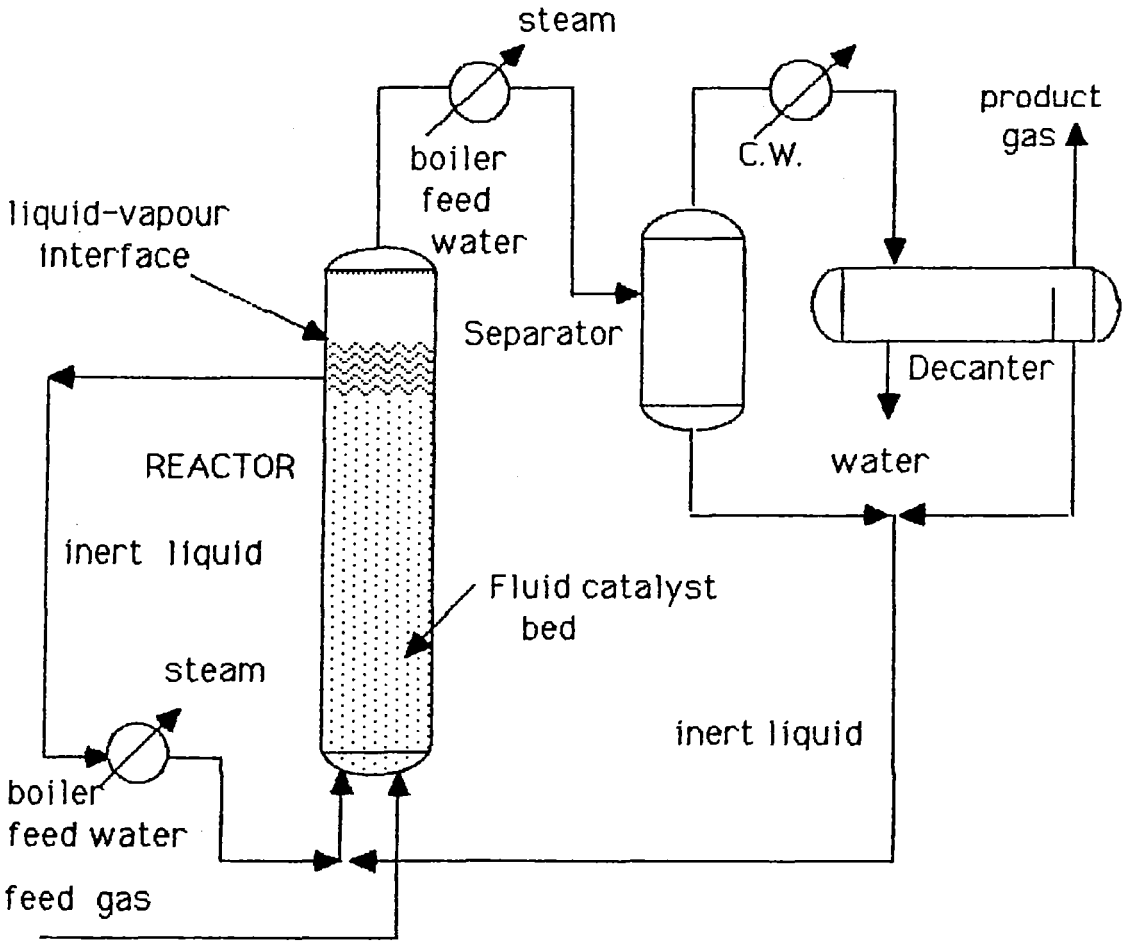

Fig. 2 Chem systems process (Liquid phase approach)

(iv) Steam moderated method(Iammartino,(1974):

a. RM process:

This process was developed by Ralph M. Parsons Co. (Pasadena, California). It was cosponsored by Texaco Inc. This dual purpose technique provides shift conversion simultaneous with methanation, avoiding the need for separate units to increase the H_2/CO of high-CO synthesis gases. The feed gas passes through a series of fixed bed adiabatic catalytic reactors(shown in fig.3). No gas is recycled. Final methanation occurs in a clean up reactor. The main advantages of this process are:

.Efficient utilization and production of steam.

.Removal of CO from the system in a one stage operation, at a point where gas volume for treatment is minimal.

.Minimal catalyst volume requirement because of once-through operation at high space velocity.

b. The high CO direct methanation scheme(HCM), (Tart and Rampling(1981))

This is a proprietary direct methane synthesis route from British Gas Corporation especially suitable for the production of SNG from synthesis gas manufactured from the British gas/Lurgi slagging coal gasifier. This scheme is shown in fig.4. The HCM route offers the following advantages:

1. Net process steam requirement is lower.
2. A major part of the process steam requirement for methane synthesis can be generated by using the otherwise difficult to-recover low grade heat by means of a saturator.
3. A seperate CO-shift stage with all its ancillary equipment is not needed; thus causing reduction in capital cost and in the volume of phenolic liquor produced.

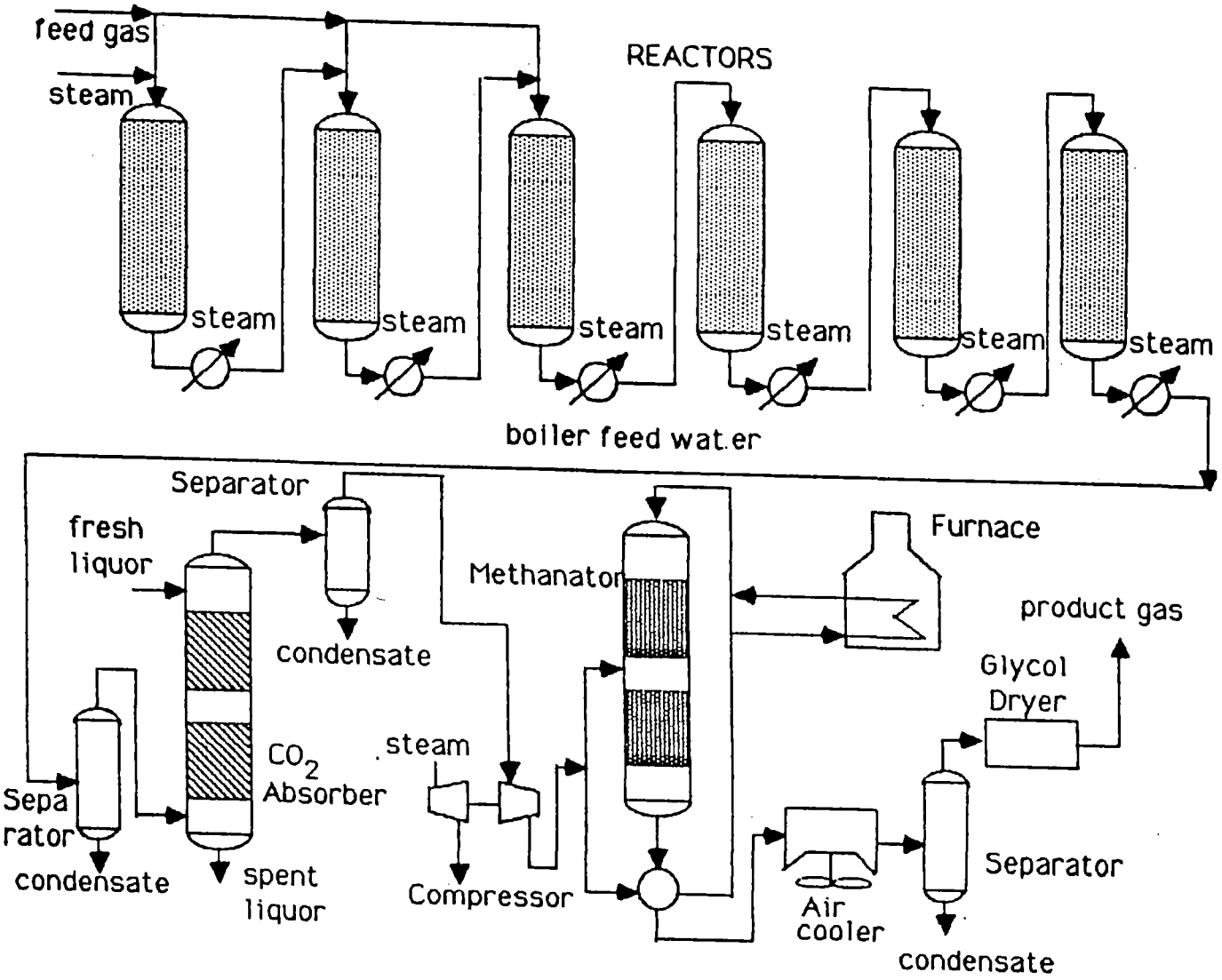

Fig. 3 Parsons Process

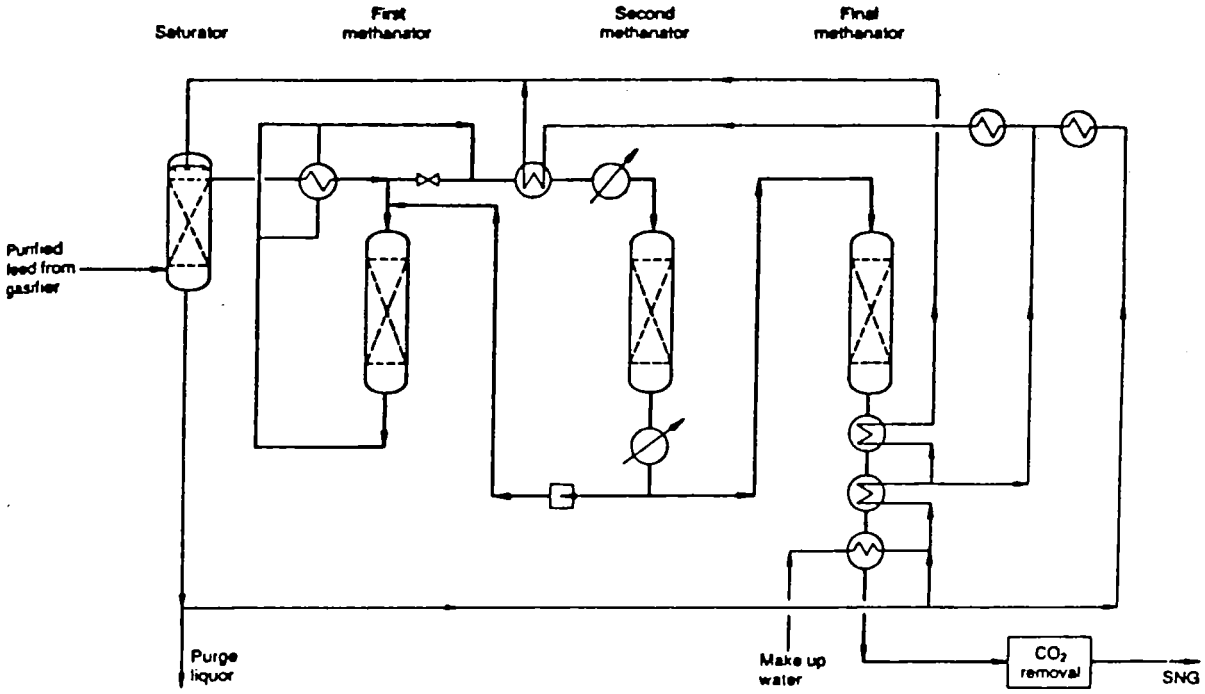

Fig. 4 HCM direct methanation scheme.

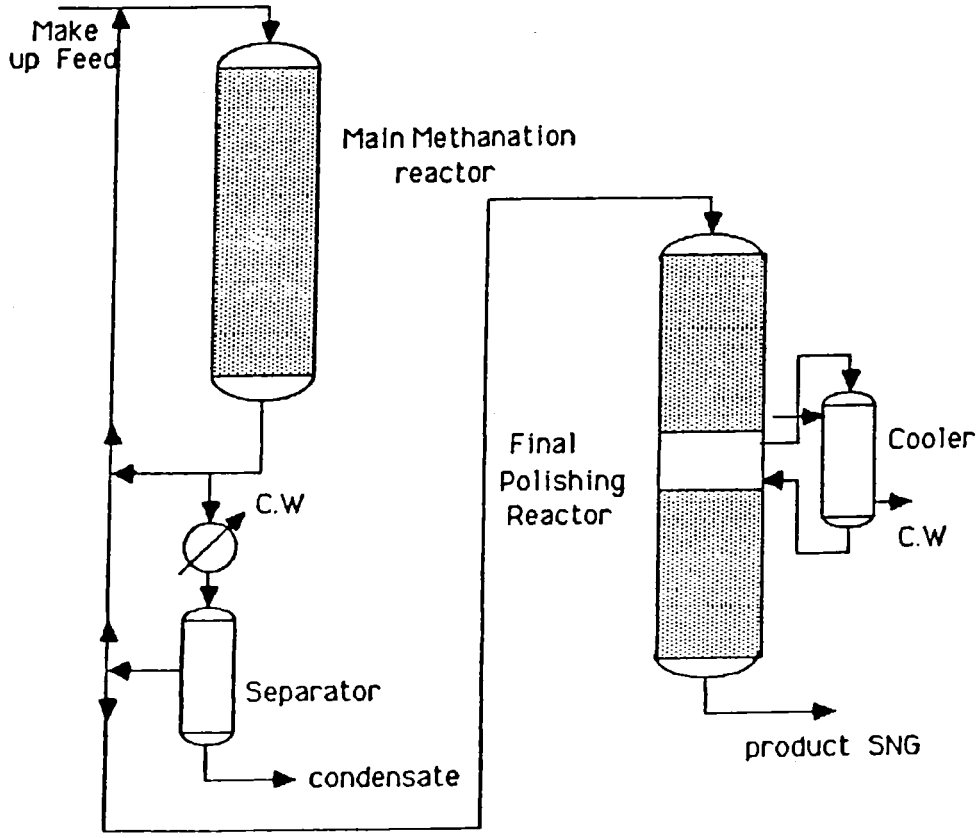

Fig. 5 Schematic flow diagram of the recycle methanation reactor system.

4. Gas purification costs are lower due to a lower throughput and a lower CO feed concentration that favors production of a H_2S rich side stream.

5. Volume of CO_2 removed is similar but the volume of gas from which it is removed is substantially lower.

Since the methanation reaction is a highly exothermic reaction, the heat removal method from the reacting gases can become a major criterion in reactor selection. Wen et al.(1968) did an economic optimization of different catalytic fixed bed methanation reactors and concluded that the recycle methanation scheme was the only suitable system for methanation of synthesis gas with CO concentration higher than 15% (by vol.), typical of Lurgi and other coal gasification processes.

It can be easily shown that it is impossible to methanate a typical synthesis gas to pipeline quality SNG in a single adiabatic reactor as well as in a multibed reactor with cold shot cooling by simple mathematical analysis (Shown in Appendix IV-A).

The following recycle reactor system (shown in fig.5) was chosen for modeling purposes because it is a commercially successful system and is suitable for a wide range of CO concentration.

2.0 THERMODYNAMICS

The catalytic production of methane from CO and CO_2 hydrogenation can be described by the following reactions:

$$3H_2 + CO \rightleftharpoons CH_4 + H_2O \quad \ldots\ldots\ldots (1)$$

$$2H_2 + 2CO \rightleftharpoons CH_4 + CO_2 \quad \ldots\ldots\ldots (2)$$

$$4H_2 + CO_2 \rightleftharpoons CH_4 + 2H_2O \quad \ldots\ldots\ldots (3)$$

Hydrogenation of CO_2 does not occur in the presence of CO(Mills and Steffgen(1974), Greyson(1956). According to Greyson(1956) reaction (2) is not a primary reaction, rather it can be considered to be a combination of reaction (1) and the water gas shift reaction

$$CO + H_2O \rightleftharpoons CO_2 + H_2 \quad \ldots\ldots\ldots (4)$$

Although the water gas shift reaction does not produce methane, it plays an important role in methane synthesis by altering the H_2/CO ratio with far reaching impact on reaction products.

Another reaction that does occur to a varying extent during the catalytic synthesis of methane is the decomposition of CO to carbon and CO_2.

$$2CO \rightleftharpoons C + CO_2 \quad \ldots\ldots\ldots (5)$$

This reaction is important because it tends to reduce the efficiency of the process by unnecessarily consuming CO and because the deposition of carbon on the catalyst particle can plug the reactor as well as foul the catalyst.

Thermodynamic values for reactions (1) to (5) are given in the following figures (fig.6, fig.7, fig.8, fig.9) (Greyson, 1956; Mills and Steffgen, 1974). The free energy values of all the above reactions have large negative values for a wide temperature range; however the reactions are relatively slow and catalysts are needed to accelerate the reactions to acceptable commercial rates. From the heat of reaction vs. temperature curves it is evident that all except

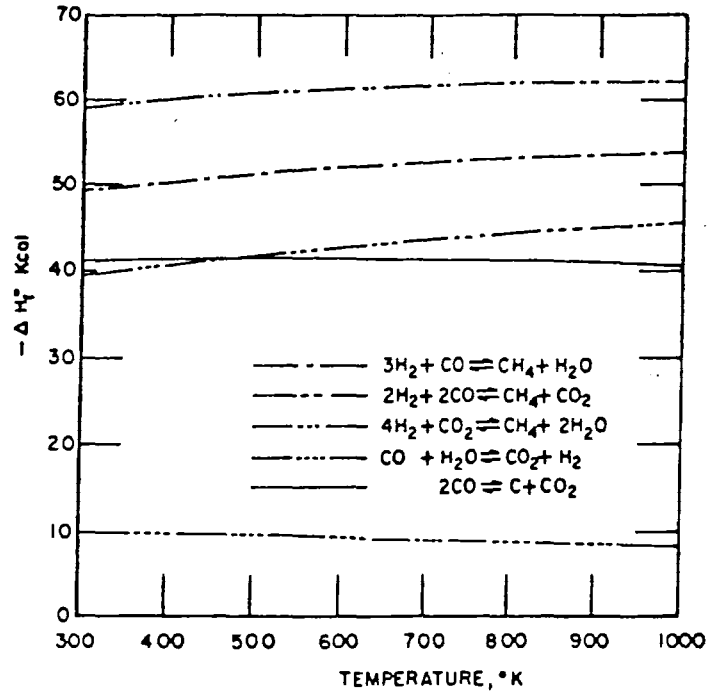

FIG. 6 Heats of reactions as functions of temperature.

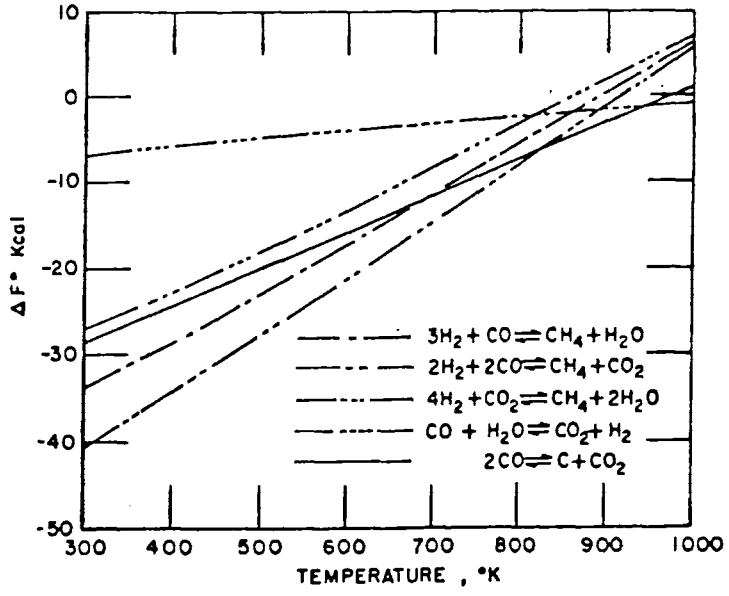

FIG. 7 Free energy changes as functions of temperature.

reaction (4) are highly exothermic. This high heat release makes it difficult to prevent overheating and inactivation of the catalysts and also it can make temperature rise to such a degree that methanation becomes limited due to thermodynamic equilibrium. Greyson(1956) presented graphically (fig.9) the theoretical equilibrium methane yield with H_2/CO ratio as a function of temperature and pressure.

Though temperature and pressure have some impact on carbon deposition, the degree of carbon deposition is primarily a function of H_2/CO ratio in the synthesis gas. The carbon deposition boundaries, or limiting H_2/CO ratios above which carbon will not deposit are shown in (fig.10) for the temperature range 500-1400 K and for pressures of 1, 10 and 25 atmospheres.

The following conclusions can be drawn from the preceeding figures of thermodynamic data:

(i) Catalyst beds should be operated at the lowest temperature that are consistent with acceptable activity and with H_2/CO ratio at or above the limiting boundary ratio.

(ii) Pressure is, as a general rule, not very important under the normal operating conditions but operation at high pressure tends to permit the use of lower H_2/CO ratios without the deposition of carbon on the catalyst.

Unfortunately operation at elevated pressure releases a large quantity of heat per unit volume of bed which, unless adequate means of removal are available, increases catalyst bed temperature, decreases methane yield and also deactivates the catalyst by depositing excessive amounts of carbon.

Equilibrium constant expressions:

The following equilibrium constant expressions for reaction (1) in terms of mole fraction of components involved from Wen et al.(1969) are used in this work:

Experimental equilibrium constant (for a pressure of 7440 kPa):

$$K = 10^{(1.283 \times 10^4/T - 10.77)}$$

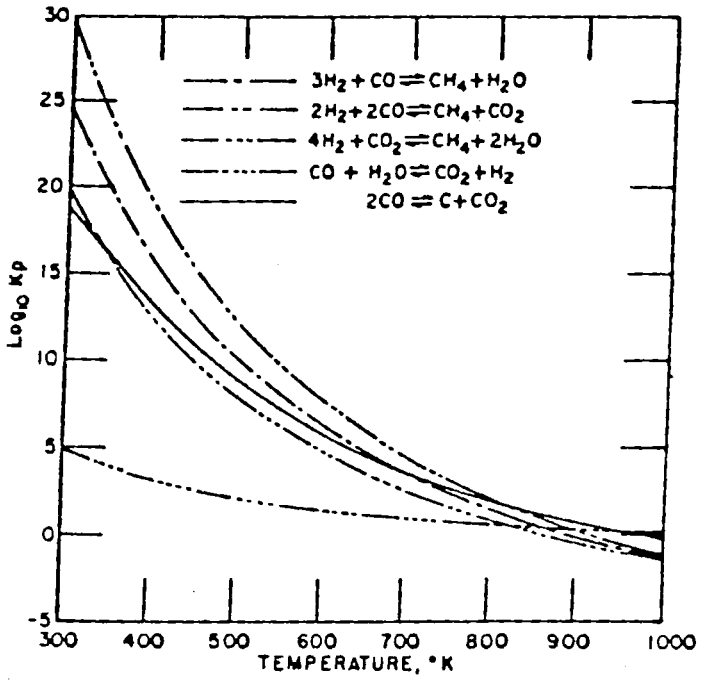

FIG 8 Equilibrium constants as functions of temperature.

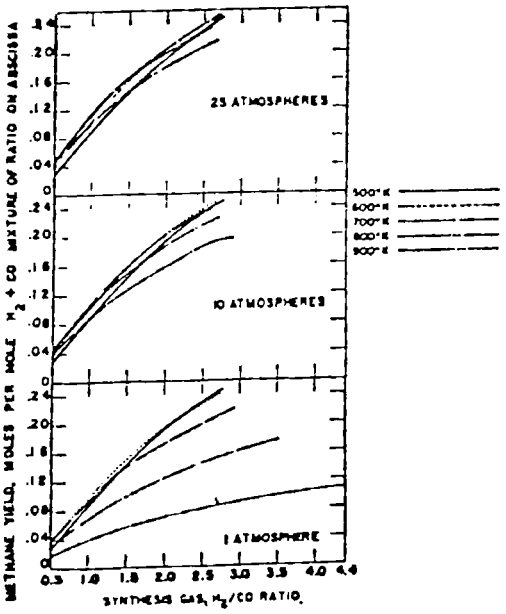

Figure 9 Equilibrium methane yields.

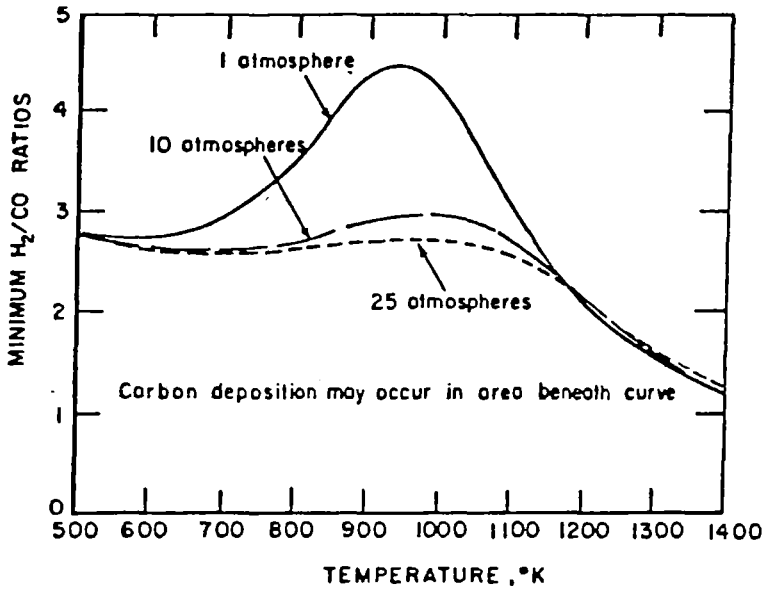

FIG. 10 Carbon deposition boundaries

Calculated equilibrium constant expression:

$$K_{ca} = \frac{Y_{CH_4}^{*} \; Y_{H_2O}^{*}}{Y_{CO}^{*} \; (Y_{H_2}^{*})^3}$$

3.0 KINETICS AND REACTION RATE EXPRESSIONS

A number of kinetic studies of the methanation reaction have been conducted over a wide range of temperature, pressure, H_2/CO ratios, and a variety of catalysts. Lee(1973), Vanice(1976), Vatcha(1976) compiled the results and experimental conditions of most of these studies. Some of these studies are briefly discussed here.

Akers and White(1948) explained the kinetics of CO methanation by considering CO methanation reaction(1) and shift reaction(4). The rate of methane synthesis and that of CO_2 were expressed by:

$$r_{CH_4} = \frac{P_{CO}\, P_{H_2}{}^{3} \rho_c}{\left(3600\ A + B\, P_{CO} + D\, P_{CO_2} + E\, P_{CH_4}\right)^4} \qquad \ldots(6)$$

$$r_{CO_2} = \frac{A'\,(P_{CO} - B')\,\rho_c}{3600} \qquad \ldots(7)$$

Pursley et al.(1952) examined the rate of the methanation reaction from mixtures of CO and H_2 with Nickel based catalysts (Harshaw chemical co.) at pressures between 1 and 27 atm. and at temperatures between 533 and 644 K and proposed the following rate expression:

$$r_{CH_4} = \frac{1.1\, P_{CO}\, P_{H_2}{}^{0.5}\, \rho_c}{3600\ (1 + 1.5\, P_{H_2})} \qquad \ldots. (8)$$

Wen et al.(1969) proposed the following rate expressions for the methanation reaction based on the Institute of Gas Technology (U.S.A) data.:

$$r_{CH_4} = \frac{120\, \exp(-65521/RT)\, P_{CO}{}^{0.7} P_{H_2}{}^{0.3} \rho_c}{3600} \qquad \ldots(9)$$

for 561 - 589 K.

$$= \frac{0.07\ P_{CO}^{0.7}\ P_{H_2}^{0.3}\ \rho_c}{3600} \qquad \ldots\ (10)$$

for 589 - 728 K.

Herwijen et al.(1973) studied the kinetics of the CO and CO_2 methanation reactions (1 and 2) separately at very low concentrations of CO and CO_2 at atmospheric pressure and at temperatures between 473 and 503 K. The results were represented by the following Langmuir-type rate expressions:

$$-r_{CO} = \frac{2.09\times10^{5}\ \exp(-42258/RT)\ P_{CO}\rho_c}{3600\ (1 + 4.56\times10^{-4}\ \exp(51882/RT)\ P_{CO})^2} \qquad \ldots\ (11)$$

$$-r_{CO_2} = \frac{1.36\times10^{12}\ \exp(-105855/RT)\ P_{CO_2}\rho_c}{3600\ (1 + 1270\ P_{CO_2})} \qquad \ldots(12)$$

Lee (1973) formulated the following simple rate expresion for reaction(1) based on a large number of experimental results:

$$-r_{CO} = \frac{270.87\ \exp(-29054/RT)\ P_{CO}\ P_{H_2}^{0.5}\rho_c}{3600\ (1 + 1.469P_{H_2} + 0.734P_{CH_4})} \qquad \ldots\ (13)$$

Some important features of this rate expression are mentioned below:

(i) It was tested with a large number of commercial methanation catalysts.

(ii) It was tested with eleven (CO, CO_2, H_2, CH_4, C_2H_6, C_3H_8, H_2O, C_6H_6, N_2, He, C_2H_5CH) to fifteen component (C_4H_4S, CS_2, COS, H_2O) feed gases unlike most of the literature rate expressions which have been fomulated with three to four components(CO, CO_2, H_2, CH_4) feed gas.

(iii)It was found to be valid over a wide temperature

range (492 - 978 K) and also valid over a wide pressure range (1 - 68 atm.).

This rate expression does not apply when:

(1) The feed gas contain the following components at a higher level than that given here.

a. Benzene(1.5 vol %)
b. water (5.0 vol %)
c. CO_2 (20 vol %)
d. N_2 (50 vol %)
e. H_2S (0.5 ppm)
f. mercaptans(2 ppm)
g. ammonia, phenol and HCN (individually at any conc.)

(2) If H_2/CO ratio is less than 2.85 in the feed gas.

Vatcha(1976) divided the existing rate expressions for the methanation reaction into two categories e.g, Langmuir-Hinshelwood form and Power law form and after some analysis concluded that Langmuir-Hinshelwood form is superrior to Power law form for heterogenous catalytic kinetics. He modified the rate expression proposed by Lee(1973) by multiplying by a term which takes into account the effect of the reverse reaction, thereby making it thermodynamically consistent. This rate expression for CO methanation reaction(1) is given below:

$$-r_{CO} = \frac{270.87 \exp(-29054/RT)\, P_{CO}\, P_{H_2}^{0.5} \rho_c}{3600\,(1 + 1.469 P_{H_2} + 0.734 P_{CH_4})} \times \left(1 - \frac{Y_{CH_4}\, Y_{H_2O}}{K\,(Y_{CO}\, Y_{H_2}^{3})}\right) \quad \ldots\ldots (14)$$

It is apparent that there ia a great diversity among the proposed rate expressions; most of these variations can be attributed to the following factors:

(i) Vast differences in the reaction parameters e.g., temperature, pressure, composition of synthesis gas.

(ii) Wide differences in catalysts compositions, supports and pretreatments.

(iii) Insufficient characterization of the surface intermediates and the rate controlling step.

(iv) Complications due to carbon deposition and metal carbide formation.

(v) Complications due to mass and heat transfer limitations since most of these rate expressions were formulated from data obtained at high conversions.

Dalla Betta et al.(1975) examined the activity of 2% Ni/Al_2O_3, 5% Ni/ZrO_2, Raney Ni, and 1.5% Ru/Al_2O_3 catalysts in the presence of sulphur poisons. When 10 ppm H_2S was included in the syngas feed stream, the activity of Ru/Al_2O_3 catalysts declined two orders of magnitude at 673 K. Raney Ni and 2% Ni/Al_2O_3 exhibited similar behavior while the 5% Ni/ZrO_2 catalysts was much less affected by the presence of sulphur. In no case did the activities return to their initial steady state levels after the H_2S was removed from the feed stream. An interesting observation was that the relative inhibition of methane formation, compared to C_2^+ hydrocarbons formation, in the presence of H_2S.

Agrawal et al.(1982) studied the kinetic behavior of CO hydrogenation over alumina-supported Cobalt. Under sulphur free reaction conditions, two steady states were observed:

(i) An upper pseudo steady state (very short duration five hours at 673 K).

(ii) A lower pseudo steady state.

A third steady state was observed for sulphur poisoned Cobalt catalyst. The results are shown in the table 1.

Table 1.
Kinetic behavior of Co/Al_2O_3 in different regions of methanation activity.

	Fresh catalyst	carbon deactivated	sulphur poisoned
N_{CH_4}, (s^{-1})	10.0	0.10	0.001
E_a, (kcal mol^{-1})	28.2±2	16±2	16±2
Effect of P_{CO}, $N_{CH_4} \propto P_{CO}^{n}$	-0.24	0.3 to 1.0	0.3 to 1.0
Effect of P_{H_2}, $N_{CH_4} \propto P_{H_2}^{m}$	0.5	0.5	

Inoue et.al.(1984) investigated the kinetics of reactions of CO and CO_2 with H_2 in a tube wall reactor sprayed with nickel catalyst. The observed rate laws were

For reaction (1)

$$-r_{CO} = \frac{3.21\times10^{-5}\, k_1\, P_{H_2}\, P_{CO}^{0.5}}{1 + K_{CO}\, P_{CO}} \qquad \ldots\ldots (15)$$

For reaction (3)

$$-r_{CO_2} = \frac{4.708\times10^{-5}\, k'\, P_{H_2}\, P_{CO_2}^{0.33}}{1 + K_{CO_2} P_{CO_2} + K_{H_2} P_{H_2} + K_{H_2O} P_{H_2O}} \qquad \ldots\ldots\ldots (16)$$

These reaction rate expressions were derived theoretically from a reaction mechanism. For a mixture of CO and CO_2 the kinetics of the methanation reactions were found to be well accounted for by the above reaction rate expressions.

In this work the rate expression of Vatcha (1976) was used for CO methanation reaction(1) and for shift reaction the rate expression of Rase (1977) was used.

4.0 CATALYSIS

Sabatier and Senderens(1902) are the pionears in using Nickel as a catalyst to produce methane by the hygrogenation of CO and CO_2. They extended their study to other metals and showed that Cobalt also promoted the methanation reaction but that Copper, Iron, Platinum and Palladium did not form active catalysts.

Early in the 1920's Fischer, Tropsch and Dilthey (1925) compared the methanation properties of various metals at temperature upto 1073 K. The decreasing order of methanation activity was Ru, Ir, Rh, Ni, Co, Pt, Fe, Mo, Pd, Ag. In terms of metals important for methanation, the list can be shortened to Ru, Ni, Co, Fe, and Mo (Mills and Steffgen, 1974).

Over the past 60 years further progress had been made regarding preferred promoters, supports, and preparation conditions to obtain high selectivity and to maintain longer catalytic activity. Significant advances were made, particularly where methane-enriched fuel is desired regarding operating conditions, reactor design, and removal of catalyst poisons, especially sulphur compounds from the feed stream. These developments of catalysis are described systemetically by Greyson(1956) upto 1950 and by Mills and Steffgen(1974) from 1950 to 1973. Vannice(1976) gives a concise description of the catalytic research, occured during the 1970-75 period. A brief description of nickel based catalysts is given below:

4.1 Nickel

Although less active than ruthenium, Nickel has been by far the preferred active constituent in commercial catalysts for methanation of CO because of its relative cost, high activity for specific surface and selectivity.

Main drawbacks of Nickel based catalysts are:

(i) Readily poisoned by sulphur compounds.
(This fault is common to all of the more active methanation catalysts)

(ii) Nickel can react with CO to form nickel cabonyl, $Ni(CO)_4$, nickel carbide, Ni_3C or even free carbon.
(These faults can be avoided through the proper selection of reaction temperature and use of an excess of H_2 over the stoichiometric H_2/CO ratio 3:1.)

Commercial catalysts consist of rather high concentrations, (25-77 wt.%) of nickel disperesed on refractory support such as alumina or kieselguhr having high surface area. Mills and Steffgen(1974) list some noteworthy nickel based catalysts at different levels of development.

5.0 MODEL DEVELOPMENT

The mathematical model of the hot gas recycle methanation reactors system is developed assuming:

1. Steady state.
2. No temperature or concentration gradient in the radial direction of the reactor i.e. temperature and concentration are uniform at any cross section.
3. No axial heat and mass transfer due to axial temperature and concentration gradients.
4. Carbon dioxide is not hydrogenated directly; rather it is converted to carbon monoxide by reverse shift reaction.
5. Global rate expressions for CO methanation and shift reaction are used, neglecting heat and mass transfers within the catalyst and also from bulk phase to the catalyst.
6. Momentum balance is neglected in the reactor. Average pressure is used in all calculations.
7. Adiabatic reactor i.e no heat loss from the reactor wall.

5.1 Model Equations And Method Of Solution

The various chemical and physical processes taking place in the reactor can be described mathematically (Bird et al.,1960) by performing mass balances for CO and CO_2 and also an overall energy balance over a differential height Δz of the reactor (shown in fig.11).

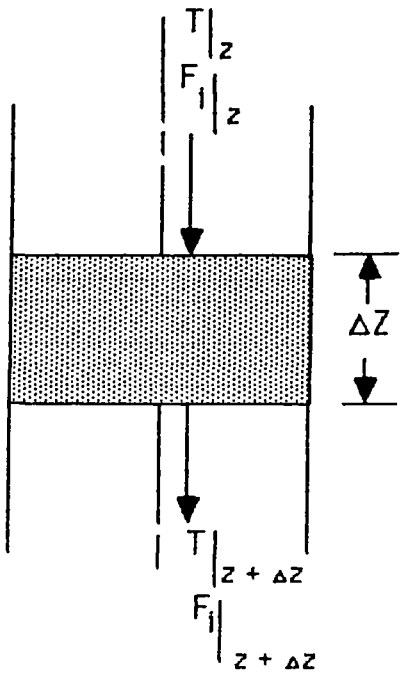

Fig. 11 Schematic diagram of a differential reactor height Δz for mass and energy balance

Mass balances:

1. For CO,

$$\frac{dF_{CO}}{dZ} = (r_1 + r_2) \qquad \ldots\ldots (17)$$

2. For CO_2,

$$\frac{dF_{CO_2}}{dZ} = r_2 \qquad \ldots\ldots (18)$$

Energy balance:

$$\frac{dT}{dZ} = \frac{\sum_{j=1}^{m} \Delta H_j r_j}{\sum_{i=1}^{n} F_i C_{pi}} \qquad \ldots\ldots (19)$$

These three coupled first order non-linear differential equations are solved simultaneously by a fourth order Runge-Kutta-Gill method (Carnahan et al., 1969) with the

following boundary conditions:

At $Z=0$ $\quad F_i = F_{io}$ and $T = T_o$

$Z = L$ (max. arbitrary reactor length) $\quad T < T_{max}$ and
calculated equilibrium constant x 10.
< experimental equilibrium constant.

Once the differential equations are solved the other components are determined from reaction stoichiometries.

6.0 FLOW DIAGRAM OF THE COMPUTER PROGRAM

The mathematical representation of the methanation reactor is translated into a computer program. This program can be summarized by the following flow diagram:

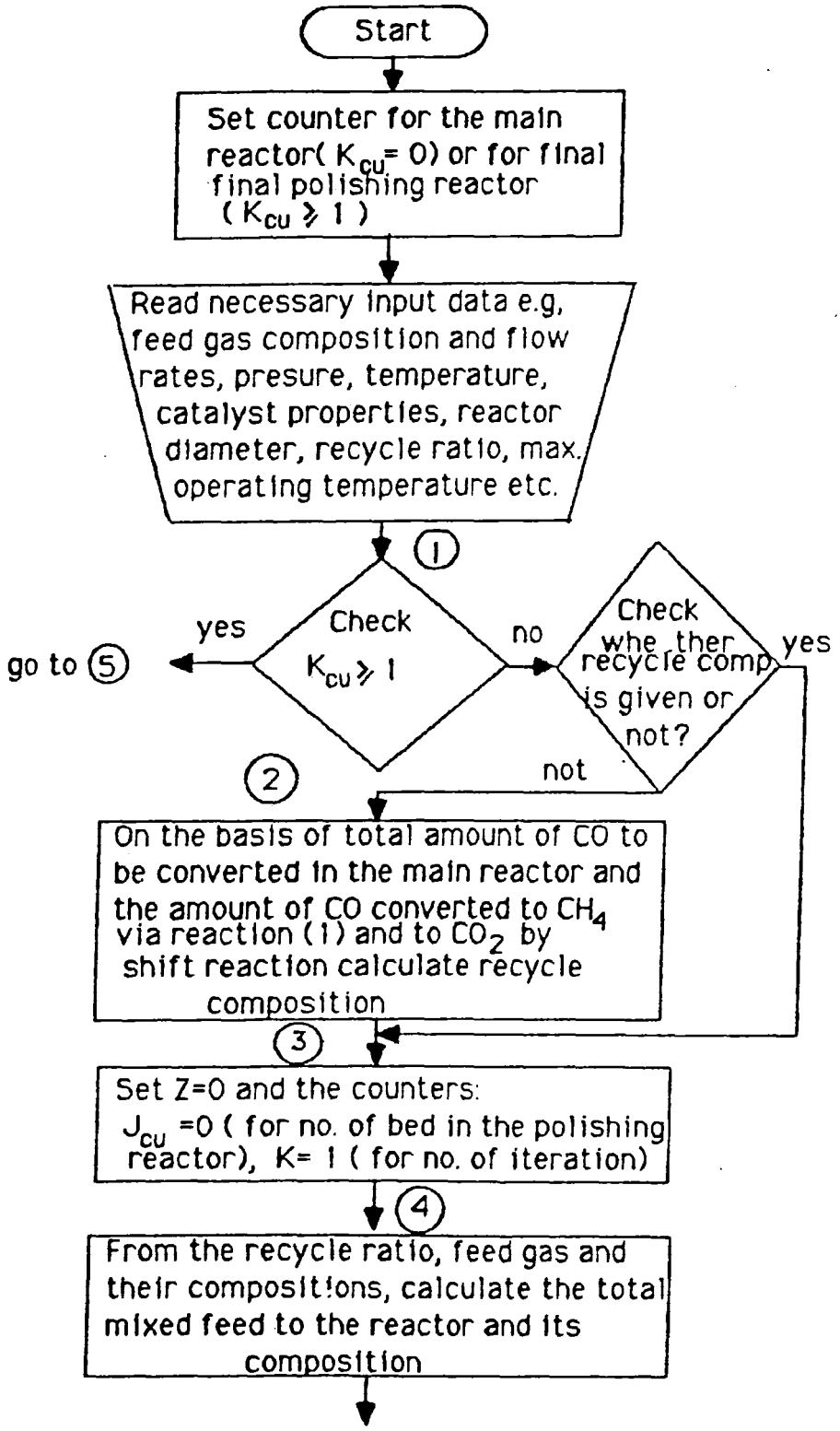

cont..

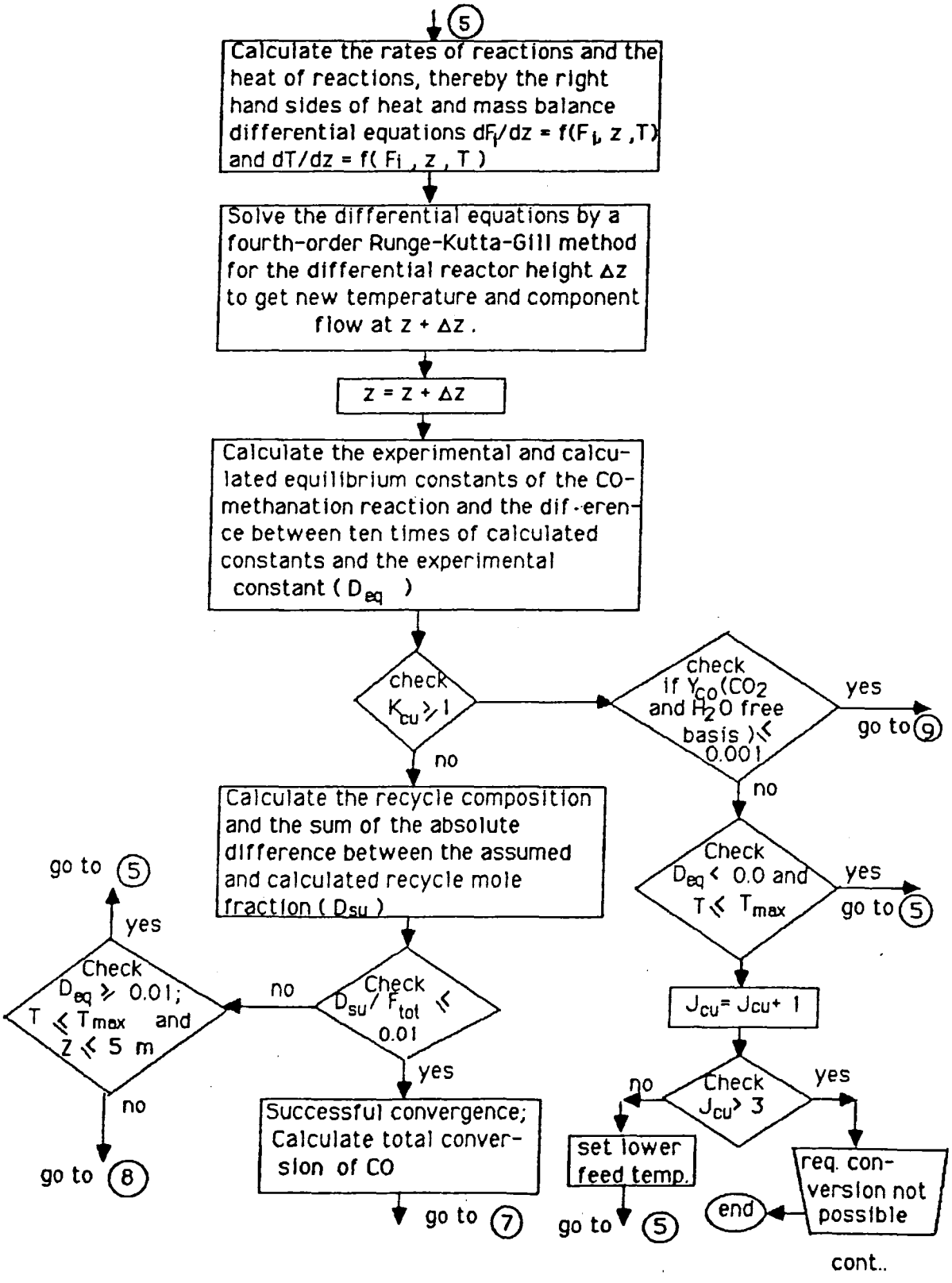
5
Calculate the rates of reactions and the heat of reactions, thereby the right hand sides of heat and mass balance differential equations $dF_i/dz = f(F_i, z, T)$ and $dT/dz = f(F_i, z, T)$
Solve the differential equations by a fourth-order Runge-Kutta-Gill method for the differential reactor height Δz to get new temperature and component flow at $z + \Delta z$.
$z = z + \Delta z$
Calculate the experimental and calculated equilibrium constants of the CO-methanation reaction and the difference between ten times of calculated constants and the experimental constant (D_{eq})
check $K_{cu} \geq 1$
yes
check if Y_{CO} (CO_2 and H_2O free basis) $\leq$ 0.001
yes
go to 9
no
Calculate the recycle composition and the sum of the absolute difference between the assumed and calculated recycle mole fraction (D_{su})
Check $D_{eq} < 0.0$ and $T \leq T_{max}$
yes
go to 5
$J_{cu} = J_{cu} + 1$
Check $D_{su} / F_{tot} \leq$ 0.01
no
yes
Check $D_{eq} \geq 0.01$; $T \leq T_{max}$ and $Z \leq 5$ m
yes
go to 5
no
go to 8
Successful convergence; Calculate total conversion of CO
go to 7
Check $J_{cu} > 3$
no
yes
set lower feed temp.
go to 5
req. conversion not possible
end
cont..

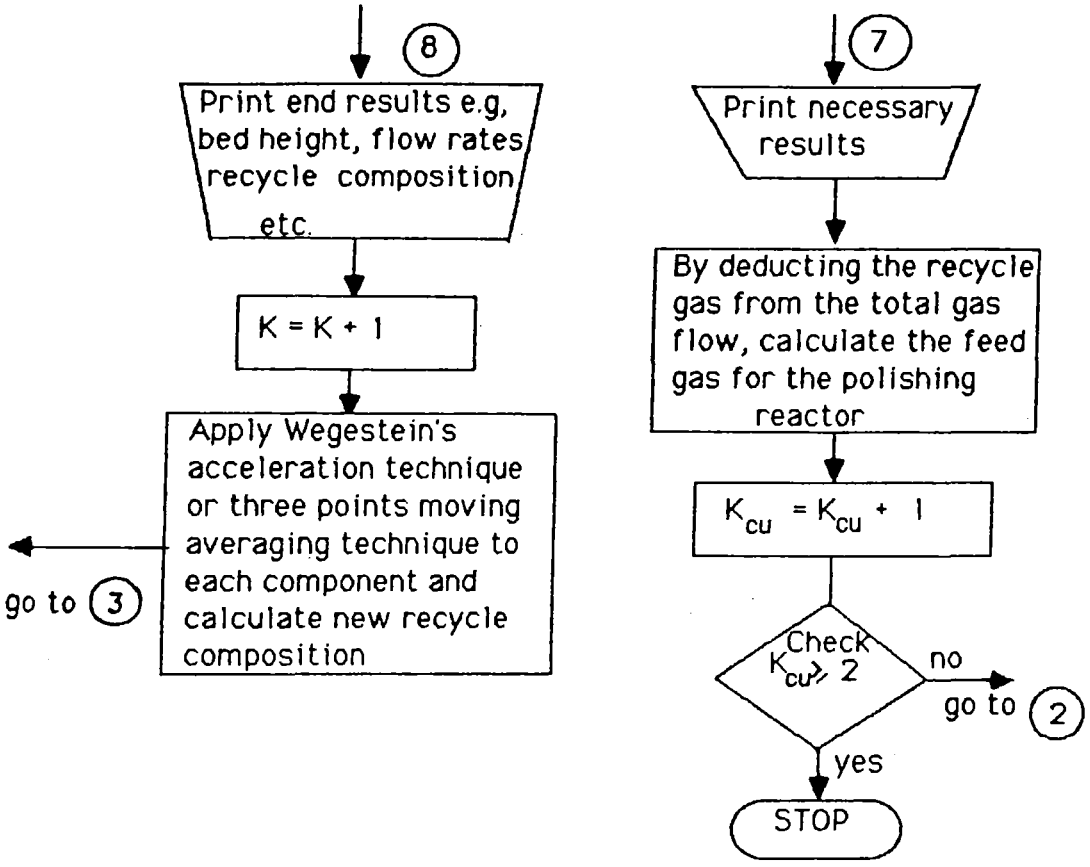

Fig. 12 Flow diagram of the methanation reactors system process module.

7.0 RESULTS AND DISCUSSIONS

The model was used to design a methanation reactor system capable of producing 7.08×10^6 m^3/day SNG (250×10^6 ft^3/day) from purified synthesis gas obtained by coal gasification on the basis of following assumptions:

1. The system consists of one main recycle reactor and one single or multibed polishing reactor, with interstage cooling, (max. no. of bed is 5) (flow diagram is shown in fig.5).
2. Maximum amount of catalyst used in the main reactor is equal to 42410 kg (typical reactor dimensions; 3m ID, 5m tan to tan height).
3. Maximum allowable bed temperature is 755 K.
4. In the case of the main reactor, if assumption no.2 or assumption no.3 is violated or the calculated equilibrium constant (calculated from component mole fractions) of CO methanation reaction(1) comes within 1/10th of the experimental equilibrium constant (calculated from theoretical equilibrium constant expression), the methanated gas is passed through the polishing reactor.
5. In the case of the polishing reactor, if assumption no.3 or the calculated equilibrium constant of reaction(1) comes with in 1/10th of the experimental equilibrium constant, new bed with interstage coling is used.
6. The catalysts in the reactors is adjusted in accordance with the actual and the required SNG production.
7. When the mole fraction of CO (H_2O and CO_2 free basis) becomes less than or equal to 0.1%, calculation stopped.

Operating conditions and results are shown in table 2. Typical composition profiles and temperature profile in the main reactor are shown in fig. 13 and fig. 14.

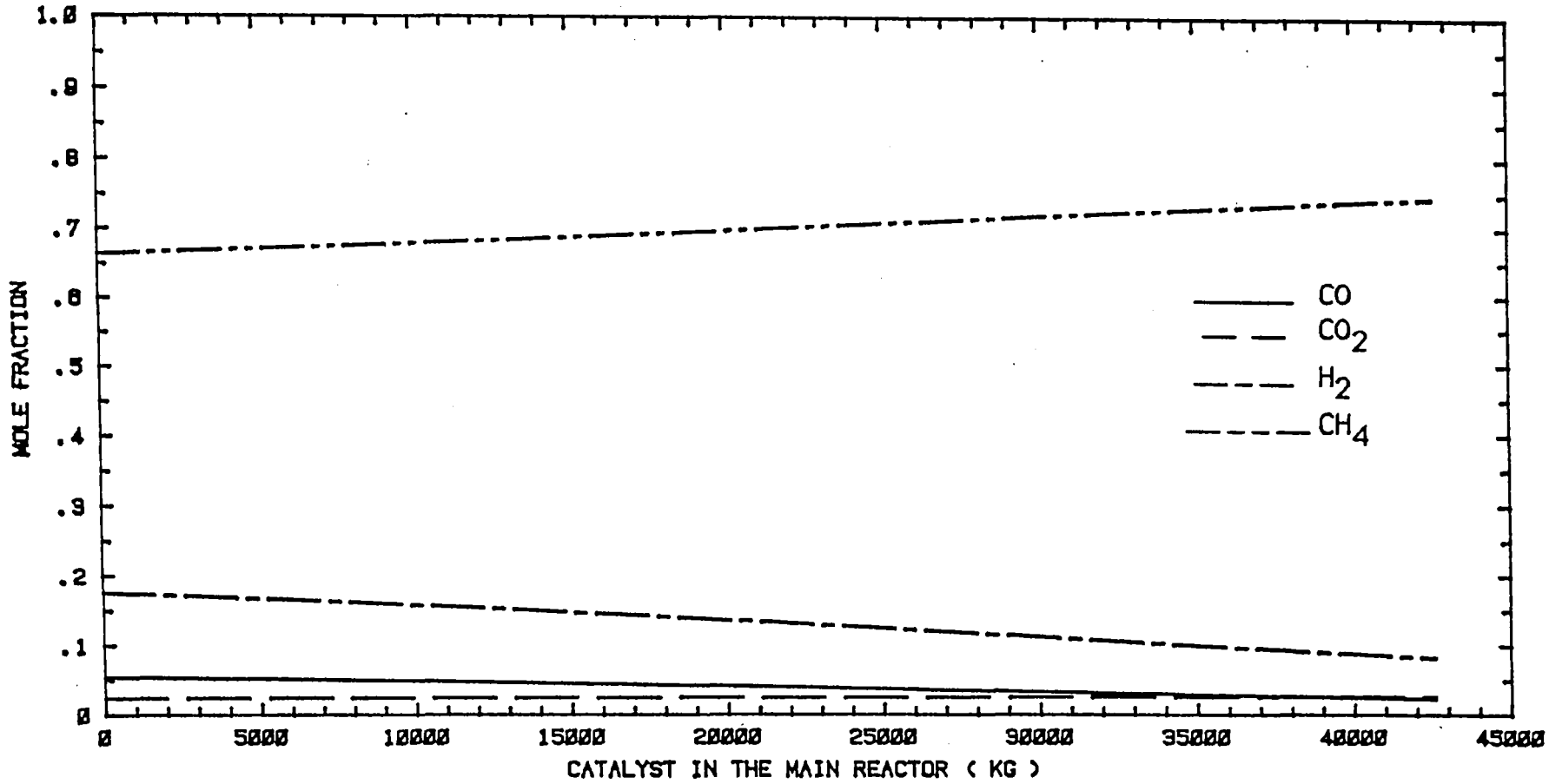

Fig. 13 Composition profiles in the main methanation reactor for the conditions of table 2.

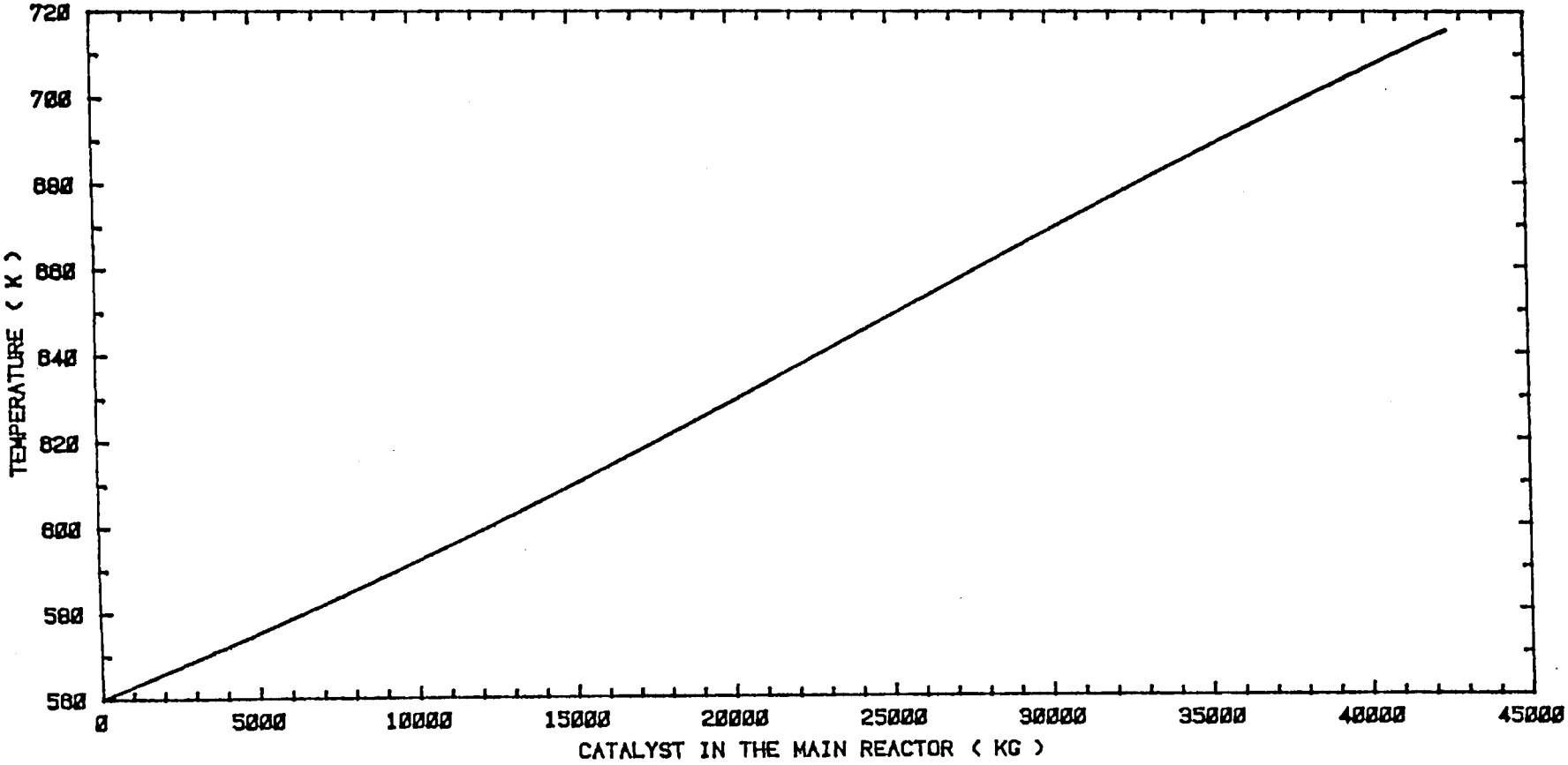

Fig. 14 Temperature profile in the main methanation reactor for the conditions of table 2.

Table 2. Operating conditions and results for the base case design of methanation reactors system.

Fresh make up feed rate	:	9.93 kmol s^{-1}
Feed gas composition:		Mole fraction
CO	:	0.21
CO_2	:	0.01
H_2	:	0.63
CH_4	:	0.134
H_2O	:	0.001
N_2	:	0.015
Main reactor inlet gas temp.	:	560 K
Average operating pressure of the reactor	:	7440 kPa
Catalyst : Hirshaw Nickel based Catalyst bulk density	:	1200 kg m^{-3}
Recycle ratio (Recycle/ Fresh make up feed, mole $mole^{-1}$)	:	5
Mole fraction of H_2O in the mixed feed to the main reactor	:	0.05
Polishing reactor inlet feed temp.	:	560 K
Mole fraction of H_2O in the feed to the polishing reactor	:	0.001
SNG production	:	7.08 x 10^6 m^3/day
SNG compositions :		Mole fraction (dry basis)
CO	:	0.001
CO_2	:	0.010
H_2	:	0.017
CH_4	:	0.932
N_2	:	0.040
Total catalyst required	:	58395 Kg
No. of bed needed in the polishing reactor	:	1

The model was also used to test the effects of different operating variables e.g., recycle ratio, main reactor inlet gas temperature, polishing reactor inlet gas temperature, H_2O level in the mixed feed to the main reactor, H_2O level in the feed to the polishing reactor, H_2/CO ratio in the make up feed, CO_2 level in the make up feed on methanation reactors system performance.

7.1 The effects of recycle ratio on reactor performance

Effects of recycle ratio on reactor performance are shown in table 3 for the conditions of table 2. (except those mentioned in table 3)

Table 3. The effects of recycle ratio on reactor performance.

	Recycle ratio			
	3	4	5	6
Fresh feed needed, kmol s^{-1} :	9.94	9.91	9.93	9.95
Catalyst used in the main reactor, kg :	5645	39808	39725	39815
Main reactor Exit temperature, K :	755	748	716	693
% of total CO in the fresh make up feed converted in the main reactor :	67.04	96.56	95.10	94.05
Equilibrium constants; Experimenal :	1.7×10^{6}	2.4×10^{6}	1.4×10^{7}	5.61×10^{7}
Calculated :	9.975	1.6×10^{4}	5.0×10^{3}	2.45×10^{3}
Catalyst required in the polishing reactor, kg :	29100	20617	18671	18315
No. of bed needed in the polishing reactor :	4	1	1	2
Total catalyst needed, kg :	34745	60426	58396	58130
Reasons for multiple beds in the polishing reactor :	Max. allowable temp. violation. —		— Equilibrium violation	

It is obvious from table 3 that:

— Better reactor performance in terms of catalyst requirement and reactor operation lies around recycle ratio equal to 5.

— Although the catalyst requirement in the case of a recycle ratio of 3 is much less than the other cases because of higher reactant concentrations, it would be difficult to operate the reactors because of a much higher temperature level and also due to the added complications of mutlistage operation.

It would be worthwhile to see the effects of a larger main reactor in case higher recycle ratio (more than 5) and the

effects of lower bed inlet temperature in case of lower recycle ratio (less than 4) on reactors performance

7.2 The effects of main reactor feed inlet temperature on methanation reactor performance

The effects of main reactor feed inlet temperature on reactor performance are shown in table 4 for the conditions of table 2.

Table 4. Effects of main reactor inlet temperature on reactor performance.

	Main reactor feed inlet temp. (K)				
	500	520	540	560	600
Fresh feed needed, kmol s^{-1}	9.96	9.95	9.94	9.93	9.90
Catalyst used in the main reactor, kg	39845	39815	39785	39725	39699
Main reactor Exit temperature, K	659	678	697	716	752
% of total CO in the fresh make up feed converted in the main reactor	90.1	92.2	93.9	95.1	96.9
Equilibrium constants; Experimenal	5.0×10^{8}	1.4×10^{8}	4.3×10^{7}	1.4×10^{7}	1.9×10^{6}
Calculated	484	1.1×10^{3}	2.5×10^{3}	5.0×10^{3}	1.9×10^{4}
Catalyst required in the polishing reactor, kg	31477	27074	19495	18671	20919
No. of beds needed in the polishing reactor	2	2	2	1	1
Reasons of multiple beds in the polishing reactor	Max. temp and equilb. vilolations.	Equilb. violation.		—	—
Total catalyst needed, kg	71322	66889	59280	58396	60618

It is evident from table 4 that:

___ The best reactor performance is obtained about a main reactor feed inlet temperature of 560 K.

___ Since the calculated equilibrium constant is far away from the experimental equilibrium constant (except in case of 600 K), higher inlet temperature (more than 540 K) favors the reactors performance.

It may be worthwhile to examine the effects of higher inlet temperature (more than 560 K) for the polishing reactor on reactor performance in case 600 K main reactor feed inlet temperature.

7.3 The effects of Polishing reactor feed temperature on reactor performance

The effects of polishing reactor feed temperature on reactor performance are shown in table 5 for the conditions of table 2.

Table 5. Effects of Polishing reactor feed temperature on reactorsd performance.

	Polishing reactor feed temp. (K)				
	500	520	540	560	600
Fresh feed needed, Kmol S^{-1} :	9.92	9.92	9.92	9.93	9.92
Catalyst required in the polishing reactor, kg :	31608	26208	21919	18671	14778
No. of bed needed in the polishing reactor :	1	1	1	1	2
Reasons for mulibeds in polishing reactor :	—	—	—	—	Equilib. violation.
Total catalyst needed, kg :	71476	66076	61786	58396	54504

It is evident from the table 5 that:

— Better overall reactor performance lies around 560 K polishing reactor feed temperature in terms of catalyst requirement and polishing reactor operation.

— If the polishing reactor feed inlet temperature is raised too high e.g., to 600 K or higher, polishing reactor performance improves but at the cost of multibed operation with added operation problem.

7.4 The effects of H_2/CO ratio in the fresh make up feed on reactor performance

The effects of H_2/CO ratio in the fresh make up feed on overall reactor performance are shown in table 6 for the condition of table 2.

Table 6. Effects of H_2/CO ratio on overall reactors performance; (CO, CO_2, H_2O, N_2 are kept constant, H_2 varies according to the required ratio; rest is balanced by CH_4.)

	H_2/CO mole ratio		
	2.93	3.0	3.14
Fresh feed needed, kmol s^{-1}	Required conversion of CO is not possible because of equilibrium violation.	9.93	9.95
Catalyst used in the main reactor, kg		39725	39985
Main reactor Exit temperature, K		716	721
% of total CO in the fresh make up feed converted in the main reactor		95.1	96.2
Equilibrium constants; Experimenal		1.4×10^7	1.0×10^7
Calculated		5.1×10^3	1.4×10^2
Catalyst required in the polishing reactor, kg		18671	12108
No. of bed needed in the polishing reactor		1	1
Total catalyst needed, kg		58396	52095
Residual hydrogen in the purified product (mole frac., dry basis)		0.017	0.098

It is evident from table 6 that:

__ The best reactor performance occurs about a ratio of 3 (stoichiometric H_2/CO ratio for CO methanation reaction (1).

__ If H_2/CO ratio in the fresh feed is below 3, required CO conversion will be difficult to meet.

__ At higher H_2/CO ratios (more than 3), though the catalyst requirements are comparatively lower because of higher methanation rate, higher residual hydrogen is left in the final SNG product making it dangerous to use.

7.5 The efffects of CO_2 concentration in the make up feed on reactor performance

The effects of CO_2 level in the make up feed on reactor performance are shown in table 7 for the conditions of table 2. (CO, H_2, H_2O, N_2 are kept constant in the make up feed, rest is balanced by CH_4).

Table 7. Effects of CO_2 level in the make up feed on reactors performance.

	CO_2 mole fraction in the make up feed		
	0.01	0.02	0.05
Fresh feed needed, kmol s^{-1} :	9.93	10.23	11.21
Catalyst used in the main reactor, kg :	39725	41081	45050
Main reactor Exit temperature, K :	716	716	718
% of total CO in the fresh make up feed converted in the main reactor :	95.1	95.3	95.7
Equilibrium constants; Experimenal :	1.4×10^7	1.4×10^7	1.3×10^7
Calculated :	5.1×10^3	5.8×10^3	7.9×10^3
Catalyst required in the polishing reactor, kg :	18671	19640	22615
No. of bed needed in the polishing reactor :	1	1	1
Total catalyst needed, kg :	58396	60721	67665

It is evident from the table 7 that:

- CO_2 almost acts as an inert. Both make up feed and catalyst requirements increase with an increase in CO_2 in the make up feed.
- It is not wothwhile to decrease CO_2 level in the make up feed below 0.01 mole fraction level because it would be necessary to add CO_2 in the final product to maintain the required CO_2 level.

7.6 **The effects of** H_2O concentration in the mixed feed to the main reactor on reactor performance

The effects of H_2O concentration in the mixed feed to the main reactor on overall reactor performance are shown in table 8 for the conditions of table 2.

Table 8. Effects of H_2O concentration in the mixed feed to the main reactor on overall reactors performance.

	H_2O (mole frac.) in the feed to the main reactor		
	0.01	0.03	0.05
Fresh feed needed, kmol s^{-1} :	10.0	9.97	9.93
Catalyst used in the main reactor, kg :	40040	39874	39725
Main reactor Exit temperature, K :	714	715	716
% of total CO in the fresh make up feed converted in the main reactor :	95.0	95.0	95.0
Equilibrium constants; Experimenal :	1.5×10^7	1.5×10^7	1.4×10^7
Calculated :	2.7×10^3	3.8×10^3	5.1×10^3
Catalyst required in the polishing reactor, kg :	24024	19937	18671
No. of bed needed in the polishing reactor :	2	1	1
Reasons for multi beds in the polishing reactor :	Equilb. violation.	—	—
Total catalyst needed, kg :	64064	59811	58396

It is evident from table 8 that:

— Higher H_2O level in the main reactor feed improves the overall reactor performance, because more CO is converted via shift reaction thereby helped to meet the CO conversion criterion quickly.

— Higher H_2O level in the main reactor feed does not affect reactor performance adversely bacause the

calculated equilibrium constant of methanation reaction is far away from the experimental equilibrium constant.

If the rate expression were valid for a H_2O level more than 0.05 mole fraction, it would be wothwhile to see the effects of higher H_2O level on reactors performance.

7.7 **The effects of H_2O** concentration in the polishing reactor feed on reactor performance

The effects of H_2O concentration in the polishing reactor feed on reactors performance are shown in table 9 for the conditions in table 2.

Table 9. Effects of H_2O concentration in the polishing reactor feed on overall reactors performance.

	H_2O (mole frac.) in the polishing reactor feed		
	0.001	0.01	0.05
Fresh feed needed, kmol s^{-1} :	9.93	9.93	9.92
Catalyst used in the main reactor, kg :	39725	39885	39868
Catalyst required in the polishing reactor, kg :	18671	18592	19219
Equilibrium constants at the exit of polishing reactor :			
Experimenal :	2.7×10^8	2.9×10^8	3.7×10^8
Calculated :	3.6×10^6	4.9×10^6	1.1×10^6
No. of bed needed in the polishing reactor :	1	1	1
Total catalyst needed, kg :	58396	58477	59087

It is evident from the table 9 that:

__ H_2O concentration (mole frac. 0.001 to 0.05) in polishing reactor feed does not affect the reactor

performance significantly.

__ At 0.05 mole frac. H_2O level the calculated equilibrium constant of methanation reaction(1) at the exit of polishing reactor comes closer to the experimental value.

8.0 CONCLUSIONS AND SUGGESTIONS FOR FURTHER WORK

Almost all the varibles considered in the discussion section e.g recycle ratio, main reactor feed inlet temperature, polishing reactor feed inlet temperature, H_2/CO ratio and CO_2 level in the make up feed, H_2O level in the mixed feed to the main reactor affect the methanation reactor performance significantly. By analyzing the results, it is possible to use the trends of operating and process conditions for better and efficient operation of the methanation reactors.

Limitations and suggestions for further work

- Although the rate expressions used in this work have been tested in laboratory measurements under widely different conditions, there are no data available in the open literature to validate the model results for a full scale reactor system.
- Just by changing one variable at a time, it will be very difficult to pinpoint quantitatively the optimum operating conditions of the methanation reactors system because of varied nature of the effects of different variables on reactors performance at different levels. Optimum operating conditions can be obtained by optimizing the total annual operating cost of the methanation system over the acceptable domains of the variables concerned as has been done for shift reactors in chapter V.

More works should be done in the following area:

- Testing the rate expressions under industrially comparable conditions.
- Analyzing the deactivation behavior of the catalyst with the age of use under industrially comparable conditions.
- Modifying the intrinsic rate expressions to global rate expressions by using effectiveness factors and/or by using appropriate parameters in the rate expressions.
- Examining the effects of CO_2 and H_2O levels in the feed on reactor performance in more detail.

9.0 NOMENCLATURE

$A, A', B, B', D, E, k, k'$ = Constants in rate expresions.

C_{pv} = Average sp. heat of the gaseous mixture, kJ $kmol^{-1}$ K^{-1}

C_{pi} = Specific heat of component i, kJ $kmol^{-1}$ K^{-1}

C_a = Concentration of CO, kmol m^{-3} (o refers to initial condition)

ΔZ = Differential bed height, m

ΔH_j = Heat of reaction j, kJ $kmol^{-1}$ (o refers to standard conditions; j=1 for reaction (1), j=2 for reaction (4))

F_i = Molal flux of component i, kmol m^{-2} s^{-1} (o, refers to initial condition; i=1 for CO, i=2 for CO_2, i=3 for H_2, i=4 for CH_4, i=5 for O_2, i=6 for H_2O, i=7 for C_2H_6, i=8 for H_2S, i=9 for N_2, i=10 for CH_3OH)

f = Fractional molal conversion of CO

G = Gaseous mass flux in the reactor, kg m^{-2} s^{-1}

K = Experimental equilibrium constant of reaction (1) in terms of mole fracion of components involved.

K_{ca} = Calculated equilibrium constant of reaction (1) in terms of mole fraction of components involved.

K_i = Constants for component i in the rate expression

P = Average reactor operating pressure, kPa

P_i = Partial pressure of component i, atm.

r_1, r_2 = Rate of reactions (1) and (4), kmol m^{-3} s^{-1}

r_{CH_4}, r_{CO_2} = rate of formation of CH_4 and CO_2 respectively, kmol m^{-3} s^{-1}

r_m = Rate of reation (1), kmol kg. cat^{-1} s^{-1}

R = Unversal gas constant, kJ $kmol^{-1}$ K^{-1}

S_c = BET surface area of the catalyst, m^2 kg^{-1}

T = temperature, K

u = Velocity of CO in the reactor, m s^{-1} (o refers to intial condition)

Y_i = Mole fraction of component i (* refers to equilibrium values)

Z = instantaneous bed height, m

Greek letters

ρ_c = Bulk density of the catalyst, kg m^{-3}(reactor)

ν_a = Stoichiometric coefficient for CO in reaction (1)

δ_a = Expansion coeffocient for CO in reaction (1)

10.0 REFERENCES

Agrawal, P. K, J. R. Katzer and W. H. Manogue, " Methanation over transition-metal catalysts. 4. Co/Al_2O_3. rate behavior and kinetic modeling", Ind. eng. chem. Fundam, vol.21, pp 385-390, (1982).

Allen, D. W and W. H. Yen, "Methanator design and operation", C.E.P, vol.69, no.1, pp 75-, (1973).

Bajpai, P. K, N. N. Bakhshi, Liu dan-chu and J. F. Mathews, "Methanation of carbon monoxide over alumina supported Ni-Cu catalysts", Cand. J. of chem eng. vol.60, pp 613-, (Oct,1982).

Bird, R. B, W. E. Stewart and E. N. Lightfoot, "Transport phenomena", chapters 9 and 17, John wiley & sons Inc., Wiley International edition, (1960).

Fischer, F, H. Tropsch, and P. Dilthey, Brennstoff-chem., vol.6, pp 265- , (1925).

Haynes, W. P, J. J. Elliot and A. J. Forney, "Experience with methanation catalysts", American chemical society, Div. of fuel chem., preprints of papers presented in the national meeting, Boston, Massachusettes, (April, 1972).

Haynes, W. P, R. R. Schehl, J. K. Weber and A. J. Forney, "The study of an adiabatic parallel plate methanation reactor", Ind. Eng. chem. Process Des. Dev., vol.16, no.1, pp 113-, (1977).

Hegarty, W. P and B. E. Moody, "Evaluating the Bi-Gas SNG process", C.E.P, vol.69, no.3, pp 37-, (1973).

Iammartino, N. R, "Methanation routes ready", Chemical Engg., Oct 14, pp 68-, (1974).

Kark, F. S, J. F. Shultz and R. B. Anderson, Ind. Eng. chem. prod. res. Devolop., vol.4, pp 265-269, (1965).

Kurita, H and Y. Tsutsumi, Nippon Kogaku Zasshi, vol.82, pp 1461-63, (1961).

Lee, A. L, "Methanation for coal gasification", symposium papers, "clean fuels from coal", Chicago, Illinois, pp 341-351, (Sep, 1973).

Mills, G. L and F. W. Steffgen, "Catalytic methanation", Catalysis reviews, Edited by H. Heinemann, vol.8, Mercell and Dekker, Inc., New york, pp 159-209, (1974).

Moeller, F. W, H. Roberts and B. Britz, "Methanation of coal gas for SNG", Hydrocarbon processing, pp 69-, (April,1974).

Rehmat, A and S. S. Randhava, Ind. Eng. chem. prod. res. develop., vol.4, pp 265-269, (1965).

Ross, J. R. H, "A modified kinetic expression for the carbon monoxide over group viii metal catalysts", J. of cat., vol.71, pp 205-208, (1981).

Sabatier and J. B. Senderens, C.R. Acad. Sci., Paris, vol.134, p 514- , (1902).

Schehl, R. R, J. K. Weber, M. J. Kuehta and W. P. Haynes, "Application of a diffusion limiting model to a tube-wall methanation reactor", Ind. Eng. chem. Process Des. Dev., vol.16, no.2, pp 227-, (1977).

Schlesinger, M. D, J. J. Demeter and M. Greyson, Ind. Eng. chem., vol.48, pp 68-70, (1956).

Senkan, S. M, L. B. Evans and J. B. Howard, "An analysis of the tube-wall reactor under diffusion limiting conditions", Ind. Des. Dev., vol.15, no.1, pp 184-187 (1976).

Shultz, J. F, F. S. Karn and R. B. Anderson, U.S Bureau of mines Rept. Invest. 6974, 20 pages, (1967).

Tart, K. R and T. W. A. Rampling, "Methanation key to SNG success", Hydrocarbon Proc., pp 114-, (April, 1981).

Vannice, M. A, "The catalytic synthesis of hydrocarbons from H_2/CO mixtures over the group viii metals", J. of catalysis, vol.37, pp 449-461, (1975); vol.37, pp 462-473, (1975); vol.44, pp 152-162, (1976).

Vatcha, S. R, "Analysis and design of methanation processes in the production of substitute natural gas from coal", Ph.D thesis, Chemical engineering, California institute of technology, Pasedona, California, (1976).

Wen, C. Y, P. W. Chen, K. Kato and A. F. Galli, "Optimization of fixed bed Methanation processes", Engg. Expt. station,West Virginia University, Morgantown, report 7, (March, 1969).

APPENDIX IV-A

Analysis of an adiabatic methanation reactor:

Basis : 1 Sec operation of a reactor producing 7.08×10^6 m^3/day SNG (250×10^6 scft/day).

Production (applying ideal gas law)= 3.46 Kmol S^{-1}(dry)

For a Lurgi dry ash coal gasifier, typical gas composition after shift conversion and purification is:

		mole %
CO	:	21.34
CO_2	:	0.3
H_2	:	64.02
CH_4	:	11.4
H_2O	:	0.1
N_2	:	2.84

H_2/CO = 3.0 mole $mole^{-1}$

Calculation of feed gas requirement:

Let X kmole of feed gas required

According to the specification of SNG(CO content < 0.01% on dry basis); so CO in dry SNG = 3.46 x 0.001 = 0.00346 kmol
Thus amount of CO converted in methanation reaction(1) =
(0.2134X - 0.00346) kmol

Products after methanation(assuming $CO + 3H_2 \rightarrow CH_4 + H_2O$) is the only reaction):

		kmole
CO	:	0.00346
CO_2	:	0.003X
H_2	:	0.0104
CH_4	:	0.3274X - 0.00346
H_2O	:	0.2144X - 0.00346
N_2	:	0.0284

Total dry product gas : 0.3588X + 0.0104 which is equal to 3.46

or, X = 9.615 kmol

So total feed gas to be used = 9.615 kmol

Calculation of total required conversion of CO:

Mole table at a fractional conversion of CO, f

		Initail feed(kmol)	Product(kmol)
CO	:	2.0518	2.0518(1 - f)
CO_2	:	0.0288	0.0288
H_2	:	6.1554	6.1554(1 - f)
CH_4	:	1.0962	1.0962 + 2.0518f
H_2O	:	0.0097	0.0097 + 2.0518f
N_2	:	0.2731	0.2731

Total product = 9.615 - 4.1026f(wet)
= 9.6053 - 6.1554f(dry)

According to CO mole fraction (dry basis) in SNG

2.0518(1 - f)/(9.6053 - 6.1554f) = 0.001

or, f = 0.999

Product moles table:

	kmoles	Mole fraction (wet basis)	mole fraction (dry basis)
CO	0.0021	0.0004	0.001
CO_2	0.0288	0.0052	0.008
H_2	0.0062	0.0011	0.002
CH_4	3.1459	0.5704	0.91
H_2O	2.0594	0.3734	---
N_2	0.2731	0.0495	0.079

Dry product gas = 3.4561 kmoles

Case I : For Adiabatic reactor

Applying the assumptions of plug flow reactor, the following mass and heat balance equations can be written:

Mass balance (for CO)

$$\frac{d(C_a u_z)}{dz} = \nu_a r_m \rho_c \qquad \ldots\ldots \quad (A\text{-}1)$$

where,

$$u_z = u_o\,(1 + \delta_a f) T/T_o$$

$$C_a = N_a/V = \frac{N_{ao}\,(1 - f)}{V_o\,(1 + \delta_a f) T/T_o}$$

$$= \frac{C_{ao}\,(1 - f)\,T_o}{(1 + \delta_a f)\,T}$$

$$\nu_a = -1 \text{ (for CO)}$$

So eqn. (A-1) becomes

$$\frac{C_{ao} u_o}{\rho_c} \frac{df}{dz} = r_m \qquad \ldots\ldots\ldots \quad (A\text{-}2)$$

Energy balance:

$$G \frac{d(C_p T)}{dz} = r_m \rho_c (-\Delta H_1) \qquad \ldots\ldots \quad (A\text{-}3)$$

where , G = Mass velocity of feed gases, kg m^{-2} s^{-1}
using 2m reactor diameter, G = 30.683

Calculation of average specific heat of the gaseous mixture:

$$C_{pv} = X_i\, C_{p,i} \,/\, M_v$$

Thus $C_{pv}\,(f=0) = 2.704 + 8.931 \times 10^{-4} T - 9.182 \times 10^{-8} T^2 + 6.052 \times 10^{-11} T^3$

$$C_{pv}\ (f=1) = 1.412 + 1.724\times10^{-3}T + 6.77\times10^{-7}T^2 - 4.745\times10^{-10}T^3$$

Temperature range, 533 - 755 K
so average temperature = 644 K

Thus, C_{pv} (f=0, 644 K) = 3.257 kJ kg^{-1} K^{-1}

C_{pv} (f= 1, 644 K) = 2.676 kJ kg^{-1} K^{-1}

So the average specific heat value of the gaseous mixture

= 2.967 kJ kg^{-1} K^{-1}

Calculation of heat of reaction of methanation reaction(1) at temperature T

$\Delta H^0 = -2.0615 \times 10^5$ kJ $kmol^{-1}$

$$\Delta H_T = \Delta H^0 + \int ((C_p)_{prod} - (C_p)_{reac})\, dT$$

$$= -1.9 \times 10^5 - 60.764\ T + 1.953 \times 10^{-2}\ T^2 + 1.201 \times 10^{-5} T^3 - 6.279 \times 10^{-9}\ T^4$$

For the temperature range 530 - 755 K, ΔH_T can be represented with the linear relationship

$$\Delta H_T = -2.007 \times 10^5 - 28\ T$$

Calculation of $C_{ao}u_o$ (molal velocity of reactant CO)

= 0.6531 kmol CO m^{-2} s^{-1}

Combinining equations A-2 and A-3, and using rate expression of Lee(1973), One can get by applying finite difference technique

$$T = \frac{T_o + 1440.023\ (f - f_o)}{1 - 0.201\ (f - f_o)} \qquad \ldots\ (A\text{-}4)$$

Using T_o = 560 K and T = T_{max} = 755 K One can get from eqn. A-4, $(f - f_o)$ = 0.1225

Thus it is impossible to achieve the required CO conversion in a single adiabatic reactor.

Case II : Cold quench reactor

Assuming 10% of the total feed is used in the first bed

Then $G = 9.615 \times 0.1 \times M_v$ / Cross sectional area

$= 3.068 \text{ kg m}^{-2} \text{ s}^{-1}$

$C_{a0}u_0 = 0.9615 \times 0.2134$ / cross sectioanal area

$= 0.0653 \text{ kmol CO m}^{-2} \text{ s}^{-1}$

$C_{pv} = 2.967 \text{ kJ kg}^{-1} \text{ K}^{-1}$

$\Delta H_T = -2.007 \times 10^5 - 28 \text{ T kJ kmol}^{-1}$

Thus again combining eqn. A-2 and A-3 and using rate expression of Lee(1973) One can get assuming $T = T_{max}$ $(f - f_0) = 0.1225$

Calculation of cold shot after 1st bed:

Let X Kmoles (at 422 K) are required to bring down the temperature of the exit gases from 755 K to 560 K.

Making a heat balance at the quenching zone, One can get X = 1.372 kmol

Thus again combining eqn. A-2 and A-3 and assuming T = 755 K, one can get $(f-f_0) = 0.1335$

In the similar way, cold shot after 2nd bed = 3.269 kmol.

Thus it is evident that large number of beds are to be used to achieve the required CO conversion, which is impractical.

CHAPTER V

OPTIMIZATION OF THE REACTING SYSTEMS OF A COAL TO METHANOL PLANT

ABSTRACT

Using comprehensive process modules, developed in chapters I to III three cost studies have been performed for a 1200 tonne/day methanol-from-coal plant to observe the effects of different variables on the annual operating costs for:

(i) The Lurgi dry ash coal gasification system. (variables considered here are coal particle size, H_2O/O_2 and carbon/O_2.)

(ii) The Shift reactor system. Variables considered here are H_2O/CO in the feed, CO_2 concentration in the feed and feed gas inlet temperature. In addition constrained Box optimization technique (Box, 1965) was applied to determine the optimum operating conditions of the shift reactor system for different steam and catalyst costs.

(iii) The methanol synthesis section. (variables considered here are recycle ratio, feed/cold shot distribution in the beds).

TABLE OF CONTENTS

page

(i) ABSTRACT .....

1.0 INTRODUCTION V-1

1.1 Optimization in chemical plant design. V-1

2.0 MAIN ASSUMPTIONS IN THIS OPTIMIZATION V-4

3.0 LURGI DRY ASH GASIFICATION SYSTEM OPTIMIZATION V-7

3.1 Results and Discussions V-8

3.1.1 The effect of coal particle size on the annual operating cost of the gasification system. V-8

3.1.2 The effect of Steam/Oxygen ratio (mole/mole) ratio on the annual operating cost of the gasification system. V-9

3.1.3 The effect of Fixed carbon/Oxygen (mole/mole) ratio on the annual operating cost of the gasification system. V-9

3.1.4 The effect of gasifying medium inlet temperature on the annual operating cost of the gasification system. V-10

4.0 SHIFT REACTOR SYSTEM OPTIMIZATION V-12

4.1 Results and Discussions V-13

4.1.1 Part I. V-14

4.1.2 Part II. V-19

5.0 METHANOL SYNTHESIS SECTION OPTIMIZATION V-22

5.1 Results and Discussions V-24

5.1.1 The effect of recycle ratio (recycle/make up feed), mole/mole on the annual operating cost of the methanol synthesis section. V-24

5.1.2 The effects of feed/cold shot distributions in the reactor beds on the annual operating cost of the methanol synthesis section. V-25

6.0 CONCLUSIONS V-26

7.0 NOMENCLATURE V-27

8.0 REFERENCES V-32

9.0 APPENDICES :

APPENDIX V-A1: Module for a centrifugal compressor. V-34

APPENDIX V-A2: Module for a surface air cooler/condenser. V-36

APPENDIX V-A3: Module for a shell and tube heat exchanger. V-44

APPENDIX V-A4: Module for a distillation column. V-50

APPENDIX V-A5: Module for a process vessel. ... V-52

APPENDIX V-A6: Module for a gas liquid separator. V-55

1.0 INTRODUCTION

What is optimization ?

Optimization is the collective process of finding the set of conditions required to achieve the best result from a given situation. (Beveridge and schechter, 1970).

Application

Almost any problem in the design, operation of industrial processes can be reduced in the final analysis to the problem of determining the largest or smallest value of a function of several variables i.e to an optimization problem.

What is the need of optimization ?

In most aspects of industrial life, continual improvement is an important feature. Thus one may want to get the maximum production from given raw materials, the largest profit from a fixed investment, the minimum energy or utility usage for a fixed production, and so on. Optimization is a formal presentation of these ideas.

Precautions

- In many cases formal optimization methods are not worthwhile applying.
- Care should be taken about inaccurate data and over simplified assumptions.
- Care should be taken in the interpretation and application of optimization results.
  (It may be impossible to attain optimum conditions)

1.1 Optimization In Chemical Plant Design

Though the optimization theory has been extensively developed (Beveridge and Schechter, 1970; Himmelblau, 1972; Beightler, 1979) and is potentially very useful for design, it is not being used to a significant extent in industrial practices

(Westerberg, 1980). There are different reasons behind this, some of which are given below:

(i) Firstly, performance of plant optimization studies largely depends on the reliability and accuracy of the process models. It is a difficult and time consuming task to construct resonably accurate and reliable process models. Industry may not have enough technical manpower for this purpose.

(ii) Secondly, execution of an optimizer can be slow and costly particularly with processes requiring a large number of internal recycle calculations and for processes with large number of optimizing variables. The computing cost for finding optimum conditions of a chemical plant may be up to U.S $ 10000 per run (Westerberg, 1981).

Westerberg (1981) suggested the following characteristics of an optimization tool to increase its usefulness and acceptibility to the designer:

(i) The optimization program should be relatively inexpensive to execute, so that when errors are made, the designer can detect them easily and correct them without excessive cost.

(ii) The program should allow for any variable in the problem description to become the objective function.

(iii) Arbitrary constraints should be easy to add and detect.

(iv) Problem modification should be easy so the designer is not inhibited in making changes in the structure as new ideas occur. This requirement clearly suggests a flowsheeting format for the problem.

(v) As the designer builds up his problem, he should be able to use past answers to initiate the current search.

(vi) The designer should be able to evolve toward his problem definition and solution.

(vii) The designer should be able to view the optimization exercise as a learning exercise so he can be a

realistic critic of the final result. This suggests the system should not apper to be a black box to him. Easy access to the various numbers generated is required.

Meaningful communication with the user is necessary.

2.0 MAIN ASSUMPTIONS IN THIS OPTIMIZATION

(i) Base temperature for heat balance was taken as 298 K.

(ii) Appropriate lang factors were used to convert equipment cost to total investment cost.

(iii) Capital cost and and all utility costs were updated to 3rd. quarter of 1984 using Marshall and Swift all industry cost indexes.

(iv) 20% of total fixed capital investment was included as the annual capital charge in the annual operating cost of the system.

(v) The costs of all the vessels e.g. reactors, separators, distillation columns etc. were calculated assuming them as pressure vessels.

(vi) When actual production was different from the required production, then fixed capital costs were adjusted using 6/10th rule (Peters and Timmerhaus, 1980) whearas utility costs were adjusted proportionately comparing actual production to the required production.

(vii) Steam generating efficiency of the boilers was taken as 75%.

Cost data and other relevent data for optimization are given in table 1.

Table 1. Cost data (in U.S dollars for the year 1979) and other relevent data for this optimization study. (Peters and Timmerhaus, 1980; Backhurst and Harker, 1983; Rase, 1977; Chemical engg., Nov. 26, 1984; Wham, 1981)

Cost Data :

Steam (high pressure, more than 500 kPa) = 4.21×10^{-3} \$ kg^{-1}

Steam (low pressure, less than 500 kPa) = 2.10×10^{-3} \$ kg^{-1}

Electricity (purchased) = 0.05 \$ kWh^{-1}

Cooling water = 2.64×10^{-5} \$ kg^{-1}

Coal = 0.03 \$ kg^{-1}

Catalyst :

Shift = 1234 \$ m^{-3}

methanol = 1 \$ ton^{-1} of methanol

Inerts used in shift reactor = 561 \$ m^{-3}

Other relevent data:

Marshall and Swift all industry cost indexes: (Peters and Timmerhaus 1980)

For the year, 1979 = 561

For the 3rd quarter of 1984 = 811.2

Lang factors:

For reactors = 5.6

For boilers = 5.6

For heat exchangers = 3.5

For distillation columns = 4.0

For separators = 4.0

For compressors = 2.5

Direct field cost of one Lurgi gasifier = 7.86×10^{6}

Direct field cost of an Oxygen plant (capacity, 2177 tons/day) = 44.65×10^{6}

Utility requirement of Oxygen plant :

Steam = 2.20 kg kg^{-1} of O_2

Electricity = 0.485 kWh kg^{-1} of O_2

water = 130.0 kg kg^{-1} of O_2

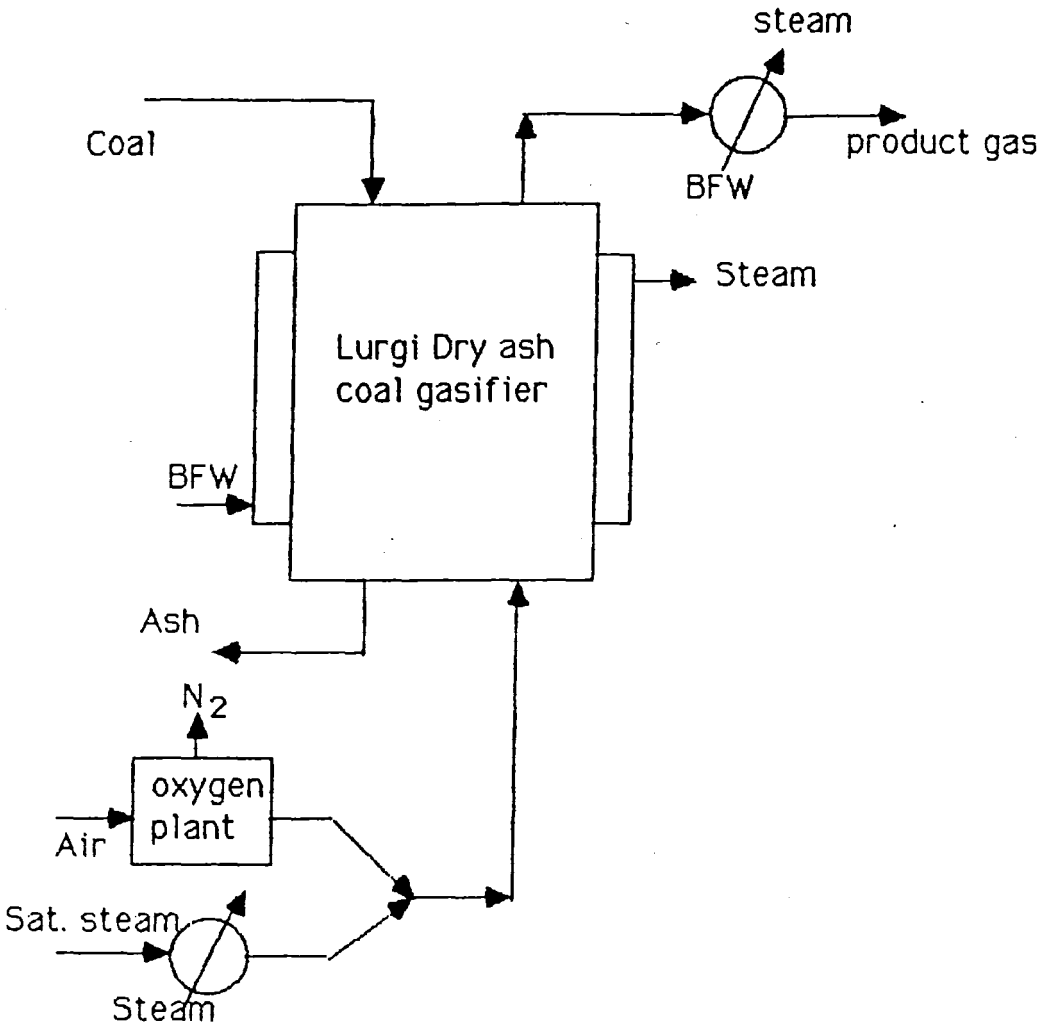

Fig. 1 Simplified flow diagram of the coal gasifier system

3.0 LURGI DRY ASH GASIFICATION SYSTEM OPTIMIZATION

The process module of the dry ash Lurgi coal gasifier, developed in chapter I has been used to optimize the annual operating cost of the gasification system (shown in fig. 1), producing synthesis gas for 1200 tonne/day methanol plant on the basis of following assumptions:

(i) The number of gasifiers were determined by dividing the total amount of CO + H_2 required for 1200 tonne/day methanol plant (which is equal to 1.8 kmol s^{-1} from table 7 of chapter III) by the amount of CO + H_2 produced by a single gasifier. For comparison, the number of gasifiers were not converted to whole number.

(ii) On the basis of the total number of gasifiers, requirement of raw materials, e.g. coal, oxygen and steam were determined.

(iii) Annual operating cost ($) of the gasification system was determined by the following expression:

$$C_{anopg} = C_{fg} + C_{cl} + C_{st} + C_{ox} + C_{ss} - C_{st} + C_{fb} - C_{sp} \quad \ldots(1)$$

where,

C_{fg} = annual fixed cost of the gasifiers. (Wham et al., 1981; Direct field cost was multiplied by a factor of 2 to get total investment cost)

C_{cl} = annual cost of coal

C_{st} = annual cost of saturated steam

C_{ox} = annual cost of oxygen (fixed and operating) (Wham et al., 1981; Backhurst and Harker, 1980, Direct field cost was multiplied by a factor of 2 to get total investment cost)

C_{ss} = annual steam equivalent cost of raising the temp. of saturated steam temperature to the required temp. (no cost was added for heat exchanger).

C_{st} = annual cost of steam recovered from the jackets of the gasifiers.

C_{sp} = annual cost of steam equivalent recovered from the heat content of the product gas (down to the condensing temperature of steam).

C_{fb} = annual fixed cost of waste heat boilers for the product gas.

3.1 Results And Discussions

The following variables were chosen for the minimisation of annual operating cost of the coal gasification system (shown in fig. 1).

(i) Coal particle size.

(ii) Steam/Oxygen ratio.

(iii) Fixed carbon in coal/Oxygen ratio.

(iv) Gasifying medium inlet temperature.

3.1.1 The effect of coal particle size on annual operating cost of the gasification system

The effect of coal particle size on annual operating cost of the gasification system is shown in table 2. (process conditions are the same as in fig. 9 of chapter I).

Table 2.

Particle size (m)	No. of gasifiers needed	Annual operating cost ($/year)
0.01	9.01	1.199×10^8
0.015	9.05	1.202×10^8
0.020	9.21	1.218×10^8

3.1.2 The effect of Steam/Oxygen ratio on annual - operating cost of the gasificaion system

The effect of Steam/Oxygen ratio on annual operating cost of the gasification system is shown in table 3. (process conditions are the same as in fig. 11 of chapter I.)

Table 3.

Steam/Oxygen ratio (mole mole^{-1})	No. of gasifiers needed	Annual operating cost ($/year)
7.0	9.01	1.199×10^8
8.0	9.40	1.254×10^8
9.0	10.00	1.334×10^8

3.1.3 The effect of Fixed carbon/Oxygen on annual - operating cost of the gasification system

The effect of Fixed carbon/Oxygen ratio on annual operating cost of the gasification system is shown in table 4. (process conditions are the same as in fig. 14 of chapter I).

Table 4.

Fixed carbon/ Oxygen ratio. (mole mole^{-1})	No. of gasifiers needed	Annual operating cost ($/year)
2.729	9.01	1.199×10^8
2.900	8.77	1.205×10^8
3.014	8.71	1.217×10^8

3.1.4 The effect of gasifying medium inlet temp. on - annual operating cost of the gasification system

The effect of gasifying medium inlet temperature on annual operating cost of the gasification system is shown in table 5. (process conditions are the same as in fig. 17 of chapter I).

Table 5.

Gasifying medium inlet temperature(K)	No. of gasifiers needed	Annual operating cost ($/year)
520	11.24	1.411×10^8
560	9.69	1.258×10^8
600	9.35	1.228×10^8
644	9.01	1.199×10^8

It is evident from tables 2 to 5 that :

- Annual operating cost of the gasification system decreases with the decrease in particle size, steam/O_2 ratio because of efficient carbon conversion.
- Annual operating cost of the gasification system increases with the increase in Fixed carbon/O_2 ratio, and with the decrease in gasifying medium inlet temperature because of less efficient carbon conversion.

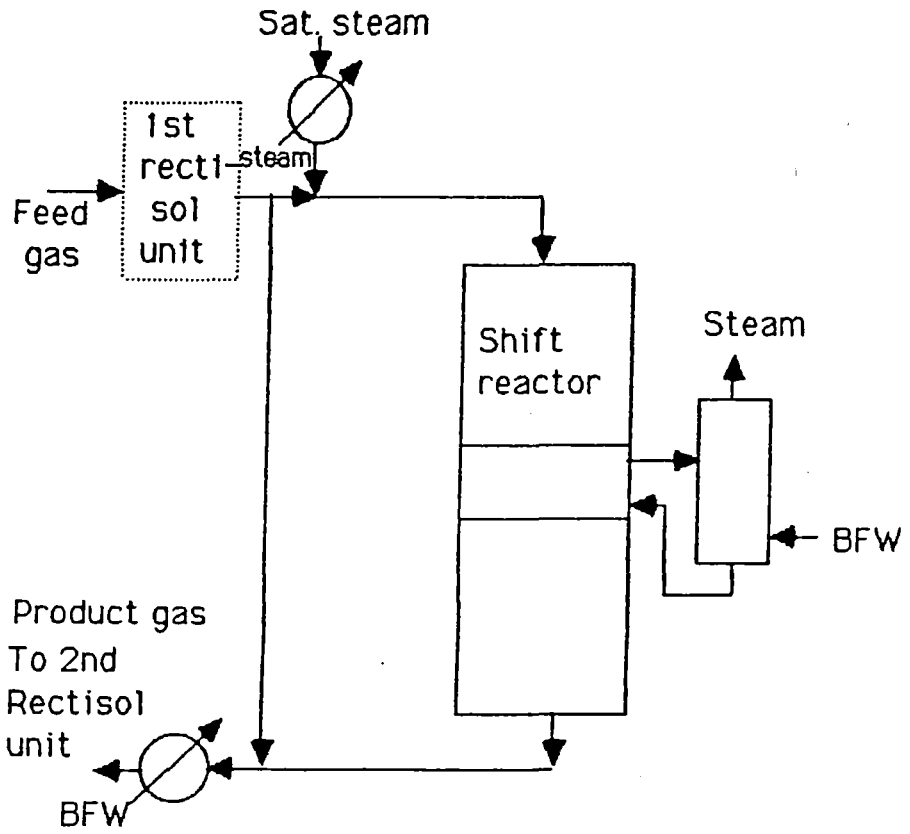

Fig. 2 Simplified flow diagram of the shift reactor system

4.0 SHIFT REACTOR SYSTEM OPTIMIZATION

The shift reactor module developed in chapter II was used to optimize the annual operating cost of the shift reactor system (shown in fig. 2), producing 2.5 kmol s^{-1} synthesis gas (H_2/($CO + CO_2$) = 3.05, CO/CO_2 = 1.87) suitable for the production of 1200 tons/day methanol on the basis of the following assumptions:

(i) Purified feed gas was first passed through a Rectisol unit to remove all H_2S and the necessary CO_2 from the the gas before passing through the shift reactor.

(ii) Purified feed gas was available at 500 K.

(iii) Shift catalyst life was 3 years (Rase, 1977).

(iv) 2500 kPa saturated steam was available for process steam. This process steam was heated to the necessary degree of superheat so that after mixing with the inlet feed gas, the temperature of the mixed gas could be raised to the required reactor inlet temperature.

(v) Costs of Rectisol units were not considered.

(vi) Maximum reactor I.D was taken as 3.5 m.

(vii) Minimum reactor I.D was taken as 2.5 m.

(viii) Maximum allowable pressure drop in the bed was taken as 150 kPa.

(ix) Minimum allowable pressure drop in the reactor bed was taken as 20 kPa.

(x) Even using max. reactor I.D, if the max. allowable pressure drop criterion was violated, more reactors in parallel were used.

(xi) Reactor I.D was changed until the pressure drop in the bed was within the allowable pressure drop criteria.

(xii) Pressure drop in the bed was converted to equivalent steam cost. Half of the normal steam cost was used for this purpose, assuming that the steam used in the

turbine used for driving the compressor could be used for other purposes after expansion.

(xiii) Annual operating cost of the shift reactor system was determined using the following expression:

$$C_{anops} = C_{sf} + C_{ss} + C_{ps} + C_{ct} + C_{in} + C_{fr} + C_{pr} - C_{rs} + C_{fb} \quad .... (2)$$

where,

C_{sf} = annual steam equivalent cost for the heat content of the feed.

C_{ss} = annual steam equivalent cost for raising the saturated steam temperature to the required superheat.

C_{ps} = annual cost of the process steam.

C_{ct} = annual cost of the catalyst.

C_{in} = annual cost of the inert. (used as catalyst support).

C_{fr} = annual fixed cost of the reactor.

C_{pr} = annual steam equivalent cost for the pressure drop in the reactor bed.

C_{fb} = annual fixed cost for the waste heat boilers. (interstage coolers and product cooler)

C_{rs} = annual recovered steam cost from the intermediate and final product gas.

4.1 Results And Discussions

For a fixed rate, the following three variables were chosen for optimization of the shift reactor sysrem:

(i) Steam/CO ratio in the feed.

(ii) Inlet feed temperature.

(iii) CO_2 concentration in the feed.

This optimization study was divided into two parts; in the first part the effects of different variables on the annual operating cost was studied, while in the second part a Box contrained optimization technique (Box, 1965; Kuester et al., 1973) was used to find the optimum operating conditions.

4.1.1 Part I -

The effect of Steam/CO ratio in the feed on annual operating cost of the shift reactor system

The effects of Steam/CO ratio ratio on the annual operating cost of the shift reactor system are shown in fig. 3 for two levels of inlet tempearture and for two levels of steam costs (process conditions are the same as in fig. 7 of chapter II).

It is evident from fig. 3 that :

- The annual operatiing cost is a strong function of Steam/CO ratio because process steam cost is the most predominant cost item in the annual operating cost.
- The minimum annual operating cost lies near a Steam/CO ratio of 0.8 (close to minimum ratio of 0.5) for all cases considered.
- With normal steam costs (given in table 1), the lower inlet temperature (520 K) is more favourable for the annual operating cost, whearas with lowe steam costs, the effect of inlet temperature on annual operating cost becomes less significant.

The effect of feed inlet temperature on the annual operating cost of the shift reactor system

The effects of feed inlet temperature on the annual operating cost of the shift reactor system are shown in fig. 4 for two levels of Steam/CO ratio, and for two levels of steam cost (process conditions are the same as in fig. 9 of chapter II).

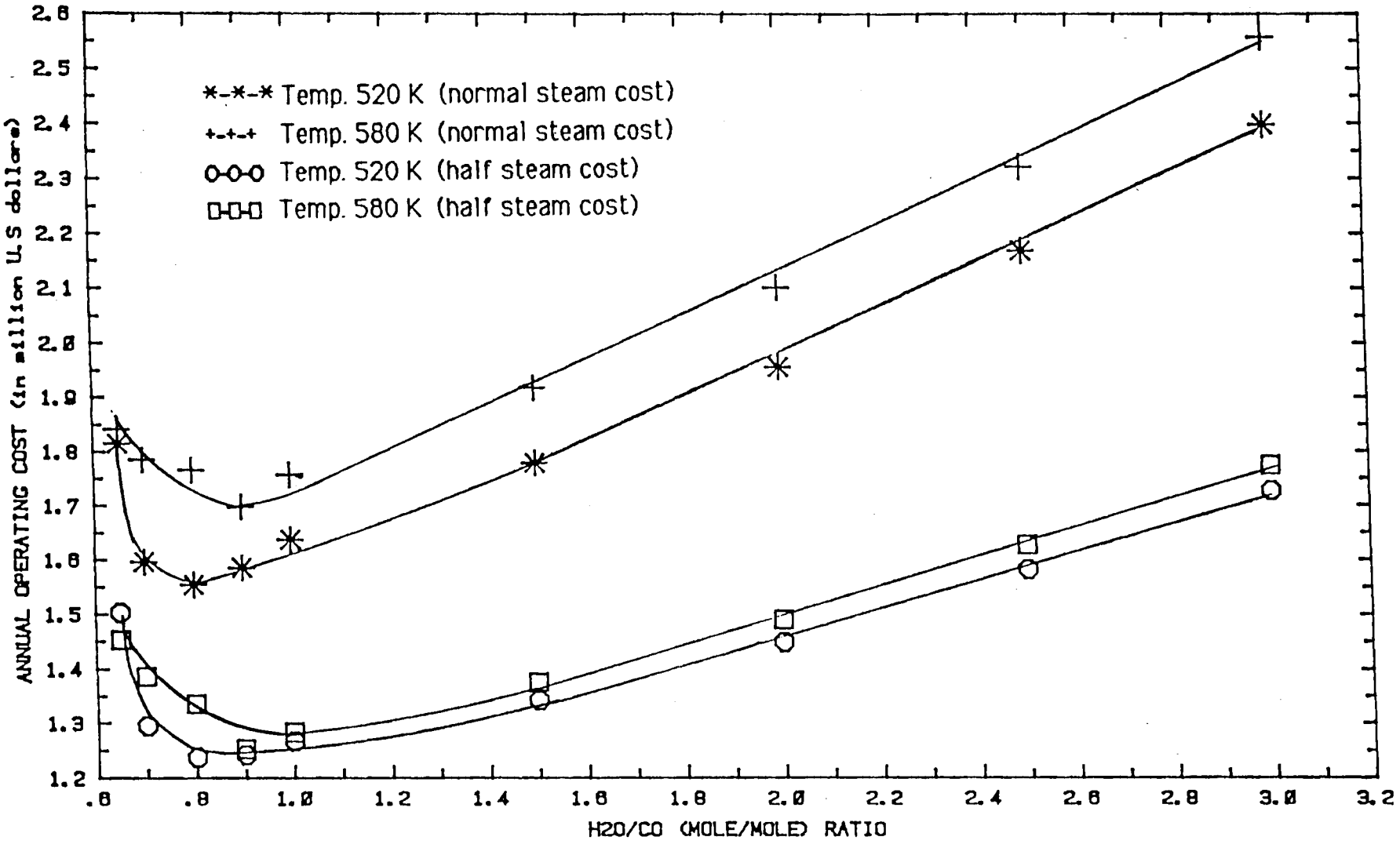

Fig. 3 Effect of H_2O/CO (mole $mole^{-1}$) ratio on annual operating cost of the shift reactor system for the conditions of table 1 and fig. 7 of chap. II.

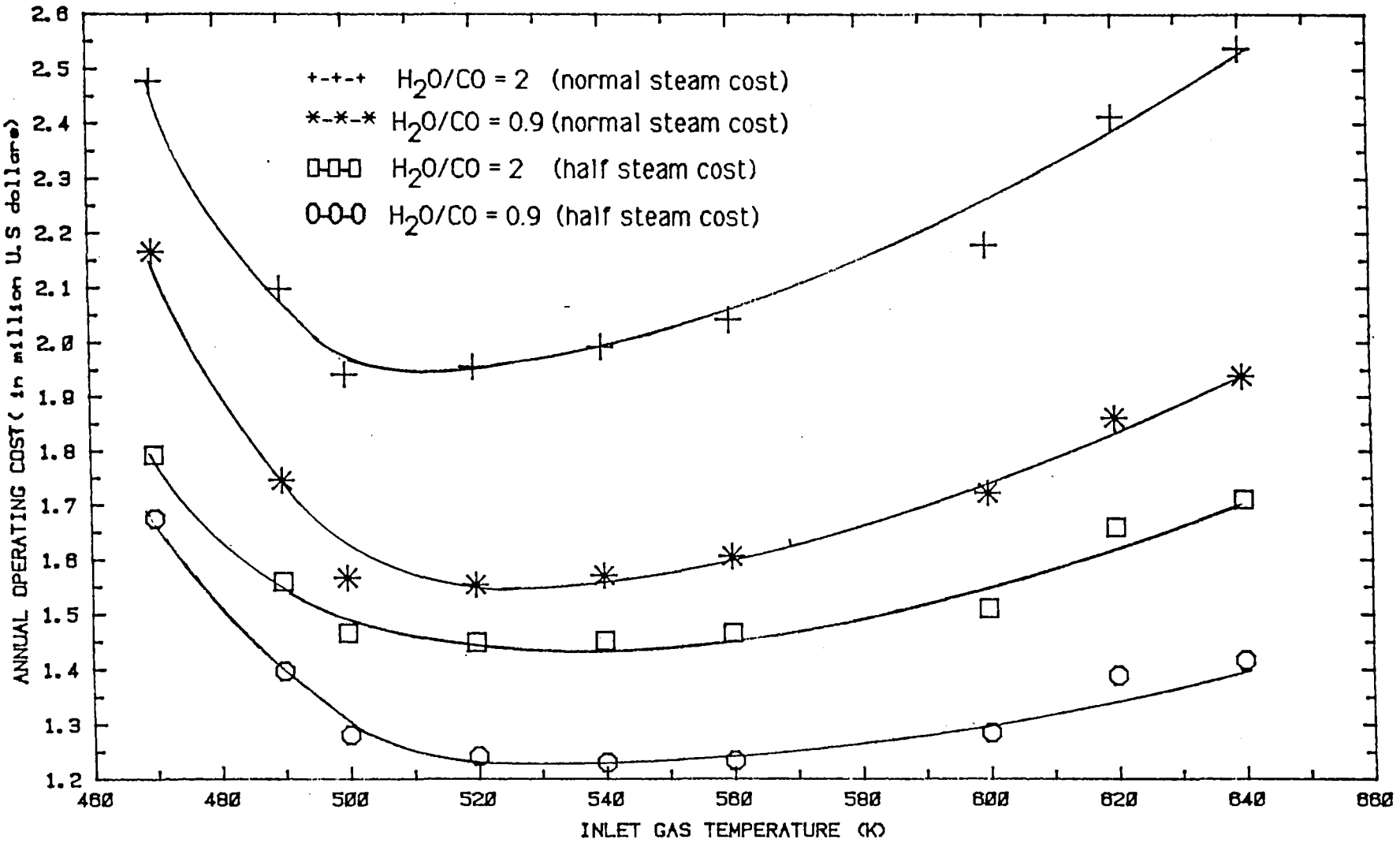

Fig. 4 Effect of feed inlet temperature on annual operating cost of the shift reactor system for the conditions of table 1 and fig. 9 of chapter II.

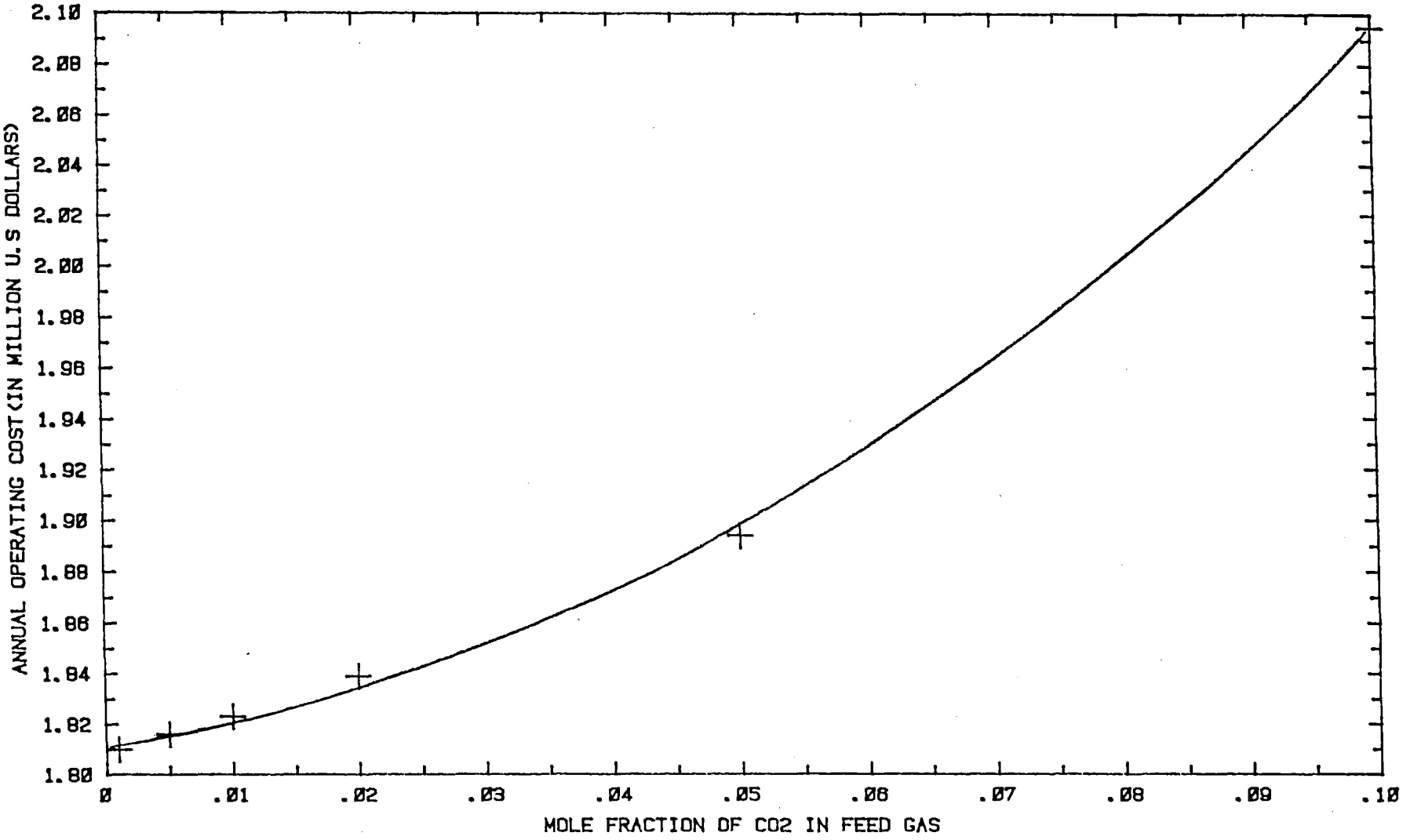

Fig. 5 Effect of CO_2 level (mole fraction) in the feed on annual operating cost of the shift reactor for the conditions of table 1 and fig. 11 of chap. II

It is evident from fig. 4 that:

___ Minimum annual operating cost lies between 500 K and 520 K feed inlet temperature for all cases considered.

___ Lower Steam/CO ratio favors the annual operating cost.

The effect of CO_2 concentration in the feed on the annual operating cost of the shift reactor system

The effect of CO_2 concentration in the feed on the annual operating cost of the shift reactor system is shown in fig. 5 (process conditions are the same as in fig. 11 of chapter II).

It is evident from fig. 5 that:

___ Annual operating cost of the shift reactor system decreases monotonically with the decrease in CO_2 concentration since costs of the Rectisol units are not considered.

___ The effect becomes less significant at lower CO_2 concentration.

4.1.2 Part II -

The parameter values used in the Box constrained optimization technique are given in table 6. The original program of the Box optimization technique is in Kuester et al., (1973).

Table 6. Parameters used in Box constrained optimization study

No. of explicit variables	:	3
No. of constraints	:	3
Total no. of points in the complex	:	6
Reflexion parameter (α)	:	1.3
Convergence parameter (β)	:	0.01
Explicit constraint violation Correction terms	:	
δ_1 (for Steam/CO ratio)		8×10^{-4}
δ_2 (for feed inlet temperature)		0.1
δ_3 (for CO_2 mole fraction in the feed)		5×10^{-5}
Convergence parameter (γ)	:	4
Feasible starting point	:	
Steam/CO ratio		0.8
Feed inlet temperature (K)		500
CO_2 mole fraction in the feed		0.01

Problem statement

Maximize $-C_{anops}$ (Steam/CO ratio, feed inlet temp., CO_2 mole fraction n the feed)

subject to,

$0.65 < \text{Steam/CO} < 3.0$

$480.0 < \text{Feed inlet temp.} < 640.0$

$0.001 < CO_2 \text{ mole fraction in the feed} < 0.05$

This problem was run on a Vax 11/730 computer with the results

given in table 7.

table 7. Results of optimixzation study of shift reactor system.

	Case I	Case II	Case III
	Normal cost data from table 1.	half the steam cost, all other costs are same as in case I.	half the steam cost, and double the catalyst cost, all other costs are same as in case I
Minimum annual operating cost (million $/year)	1.538	1.190	1.263
Optimum operating conditions:			
Steam/CO ratio:	0.804	0.841	0.843
Feed inlet temp. (K) :	506.9	544.4	570.5
CO_2 mole fraction in the feed :	0.011	0.0011	0.0031
Elapsed CPU time, hr:min. :	2:34	3:05	2:16

It is evident from table 7. that:

___ As the steam cost is halved, and the catalyst cost was doubled, optimum conditions move toward higher Steam/CO ratio, and higher feed inlet temperature, necessitating lower catalyst height.

___ Steam cost is the predominant item of the annual operating cost of the shift reactor system.

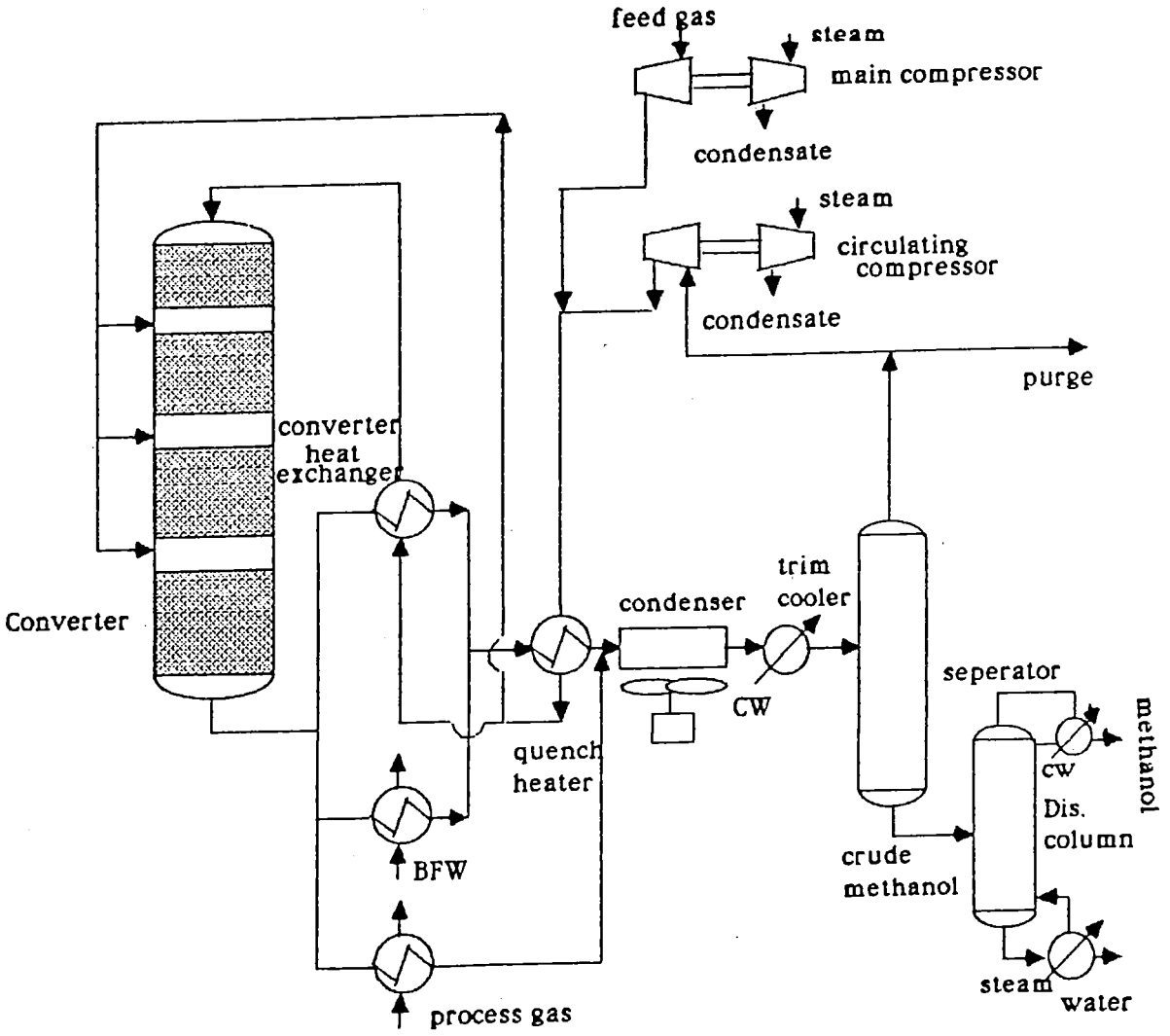

Fig. 6 Simplified flow diagram of ICI Low Pressure Methanol synthesis section

5.0 METHANOL SYNTHESIS SECTION OPTIMIZATION

The methanol reactor module described in chapter III, along with modules of presure vessels, heat exchangers, surface condensers, separators, distillation columns, and of compressors (given in Appendices V-A1 to V-A6) have been used to optimize the annual operating cost of the methanol synthesis section (shown in fig. 6) of a 1200 tonne/day methanol plant on the basis of the following assumptions:

(i) An ICI 4-bed quench reactor (dimensions given in table 7. of chapter III) was used.

(ii) All the studies have been started with a fixed feed rate of 2.5 kmol s^{-1} (compositions given in table 9. of chapter III).

(iii) The necessary amount of reactor exit gas was used in the in the converter heat exchanger and the rest was divided into two parts to be used in the BFW heat exchanger and in the process gas heat exchanger.

(iv) Fixed heat transfer coefficients from Bell, (1983) were used in heat exchanger calculations.

(v) 90% methanol produced was considered as recoverable product.

(vi) Annual operating cost ($) was determined using the following expression :-

$$C_{anopm} = C_{fr} + C_{fch} + C_{fbh} - C_{sbh} + C_{fph} - C_{sph} + C_{fqh} + C_{fsc} + C_{osc} + C_{ftc} + C_{cwt} + C_{fsp} + C_{fdc} + C_{opd} + C_{fcm} + C_{mnc} + C_{opc} \quad \ldots (3)$$

where,

C_{fr} = annual fixed cost of the methanol reactor, $

C_{fch} = annual fixed cost of the converter heat exchanger, $

C_{fbh} = annual fixed cost of the boiler feed water heat exchanger, $

C_{sbh} = annual recovered steam cost from the boiler feed water heat exchanger, $

C_{fph} = annual fixed cost of the process gas heat exchanger, $

C_{sph} = annual recovered steam cost from the process gas heat exchanger, $

C_{fqh} = annual fixed cost of the quench gas heat exchanger, $

C_{fsc} = annual fixed cost of the air surface condenser, $

C_{osc} = annual operating cost of the air surface condenser, $

C_{ftc} = annual fixed cost of the trim cooler, $

C_{cwt} = annual cost of cooling water used in trim cooler, $

C_{fsp} = annual fixed cost of the separator, $

C_{fdc} = annual fixed cost of the distillation column, $

C_{opd} = annual operating cost of the distillation column, $

C_{fcm} = annual fixed cost of the compressors, $

C_{mnc} = annual maintainence cost of the compressors, $

C_{opc} = annual operating cost of the compressors, $

5.1 Results And Discussions

The folowing variables were chosen for the annual operating cost optimization of methanol systhesis section:

(i) recycle ratio
(ii) distribution of feed/cold shot in the reactor beds.

5.1.1 The effects of recycle ratio (recycle/make up feed), on annual operating cost of methanol synthesis section

The effect of recycle ratio on annual operating cost of the methanol synthesis section is shown in table 8. (process conditions are same as in table 10. of chapter III).

Table 8. The effect of recycle ratio on annual operating cost of the methanol synthesis section.

Recycle ratio	Annual operating cost ($)
4.0	1.373×10^7
4.5	1.389×10^7
5.0	1.434×10^7

It is evident from table 8 that in spite of increase in methanol production with an increase in recycle ratio (table 10. of chapter III), the annual operating cost of the methanol synthesis section increases with the increase in recycle ratio because of an increase in operating costs as well as fixed costs.

5.1.2 The effect of feed/cold shot distribution in the reactor beds on the annual operating cost of methanol synthesis section

The effect of feed/cold shot distribution in the reactor beds on the annual operating cost of the methanol synthesis section is shown in table 9. (process conditions are same as in table 11 of chapter III).

Table 9. Effect of feed/cold shot distribution in the reactor beds on the annual operating cost of the methanol synthesis section.

Fraction of total mixed feed, fed into the first bed.	Annual operating cost ($/year)
0.38	1.382×10^7
0.40	1.389×10^7
0.42	1.397×10^7

It is evident from table 9 that annual operating cost of the methanol synthesis section increases with the increase in feed to the first bed because of comparatively lower production.

6.0 CONCLUSIONS

Merits and demerits of both perturbation type (studying the effects one variable at a time on objective function) and partial optimization are briefly mentioned below:

Merits

(i) These studies give a good idea of trends of change of the objectives e.g operating cost, profit etc. of the system under consideration with different variables, and thereby help in finding the important variables and their ranges worthy of further study using formal optimization techniques.

(ii) The results of perturbation type optimization study can be used to check the final converged solutions of formal optimization studies, because sometimes formal optimization techniques may converge to totally wrong values depending on the initial starting conditions, convergence criterion etc.

(iii) Because of comparatively less execution times, these studies can be used to check the robustness and reliability of individual modules of the system; which are essential for large plant optimization.

Demerits

(i) As the number of variables increase and their domain range increase, it can become very difficult to pinpoint the optimum operating conditions of a system by simply performing perturbation type optimization and also it becomes difficult to keep track of different results.

(ii) There are dangers of partial optimization, because optimum operating conditions in one part of the plant do not usually give optimum conditions for other parts of the plant.

7.0 NOMENCLATURE

Optimization:

C_{anopg} = annual operating cost of the gasification system, $

C_{anops} = annual operating cost of the shift reactor system, $

C_{anopm} = annual operating cost of the methanol synthesis section, $

Compressor:

C_v, C_p = Sp. heat of gas at contant volume and pressure respectively, kJ $kmol^{-1}K^{-1}$

F_g = molal flow of gas ,kmol s^{-1}

k = gas specific heats ratio

n = equivalent to k

N_s = no. of compression stages.

r_c = compression ratio

R = universal gas constant,kJ $kmol^{-1}s^{-1}$

T_d = outlet temperature, K

T_s = inlet temperature, K

V_F = volumetric flow rate of gas, m^3s^{-1}

Greek letters:

η_p = Compressor cycle polytropic efficiency

η_F = overall efficiency of the compressor.

Air surface condenser and/or cooler:

A_{tot} = total heat transfer surface area, m^2

A_i = heat transfer surface area in region i, m^2

A = fin tube total outside surface area, m^2

C = constant in Martinelli equation

C_1, C_2 = constants

$C_{p,a}$ = sp.heat of air, kJ $kmol^{-1}K^{-1}$

$C_{p,i}$ = sp.heat of gaseous component i, kJ $kmol^{-1}K^{-1}$

$C_{pl,j}$ = sp. heat of liquid component j, kJ $kmol^{-1}K^{-1}$

D_i = inside equivalent tube diameter, m

F_i = molal flow of component i, kmol s^{-1}

f = tube side friction factor

f_g, f_l = friction factors of gas and liquid respectively

h_a = air side heat transfer coeffcient, kW $m^{-2}K^{-1}$

$h_{t,}$ = tube side heat tranfer coefficient, kW $m^{-2}K^{-1}$

h_t = effective tube side heat transfer coefficient, kW $m^{-2}K^{-1}$

h_{fl} = tube side fouling resistance, m^2K kW^{-1}

$HV_{l,j}$ = heat of vaporization of liquid j, kJ $kmol^{-1}$

K = coolant design number

L = length of the tube, m

L_j = molal flow of liquid component j, kmol s^{-1}

m = mass flux in the tube, kg $m^{-2}s^{-1}$

N_{tu} = no. of transfer unit

N_R = no. of tube rows

O_{pf} = optimum fune tube extension ratio

Q_i = heat load in region i , kW

R_j = fouling resistances, m^2K kW^{-1}

$R_{e,g}$ = gas phase Reynolds number

$R_{e,l}$ = liquid phase Reynolds number

r_{foul} = additional tube side fouling resistance, m^2K kW^{-1}

$T_{a,i}$ = air inlet temperature, K

$T_{lm,i}$ = log mean temperature difference in region i, K

$T_{p,b}$ = temperature of the product at the end of condensation, K

$T_{p,d}$ = dew point temperature of the product, K

$T_{p,i}$ = inlet temperature of the product, K

$T_{p,o}$ = oulet temperature of the product, K

u = velocity of products in the tube, m s^{-1}

u_a = velocity of air, m s^{-1}

U_i = overall heat transfer coefficient in region i, kW $m^{-2}K^{-1}$

X = Martenelli parameter

X_g = fraction of gas in the fluid flowing in the tube

Greek letters:

η_f = fin efficiency

ΔP_a = air side pressure pressor drop, kPa

ΔT_a = air temperature change, K

Δv_o = difference between product inlet temperature and air inlet temperature, K

ΔP_t = tube side pressor drop, kPa

ϕ_a = coolant thermal design number

ϕ_g, ϕ_l = Lockhart-Martenelli dimesionless parameter.

μ_a = viscosity of air, kg $m^{-1}s^{-1}$

ρ_a = density of air, kg m^{-3}

ρ_g, ρ_l = density of gas and liquid, kg m^{-3}

τ = dimensionless number

Heat exchanger:

A = heat transfer surface area, m^2

A_o = heat transfer surface area based on outside tube area, m^2

A_i = heat transfer surface area based on inside tube area, m^2

B_c = fraction of baffle cut

C_1 = constant

$C_{p,s}$ = sp.heat of fluid in the shell side, kJ $kmol^{-1}K^{-1}$

$C_{p,t}$ = sp.heat of fluid in the tube side, kJ $kmol^{-1}K^{-1}$

$D_{t,o}$ = outside tube diameter, m

$D_{s,i}$ = inside shell diameter, m

$D_{t,i}$ = tube inside diameter, m

F = dimensionless log mean temperature difference correction factor

f_s, f_t = shell and tube side friction factors respectively

h_s, h_t = shell and tube side heat tranfer coefficients respectively, kW $m^{-2}K^{-1}$

L_{bb} = inside shell diameter to tube bundle by pass clearance, m

L_{bc} = baffle spacing, m

L_t = Tube length, m

L_{tp} = tube pitch, m

M_s, M_t = molal flow in the shell and tube side, kmol s^{-1}

$N_{Re,s}$ = shell side reynolds number

$N_{Re,t}$ = tube side Reynolds number

N_{cc} = no. of crosses made by shell side fluid.

N_{tt} = total number of tubes in the heat exchanger

P = dimensionless factor

Q = total heat load of the heat exchanger, kW

R = dimensionless factor

R_s, R_t = shell and tube side fouling resistances, $m^2K\ kW^{-1}$

S_m = shell side cross-sectional flow area, m^2

$T_{s,i}$ = shell side fluid inlet temperature, K

$T_{t,i}$ = tube side fluid inlet temperature, K

$T_{s,o}$ = shell side fluid outlet temperature, K

$T_{t,o}$ = shell side fluid outlet temperature, K

U = overall heat transfer coefficient, $kW\ m^{-2}K^{-1}$

U_o = overall heat transfer coefficient based on outside tube surface area, $kW\ m^{-2}K^{-1}$

V_t = tube side fluid velocity, $m\ s^{-1}$

Greek letters:

Δh = latent heat change, $kJ\ kmol^{-1}$

Δ_{lm} = log mean temperature difference, K

$\Delta P_s, \Delta P_t$ = shell and tube side pressure drop, kPa

δ = a correlating variable

η = a correlating variable

ψ_c = a correlating variable

μ_t = tube side fluid viscosity, $kg\ m^{-1}s^{-1}$

ρ_t = tube side pressure drop, $kg\ m^{-3}$

Distillation column:

B = bottom product rate, $kmol\ s^{-1}$

D = Top product rate, $kmol\ s^{-1}$

F = Feed rate, $kmol\ s^{-1}$

q = ratio of the heat required to vaporize one mole of feed and the molal latent heat of the feed.

R = operating reflux ratio

R_m = minimum reflux ratio

S_m = minimum no. of trays

x_{lk} = mole fraction of light key component

x_{hk} = mole fraction of heavy key component

X_i = molal flow of component i, $kmol\ s^{-1}$

XX = dimensionless parameter

Y = dimensionless parameter

Greek letters:

α_{lk} = volatility of the light key with respect to heavy key

α_i = volatility of component i with respect to heavy key

θ = a correlating variable

Pressure vessel:

C_c = corrosion allowance, m

C_{tv} = total cost of the vessel, $

C_{tr} = Installed cost of trays, $

D_a = major axis of the ellipsoidal head, m

D_i = inside diameter of the vessel, m

E = welded joint efficiency(fraction)

H_t = height of the vessel, m

L_a = inside radius of hemispherical head, m

n = parameter constant

P = design pressure, kg m^{-2}

R_i = indide radius of the vesesl, m

S = allowable working stress of the pressure vessel material, kg m^{-2}

W_t = wall thickness, m

W_{th} = weight of the head portion, kg

W_{tt} = Total weight of the installed vessel, kg

W_{tv} = total cost of the vessel, $

Greek letters:

ρ_{mt} = density of the vesssel material, kg m^{-3}

Gas liquid Seperator:

V_g = maximum allowable gas velocity, m s^{-1}

V_{ag} = operating gas velocity, m s^{-1}

K_v = constant

D_{sp} = inside diameter of the seperator vessel, m

G_{gf} = mass flow rate of gas in the seperator, kg s^{-1}

H_{sp} = height of the seperator, m

P_{sr} = operating pressure of the seperator, kPa

Greek letters:

ρ_g, ρ_l = gas and liquid density, kg m^{-3}

ΔP_{sr} = pressure drop of fluid in the seperator , kPa

8.0 REFERENCES

Backhurst, J. R., J. H. Harker, "Process plant design," Heinemann books, London, (1973, 1983).

Beightler, C. S. et al., "Foundation of optimization," 2nd. edition, Prentice-Hall Inc., N.J., (1979).

Bell, K. J., "Approximate sizing of shell-and-tube heat exchanger," Heat exchanger design handbook, Hemisphere publishing corp., pp 3.1.4-1 to 3.1.4-9, (1983).

Beveridge, G. S., and R. S. Schechter, "Optimization: Theory and practice," McGraw-Hill book company, N.Y., (1970).

Box, M. J., "A new method of constrained optimization and a comparison with other methods," Computer J, vol. 8, pp 42-52, (1965).

Fenske, Ind. eng. chem. vol. 24, pp 482-, (1932).

Gilliland, Ind. eng. chem. vol. 32, pp 1220-, (1940).

Himmelblau, D. M., "Applied Nonlinear programming," Mcgraw-Hill book company, N.Y., (1972).

Holland, F. A. et al., "Heat transfer," Heinemann educational books ltd., London, (1970).

Kuester, J. L., and J. A. Mize, "Optimization techniques using FORTRAN," McGraw-Hill book company, N.Y., (1973)

Molokanov, Y.K. et al., International chemical engineering, vol. 12, no. 2, pp 209-, (1972).

Neerken, R. F., "Compressor selection for the chemical process industries," Chemical engg., pp 78-94, (Jan 20,1975).

Paikert, P., "Air cooled heat exchanger," Heat exchanger design handbook, Hemisphere publishing corp., pp 3.8.2-1 to 3.8.9-3, (1983).

Perry, R. H., and D. Green, "Perry's chemical engineers handbook," McGraw-Hill book company, 6th edition, (1984).

Peters, M. S. and K. D. Timmerhaus, " Plant design and economics for chemical engineers," 3rd edition, McGraw-Hill book company, N. Y., (1980).

Taborek, J., "Shell-and-tube heat exchanger", Heat exchanger design handbook, Hemisphere publishing company, pp 3.3.2-1 to 3.3.10-8, (1983).

Underwood, J. of the institute of petroleum, vol. 32, pp 614-, (1946).

Westerberg, A. W., "Optimization in computer-aided-design," Foundation of computer aided chemical process design, vol. I, pp 149-183, (1981).

Wham, R. M., "Liquefaction Technology Assessment - phase 1: Indirect liquefaction of coal to methanol and gasoline using available technology," Oak Ridge National laboratory, ORNL - 5664, (Feb, 1981).

9.0 APPENDICES

APPENDIX V-A1: Module for a centrifugal compressor.

Some compressors perform closely to adiabatic conditions; many others deviate significantly from adiabatic conditions, and must be considered polytropic (Neerken, 1975). In this work the compression cycle was assumed to be polytropic.

Compressor design here was based on the following steps:

(i) Calculation of the number of compression stages.

According to Peters and Timmerhaus(1979), multistage comression is necessory if the ratio of the delivery pressure and intake pressure exceeds approximately 5:1. For this work a ratio of 4:1 was chosen. We can thus easily calculate the number of compression stages necessary.

(ii) Calculation of outlet temperature.

Assuming equal division of work in each stage and intercooling in between stages are such that inlet temperature to each stage is identical to the initial temperature, the outlet temperature was calculated by the following expression:

$$T_d = T_s(r_c)^{n-1/(n \times N_s)} \qquad .....(4)$$

$$\text{Where, } r_c = \frac{P_o}{P_i}$$

$$\frac{n-1}{n} = \frac{k-1}{k}\left(\frac{1}{\eta_p}\right) \quad ; \quad k = \frac{C_p}{C_v}$$

η_p for centrifugal compressor having backward-curved impellers can be obtained from Neerken's (1975) curve. This curve was represented by the following correlation,

$$\eta_p = 0.645 + 0.25\log_{10}(0.59\ V_F) \qquad .....(5)$$

(iii)Calculation of power requirement:

The power (kW) required to compress the fluid was calculated using the following correlation:

$$\text{Power(kW)} = -\frac{1}{\eta_F}\left(\frac{n}{n-1}\right)\left(\frac{Z_s+Z_d}{2}\right) \times R \times N_s \times T_s\left(r_c^{n-1/(nN_s)} - 1\right) \times F_g \quad \ldots\ldots(6)$$

where $R = 8.314$ kJ $kmol^{-1}K^{-1}$

(iv) Calculation of total cost of the compressor:

Compressor cost was calculated using, (Backhurst et al., 1973)

$$\text{Base price(\$ / kW)} = 2260.0\ kW^{-0.5} \quad \ldots\ldots(7)$$

Cost was incresed for pressure more than 6893 kPa.

$$\%\ \text{increase in price} = 0.064\ P^{0.68}$$

Where, P = highest operating pressure, kPa.

APPENDIX V-A2: Module for a surface air cooler/condenser

1.0 Introduction

When the gas/vapour mixture is cooled or condensed, the temperature vs. heat load curves (T/Q curve shown in fig. 7 for a typical gas/vapor mixture), are highly curved. For these systems, the effective mean temperature difference (T_{lm}) and the exchanger surface area are to be determined in several steps after the T/Q curve is linearized. Thus total area of the heat exchanger will be given by

$$A_{tot} = \sum_{i=1}^{3} A_i = \sum_{i=1}^{3} \frac{Q_i}{U_i \, T_{lm,i}} \qquad .....(8)$$

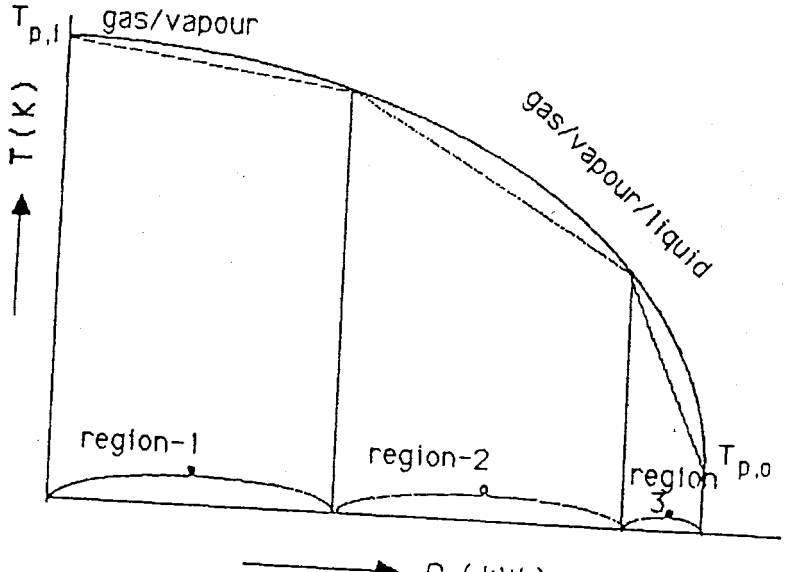

Fig. 7 Temperature distribution for cooling and condensing gas/vapour mixture

Region 1: From the product entering temperature to the dew point of the mixture.

Region 2: From dew point temperature to the end of condensation.

Region 3: subcooling of the gas/condensed vapor mixture.

2.0 Design of the surface air cooler/condenser.

The design strategy for the cooler/condenser is briefly described below:

(i) Estimation of the tube side heat transfer coefficient and fouling resistance:

Approximate values for heating/cooling, condensing, vaporizing heat transfer coefficients were chosen from Bell's (1983) article.

(ii) Heat load calculation:

For region 1,

$$Q_1 = \sum_{i=1}^{N} F_i C_{pi} (T_{p,i} - T_{p,d}) \qquad .....(9)$$

for region 2,

$$Q_2 = \sum_{i=1}^{N} F_i C_{p,i} (T_{p,d} - T_{p,b}) + \sum_{j=1}^{M} L_j HV_{1j} \qquad .....(10)$$

for region 3,

$$Q_3 = \sum_{i=1}^{N} F_i C_{p,i} (T_{p,b} - T_{p,o}) + \sum_{j=1}^{M} L_j C_{pl,j} (T_{p,b} - T_{p,o}) \qquad ...(11)$$

(iii) Selection of Fin tubes:

The optimium surface extension of fin tubes (ratio of total fin surface area and bare tube surface area) was calculated using plots of Paikert(1982). These curves were correlated by the following correlation:

$$O_{pf} = \frac{(1.734 - 0.0232\ h_t)}{(1.0 + 7.8 \times 10^{-4}\ h_t)} \qquad .....(12)$$

(iv) Selection of cooling air velocity, u_a:

Due to the low static pressure of 100 to 200 Pascal developed by conventional fans, the air velocity ranges mostly from 2 to 4 m s^{-1}. In this work u_a was taken equal to 4 m s^{-1}.

(v) Calculation of overall heat transfer coefficient, U:

The overall heat transfer coefficient was calculated using,

$$\frac{1}{U\,A} = \frac{1}{\eta_f h_a A} + \frac{1}{h_t A_i} + R_j \qquad .....(13)$$

Since h_a, η_f etc. are not known, (generally these values are provided by the heat exchanger manufacturers), the following type of fin tube characteristics were chosen for which U and air side pressure drop were obtained from the curves plotted by Paikert (1983). (shown in fig. 8)

L- foot single

$\frac{A}{A_i} = 28$

$\frac{A}{S} = 27.8$

D = 57 mm

d_o = 25 mm

d_i = 20 mm

S = 67 mm

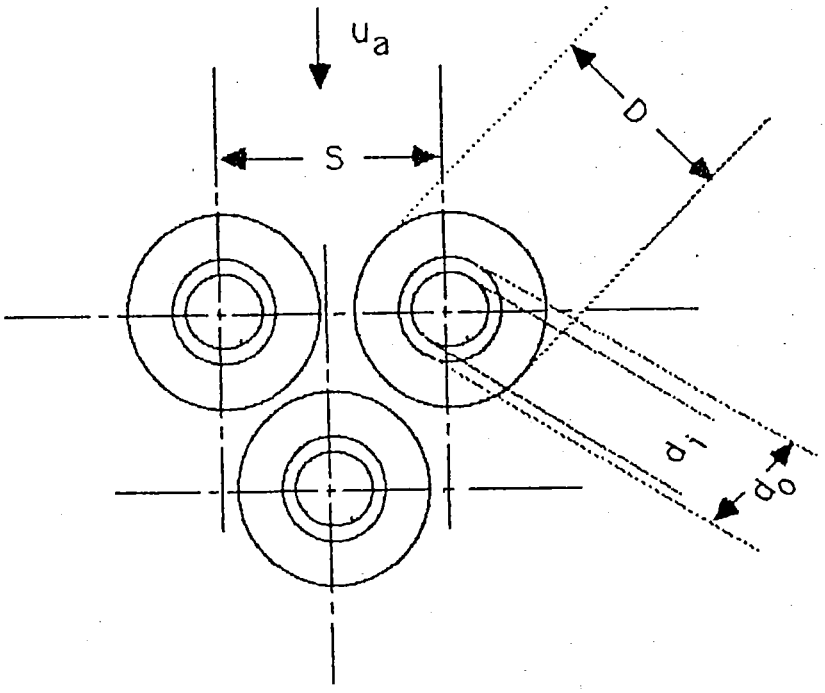

Fig. 8 Fin tube characteristics

When an additional product side fouling resistance r_{foul} needs to be considered, the actual h_t' was determined by,

$$\frac{1}{h_t'} = \frac{1}{h_t} + r_{foul}.$$

For u = 4 m s^{-1}, U was correlated with h_t' from Paikert's plot as

$$U = 10^{-3}\frac{(1.226 + 30.3\ h_t')}{(1.0 + 0.7971\ h_t')} \qquad .....(14)$$

ΔP_a = 0.033 kPa.

(vi) Number of tube rows, N_R (Paikert, 1983).

The number of tube rows can be determined from the empirical correlation,

$$N_R = C_1\ a^{C_2} \qquad .....(15)$$

$$\text{Where, } a = \frac{T_{p,i} - T_{a,i}}{\frac{U\ A}{S}} = \frac{\Delta v_o}{\frac{U\ A}{S}}$$

C_1 = 24 ; C_2 = 0.49 for the type of fin tubes considered here.

For the sake of simplicity N_R was chosen to be 6.

(vii) Number of transfer units, N_{tu}, (Paikert, 1983).

The number of transfer units was determined by,

$$N_{tu} = N_R\ K = \frac{\Delta T_a}{T_{lm,i}} \qquad .....(16)$$

$$\text{where, K is coolant design number} = \frac{U\ A\ /\ S}{\mu_a \rho_a}$$

For optimium design, N_{tu} should lie in the range $0.8 < N_{tu} < 1.5$

(viii) Coolant thermal number, ϕ_a (Paikert, 1983).

The dimensionless value $\phi_a = \Delta_a/\Delta v_o$ depends on the types of air flow through the heat exchanger. For cross flow arrangement, (shown in fig. 9)

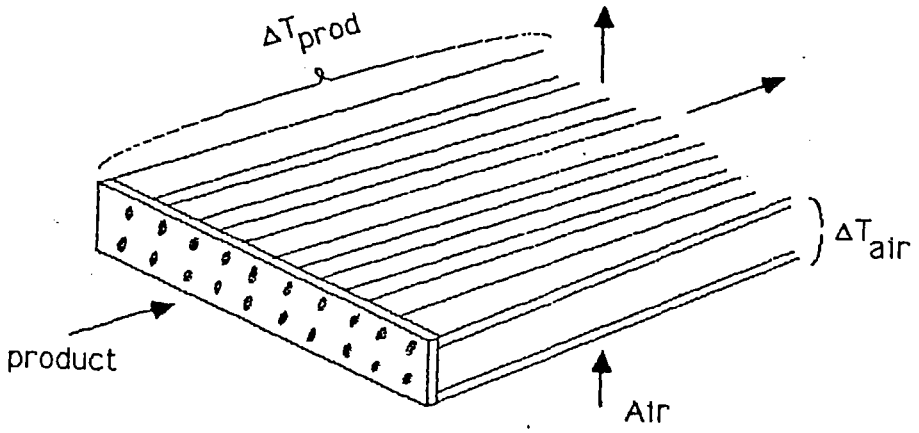

Fig. 9 Cross flow arrangement

$$\phi_a = \frac{1 - \exp[-\tau\,(1 - \exp^{-N_{tu}})]}{\tau} \qquad \ldots.(17)$$

where, $\tau = \Delta_{tp}/\Delta T_a$

Expressions for other types of arrangements e.g, cross counter flow return bend and counter flow return are given by Paikert (1983).

(ix) Effective mean temperature difference, $T_{lm,i}$ (Paikert, 1983)

$$T_{lm,i} = \frac{\Delta T_a}{N_{tu}} = \frac{\phi_a\ \Delta v_o}{N_{tu}} \qquad \ldots..(17a)$$

(x) Surface area of fin tubes, A_i.

$$A_i = \frac{Q_i}{U_i \times T_{lm,i}} \qquad .....(18)$$

(xi) Face area, S.

$$S = \frac{A}{\frac{A}{S} \times N_R} \qquad .....(19)$$

Face area of the heat exchanger was so apportioned to length and width that reasonable bundle dimensions were obtained.

(xii) Tube side pressure drop:

Single phase pressure drop was calculated from the standard formulae,

$$\Delta P_t = \frac{2 f L u^2}{D_i} \qquad .....(20)$$

Two phase pressure drop was calculated from the Lockhart-Martinelli correlations (Paikert, 1983).

$$\phi_g^2 = \frac{\frac{dP_F}{dZ}}{\frac{dP_F}{dZ}} \quad ; \quad \phi_l^2 = \frac{\frac{dP_F}{dZ}}{\frac{dP_F}{dZ}} \qquad .....(20a)$$

Where $\frac{dP_F}{dZ}$ is the two phase frictional pressure gradient.

The single phase pressure gradients was calculated from the standard formulas,

$$-\frac{dP_F}{dZ} = \frac{2 f_g m^2 X_g^2}{D_i \rho_g} \qquad .....(21)$$

$$-\frac{dP_F}{dZ} = \frac{2 f_l m^2 (1 - X_g)^2}{D_i \rho_l} \qquad .....(22)$$

For Laminar flow $N_{Re} < 2000$, f_g or $f_l = \frac{16}{N_{Re}}$

For turbulent flow $N_{Re} > 2000$, f_g or $f_l = 0.079 (N_{Re})^{-0.25}$

Reynolds numbers for different phases can be correlated as

$$N_{Re,g} = \frac{m X_g D_i}{\mu_g} \qquad .....(23)$$

$$N_{Re,l} = \frac{m (1 - X_g)}{\mu_l} \qquad .....(24)$$

A simple and accurate analytical representation of the Lockhart- Martinelli curve is suggested by Chisholm (Paikert, 1983),

$$\phi_l^2 = 1 + C X^{-1} + X^{-2} \qquad .....(25)$$

$$\phi_g^2 = 1 + C X + X^2 \qquad .....(26)$$

Where X is the Martinelli parameter = $\frac{dP_F}{dZ} \div \frac{dP_F}{dZ}$

Values of C for different flow conditions for gas and liquid phases:

Liquiid phase	Gas phase	value of C
Turbulent	Turbulent	20
Laminar	Turbulent	12
Turbulent	Laminar	10
Laminar	Laminar	5

(xiii) Costing : Cost data for extended surface heat exchangers (including fans and motors casing) are given in graphical forms by Peters and Timmerhaus (1980) for different no. of rows (4 - 8 rows) and for the following conditions:

Tube length = 7.32 m

Pressure = 1034 kPa

Material, Carbon steel.

For 6 rows of tubes, the cost data (U.S $, Jan, 1979) were correlated by $Y\ (\$/m^2) = 212.99\ (3.281\ A_i)^{-0.279}$ ...(27) Costs were updated using factors for tube length, pressure, and material of construction.

APPENDIX V-A3: Module for a Shell and tube heat exchanger (All expressions unless otherwise stated were obtained from Taborek, 1983).

This preliminary design algorithm of a shell and tube heat exchanger assumes :-

1. The overall heat transfer coefficient U, the flow rate, and specific heat of the two streams are constant throughout the heat exchanger.

2. For pure countercurrent flow or cocurrent flow, the temperature of either fluid is uniform over any cross section of its path.

3. For a baffled shell and tube exchanger, the heat transferred in each baffle compartment is small compared to the overall heat load i.e. the no. of baffles is large (usally more than 5).

4. Isothermal boiling or condensation occurs uniformly over the whole length of the exchanger.

5. There is equal heat transfer in each tube or shell pass.

6. Heat losses to the surrounding are negligible.

Steps for heat exchanger design

(i) The overall heat transfer coefficient, U was calculated using, (individual heat transfer coefficients were obtained from Bell, 1983)

$$\frac{1}{U} = \frac{1}{h_t} + \frac{1}{h_s} + R_t + R_s \quad \ldots\ldots\ldots\ldots (28)$$

(ii) The heat duty, Q was calculated using,

$$Q = M_s C_{p,s} (T_{s,i} - T_{s,o}) \text{ or}$$

$$M_t C_{p,t} (T_{t,o} - T_{t,i}) \quad \ldots\ldots\ldots (29)$$

or for condensing vapors, $Q = M \Delta h$

(iii) The log mean temperarture difference, T_{lm} and the correction factor for T_{lm} if there are more than one tube or shell passes were calculated. For true cocurrent or countercurrent flow the rate equation for heat transfer is,

$$Q = U\ A\ \Delta T_{lm} \qquad .....(30)$$

For multipass shell and tube heat exchangers eqn. (30) is modified to,

$$Q = U\ A\ F\ \Delta T_{lm} \qquad .....(31)$$

The correction factor F is a function of two dimesionless factors R and P defined as

$$R = \frac{(T_{s,i} - T_{s,o})}{(T_{t,o} - T_{t,i})} \quad ; \quad P = \frac{(T_{t,o} - T_{t,i})}{(T_{s,i} - T_{t,i})}$$

The values of F were obtained from Bell, (1983).

(iv) The heat transfer area (based on outside tube surface area) was estimated using,

$$A_o = \frac{Q}{U_o \Delta T_{lm}\ F} \qquad .....(32)$$

(v) Approximate tube and shell geometries (shown in fig. 10) was estimated using,

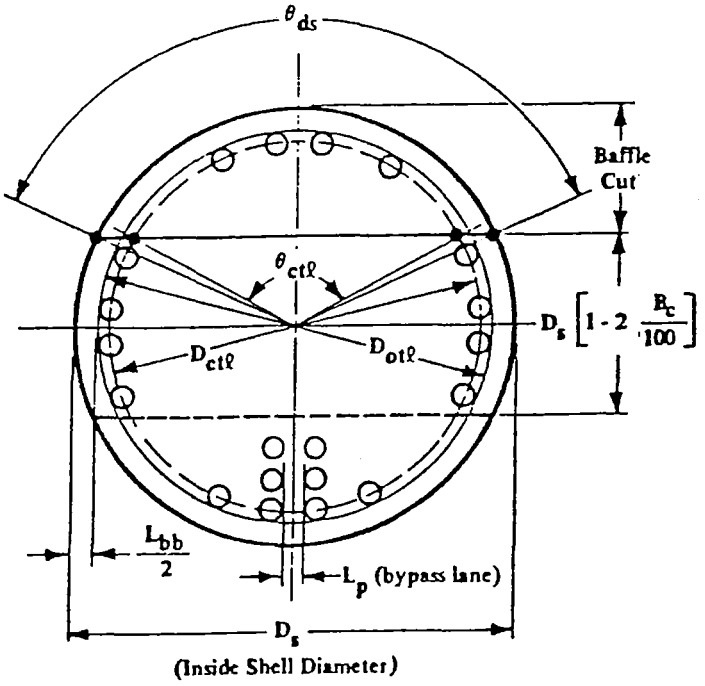

Fig. 10 Basic baffle geometry relation

-- calculation of no. of tubes (using D_{to}=0.02 m, and L_t= 8 m)

$$N_{tt} = \frac{A_o}{\pi D_{t,o} L_t} \qquad .....(33)$$

-- calculation of inside shell diameter, D_{is} (using L_{tp} = 1.35 D_{to}, L_{bb} = 0.042 m),

The following relationships were used:

$$N_{tt} = \frac{0.78}{C_1 L_{tp}^2} \times D_{ctl}^2 \qquad .....(34)$$

$$D_{si} = D_{ctl} + L_{bb} + D_t$$

Where, L_{bb} varies with types of heat exchanger head and shell outside diameter; for split ring and packed floatir head, it can be expressed by a straight line,

$$L_{bb} = 0.025 + 0.017 D_{s,i}$$

C_1 = 0.866 for 30 deg. tube layout chracteristic angle
= 1.0 for 45 and 90 deg. tube layout angle.

(vi) The correction factor, Ψ_c for the reduction in no. of tubes due to tube pass partitions was calculated using the following correlations :-

$$\text{for } D_{ctl} = 2 \text{ m} \; ; \quad \Psi_c = 0.014 + 0.0115 \, (N_{tp} - 2)$$

$$\text{for } D_{ctl} = 1.5 \text{ m}; \quad \Psi_c = 0.018 + 0.016 \, (N_{tp} - 2)$$

$$\text{for } D_{ctl} = 1 \text{ m} \; ; \quad \Psi_c = 0.025 + 0.023 \, (N_{tp} - 2) \qquad \ldots\ldots(35)$$

$$\text{for } D_{ctl} = 0.8 \text{ m}; \quad \Psi_c = 0.033 + 0.028 \, (N_{tp} - 2)$$

so,

actual N_{tt} = previously calculated N_{tt} $(1 - \Psi_c)$

(vii) Effective tube length was calculated using,

$$L_{tt} = \frac{A_o}{\pi \, D_{t,o} N_{tt}} \qquad \ldots\ldots(36)$$

(viii) The tube length was adjusted within 3m and 12m and consequently other shell and tube side specifications.

(ix) The shell side pressure was calculated using,

(a) Average baffle spacing was calculated using,

$$L_{bc} = 0.6 \, D_{s,i}$$

(b) Shell side cross-sectional flow area, S_m was calculated using,

$$S_m = L_{bc} \left[L_{bb} + \frac{D_{ctl}}{L_{tp}} \times (L_{tp} - D_{t,o}) \right] \qquad \ldots\ldots(37)$$

(c) Shell side Reynolds no., $N_{Re,s}$ was calculated using,

$$N_{Re,s} = \frac{D_{t,o} m_s}{\mu_s}$$

$$\text{Where, } m_s = \frac{M_s}{S_m}$$

(d) Shell side fluid friction factor, f_s was calculated in accordance to $N_{Re,s}$.

(e) Number of crosses by shell side fluid, T_{cc} (using segmental baffle cut fraction, B_c=0.25) was calculated using,

$$T_{cc} = \frac{D_{s,o} (1 - 2 B_c)}{L_{pp}} \qquad .....(38)$$

Shell side pressure drop was calculated using,

$$\Delta P_s = \frac{2 \times 10^{-3} f_s T_{cc} m^2}{\rho_s} \qquad .....(39)$$

(x) Tube side pressure drop was calculated using,

(a) Tube side fluid velocity, V_t was calculated using,

$$V_t = \frac{M_t}{0.786 D_{t,i}^2 \rho_t \frac{N_{tt}}{N_{tp}}} \qquad .....(40)$$

(b) Tube side Reynolds number, $N_{Re,t}$ was calculated using,

$$N_{Re,t} = \frac{V_t \rho_t D_{t,i}}{\mu_t} \qquad .....(41)$$

(c) Tube side friction factor ,f_t was calculated using, (Holland, 1970)

For $10^2 < N_{Re,t} < 10^6$,

$$f_t = \frac{0.05573}{N_{Re,t}^{0.261}} \qquad .....(42)$$

Tube side frictional pressure drop, ΔP_t was calculated using,

$$\Delta P_t = \frac{4 f_t L_t \rho V_t^2}{D_{t,i}} \qquad .....(43)$$

Pressure drop due to change in direction (four velocity head

for each tube pass) was added to the tube side pressure drop using,

$$\Delta P_t = \Delta P_t + \frac{4\ N_{tp}\ V_t^2}{2\ \rho_t} \qquad .....(44)$$

(xi) Purchasing cost of the heat exchanger was calculated assuming a floating head heat exchanger using total heat transfer area based on tube inner diameter (Peters and Timmerhaus, 1980).

$$C_{Ex} = 1621.81\ A_i^{0.582} \qquad .....(45)$$

Correction factors for different tube lengths, operating pressure, tube diameter, material of construction was applied to the cost.

APPENDIX V-A4: Process module for a distillation column

Assumptions:

1. Constant relative volatilities.
2. Optimum feed stage location.
3. Constant molal overflow.
4. Feed is liquid i.e at its bubble point.

Distillation column was designed based on the following steps:

(i) The following data were passed to the distillation subroutine:

No. of components, component no. of light key, component no. of heavy key, distillate recovery of light and heavy keys (moles), feed condition, feed rates (moles), Equilibrium values (K values, volatility of components).

Both feed and equilibrium values must be in descending order of volatility.

(ii) Fenske equation (Fenske, 1932) for total reflux was used to get minimum number of theoritical trays.

(iii) Underwood equation (Underwood, 1940) was used to get the minimum reflux ratio at infinite no. of stages.

(iv) Gilliland's curve equivalent equation (Molokanov et al., 1972 fitted Gilliland's curves into an equation) was used to find out the number of theoretical plates at the operating reflux ratio($R = 1.5\ R_{min}$).

Gilliland's curve is approximated by the equivalent equation:

$$Y = 1 - \exp\left| \frac{(1 + 54.4\ XX)\ (XX - 1)}{(11 + 117.2\ XX)\ \sqrt{XX}} \right| \quad \ldots.(46)$$

$$\text{Where. } XX = \frac{R - R_m}{R + 1} \; ; \quad Y = \frac{S - S_m}{S + 1}$$

(v) Using an overall column efficiency, the actual number of plates to be used was calculated.

(vi) Using actual reflux ratio and feed, top and bottom products flows and their conditions, the allowable velocity of vapor and correspondingly allowable diameter (using 70 % of allowable velocity as actual operating velocity) were determined based on some assumed tray spacing.

(vii) Based on the assumed tray spacing, the total height of the column was determined.

(viii) Using typical overall heat transfer coefficients and T_{lm} heat transfer surface area of both condenser and reboiler were calculated from their corresponding heat duties.

(ix) The total cost of the column, trays, condenser and reboiler etc. were calculated.

APPENDIX V-A5: Module for a pressure vessel

Assumptions:

(1) Design pressure is 10% more than the maximum operating pressure (Backhurst et al., 1973).

(2) For vessels operating between 245 K and 615 K, the design temperature was taken as the maximum temperature plus 28 K (Backhurst et al., 1973).

(3) Construction material was assumed to be carbon steel (SA - 285, Gr. C).

(4) Corrosion allowance was taken as 0.004 m.

Pressure vessel was designed on the basis of the following steps :-

(i) The following data were passed to the pressure vessel subroutine:

Shape of the vessel (Cylindrical or Spherical), shape of the head in case of cylindrical vessel (Elliptical or Hemispherical), maximum operating temperature and pressre, diameter and height of the vessel, allowable stress value of the material concerned, efficiency of the welding joint, corrosion allowance, no. of trays and types (if used), density of the material concerned.

(ii) Wall thickness, W_t (Peters and Timmerhaus, 1980) was calculated using,

For cylindrical shells :

$$W_t = \frac{P \times R_i}{S \times E - 0.6\ P} + C_c \quad \text{for } W_t < 0.5\ R_i \text{ or } P < 0.385\ S \times E \quad ..(47)$$

$$= R_i \frac{S \times E + P}{S \times E - P} - R_i + C_c \quad \text{for } W_t > 0.5\ R_i \text{ or } P > 0.385\ S \times E \quad ..(48)$$

For Spherical vessels:

$$W_t = \frac{P \times R_i}{2\,S \times E - 0.2\,P} + C_c \quad \text{for } W_t < 0.356\,R_i \text{ or } P < 0.665\,S \times E \quad ...(49)$$

$$= \frac{2\,S \times E + 2\,P}{2\,S \times E - P} - R_i + C_c \quad \text{for } W_t > 0.5\,R_i \text{ or } P > 0.385\,S \times E \quad ..(50)$$

(iii) The weight of the cylindrical shell or that of the spherical vessel was calculated using,

For cylindrical shell:

$$W_{tv} = 2\pi\, R_i H_t W_t \rho_{mt} \quad .....(51)$$

For Spherical vessels:

$$W_{tv} = 4\pi\, R_i W_t\, (R_i + W_t)\, \rho_{mt} \quad .....(52)$$

(iv) The weight of the head portion in case of a cylindrical vessel was calculated using,

For Ellipsoidal head,

$$W_{th} = \frac{\rho_{mt}\, [\, \pi (n\, D_a + W_t)^2\, W_t]}{4}\ ; \quad .....(53)$$

$n = 1.2$ for $D_a < 1.524$ M
$n = 1.21$ for $1.525 < D_a < 2$
$n = 1.22$ for $2 < D_a < 2.69$
$n = 1.23$ for $D_a > 2.7$

For Hemispherical head,

$$W_{th} = \rho_{mt}\, (\, 2\pi\, L_a^{\,2}\, W_t) \quad .....(54)$$

(v) The total weight of the vessel was increased by 15% for horizontal position or by 20% for vertical position to take into account of extra weight due to nozzles, manholes and skirts or saddles.

(vi) Cost of the vessel (in U.S $, Jan, 1979, Peters and Timmerhaus, 1980). was calculated using,

$$C_{tv} = 110.2 \, (\, 2.204 \, W_{tt})^{-0.34} \, W_{tt} \qquad .....(55)$$

(vii) The cost was updated using factors for material of construction:

(vii) Installed cost of the vessel was calculated from the purchasing cost using lang factors.

Lang factor = 3 for horizotally installed vessels.

Lang factor = 4 for vertically installed vessels.
(Peters and Timmerhaus, 1980).

(viii) Installed cost of trays, (Peters and Timmerhaus, 1980) was calculated using,

$$C_{tr} = N_{tr} \frac{(-67.2 + 350.39 \, D_i)}{(\, 1.0 \, - 0.146 \, D_i)} \qquad .....(56)$$

(ix) The total cost of both vessel and trays were updated using cost indexes.

APPENDIX V-A6: Module for a Gas liquid separator

Gas liquid separator was designed on the basis of following steps:

(i) Gaseous and liquid flow, operating pressure and temperature were passed to the separator subroutine as input data.

(ii) Maximum allowable superficial gas velocity was calculated using, (Peters and Timmerhaus, 1980)

$$V_g = K_g \frac{\rho_l - \rho_g}{\rho_g} \qquad .....(57)$$

The necessary diameter of the separator was calculated using allowable operating gas velocity (70% of the maximum velocity) and volumetric gas flow rate.

$$D_{sp} = \frac{4\ G_{gf}}{\pi\ V_g} \qquad .....(58)$$

(iv) Height of the separator was calculated assuming height is equal to three times of diameter.

$$H_{sp} = 3\ D_{sp} \qquad .....(59)$$

(vi) The pressure drop in the wire demister was calculated using the following correlation for wetted and drained demister (Perry, et al., 1984).

$$\Delta P_{sr} = 0.0115\ (3.28\ V_{ag})^{1.771} \times 0.0254\ kPa \qquad ....(60)$$

(vii) The cost of the separator was calculated similar way like a pressure vessel; and also that of wire demister assuming its cost was around four to five times that of sieve tray.

1.0 SUGGESTIONS FOR FURTHER WORK

More work should be done in the follwing areas:

(i) The performance of the chemical plant optimization study depends on the reliability and accuracy of the process models of the reacting systems which in turn rely heavily on the rate expressions of the reactions concerned (in case of rate models). It is evident from the previous chapters that there are large numbers of rate expressions for the different reacting systems in the literature, but most of these rate expressions have been developed in the laboratory under controlled environments, vastly different from industrial situations. To make the model resuls more meaningful and realistic attention must be paid to the following areas:

(a) estimating the parameters in the rate expressions matching models to plant data or pilot plant data.

(b) analyzing the deactivation behavior of the catalyst with time, total yield and other operating conditions from actual plant or pilot plant data.

(ii) There are not enough reliable cost correlations for reactors and other processing units in the literaure, e.g. in case of a coal-to-methanol and coal-to-SNG plants, costs of coal preparation plant, ash disposal units and Rectisol units. These cost correlations should not only give cost but also reflect the effects of different optimizing variables on costs e.g., the effects of coal particle size on the cost of coal preparation plants, the effects of unreacted carbon in the ash on the cost of ash disposal units, the effects of CO_2 and H_2S concentrations in the synthesis gas on the cost of Rectisol units. These correllations can better be obtained directly from the manufacturers.

(iii) One of the main barriers to performing large scale plant optimization is the excessive amount of costly processing time. The following steps can be taken to reduce

the execution time:

(a) Build simpler input-output models of the main processing units either from the plant data or from the model results using Regression analysis.

(b) Reduce the time required for inner recycle or iterative calculations using empirical correlations to get good starting solutions e.g, in the case of the coal gasifier it would seem possible to correlate the total carbon conversion (which is one of the guessed data for starting the calculation) with H_2O/O_2 ratio, carbon/O_2 ratio, coal particle size, gasifying medium inlet temperature etc., when starting with a good estimate of total carbon conversion the number of iterations in the gasifier calculations can be greatly reduced. Similarly in the case of methanol synthesis and methanation it would seem possible to correlate the recycle compositions to different operating variables to get better starting values for recycle gas composition.